Institut für Nutzpflanzenwissenschaften und Ressourcenschutz
Pflanzenernährung

Functional characterization of inositol pyrophosphate pyrophosphatases in plants

Dissertation

zur Erlangung des Grades

Doktor der Agrarwissenschaften (Dr. agr.)

der Agrar-, Ernährungs- und Ingenieurwissenschaftlichen Fakultät
der Rheinischen Friedrich-Wilhelms-Universität Bonn

von

Robin Schneider

aus

Bonn

Bonn, 2025

Referent: Prof. Dr. Gabriel Schaaf

Korreferent: Prof. Dr. Frank Hochholdinger

Tag der mündlichen Prüfung: 20.03.2025

Angefertigt mit Genehmigung der Agrar-, Ernährungs- und Ingenieurwissenschaftlichen Fakultät der Universität Bonn

This dissertation is submitted as a "semi-cumulative thesis" that covers two publications, of which the second is currently under review. The publications are listed as following:

Published paper:

Gaugler, P.*, Schneider, R.*, Liu, G., Qiu, D., Weber, J., Schmid, J., Jork, N., Häner, M., Ritter, K., Fernández-Rebollo, N., Giehl, R. F. H., Trung, M. N., Yadav, R., Fiedler, D., Gaugler, V., Jessen, H. J., Schaaf, G., Laha, D. (2022). Arabidopsis PFA-DSP-Type Phosphohydrolases Target Specific Inositol Pyrophosphate Messengers. Biochemistry 61 (12), 1213–1227. https://doi.org/10.1021/acs.biochem.2c00145. (Chapter II)

Currrently under review:

Schneider, R.*, Lami, K.*, Prucker, I.*, Stolze, S. C., Strauß, A., Langenbach, K., Lange, E., Schmidt, J. M., Ritter, K., Furkert, D., Faiß, N., Krusenbaum, L., Wege, S., Belay, Y. Z., Kriescher, S., The, J., Harings, M., Schoof, H., Gaugler, P., Kamleitner, M., Fiedler, D., Nakagami, H., Giehl, R. F. H., Lahaye, T., Jessen, H. J., Gaugler, V., Schaaf, G.: NUDIX Hydrolases Target Specific Inositol Pyrophosphates and Regulate Phosphate and Iron Homeostasis, and the Expression of Defense Genes in Arabidopsis. Submitted 2024 in JIPB. (Chapter III)

***** These authors contributed equally to the manuscripts.

Contents

List of Abbreviations

A. thaliana (*At*)	*Arabidopsis thaliana*
ABC	ATP binding cassette
ADP	Adenosine diphosphate
AM	Arbuscular mycorrhiza
ANOVA	Analysis of variance
APases	Acid phosphatases
Ap_nA	Diadenosine polyphosphates
ATP	Adenosine triphosphate
BLAST	Basic local alignment search tool
bp	Base pairs
BP	Biological processes
C-terminus	Carboxy-terminus
Ca^{2+}	Calcium ion
$CaCl_2$	Calcium chloride
CaMV	*Cauliflower mosaic virus*
Cas9	CRISPR-associated protein 9
(CE-)ESI-MS	(Capillary electrophoresis-) Electrospray ionization - mass spectrometry
Col-0	Columbia-0 (*Arabidopsis thaliana* strain)
CRISPR	Clustered regularly interspaced short palindromic repeats
DAPI	4′,6-diamidino-2-phenylindole
DDP1	Diadenosine and diphosphoinositol polyphosphate phosphohydrolase
DEG	Differentially expressed gene
DMSO	Dimethyl sulfoxide

DNA	Deoxyribonucleic acid
dpi	Days post infiltration
EDTA	Ethylenediaminetetraacetic acid.
EYFP	Enhanced yellow fluorescent protein
Fe	Iron
FER1	Ferritin 1
GO	Gene ontology
gRNA / sgRNA	Guide RNA/ single guide RNA
$H_2PO_4^-/HPO_4^{2-}$	Dihydrogen phosphate
His	Histidine
(hs)DIPP	(*homo sapiens*) diphosphoinositol polyphosphate phosphohydrolases
ICP-OES	Inductively coupled plasma - optical emission spectroscopy
ID	Identification
InsP	Inositol polyphosphate/phosphate
$InsP_6$	*Myo*-inositol hexakisphosphate
L. japonicus (*Lj*)	*Lotus japonicus*
LC-MS/MS	Liquid chromatography–mass spectrometry/mass spectrometry
Ler-0	Landsberg erecta-0 (*Arabidopsis thaliana* strain)
M. polymorpha	*Marchantia polymorpha*
MBP	Maltose binding protein
Mg^{2+}	Magnesium ion
$MgCl_2$	Magnesium chloride
MIPS	*Myo*-inositol phosphate synthase
Mn^{2+}	Manganese ion
$MnCl_2$	Manganese chloride

mRNA	Messenger RNA
mrp5	Multidrug resistance-associated protein 5
MYB	Myeloblastosis
N. benthamiana	*Nicotiana benthamiana*
N-terminus	Amino-terminus
NaF	Sodium fluoride
Nb_2O_5	Niobium (V) pentoxide
NUDIX	Nucleoside diphosphate linked to some other moiety X
NUDT	NUDIX-type hydrolase
OD_{600}	Optical density measured at a wavelength of 600 nm
OG	Orange G
ORF	Open reading frame
P	Phosphorus
P	Probability value
PAGE	Polyacrylamide gel electrophoresis
PFA-DSP	Plant and fungi atypical dual specificity phosphatase
P_i	Inorganic phosphate
Poly-P	Polyphosphate
PP	Diphosphates/Pyrophosphate
PP-InsP	Inositol pyrophosphate
PSI	Phosphate starvation-induced
PSR	Phosphate starvation response
PTP	Protein tyrosine phosphatases
(qRT)PCR	(quantitative real-time) polymerase chain reaction
RNA (-seq)	Ribonucleic acid (-sequencing)

ROS	Reactive oxygen species
S. cerevisiae (*Sc*)	*Saccharomyces cerevisiae*
(SAX)-HPLC	Strong anion exchange high performance liquid chromatography
SCF	SKP1-CUL1-F-box
SD	Standard deviation
SEM	Standard error of the mean
SPX	SYG1/Pho81/XPR1-domain containing protein
T-DNA	Transfer-DNA
TiO_2	Titanium (IV) oxide
TPM	Transcripts per million
UTR	Untranslated region
WT	Wild-type
Zn^{2+}	Zinc ion
$ZnCl_2$	Zinc chloride

List of Figures

List of Tables

Summary

The consequences of the climate and biodiversity crisis present an increasingly challenge for the agricultural sector to ensure food security for a growing world population. The optimal nutrient supply of plants is a critical factor in maintaining or increasing yields, especially of essential macronutrients such as phosphorus (P). It is therefore important to gain a deeper understanding of the processes involved in P uptake, in form of inorganic phosphate (P_i), and the mechanisms regulating P_i homeostasis in plants. Recent research has identified the involvement of the signaling molecules inositol pyrophosphates (PP-InsPs) in the process of P_i signaling and homeostasis in plants. The biosynthesis of PP-InsPs relies on balanced phosphorylation and dephosphorylation of inositol phosphates (InsPs) and PP-InsPs. However, the current state of knowledge regarding PP-InsP dephosphorylation is notably limited in comparison to InsP/PP-InsP phosphorylation. Therefore, the objective of this thesis was to identify and characterize putative PP-InsP pyrophosphatases in plants. We found that recombinant proteins of all five Arabidopsis Plant and Fungi Atypical Dual Specificity Phosphatases (PFA-DSP1-5) display pyrophosphatase activity with a high specificity for the 5-β-phosphate of PP-InsPs. Heterologous expression in *Nicotiana benthamiana* leaves provided evidence that Arabidopsis PFA-DSP1 also displays a 5-β-phosphate-specific PP-InsP pyrophosphatase activity *in planta*. Moreover, we identified a family of Arabidopsis NUDIX hydrolases (NUDTs) that group into two closely related subclades. Through *in vitro* assays, heterologous expression systems, and higher-order gene-edited mutants, we found that subclade I NUDTs preferentially hydrolyze 4-$InsP_7$, while subclade II NUDTs target 3-$InsP_7$. In higher-order mutants of subclade II NUDTs, we observed defects in both P_i and iron homeostasis, accompanied by increased levels of 1/3-$InsP_7$ and 5-$InsP_7$. Ectopic expression of NUDTs from both subclades induced local P_i starvation responses (PSRs), while RNA-seq analyses comparing WT and *nudt12/13/16* loss-of-function plants indicate additional PSR-independent roles and a potential involvement of 1/3-$InsP_7$ in the regulation of plant defense.

Collectively, the results presented in thesis show not only new insights into the roles of PFA-DSPs and NUDTs in regulating PP-InsP signaling pathways in plants, but also provide the genetic tools to uncover more general roles of PP-InsPs in plant physiology and plant development.

Zusammenfassung

Die Ernährungssicherung einer wachsenden Weltbevölkerung wird durch die Folgen der Klima- und Biodiversitätskrise zu einer zunehmenden Herausforderung für den Agrarsektor. Eine optimale Nährstoffversorgung der Pflanzen, vor allem mit essenziellen Makronährstoffen wie Phosphor (P), ist entscheidend für die Aufrechterhaltung oder Steigerung der Erträge. Um die Aufnahmeeffizienz von P, in Form von anorganischem Phosphat (P_i), zu erhöhen, ist es wichtig die Mechanismen zu verstehen, welche die P_i-Homöostase in Pflanzen regulieren. Aktuelle Forschungsarbeiten haben gezeigt, dass die Signalmoleküle Inositolpyrophosphate (PP-InsPs) an den Prozessen der P_i-Homöostase in Pflanzen beteiligt sind. Obwohl die Biosynthese von PP-InsPs auf einer ausgewogenen Phosphorylierung und Dephosphorylierung von Inositolphosphaten (InsPs) und PP-InsPs basiert, ist der Kenntnisstand über die Dephosphorylierung von PP-InsPs limitiert. Das Ziel dieser Arbeit war es, PP-InsP Pyrophosphatasen in Pflanzen zu identifizieren und zu charakterisieren. Mit *in vitro* Analysen und der heterologen Expression von Arabidopsis Plant and Fungi Atypical Dual Specificity Phosphatases (PFA-DSPs) in Hefen und Tabak haben wir gezeigt, dass diese Enzyme eine PP-InsP Pyrophosphatase Aktivität mit einer hohen Spezifität für das 5-β-Phosphat aufweisen. Darüber hinaus haben wir sieben Arabidopsis NUDIX-type (NUDT) Hydrolasen identifiziert, die eine PP-InsP Pyrophosphatase Aktivität aufweisen und sich im phylogenetischen Baum in zwei Untergruppen einteilen lassen. Mit Hilfe von *in vitro* Analysen, heterologen Expressionssystemen und Gen-Knockout-Mutanten fanden wir heraus, dass die Gruppe I NUDT Hydrolasen bevorzugt 4-$InsP_7$ hydrolysieren, während Gruppe II NUDT Hydrolasen eine Spezifität für 3-$InsP_7$ aufweisen. In der Arabidopsis dreifach Knockout-Mutante *nudt12/13/16* haben wir Defekte in der P_i- und Eisen-Homöostase beobachtet, zusammen mit erhöhten 1/3-$InsP_7$ und 5-$InsP_7$ Konzentrationen. Darüber hinaus zeigte die heterologe Expression von Arabidopsis NUDT Hydrolasen aus beiden Gruppen eine lokale P_i-Defizit Reaktion (PSR) in Tabakblättern. Die Transkriptomanalyse der Mutante *nudt12/13/16* lieferte zudem Hinweise darauf, dass PP-InsPs auch an PSR-unabhängigen Prozessen beteiligt sein könnten, wie beispielsweise 1/3-$InsP_7$ an der Regulierung der Pflanzenabwehr.

Die in dieser Arbeit vorgestellten Ergebnisse liefern nicht nur neue Erkenntnisse über die Rolle von PFA-DSPs und NUDTs bei der Regulierung von PP-InsP-Signalwegen in Pflanzen, sondern auch das genetische Werkzeug, um allgemeinere Rollen von PP-InsPs in der Pflanzenphysiologie und Pflanzenentwicklung zu erforschen.

Chapter I

General Introduction and Objectives

General Introduction

The agricultural sector faces the dual challenge of maintaining and increasing the crop yield to ensure food security for a growing world population, while also addressing the sustainability of land and resource use in the face of crisis such as climate change and biodiversity crisis. A major challenge is the optimal and sustainable nutrient supply with essential macronutrients such as phosphorus (P) (Vance *et al.*, 2003; Childers *et al.*, 2011; Heuer *et al.*, 2017). As an important structural component of nucleic acids, biomembranes, ATP, and NADPH, P is essential not only for plants but for all living organisms (Westheimer, 1987; Hawkesford *et al.*, 2023). Consequently, concentrations of cellular inorganic phosphate (P_i) affect critical cellular processes, including photosynthesis, respiration, and carbon partitioning (Hawkesford *et al.*, 2023). The acquisition of P_i by plants in the form of $H_2PO_4^-$ and HPO_4^{2-} from the surrounding soil (Hagen and Hopkins, 1955; Sentenac and Grignon, 1985) is a significant contributing factor to the agricultural yield (Holford, 1997; Tilman *et al.*, 2002; MacDonald *et al.*, 2011). However, P_i is highly reactive, which often leads to an immobilization in soils due to processes like adsorption or precipitations with minerals such as calcium, iron, or aluminum, depending on the pH of the soil (Holford, 1997; Abel *et al.*, 2002; Richardson *et al.*, 2009). Furthermore, a large proportion of the soil P contents occurs in an organic form that is unavailable to plants unless it is mineralized (Richardson *et al.*, 2009). Up to half of the soil organic P is present as phytate (Lott *et al.*, 2000), which is the salt of phytic acid, also called *myo*-inositol hexakisphosphate or $InsP_6$ (Shears, 2015). $InsP_6$ is the plants' main P_i storage form in seeds and other plant organs, and is composed of a fully phosphorylated *myo*-inositol ring (Lott *et al.*, 2000). The negative charge of the six phosphate ester groups surrounding the *myo*-inositol ring results in a strong chelation of cations, especially those with a multiple valency (Lott *et al.*, 2000). Similarly, this also occurs in the digestive tract of humans and non-ruminant animals, which can result in mineral deficiency (Raboy *et al.*, 2001). This is particularly problematic when phytate chelates minerals such as iron or zinc in the human digestive tract, which, along with vitamin A and iodine, are the primary nutrient deficiencies contributing to the so called "hidden hunger" worldwide (Lowe, 2021). The term "hidden hunger" describes the phenomenon of consuming an energy-dense diet that lacks essential nutrients, which subsequently leads to a nutrient deficiency (Lowe, 2021). Additionally, the undigested $InsP_6$ present in the manure of non-ruminant animals' functions as an optimal long-term P fertilizer (Shaji *et al.*, 2021). However, in the short term, $InsP_6$ is a suboptimal source of P_i because organic P needs to be mineralized to release P_i in soils (Richardson *et al.*, 2009). Furthermore,

the application of mineral P fertilizer results in the immobilization of a large quantity of P, leading to only 10 % of the applied fertilizer being effectively available for plants (Holford, 1997; Fageria, 2012; Haygarth *et al.*, 2013). This in turn leads to the following issues:

i) Soil erosion, surface runoff and leaching of P fertilized have the potential to result in the pollution and eutrophication of open water bodies (Vance *et al.*, 2003; MacDonald *et al.*, 2011; Cooper and Carliell-Marquet, 2013; Gregory and Nortcliff, 2013; Chen and Graedel, 2016);
ii) Mineral P fertilizer is obtained from phosphate rock, a process that is not only energy-intensive, but also dependent of a non-renewable, finite resource (Baker *et al.*, 2015; Chen and Graedel, 2016; Daramola and Hatzell, 2023). Furthermore, the majority of the world's phosphate rock reserves are located in Morocco (Figure I-1), which creates a high level of dependency in the global P fertilizer market. Besides, global disruptions such as the Russian invasion of Ukraine and the ongoing Middle East war have the potential to further stress the fertilizer market (Daramola and Hatzell, 2023; European Commission, 2024);
iii) Phosphate rock contains heavy metals such as cadmium and uranium, which are also present in mineral P fertilizer in variable concentrations, dependent on the geographical origin of the phosphate rock (McLaughlin *et al.*, 2021; Suciu *et al.*, 2022; Mwalongo *et al.*, 2024). The application of cadmium and uranium with mineral P fertilizers leads to the accumulation in arable soils (Bigalke *et al.*, 2017; Suciu *et al.*, 2022). Due to their toxicity, these heavy metals can pose risks to human health and the environment when they are taken up by crops or leached into ground and surface waters (Bigalke *et al.*, 2017; Li *et al.*, 2021; Luo and Zhang, 2021; Suciu *et al.*, 2022; Mwalongo *et al.*, 2024).

From an economic and ecological perspective, it is important to not only reduce the quantity of applied P fertilizer but also to enhance the P_i-use efficiency of crops. Consequently, it is crucial to understand the mechanisms of P_i sensing and P_i homeostasis in plants.

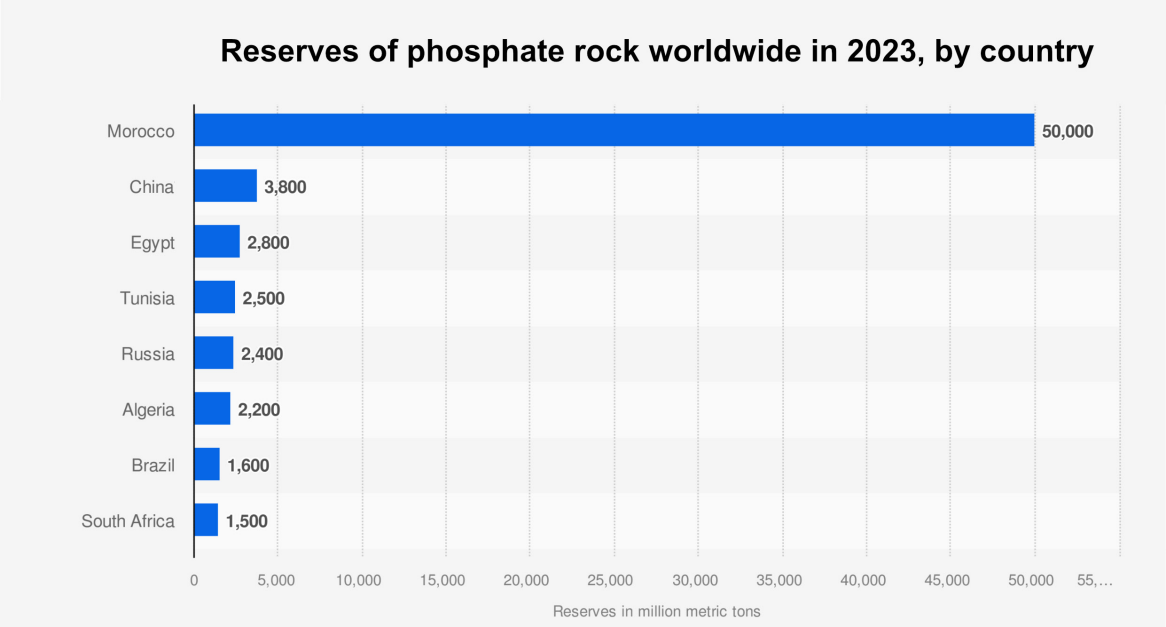

Figure I-1: Reserves of phosphate rock worldwide in 2023, by country ≥ 1,500 million metric tons. Figure with minor modifications adapted from: US Geological Survey. (2024). Reserves of phosphate rock worldwide in 2023, by country (in million metric tons). Statista. Accessed: December 09, 2024. https://www.statista.com/statistics/681747/phosphate-rock-reserves-by-country/

In response to low P_i levels, plants have evolved a range of metabolic and morphological adaption strategies. For instance, plants respond to P deficiency by modifying their root structure, such as reducing the root length and biomass and increasing the number of lateral roots and root hairs to expand the root surface area (Gilroy and Jones, 2000; Canarini *et al.*, 2019; Lopez *et al.*, 2022). The release of root exudates can solubilize P_i from the rhizosphere (Richardson *et al.*, 2001; Carvalhais *et al.*, 2011; Lyu *et al.*, 2016; Rengel *et al.*, 2023) or stimulate beneficial bacteria or fungi in the rhizosphere to solubilize P_i (Ratnayake *et al.*, 1978; Bonfante and Genre, 2010; Pantigoso *et al.*, 2023; Rengel *et al.*, 2023). Furthermore, the redistribution of P_i from older to younger tissues protects the latter from damage caused by P_i deficiency. Some plants also accumulate anthocyanin in tissues during P_i deficiency, likely as an additional form of protection for cells, particularly for nucleic acids, against damage caused by UV light (Vance *et al.*, 2003; Fang *et al.*, 2009). The maintenance of cellular P_i homeostasis is achieved through several mechanisms, including the redistribution of P_i from vacuolar stores, the replacement of membrane phospholipids with galactolipids or sulfolipids, and the bypassing of energy- or P_i-dependent reactions (Abel *et al.*, 2002; Plaxton and Tran, 2011; Fang *et al.*, 2009). These adaptations are regulated by a number of molecular signaling networks, collectively known as P_i starvation response (PSR).

An essential aspect of the PSR is the expression of P_i starvation-induced (PSI) genes, which are regulated by the MYB transcription factors PHR1 and PHL1 (Figure I-2). Under P_i deficiency, these transcription factors bind to the P1BS element located in the promoter region of PSI genes (Rubio *et al.*, 2001; Bustos *et al.*, 2010). Under P_i sufficient conditions, the transcription factor is negatively regulated by stand-alone SPX proteins (Liu *et al.*, 2010; Lv *et al.*, 2014; Shi *et al.*, 2014; Puga *et al.*, 2014; Wang *et al.*, 2014; Qi *et al.*, 2017; Zhong *et al.*, 2018; Osorio *et al.*, 2019; Ried *et al.*, 2021). The negative regulation is driven by the binding of inositol pyrophosphates (PP-InsPs) to SPX proteins, which in turn promotes the complex formation of SPX and PHR1, thereby inhibiting the expression of PSI genes (Wild *et al.*, 2016; Ried *et al.*, 2021; Dong *et al.*, 2019; Zhu *et al.*, 2019). PP-InsPs are small signaling molecules consisting of a phosphorylated *myo*-inositol ring and one or several pyrophosphate groups (Shears, 2015). The disruption of the PP-InsP synthesis in plants has been observed to result in an upregulated PSR, which indicates the important role of PP-InsP in P_i sensing (Dong *et al.*, 2019; Zhu *et al.*, 2019; Riemer *et al.*, 2021). Moreover, PP-InsPs are also involved in the accumulation of storage lipids (Couso *et al.*, 2016) and are key components regulating responses to plant hormones, such as jasmonate (Laha *et al.*, 2015; Laha *et al.*, 2016), auxin (Laha *et al.*, 2022), and salicylic acid (Gulabani *et al.*, 2021).

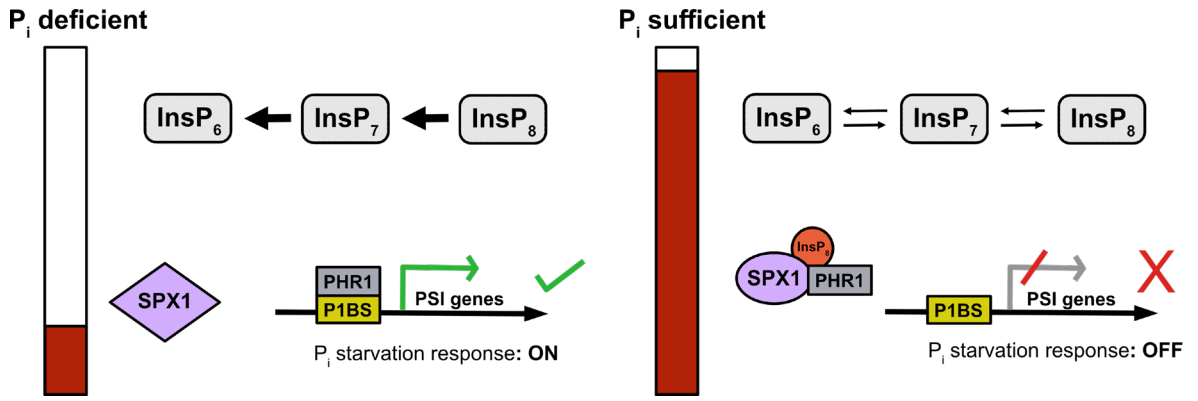

Figure I-2: PP-InsP-dependent regulation of PSR in plants. Under P_i deficiency, $InsP_8$ is hydrolyzed to $InsP_6$, which results in the binding of transcription factors PHR1/PHL1 to the P1BS element located in the promoter region of PSI genes. Under P_i sufficient conditions, the transcription factor is negatively regulated by the formation of a complex with $InsP_8$ and SPX proteins, thereby inhibiting the expression of PSI genes. Figure adapted from Riemer *et al.* (2022).

While a mechanistic understanding of PP-InsP turnover remains largely elusive in plants, evidence from experiments conducted in mammalian cells and yeast suggests a high rate of PP-InsP turnover in cells (Menniti *et al.*, 1993; Kim *et al.*, 2024). Furthermore, the low concentration of PP-InsP in plants and the high charge density present additional challenges to the analysis of PP-InsP levels in plants (Qiu *et al.*, 2020). Depending on the pyrophosphate position on the *myo*-inositol ring, it is possible that six different $InsP_7$ isomers exist in plants. However, many analytical methods are limited in their ability to distinguish isomers with an identical mass. By coupling capillary electrophoresis to an electrospray ionization mass spectrometry (CE-ESI-MS) (Qiu *et al.*, 2020), we were able to identify three $InsP_7$ isomers in plant extracts for the first time (Riemer *et al.*, 2021). In *Arabidopsis thaliana* wild-type (WT) plants, 4-$InsP_7$ (carrying the PP-moiety at the 4-position) and/or 6-$InsP_7$ (hereafter referred to as 4/6-$InsP_7$) and 5-$InsP_7$ were the most abundant $InsP_7$ isomers. Furthermore, 1-$InsP_7$ and/or 3-$InsP_7$ (hereafter referred to 1/3-$InsP_7$) was also identified in the plant extracts (Riemer *et al.*, 2021). Due to the plane of symmetry dissection at the 2 and 5 positions of $InsP_6$ (Figure I-3), the precursor of PP-InsPs, the 1/3 and 4/6 phosphates are enantiomeric and cannot be distinguished in the absence of chiral selectors (Blüher *et al.*, 2017; Ritter *et al.*, 2023). Therefore, it is unclear whether plants contain 1-$InsP_7$ or 3-$InsP_7$, 4-$InsP_7$ or 6-$InsP_7$, and also 1,3-$InsP_8$ or 3,5-$InsP_8$ or, if both isomers are present, which of them is the most abundant (Riemer *et al.*, 2021).

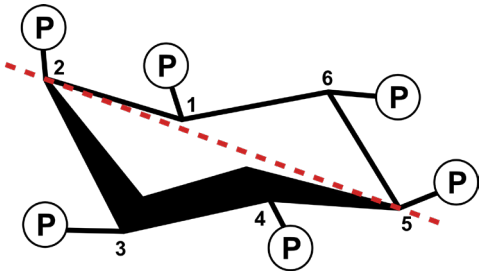

Figure I-3: Structure of *myo*-inositol hexakisphosphate demonstrating the plane of symmetry dissection at the 2 and 5 positions.

The PP-InsP synthesis pathway has been well-studied in mammals and yeast, whereas comparatively little is known about PP-InsP metabolism in plants. Of all inositol phosphates (InsPs), including also the PP-InsPs, $InsP_6$ is the most abundant in plant cells (Raboy, 2003). In mammals and yeast the phosphorylation of $InsP_6$ to 5-$InsP_7$ is catalyzed by Kcs1/IP6K-type proteins, while in plants a sequence-unrelated enzyme family was identified (Saiardi *et al.*, 1999; Draskovic *et al.*, 2008). *In vitro* and yeast-based studies have demonstrated that various Arabidopsis and rice inositol (1,3,4) trisphosphate 5/6-kinases (ITPKs) possess the ability to catalyze the phosphorylation of $InsP_6$ to 5-$InsP_7$ (Laha *et al.*, 2020; Whitfield *et al.*, 2020). Additionally, this activity was observed *in planta* with Arabidopsis ITPK1 and ITPK2 (Riemer *et al.*, 2021; Laha *et al.*, 2022). In contrast, the phosphorylation of $InsP_6$ to 1/3-$InsP_7$ and 5-$InsP_7$

to $InsP_8$ by VIP1/PPIP5K-type kinases appear to be largely conserved in eukaryotes (Mulugu *et al.*, 2007; Lin *et al.*, 2009; Wang *et al.*, 2011). Two PPIP5K isoforms were identified in Arabidopsis, namely VIH1 and VIH2, which catalyze the synthesis of $InsP_8$ *in planta* (Desai *et al.*, 2014; Laha *et al.*, 2015; Dong *et al.*, 2019; Zhu *et al.*, 2019) and are likely involved in the 1/3-$InsP_7$ synthesis as well (Riemer *et al.*, 2021). Furthermore, a recent study has demonstrated that IPK2α phosphorylates $InsP_6$ to 4/6-$InsP_7$ *in vitro* and reported a 30 % and 40 % reduction of 4/6-$InsP_7$ in Marchantia *IPMK* knockout mutants and Arabidopsis *ipk2β*$^{-/-}$ *ipk2α*^{kd} (*IPK2α* knockdown in *IPK2β* knockout mutants), respectively, indicating a potential regulatory role of 4/6-$InsP_7$ *in vivo* (Yadav *et al.*, 2023). Although PP-InsP biosynthesis is based on a balanced phosphorylation and dephosphorylation of InsP/PP-InsPs, the current state of knowledge regarding PP-InsP dephosphorylation is notably limited (Figure I-4).

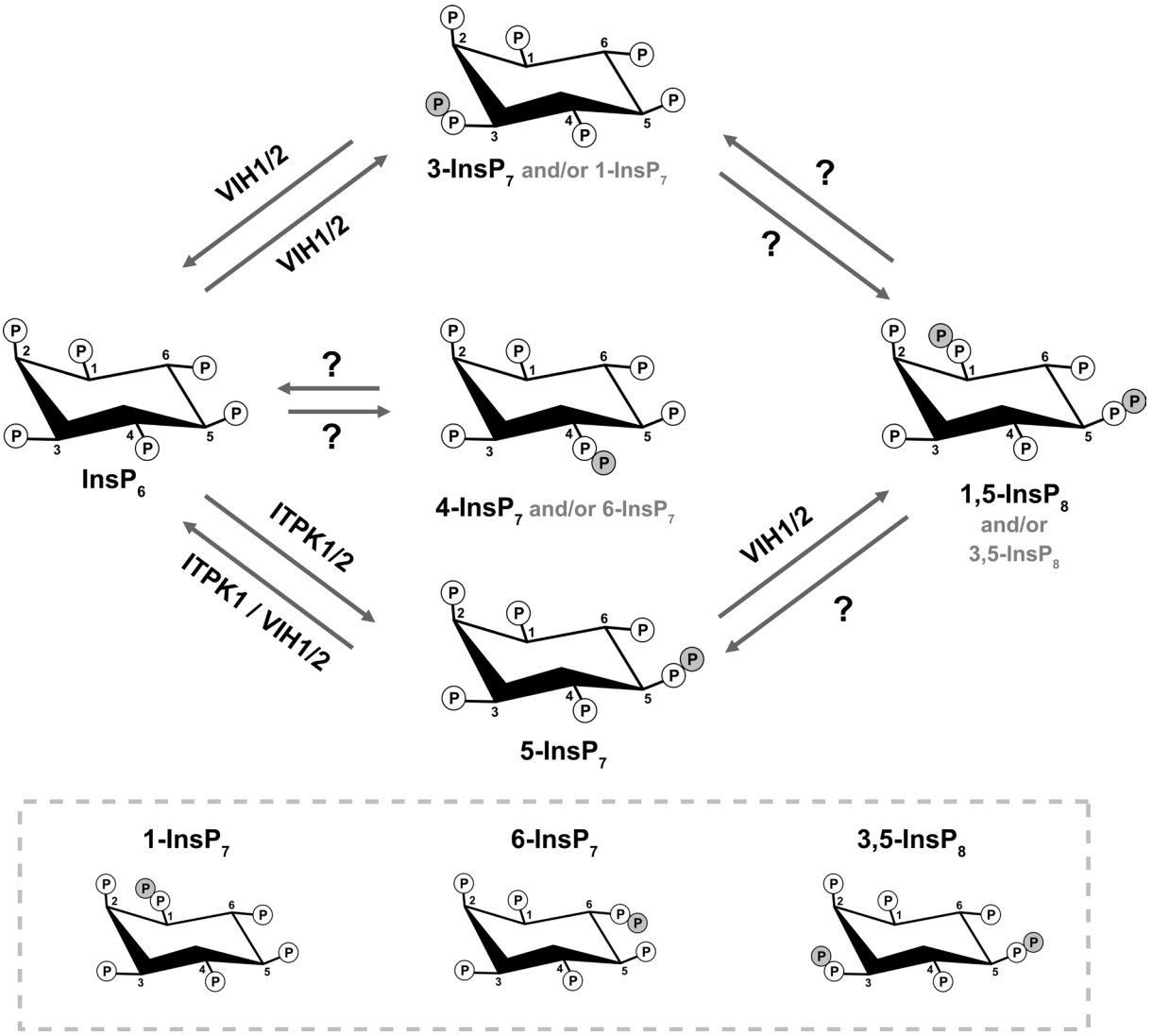

Figure I-4: Current state of knowledge about PP-InsP biosynthesis in plants by ITPK1/2 and VIH1/2.

Similar to yeast and mammalian PPIP5Ks, the Arabidopsis VIH1 and VIH2 are bifunctional enzymes harboring an N-terminal ATP-grasp kinase domain and a C-terminal phosphatase-like domain (Fridy *et al.*, 2007; Mulugu *et al.*, 2007; Wang *et al.*, 2011; Laha *et al.*, 2015; Zhu *et al.*, 2019), the latter of which was shown to hydrolyze 1-$InsP_7$ and 5-$InsP_7$ to $InsP_6$ *in vitro* (Wang *et al.*, 2015; Pascual-Ortiz *et al.*, 2018; Zhu *et al.*, 2019). Moreover, at low adenylate energy charge, ITPK1 has been shown to transfer the β-phosphate from 5-$InsP_7$ to ADP in order to generate $InsP_6$ and ATP (Figure I-4) (Riemer *et al.*, 2021). However, the physiological relevance of these activities in the turnover of PP-InsP *in planta* remains unresolved.

In this thesis, I focus on the functional characterization of putative PP-InsP pyrophosphatases in plants belonging to two conserved phosphatase families. In baker's yeast, the pyrophosphatase Siw14 was identified with a high specificity for the 5-β-phosphate of 5-$InsP_7$ (Steidle *et al.*, 2016; Wang *et al.*, 2018). Siw14 is a member of the Plant and Fungi Atypical Dual Specificity Phosphatases (PFA-DSPs) that belong to a large, conserved family of protein tyrosine phosphatases (PTPs) (Romá-Mateo *et al.*, 2007; Romá-Mateo *et al.*, 2011; Wang *et al.*, 2018). BLAST search analyses revealed that the *Arabidopsis thaliana* genome encodes five PFA-DSPs (Romá-Mateo *et al.*, 2007; Romá-Mateo *et al.*, 2011). Aceti *et al.* (2008) investigated the PFA-DSP1 activity in the presence of a variety of phosphatase substrates and observed the highest phosphatase activity with polyphosphate, deoxyribo- and ribonucleoside triphosphates. However, a putative PP-InsP pyrophosphatase activity was not tested. Thus, chapter II of this thesis is dedicated to the investigation of the potential role of the Arabidopsis PFA-DSP homologues as PP-InsP pyrophosphatases.

A second conserved group of proteins that target different pyrophosphates is the NUDIX-type hydrolases family (hereafter referred to as NUDTs) (Bessman *et al.*, 1996; Sheikh *et al.*, 1998; Yoshimura *et al.*, 2007; Fonseca and Dong, 2014). In Arabidopsis, 29 genes were identified encoding NUDT proteins, whereas one member, NUDT26 (At2g04440), harbors only partly the conserved NUDT motif (GX_5EX_7REUXEEXGU, where U represents a hydrophobic residue such as leucine, isoleucine or valine and X represents any amino acid) (Bessman *et al.*, 1996; Gunawardana *et al.*, 2009; Yoshimura and Shigeoka, 2015). These proteins have been partly characterized in plants and were shown to be involved in oxidative DNA and RNA damage protection, mRNA turnover, abiotic and biotic stress response, starch synthesis, flavin synthesis and protein N-glycosylation, as consequence of 8-oxo-dGTP (Yoshimura *et al.*, 2007), capped mRNA (Xu *et al.*, 2006; Gunawardana *et al.*, 2008), ADP-ribose, NADPH and NADH

(Ge *et al.*, 2007; Ishikawa *et al.*, 2009; Ogawa *et al.*, 2009; Ishikawa *et al.*, 2010b; Ishikawa *et al.*, 2010a; Maruta *et al.*, 2016), ADP-glucose (Muñoz *et al.*, 2006), FAD (Maruta *et al.*, 2012) and GDP-D-mannose (Tanaka *et al.*, 2015) hydrolysis. It has been demonstrated that baker's yeast (ScDdp1) and human (hsDIPP1, 2α, 2β, 3α, and 3β) members of the NUDT family are PP-InsP pyrophosphatases with a preference for the β-phosphate of 1-$InsP_7$ (Safrany *et al.*, 1999; Lonetti *et al.*, 2011; Kilari *et al.*, 2013; Andreeva *et al.*, 2019). Nevertheless, no NUDT hydrolase was identified in plants displaying a PP-InsP pyrophosphatase activity. Therefore, the aim of the third chapter is to determine whether Arabidopsis NUDT hydrolase family members demonstrate a PP-InsP pyrophosphatase activity *in vitro* and *in vivo*. Furthermore, the potential impact of the tested NUDT hydrolases on the plants' P_i homeostasis and other signaling pathways will be demonstrated.

Objectives

The general objective of this work was to identify and functionally characterize PP-InsP pyrophosphatases in plants. Therefore, putative inositol pyrophosphatases of the PFA-DSP family (chapter II) and NUDT hydrolase family (chapter III) were analyzed.

In chapter II, the following specific objectives were addressed:

1. Determine whether *Arabidopsis thaliana* PFA-DSPs are able to hydrolyze $InsP_7$ and $InsP_8$ *in vitro*.
2. Evaluate whether such a pyrophosphatase activity is specific for a β-phosphate of PP-InsPs and dependent on the presence of a divalent cation.
3. Identify whether Arabidopsis PFA-DSPs are able to complement the yeast *siw14Δ*-associated wortmannin sensitivity in yeast and if so, whether this sensitivity is dependent on the presence of a specific PP-InsP.
4. Investigate whether overexpression of Arabidopsis PFA-DSPs affects PP-InsP levels *in planta*.

In chapter III, the following specific objectives were addressed:

1. Validate whether *Arabidopsis thaliana* NUDT hydrolases bind to a non-hydrolysable $InsP_7$ isomer.
2. Evaluate whether NUDT4, NUDT17, NUDT18, and NUDT21 (subclade I), as well as NUDT12, NUDT13, and NUDT16 (subclade II) are able to rescue the metabolic defects of the yeast *ddp1Δ* mutant.
3. Determine whether subclade I and II NUDTs are able to hydrolyze $InsP_7$ and $InsP_8$ *in vitro*, as well as investigate the specificity of a pyrophosphatase activity towards a β−phosphate of PP-InsP, and its dependence on the presence of a divalent cation.
4. Evaluate whether the knockout or the transient overexpression of subclade I and II NUDTs affects InsP/PP-InsP levels *in planta*.
5. Identify whether subclade II NUDTs are transcriptionally responsive to the plant P status and to determine whether the ectopic expression of subclade I or II NUDT hydrolases activates the PSR reaction in *N. benthamiana*.
6. Investigate whether the altered PP-InsP synthesis in *nudt12/13/16* has a regulatory influence on metabolic processes and lead to altered mineral concentrations in shoots.

7. Determine whether the enzyme activity with respect to the 3PP-position of PP-InsPs is specific for subclade II NUDT hydrolases or whether other enzymes also interact with the 3PP-moiety.
8. Identify whether NUDT effectors of pathogenic ascomycete fungi directly interfere with PP-InsPs synthesis in plants by targeting a specific $InsP_7$ isomer.

Finally, I envisage that the fulfillment of these objectives will contribute to a comprehensive understanding of the physiological role of PP-InsPs and the regulation of P_i homeostasis in plants. Additionally, the results presented here may lay the basis for novel approaches for crop engineering to enhance the P_i-use efficiency in plants, thereby contributing to a sustainable reduction in the application of P fertilizer.

References

Abel, S., Ticconi, C. A. and Delatorre, C. A. (2002). Phosphate sensing in higher plants. Physiologia plantarum. 10.1034/j.1399-3054.2002.1150101.x.

Aceti, D. J., Bitto, E., Yakunin, A. F., Proudfoot, M., Bingman, C. A., Frederick, R. O., Sreenath, H. K., Vojtik, F. C., Wrobel, R. L., Fox, B. G., Markley, J. L. and Phillips, G. N. (2008). Structural and functional characterization of a novel phosphatase from the *Arabidopsis thaliana* gene locus At1g05000. Proteins: Structure, Function, and Bioinformatics. 10.1002/prot.22041.

Andreeva, N., Ledova, L., Ryazanova, L., Tomashevsky, A., Kulakovskaya, T. and Eldarov, M. (2019). Ppn2 endopolyphosphatase overexpressed in *Saccharomyces cerevisiae*: Comparison with Ppn1, Ppx1, and Ddp1 polyphosphatases. Biochimie. 10.1016/j.biochi.2019.06.001.

Baker, A., Ceasar, S. A., Palmer, A. J., Paterson, J. B., Qi, W., Muench, S. P. and Baldwin, S. A. (2015). Replace, reuse, recycle: improving the sustainable use of phosphorus by plants. Journal of Experimental Botany. Advanced Access published May 4, 2015: 10.1093/jxb/erv210.

Bessman, M. J., Frick, D. N. and O'Handley, S. F. (1996). The MutT proteins or "Nudix" hydrolases, a family of versatile, widely distributed, "housecleaning" enzymes. Journal of Biological Chemistry. 10.1074/jbc.271.41.25059.

Bigalke, M., Ulrich, A., Rehmus, A. and Keller, A. (2017). Accumulation of cadmium and uranium in arable soils in Switzerland. Environmental pollution (Barking, Essex: 1987). Advanced Access published November 28, 2016: 10.1016/j.envpol.2016.11.035.

Blüher, D., Laha, D., Thieme, S., Hofer, A., Eschen-Lippold, L., Masch, A., Balcke, G., Pavlovic, I., Nagel, O., Schonsky, A., Hinkelmann, R., Wörner, J., Parvin, N., Greiner, R., Weber, S., Tissier, A., Schutkowski, M., Lee, J., Jessen, H., Schaaf, G. and Bonas, U. (2017). A 1-phytase type III effector interferes with plant hormone signaling. Nature Communications. 10.1038/s41467-017-02195-8.

Bonfante, P. and Genre, A. (2010). Mechanisms underlying beneficial plant-fungus interactions in mycorrhizal symbiosis. Nature Communications. Advanced Access published July 27, 2010: 10.1038/ncomms1046.

Bustos, R., Castrillo, G., Linhares, F., Puga, M. I., Rubio, V., Pérez-Pérez, J., Solano, R., Leyva, A. and Paz-Ares, J. (2010). A Central Regulatory System Largely Controls Transcriptional Activation and Repression Responses to Phosphate Starvation in Arabidopsis. PLoS Genetics. 10.1371/journal.pgen.1001102.

Canarini, A., Kaiser, C., Merchant, A., Richter, A. and Wanek, W. (2019). Root Exudation of Primary Metabolites: Mechanisms and Their Roles in Plant Responses to Environmental Stimuli. Frontiers in plant science. Advanced Access published February 21, 2019: 10.3389/fpls.2019.00157.

Carvalhais, L. C., Dennis, P. G., Fedoseyenko, D., Hajirezaei, M.-R., Borriss, R. and Wirén, N. von (2011). Root exudation of sugars, amino acids, and organic acids by maize as affected by nitrogen, phosphorus, potassium, and iron deficiency. Journal of Plant Nutrition and Soil Science. 10.1002/jpln.201000085.

Chen, M. and Graedel, T. E. (2016). A half-century of global phosphorus flows, stocks, production, consumption, recycling, and environmental impacts. Global Environmental Change. 10.1016/j.gloenvcha.2015.12.005.

Childers, D. L., Corman, J., Edwards, M. and Elser, J. J. (2011). Sustainability Challenges of Phosphorus and Food: Solutions from Closing the Human Phosphorus Cycle. BioScience. 10.1525/bio.2011.61.2.6.

Cooper, J. and Carliell-Marquet, C. (2013). A substance flow analysis of phosphorus in the UK food production and consumption system. Resources, Conservation and Recycling. 10.1016/j.resconrec.2013.03.001.

Couso, I., Evans, B. S., Li, J., Liu, Y., Ma, F., Diamond, S., Allen, D. K. and Umen, J. G. (2016). Synergism between Inositol Polyphosphates and TOR Kinase Signaling in Nutrient Sensing, Growth Control, and Lipid Metabolism in Chlamydomonas. The Plant Cell. 10.1105/tpc.16.00351.

Daramola, D. A. and Hatzell, M. C. (2023). Energy Demand of Nitrogen and Phosphorus Based Fertilizers and Approaches to Circularity. ACS Energy Letters. 10.1021/acsenergylett.2c02627.

Desai, M., Rangarajan, P., Donahue, J. L., Williams, S. P., Land, E. S., Mandal, M. K., Phillippy, B. Q., Perera, I. Y., Raboy, V. and Gillaspy, G. E. (2014). Two inositol hexakisphosphate kinases drive inositol pyrophosphate synthesis in plants. The Plant Journal. 10.1111/tpj.12669.

Dong, J., Ma, G., Sui, L., Wei, M., Satheesh, V., Zhang, R., Ge, S., Li, J., Zhang, T.-E., Wittwer, C., Jessen, H. J., Zhang, H., An, G.-Y., Chao, D.-Y., Liu, D. and Lei, M. (2019). Inositol Pyrophosphate $InsP_8$ Acts as an Intracellular Phosphate Signal in Arabidopsis. Molecular Plant. 10.1016/j.molp.2019.08.002.

Draskovic, P., Saiardi, A., Bhandari, R., Burton, A., Ilc, G., Kovacevic, M., Snyder, S. H. and Podobnik, M. (2008). Inositol hexakisphosphate kinase products contain diphosphate and triphosphate groups. Chemistry & biology. 10.1016/j.chembiol.2008.01.011.

European Commission (2024). Short-term outlook for EU agricultural markets, Autumn 2024. European Commission, DG Agriculture and Rural Development, Brussels.

Fageria, N. K. (2012). The Role of Plant Roots in Crop Production. CRC Press.

Fang, Z., Shao, C., Meng, Y., Wu, P. and Chen, M. (2009). Phosphate signaling in Arabidopsis and *Oryza sativa*. Plant Science. 10.1016/j.plantsci.2008.09.007.

Fonseca, J. P. and Dong, X. (2014). Functional characterization of a Nudix hydrolase AtNUDX8 upon pathogen attack indicates a positive role in plant immune responses. PloS one. Advanced Access published December 1, 2014: 10.1371/journal.pone.0114119.

Fridy, P. C., Otto, J. C., Dollins, D. E. and York, J. D. (2007). Cloning and Characterization of Two Human VIP1-like Inositol Hexakisphosphate and Diphosphoinositol Pentakisphosphate Kinases. Journal of Biological Chemistry. 10.1074/jbc.m704656200.

Ge, X., Li, G.-J., Wang, S.-B., Zhu, H., Zhu, T., Wang, X. and Xia, Y. (2007). AtNUDT7, a negative regulator of basal immunity in Arabidopsis, modulates two distinct defense response pathways and is involved in maintaining redox homeostasis. Plant Physiology. Advanced Access published July 27, 2007: 10.1104/pp.107.103374.

Gilroy, S. and Jones, D. L. (2000). Through form to function: root hair development and nutrient uptake. Trends in Plant Science. 10.1016/S1360-1385(99)01551-4.

Gregory, P. J. and Nortcliff, S. (eds.) (2013). Soil conditions and plant growth. Chichester: Wiley-Blackwell.

Gulabani, H., Goswami, K., Walia, Y., Roy, A., Noor, J. J., Ingole, K. D., Kasera, M., Laha, D., Giehl, R. F. H., Schaaf, G. and Bhattacharjee, S. (2021). Arabidopsis inositol polyphosphate kinases IPK1 and ITPK1 modulate crosstalk between SA-dependent immunity and phosphate-starvation responses. Plant Cell Reports. 10.1007/s00299-021-02812-3.

Gunawardana, D., Cheng, H.-C. and Gayler, K. R. (2008). Identification of functional domains in *Arabidopsis thaliana* mRNA decapping enzyme (AtDcp2). Nucleic Acids Research. Advanced Access published November 19, 2007: 10.1093/nar/gkm1002.

Gunawardana, D., Likic, V. A. and Gayler, K. R. (2009). A comprehensive bioinformatics analysis of the Nudix superfamily in *Arabidopsis thaliana*. Comparative and functional genomics. Advanced Access published July 2, 2009: 10.1155/2009/820381.

Hagen, C. E. and Hopkins, H. T. (1955). Ionic Species in Orthophosphate Absorption by Barley Roots. Plant Physiology. 10.1104/pp.30.3.193.

Hawkesford, M. J., Cakmak, I., Coskun, D., De Kok, L. J., Lambers, H., Schjoerring, J. K. and White, P. J. Chapter 6 - Functions of macronutrients. This chapter is a revision of the third edition chapter by M. Hawkesford, W. Horst, T. Kichey, H. Lambers, J. Schjoerring, I. Skrumsager Møller, and P. White, pp. 135–189. DOI: https://doi.org/10.1016/B978-0-12-384905-2.00006-6. © Elsevier Ltd. In Rengel, Z., Cakmak, I., White, P. (eds.), Marschner's Mineral Nutrition of Plants. San Diego: Academic Press, pp. 201–281.

Haygarth, P. M., Bardgett, R. D. and Condron, L. M. Nitrogen and phosphorus cycles and their management. In Gregory, P. J., Nortcliff, S. (eds.), Soil conditions and plant growth. Chichester: Wiley-Blackwell, pp. 132–159.

Heuer, S., Gaxiola, R., Schilling, R., Herrera-Estrella, L., López-Arredondo, D., Wissuwa, M., Delhaize, E. and Rouached, H. (2017). Improving phosphorus use efficiency: a complex trait with emerging opportunities. The Plant Journal. Advanced Access published February 3, 2017: 10.1111/tpj.13423.

Holford, I. C. R. (1997). Soil phosphorus: its measurement, and its uptake by plants. Soil Research. 10.1071/S96047.

Ishikawa, K., Ogawa, T., Hirosue, E., Nakayama, Y., Harada, K., Fukusaki, E., Yoshimura, K. and Shigeoka, S. (2009). Modulation of the poly(ADP-ribosyl)ation reaction via the Arabidopsis ADP-ribose/NADH pyrophosphohydrolase, AtNUDX7, is involved in the response to oxidative stress. Plant Physiology. Advanced Access published August 5, 2009: 10.1104/pp.109.140442.

Ishikawa, K., Yoshimura, K., Harada, K., Fukusaki, E., Ogawa, T., Tamoi, M. and Shigeoka, S. (2010a). AtNUDX6, an ADP-ribose/NADH pyrophosphohydrolase in Arabidopsis, positively regulates NPR1-dependent salicylic acid signaling. Plant Physiology. Advanced Access published February 24, 2010: 10.1104/pp.110.153569.

Ishikawa, K., Yoshimura, K., Ogawa, T. and Shigeoka, S. (2010b). Distinct regulation of Arabidopsis ADP-ribose/NADH pyrophosphohydrolases, AtNUDX6 and 7, in biotic and abiotic stress responses. Plant signaling & behavior. Advanced Access published July 1, 2010: 10.4161/psb.5.7.11820.

Kilari, R. S., Weaver, J. D., Shears, S. B. and Safrany, S. T. (2013). Understanding inositol pyrophosphate metabolism and function: Kinetic characterization of the DIPPs. FEBS Letters. 10.1016/j.febslet.2013.08.035.

Kim, G., Liu, G., Qiu, D., Gopaldass, N., Leo, G. de**, Hermes, J., Timmer, J., Saiardi, A., Mayer, A. and Jessen, H. J.** (2024). Pools of independently cycling inositol phosphates revealed by pulse labeling with ^{18}O-water.

Laha, D., Johnen, P., Azevedo, C., Dynowski, M., Weiß, M., Capolicchio, S., Mao, H., Iven, T., Steenbergen, M., Freyer, M., Gaugler, P., Campos, M. K. de**, Zheng, N., Feussner, I., Jessen, H. J., van Wees, S. C., Saiardi, A. and Schaaf, G.** (2015). VIH2 Regulates the Synthesis of Inositol Pyrophosphate $InsP_8$ and Jasmonate-Dependent Defenses in Arabidopsis. The Plant Cell. 10.1105/tpc.114.135160.

Laha, D., Parvin, N., Dynowski, M., Johnen, P., Mao, H., Bitters, S. T., Zheng, N. and Schaaf, G. (2016). Inositol Polyphosphate Binding Specificity of the Jasmonate Receptor Complex. Plant Physiology. 10.1104/pp.16.00694.

Laha, N. P., Dhir, Y. W., Giehl, R. F., Schäfer, E. M., Gaugler, P., Shishavan, Z. H., Gulabani, H., Mao, H., Zheng, N., von Wirén, N., Jessen, H. J., Saiardi, A., Bhattacharjee, S., Laha, D. and Schaaf, G. (2020). ITPK1-Dependent Inositol Polyphosphates Regulate Auxin Responses in *Arabidopsis thaliana*. Cold Spring Harbor Laboratory.

Laha, N. P., Giehl, R. F. H., Riemer, E., Qiu, D., Pullagurla, N. J., Schneider, R., Dhir, Y. W., Yadav, R., Mihiret, Y. E., Gaugler, P., Gaugler, V., Mao, H., Zheng, N., von Wirén, N., Saiardi, A., Bhattacharjee, S., Jessen, H. J., Laha, D. and Schaaf, G. (2022). INOSITOL (1,3,4) TRIPHOSPHATE 5/6 KINASE1-dependent inositol polyphosphates regulate auxin responses in Arabidopsis. Plant Physiology. 10.1093/plphys/kiac425.

Li, Y., Chen, W., Yang, Y., Wang, T. and Dai, Y. (2021). Quantifying source-specific intake risks of wheat cadmium by associating source contributions of soil cadmium with human health risk. Ecotoxicology and environmental safety. Advanced Access published November 13, 2021: 10.1016/j.ecoenv.2021.112982.

Lin, H., Fridy, P. C., Ribeiro, A. A., Choi, J. H., Barma, D. K., Vogel, G., Falck, J. R., Shears, S. B., York, J. D. and Mayr, G. W. (2009). Structural Analysis and Detection of Biological Inositol Pyrophosphates Reveal That the Family of VIP/Diphosphoinositol Pentakisphosphate Kinases Are 1/3-Kinases. Journal of Biological Chemistry. 10.1074/jbc.m805686200.

Liu, F., Wang, Z., Ren, H., Shen, C., Li, Y., Ling, H.-Q., Wu, C., Lian, X. and Wu, P. (2010). OsSPX1 suppresses the function of OsPHR2 in the regulation of expression of OsPT2 and phosphate homeostasis in shoots of rice. The Plant Journal. Advanced Access published February 9, 2010: 10.1111/j.1365-313X.2010.04170.x.

Lonetti, A., Szijgyarto, Z., Bosch, D., Loss, O., Azevedo, C. and Saiardi, A. (2011). Identification of an Evolutionarily Conserved Family of Inorganic Polyphosphate Endopolyphosphatases. Journal of Biological Chemistry. 10.1074/jbc.m111.266320.

Lopez, G., Ahmadi, S. H., Amelung, W., Athmann, M., Ewert, F., Gaiser, T., Gocke, M. I., Kautz, T., Postma, J., Rachmilevitch, S., Schaaf, G., Schnepf, A., Stoschus, A., Watt, M., Yu, P. and Seidel, S. J. (2022). Nutrient deficiency effects on root architecture and root-to-shoot ratio in arable crops. Frontiers in plant science. Advanced Access published January 4, 2023: 10.3389/fpls.2022.1067498.

Lott, J. N., Ockenden, I., Raboy, V. and Batten, G. D. (2000). Phytic acid and phosphorus in crop seeds and fruits: a global estimate. Seed Science Research. 10.1017/S0960258500000039.

Lowe, N. M. (2021). The global challenge of hidden hunger: perspectives from the field. The Proceedings of the Nutrition Society. Advanced Access published April 26, 2021: 10.1017/S0029665121000902.

Luo, J.-S. and Zhang, Z. (2021). Mechanisms of cadmium phytoremediation and detoxification in plants. The Crop Journal. 10.1016/j.cj.2021.02.001.

Lv, Q., Zhong, Y., Wang, Y., Wang, Z., Zhang, L., Shi, J., Wu, Z., Liu, Y., Mao, C., Yi, K. and Wu, P. (2014). SPX4 Negatively Regulates Phosphate Signaling and Homeostasis through Its Interaction with PHR2 in Rice. The Plant Cell. Advanced Access published April 1, 2014: 10.1105/tpc.114.123208.

Lyu, Y., Tang, H., Li, H., Zhang, F., Rengel, Z., Whalley, W. R. and Shen, J. (2016). Major Crop Species Show Differential Balance between Root Morphological and Physiological Responses to Variable Phosphorus Supply. Frontiers in plant science. Advanced Access published December 21, 2016: 10.3389/fpls.2016.01939.

MacDonald, G. K., Bennett, E. M., Potter, P. A. and Ramankutty, N. (2011). Agronomic phosphorus imbalances across the world's croplands. Proceedings of the National Academy of Sciences. Advanced Access published January 31, 2011: 10.1073/pnas.1010808108.

Maruta, T., Ogawa, T., Tsujimura, M., Ikemoto, K., Yoshida, T., Takahashi, H., Yoshimura, K. and Shigeoka, S. (2016). Loss-of-function of an Arabidopsis NADPH pyrophosphohydrolase, AtNUDX19, impacts on the pyridine nucleotides status and confers photooxidative stress tolerance. Scientific reports. Advanced Access published November 22, 2016: 10.1038/srep37432.

Maruta, T., Yoshimoto, T., Ito, D., Ogawa, T., Tamoi, M., Yoshimura, K. and Shigeoka, S. (2012). An Arabidopsis FAD pyrophosphohydrolase, AtNUDX23, is involved in flavin homeostasis. Plant & cell physiology. Advanced Access published April 13, 2012: 10.1093/pcp/pcs054.

McLaughlin, M. J., Smolders, E., Zhao, F. J., Grant, C. and Montalvo, D. Managing cadmium in agricultural systems. Elsevier, pp. 1–129.

Menniti, F. S., Miller, R. N., Putney, J. W. and Shears, S. B. (1993). Turnover of inositol polyphosphate pyrophosphates in pancreatoma cells. Journal of Biological Chemistry. 10.1016/s0021-9258(18)53551-1.

Mulugu, S., Bai, W., Fridy, P. C., Bastidas, R. J., Otto, J. C., Dollins, D. E., Haystead, T. A., Ribeiro, A. A. and York, J. D. (2007). A Conserved Family of Enzymes That Phosphorylate Inositol Hexakisphosphate. Science. 10.1126/science.1139099.

Muñoz, F. J., Baroja-Fernández, E., Morán-Zorzano, M. T., Alonso-Casajús, N. and Pozueta-Romero, J. (2006). Cloning, expression and characterization of a Nudix hydrolase that catalyzes the hydrolytic breakdown of ADP-glucose linked to starch biosynthesis in *Arabidopsis thaliana*. Plant & cell physiology. Advanced Access published June 13, 2006: 10.1093/pcp/pcj065.

Mwalongo, D. A., Haneklaus, N. H., Lisuma, J. B., Mpumi, N., Amasi, A. I., Mwimanzi, J. M., Chuma, F. M., Kivevele, T. T. and Mtei, K. M. (2024). Uranium Dissemination with Phosphate Fertilizers Globally: A Systematic Review with Focus on East Africa. Sustainability. 10.3390/su16041496.

Ogawa, T., Ishikawa, K., Harada, K., Fukusaki, E., Yoshimura, K. and Shigeoka, S. (2009). Overexpression of an ADP-ribose pyrophosphatase, AtNUDX2, confers enhanced tolerance to oxidative stress in Arabidopsis plants. The Plant journal: for cell and molecular biology. Advanced Access published October 14, 2008: 10.1111/j.1365-313X.2008.03686.x.

Osorio, M. B., Ng, S., Berkowitz, O., Clercq, I. de**, Mao, C., Shou, H., Whelan, J. and Jost, R.** (2019). SPX4 Acts on PHR1-Dependent and -Independent Regulation of Shoot Phosphorus Status in Arabidopsis. Plant Physiology. Advanced Access published July 1, 2019: 10.1104/pp.18.00594.

Pantigoso, H. A., Manter, D. K., Fonte, S. J. and Vivanco, J. M. (2023). Root exudate-derived compounds stimulate the phosphorus solubilizing ability of bacteria. Scientific reports. Advanced Access published March 10, 2023: 10.1038/s41598-023-30915-2.

Pascual-Ortiz, M., Saiardi, A., Walla, E., Jakopec, V., Künzel, N. A., Span, I., Vangala, A. and Fleig, U. (2018). Asp1 Bifunctional Activity Modulates Spindle Function via Controlling Cellular Inositol Pyrophosphate Levels in *Schizosaccharomyces pombe*. Molecular and Cellular Biology. 10.1128/mcb.00047-18.

Plaxton, W. C. and Tran, H. T. (2011). Metabolic adaptations of phosphate-starved plants. Plant Physiology. Advanced Access published May 11, 2011: 10.1104/pp.111.175281.

Puga, M. I., Mateos, I., Charukesi, R., Wang, Z., Franco-Zorrilla, J. M., Lorenzo, L. de**, Irigoyen, M. L., Masiero, S., Bustos, R., Rodríguez, J., Leyva, A., Rubio, V., Sommer, H. and Paz-Ares, J.** (2014). SPX1 is a phosphate-dependent inhibitor of PHOSPHATE STARVATION RESPONSE 1 in Arabidopsis. Proceedings of the National Academy of Sciences. 10.1073/pnas.1404654111.

Qi, W., Manfield, I. W., Muench, S. P. and Baker, A. (2017). AtSPX1 affects the AtPHR1-DNA-binding equilibrium by binding monomeric AtPHR1 in solution. Biochemical Journal. Advanced Access published October 23, 2017: 10.1042/BCJ20170522.

Qiu, D., Wilson, M. S., Eisenbeis, V. B., Harmel, R. K., Riemer, E., Haas, T. M., Wittwer, C., Jork, N., Gu, C., Shears, S. B., Schaaf, G., Kammerer, B., Fiedler, D., Saiardi, A. and Jessen, H. J. (2020). Analysis of inositol phosphate metabolism by capillary electrophoresis electrospray ionization mass spectrometry. Nature Communications. 10.1038/s41467-020-19928-x.

Raboy, V. (2003). *myo*-Inositol-1,2,3,4,5,6-hexakisphosphate. Phytochemistry. 10.1016/s0031-9422(03)00446-1.

Raboy, V., Young, K. A., Dorsch, J. A. and Cook, A. (2001). Genetics and breeding of seed phosphorus and phytic acid. Journal of Plant Physiology. 10.1078/0176-1617-00361.

Ratnayake, M., Leonard, R. T. and Menge, J. A. (1978). Root Exudation In Relation To Supply Of Phosphorus And Its Possible Relevance To Mycorrhizal Formation. New Phytologist. 10.1111/j.1469-8137.1978.tb01627.x.

Rengel, Z., Cakmak, I. and White, P. (eds.) (2023). Marschner's Mineral Nutrition of Plants. San Diego: Academic Press.

Richardson, A. E., Hadobas, P. A. and Hayes, J. E. (2001). Extracellular secretion of Aspergillus phytase from Arabidopsis roots enables plants to obtain phosphorus from phytate. The Plant journal: for cell and molecular biology. 10.1046/j.1365-313x.2001.00998.x.

Richardson, A. E., Hocking, P. J., Simpson, R. J. and George, T. S. (2009). Plant mechanisms to optimise access to soil phosphorus. Crop and Pasture Science. 10.1071/CP07125.

Ried, M. K., Wild, R., Zhu, J., Pipercevic, J., Sturm, K., Broger, L., Harmel, R. K., Abriata, L. A., Hothorn, L. A., Fiedler, D., Hiller, S. and Hothorn, M. (2021). Inositol pyrophosphates promote the interaction of SPX domains with the coiled-coil motif of PHR transcription factors to regulate plant phosphate homeostasis. Nature Communications. 10.1038/s41467-020-20681-4.

Riemer, E., Pullagurla, N. J., Yadav, R., Rana, P., Jessen, H. J., Kamleitner, M., Schaaf, G. and Laha, D. (2022). Regulation of plant biotic interactions and abiotic stress responses by inositol polyphosphates. Frontiers in plant science. Advanced Access published August 11, 2022: 10.3389/fpls.2022.944515.

Riemer, E., Qiu, D., Laha, D., Harmel, R. K., Gaugler, P., Gaugler, V., Frei, M., Hajirezaei, M.-R., Laha, N. P., Krusenbaum, L., Schneider, R., Saiardi, A., Fiedler, D., Jessen, H. J., Schaaf, G. and Giehl, R. F. (2021). ITPK1 is an $InsP_6$/ADP phosphotransferase that controls phosphate signaling in Arabidopsis. Molecular Plant. 10.1016/j.molp.2021.07.011.

Ritter, K., Jork, N., Unmüßig, A.-S., Köhn, M. and Jessen, H. J. (2023). Assigning the Absolute Configuration of Inositol Poly- and Pyrophosphates by NMR Using a Single Chiral Solvating Agent. Biomolecules. Advanced Access published July 19, 2023: 10.3390/biom13071150.

Romá-Mateo, C., Ríos, P., Tabernero, L., Attwood, T. K. and Pulido, R. (2007). A Novel Phosphatase Family, Structurally Related to Dual-specificity Phosphatases, that Displays Unique Amino Acid Sequence and Substrate Specificity. Journal of Molecular Biology. 10.1016/j.jmb.2007.10.008.

Romá-Mateo, C., Sacristán-Reviriego, A., Beresford, N. J., Caparrós-Martín, J. A., Culiáñez-Macià, F. A., Martín, H., Molina, M., Tabernero, L. and Pulido, R. (2011). Phylogenetic and genetic linkage between novel atypical dual-specificity phosphatases from non-metazoan organisms. Molecular Genetics and Genomics. 10.1007/s00438-011-0611-6.

Rubio, V., Linhares, F., Solano, R., Martín, A. C., Iglesias, J., Leyva, A. and Paz-Ares, J. (2001). A conserved MYB transcription factor involved in phosphate starvation signaling both in vascular plants and in unicellular algae. Genes & Development. 10.1101/gad.204401.

Safrany, S. T., Ingram, S. W., Cartwright, J. L., Falck, J. R., McLennan, A. G., Barnes, L. D. and Shears, S. B. (1999). The Diadenosine Hexaphosphate Hydrolases from *Schizosaccharomyces pombe* and *Saccharomyces cerevisiae* Are Homologues of the Human Diphosphoinositol Polyphosphate Phosphohydrolase. Journal of Biological Chemistry. 10.1074/jbc.274.31.21735.

Saiardi, A., Erdjument-Bromage, H., Snowman, A. M., Tempst, P. and Snyder, S. H. (1999). Synthesis of diphosphoinositol pentakisphosphate by a newly identified family of higher inositol polyphosphate kinases. Current Biology. 10.1016/s0960-9822(00)80055-x.

Sentenac, H. and Grignon, C. (1985). Effect of pH on Orthophosphate Uptake by Corn Roots. Plant Physiology. 10.1104/pp.77.1.136.

Shaji, H., Chandran, V. and Mathew, L. Organic fertilizers as a route to controlled release of nutrients, Controlled Release Fertilizers for Sustainable Agriculture. Elsevier, pp. 231–245.

Shears, S. B. (2015). Inositol pyrophosphates: why so many phosphates? Advances in biological regulation. Advanced Access published October 5, 2014: 10.1016/j.jbior.2014.09.015.

Sheikh, S., O'Handley, S. F., Dunn, C. A. and Bessman, M. J. (1998). Identification and characterization of the Nudix hydrolase from the Archaeon, *Methanococcus jannaschii*, as a highly specific ADP-ribose pyrophosphatase. Journal of Biological Chemistry. 10.1074/jbc.273.33.20924.

Shi, J., Hu, H., Zhang, K., Zhang, W., Yu, Y., Wu, Z. and Wu, P. (2014). The paralogous SPX3 and SPX5 genes redundantly modulate P_i homeostasis in rice. Journal of Experimental Botany. Advanced Access published December 24, 2013: 10.1093/jxb/ert424.

Steidle, E. A., Chong, L. S., Wu, M., Crooke, E., Fiedler, D., Resnick, A. C. and Rolfes, R. J. (2016). A Novel Inositol Pyrophosphate Phosphatase in *Saccharomyces cerevisiae*. Journal of Biological Chemistry. 10.1074/jbc.m116.714907.

Suciu, N. A., Vivo, R. de**, Rizzati, N. and Capri, E.** (2022). Cd content in phosphate fertilizer: Which potential risk for the environment and human health? Current Opinion in Environmental Science & Health. 10.1016/j.coesh.2022.100392.

Tanaka, H., Maruta, T., Ogawa, T., Tanabe, N., Tamoi, M., Yoshimura, K. and Shigeoka, S. (2015). Identification and characterization of Arabidopsis AtNUDX9 as a GDP-d-mannose pyrophosphohydrolase: its involvement in root growth inhibition in response to ammonium. Journal of Experimental Botany. Advanced Access published June 6, 2015: 10.1093/jxb/erv281.

Tilman, D., Cassman, K. G., Matson, P. A., Naylor, R. and Polasky, S. (2002). Agricultural sustainability and intensive production practices. Nature. 10.1038/nature01014.

Vance, C. P., Uhde-Stone, C. and Allan, D. L. (2003). Phosphorus acquisition and use: critical adaptations by plants for securing a nonrenewable resource. New Phytologist. 10.1046/j.1469-8137.2003.00695.x.

Wang, H., Falck, J. R., Hall, T. M. T. and Shears, S. B. (2011). Structural basis for an inositol pyrophosphate kinase surmounting phosphate crowding. Nature Chemical Biology. 10.1038/nchembio.733.

Wang, H., Gu, C., Rolfes, R. J., Jessen, H. J. and Shears, S. B. (2018). Structural and biochemical characterization of Siw14: A protein-tyrosine phosphatase fold that metabolizes inositol pyrophosphates. Journal of Biological Chemistry. 10.1074/jbc.ra117.001670.

Wang, H., Nair, V. S., Holland, A. A., Capolicchio, S., Jessen, H. J., Johnson, M. K. and Shears, S. B. (2015). Asp1 from *Schizosaccharomyces pombe* Binds a $[2Fe\text{-}2S]^{2+}$ Cluster Which Inhibits Inositol Pyrophosphate 1-Phosphatase Activity. Biochemistry. 10.1021/acs.biochem.5b00532.

Wang, Z., Ruan, W., Shi, J., Zhang, L., Xiang, D., Yang, C., Li, C., Wu, Z., Liu, Y., Yu, Y., Shou, H., Mo, X., Mao, C. and Wu, P. (2014). Rice SPX1 and SPX2 inhibit phosphate starvation responses through interacting with PHR2 in a phosphate-dependent manner. Proceedings of the National Academy of Sciences. Advanced Access published September 30, 2014: 10.1073/pnas.1404680111.

Westheimer, F. H. (1987). Why Nature Chose Phosphates. Science. 10.1126/science.2434996.

Whitfield, H., White, G., Sprigg, C., Riley, A. M., Potter, B. V., Hemmings, A. M. and Brearley, C. A. (2020). An ATP-responsive metabolic cassette comprised of inositol tris/tetrakisphosphate kinase 1 (ITPK1) and inositol pentakisphosphate 2-kinase (IPK1) buffers diphosphosphoinositol phosphate levels. Biochemical Journal. 10.1042/bcj20200423.

Wild, R., Gerasimaite, R., Jung, J.-Y., Truffault, V., Pavlovic, I., Schmidt, A., Saiardi, A., Jessen, H. J., Poirier, Y., Hothorn, M. and Mayer, A. (2016). Control of eukaryotic phosphate homeostasis by inositol polyphosphate sensor domains. Science. 10.1126/science.aad9858.

Xu, J., Yang, J.-Y., Niu, Q.-W. and Chua, N.-H. (2006). Arabidopsis DCP2, DCP1, and VARICOSE form a decapping complex required for postembryonic development. The Plant Cell. Advanced Access published December 8, 2006: 10.1105/tpc.106.047605.

Yadav, R., Liu, G., Rana, P., Pullagurla, N. J., Qiu, D., Jessen, H. J. and Laha, D. (2023). Conservation of heat stress acclimation by the inositol polyphosphate multikinase, IPMK responsible for 4/6-InsP_7 production in land plants.

Yoshimura, K., Ogawa, T., Ueda, Y. and Shigeoka, S. (2007). AtNUDX1, an 8-oxo-7,8-dihydro-2'-deoxyguanosine 5'-triphosphate pyrophosphohydrolase, is responsible for eliminating oxidized nucleotides in Arabidopsis. Plant & cell physiology. Advanced Access published September 5, 2007: 10.1093/pcp/pcm112.

Yoshimura, K. and Shigeoka, S. (2015). Versatile physiological functions of the Nudix hydrolase family in Arabidopsis. Bioscience, Biotechnology, and Biochemistry. Advanced Access published December 6, 2014: 10.1080/09168451.2014.987207.

Zhong, Y., Wang, Y., Guo, J., Zhu, X., Shi, J., He, Q., Liu, Y., Wu, Y., Zhang, L., Lv, Q. and Mao, C. (2018). Rice SPX6 negatively regulates the phosphate starvation response through suppression of the transcription factor PHR2. New Phytologist. Advanced Access published April 15, 2018: 10.1111/nph.15155.

Zhu, J., Lau, K., Puschmann, R., Harmel, R. K., Zhang, Y., Pries, V., Gaugler, P., Broger, L., Dutta, A. K., Jessen, H. J., Schaaf, G., Fernie, A. R., Hothorn, L. A., Fiedler, D. and Hothorn, M. (2019). Two bifunctional inositol pyrophosphate kinases/phosphatases control plant phosphate homeostasis. eLife. 10.7554/elife.43582.

Chapter II

The objective of chapter II is to determine whether *Arabidopsis thaliana* PFA-DSPs demonstrate a PP-InsP pyrophosphatase activity *in vitro* and *in planta*. This chapter is adapted from the article Gaugler *et al.* (2022) published in ACS Biochemistry. Note that the term "phosphohydrolase" has been changed to "pyrophosphatase" in the following chapter, including the header, due to a more precise and consistent labeling of the enzyme activity.

Gaugler, P.*, Schneider, R.*, Liu, G., Qiu, D., Weber, J., Schmid, J., Jork, N., Häner, M., Ritter, K., Fernández-Rebollo, N., Giehl, R. F. H., Trung, M. N., Yadav, R., Fiedler, D., Gaugler, V., Jessen, H. J., Schaaf, G. and Laha, D. (2022). Arabidopsis PFA-DSP-Type Phosphohydrolases Target Specific Inositol Pyrophosphate Messengers. Biochemistry. Advanced Access published May 31, 2022: 10.1021/acs.biochem.2c00145.

*P.G. and R.S. contributed equally to this manuscript

Own contribution: I purified the recombinant proteins and carried out and analyzed all *in vitro* pyrophosphatase assays. I prepared the figures and wrote the manuscript with P.G., R.Y., G.S., and D.L. with input from all authors.

Arabidopsis PFA-DSP-type pyrophosphatases target specific inositol pyrophosphate messengers

Abstract

Inositol pyrophosphates are signaling molecules containing at least one phosphoanhydride bond that regulate a wide range of cellular processes in eukaryotes. With a cyclic array of phosphate esters and diphosphate groups around *myo*-inositol, these molecular messengers possess the highest charge density found in nature. Recent work deciphering inositol pyrophosphate biosynthesis in Arabidopsis revealed important functions of these messengers in nutrient sensing, hormone signaling, and plant immunity. However, despite the rapid hydrolysis of these molecules in plant extracts, very little is known about the molecular identity of the pyrophosphatases that convert these messengers back to their inositol polyphosphate precursors. Here, we investigate whether Arabidopsis Plant and Fungi Atypical Dual Specificity Phosphatases (PFA-DSP1-5) catalyze inositol pyrophosphate pyrophosphatase activity. We find that recombinant proteins of all five Arabidopsis PFA-DSP homologues display pyrophosphatase activity with a high specificity for the 5-β-phosphate of inositol pyrophosphates and only minor activity against the β-phosphates of 4-$InsP_7$ and 6-$InsP_7$. We further show that heterologous expression of Arabidopsis PFA-DSP1-5 rescues wortmannin sensitivity and deranged inositol pyrophosphate homeostasis caused by the deficiency of the PFA-DSP-type inositol pyrophosphate pyrophosphatase Siw14 in yeast. Heterologous expression in *Nicotiana benthamiana* leaves provided evidence that Arabidopsis PFA-DSP1 also displays 5-β-phosphate-specific inositol pyrophosphate pyrophosphatase activity *in planta*. Our findings lay the biochemical basis and provide the genetic tools to uncover the roles of inositol pyrophosphates in plant physiology and plant development.

Introduction

Inositol pyrophosphates (PP-InsPs), such as $InsP_7$ and $InsP_8$, are molecules derived from *myo*-inositol (Ins) esterified with unique patterns of monophosphates (P) and diphosphates (PP) and have been described as versatile messengers in yeast, amoeba, and animal cells (Menniti *et al.*, 1993; Stephens *et al.*, 1993; Thota and Bhandari, 2015; Shears, 2017). With recent discoveries that PP-InsPs regulate nutrient sensing and immunity in plants, these molecules are

a novel focus of research in plant physiology (Laha *et al.*, 2015; Laha *et al.*, 2016; Couso *et al.*, 2016; Wild *et al.*, 2016; Dong *et al.*, 2019; Zhu *et al.*, 2019; Gulabani *et al.*, 2021; Riemer *et al.*, 2021; Laha *et al.*, 2022). The synthesis of PP-InsPs is partially conserved in eukaryotes, with some important distinctions in plants. In baker's yeast and mammals, 5-$InsP_7$ is synthesized by Kcs1/IP6K-type proteins, whereas Vip1/PPIP5K-type kinases phosphorylate the C1 position of both $InsP_6$ (also termed phytic acid) and 5-$InsP_7$, generating 1-$InsP_7$ and 1,5-$InsP_8$, respectively (Saiardi *et al.*, 1999; Mulugu *et al.*, 2007; Lin *et al.*, 2009; Wang *et al.*, 2011). In plants, detection, quantification, and characterization of PP-InsPs have been challenging due to the low abundance of these molecules and their susceptibility to hydrolytic activities during extraction (Laha *et al.*, 2021; Qiu *et al.*, 2021). Employing [^{3}H] *myo*-inositol labeling and subsequent analysis of plant extracts by strong-anion exchange high-performance liquid chromatography (SAX-HPLC) allowed the detection of PP-InsPs in different plant species (Flores and Smart, 2000; Lemtiri-Chlieh *et al.*, 2000; Desai *et al.*, 2014; Laha *et al.*, 2015). The recent development of capillary electrophoresis (CE) coupled to electrospray ionization mass spectrometry (ESI-MS), has enabled the detection and quantification of many InsP and PP-InsP isomers in various cell extracts including all $InsP_7$ isomers, except enantiomers (labeled, e.g., as 1/3 or 4/6-$InsP_7$) (Qiu *et al.*, 2020). Similar to yeast and mammals, the Arabidopsis PPIP5K isoforms VIH1 and VIH2 catalyze the synthesis of $InsP_8$ (Laha *et al.*, 2015; Zhu *et al.*, 2019) and are likely involved in the synthesis of 1/3-$InsP_7$ (Riemer *et al.*, 2021). However, Kcs1/IP6K-type proteins are absent in land plants. The question of how plants synthesize 5-$InsP_7$ has been partially solved by work on Arabidopsis inositol (1,3,4) triphosphate 5/6 kinases ITPK1 and ITPK2. Notably, ITPK1 and ITPK2 were reported to catalyze the synthesis of 5-$InsP_7$ from $InsP_6$ *in vitro* (Adepoju *et al.*, 2019; Laha *et al.*, 2019; Whitfield *et al.*, 2020) and consequently *itpk1* mutant plants display reduced 5-$InsP_7$ levels (Riemer *et al.*, 2021; Laha *et al.*, 2022).

In Arabidopsis, disturbances in the synthesis of $InsP_7$ and/or $InsP_8$ result in defective signaling of the plant hormones jasmonate (Laha *et al.*, 2015; Laha *et al.*, 2016) and auxin (Laha *et al.*, 2022), as well as defects in salicylic acid-dependent plant immunity (Gulabani *et al.*, 2021) and impaired inorganic phosphate (P_i) homeostasis (Dong *et al.*, 2019; Zhu *et al.*, 2019; Riemer *et al.*, 2021; Wang *et al.*, 2021). In the case of auxin and jasmonate perception, 5-$InsP_7$ and $InsP_8$, respectively, are proposed to function as co-ligands of the respective receptor complexes (Laha *et al.*, 2015; Laha *et al.*, 2016; Laha *et al.*, 2022). The role of PP-InsPs in P_i signaling is related to their ability to bind to SPX proteins, which act as receptors for these messenger molecules (Wild *et al.*, 2016; Gerasimaite *et al.*, 2017; Dong *et al.*, 2019; Zhu *et al.*, 2019; Ried *et al.*,

2021; Zhou *et al.*, 2021). $InsP_8$ has been found as the preferred ligand for stand-alone SPX proteins *in vivo* (Dong *et al.*, 2019; Zhu *et al.*, 2019; Ried *et al.*, 2021). $InsP_8$-bound SPX receptors inactivate the MYB-type transcription factors PHR1 and PHL1, which control the expression of a majority of P_i starvation-induced (PSI) genes to regulate various metabolic and developmental adaptations induced by P_i deficiency (Rubio *et al.*, 2001; Bustos *et al.*, 2010; Puga *et al.*, 2014; Ried *et al.*, 2021). The tissue levels of various PP-InsPs, including 5-$InsP_7$ and $InsP_8$, respond sensitively to the plant's P_i status (Dong *et al.*, 2019; Riemer *et al.*, 2021), suggesting that their synthesis and degradation are tightly regulated. While the steps involved in the synthesis of PP-InsPs in plants are now better understood, still little is known about how these molecules are degraded.

Vip1/PPIP5Ks are bifunctional enzymes that harbor an N-terminal ATP-grasp kinase domain and a C-terminal phosphatase domain conserved in yeast, animals, and plants (Fridy *et al.*, 2007; Mulugu *et al.*, 2007; Wang *et al.*, 2011; Laha *et al.*, 2015; Zhu *et al.*, 2019). *In vitro*, the phosphatase domain of Arabidopsis PPIP5K VIH2 hydrolyzes PP-InsPs to $InsP_6$ (Zhu *et al.*, 2019), similar to the respective C-terminal domains of fission yeast and mammalian PPIP5Ks (Wang *et al.*, 2015; Pascual-Ortiz *et al.*, 2018). Although Arabidopsis ITPK1 harbors no phosphatase domain, under conditions of low adenylate charge, it can shift its activity *in vitro* from kinase to ADP phosphotransferase activity using 5-$InsP_7$ but no other $InsP_7$ isomer (Whitfield *et al.*, 2020; Riemer *et al.*, 2021). Apart from relying on the reversible activities of ITPK1 and Vip1/PPIP5Ks, the degradation of PP-InsPs may also be controlled by specialized pyrophosphatases.

In mammalian cells, diphosphoinositol polyphosphate phosphohydrolases (DIPPs), members of the nudix hydrolase family, have been shown to catalyze the hydrolysis of the diphosphate groups of $InsP_7$ and $InsP_8$ at the C1 and C5 position (Caffrey *et al.*, 1999; Kilari *et al.*, 2013; Shears, 2017). The baker's yeast genome encodes a single homologue of mammalian DIPP1, named diadenosine and diphosphoinositol polyphosphate phosphohydrolase (DDP1), which hydrolyzes various substrates including diadenosine polyphosphates, 5-$InsP_7$ and $InsP_8$, but has a preference for inorganic polyphosphates (poly-P) and for the β-phosphate of 1-$InsP_7$ (Safrany *et al.*, 1999; Lonetti *et al.*, 2011; Andreeva *et al.*, 2019). In addition, baker's yeast has an unrelated PP-InsP pyrophosphatase, Siw14 (also named Oca3) with a high specificity for the β-phosphate at position C5 of 5-$InsP_7$ (Steidle *et al.*, 2016; Wang *et al.*, 2018). This enzyme is a member of the Plant and Fungi Atypical Dual Specificity Phosphatases (PFA-DSPs) that

belong to a large family of protein tyrosine phosphatases (PTPs) (Romá-Mateo *et al.*, 2007; Romá-Mateo *et al.*, 2011; Wang *et al.*, 2018).

Blast search analyses revealed that the *Arabidopsis thaliana* genome encodes five PFA-DSPs, with AtPFA-DSP1 sharing 61 % identity and 76 % similarity with yeast Siw14 (Romá-Mateo *et al.*, 2007; Romá-Mateo *et al.*, 2011). X-ray crystallography revealed that the protein adopts an α/β-fold typical for cysteine phosphatases, with the predicted catalytic cysteine (Cys150) residing at the bottom of a positively charged pocket (Aceti *et al.*, 2008; Romá-Mateo *et al.*, 2011). Of a number of putative phosphatase substrates tested, recombinant AtPFA-DSP1 displayed the highest activity against inorganic polyphosphate, as well as against deoxyribo- and ribonucleoside triphosphates, and less activity against phosphotyrosine-containing peptides and phosphoinositides (Aceti *et al.*, 2008). Here, we investigated whether Arabidopsis PFA-DSPs might function as PP-InsP pyrophosphatases.

Results and Discussion

Arabidopsis PFA-DSP proteins display *in vitro* PP-InsP pyrophosphatase activity with high specificity for 5-InsP$_7$

To explore the potential role of Arabidopsis PFA-DSP proteins in PP-InsP hydrolysis, we first generated translational fusions of PFA-DSPs with an N-terminal hexahistidine tag followed by a maltose-binding protein (MBP) and expressed recombinant proteins in bacteria. Corresponding His-MBP-Siw14 and free His-MBP constructs were generated as controls. All constructs allowed the purification of soluble recombinant proteins (Figure II-S1). We then tested potential PP-InsP pyrophosphatase activities of PFA-DSP1 with 1-InsP$_7$ or 5-InsP$_7$ in the presence of various divalent cations. Notably, PFA-DSP1 failed to catalyze the hydrolysis of 1-InsP$_7$ or 5-InsP$_7$ in the presence of Mn^{2+}, Ca^{2+}, or Zn^{2+}. However, in the presence of the cytoplasmic prevalent cation Mg^{2+}, PFA-DSP1 displayed a robust hydrolytic activity against 5-InsP$_7$, likely resulting in the generation of InsP$_6$, as deduced from the mobility of the reaction product compared to TiO_2-purified *mrp5* (multidrug resistance-associated protein 5) seed extract separated by polyacrylamide gel electrophoresis (PAGE) and visualized by toluidine blue staining (Figure II-1A). Seeds of Arabidopsis *mrp5* mutants that have a defective ABC-transporter involved in vacuolar loading of InsP$_6$ (Nagy *et al.*, 2009) display reduced InsP$_6$ levels and simultaneously increased InsP$_7$ and InsP$_8$ levels (Desai *et al.*, 2014; Laha *et*

al., 2019). Therefore, TiO_2-purified *mrp5* seed extract serves as a marker to visualize $InsP_6$, $InsP_7$, and $InsP_8$ on PAGE. CE-ESI-MS analysis of the reaction product spiked with a [$^{13}C_6$] $InsP_6$ standard confirmed that the resulting product indeed had the migration behavior and the mass of phytic acid (Figure II-1B). In contrast, 1-$InsP_7$ was largely resistant to PFA-DSP1 also in the presence of Mg^{2+} (Figure II-1A). In the absence of divalent cations (i.e., in buffer not supplemented with divalent cations but instead supplemented with EDTA, a condition unlikely to represent any cellular condition), both $InsP_7$ isomers were hydrolyzed to $InsP_6$, as deduced from the mobility of the reaction product by PAGE (Figure II-1A).

We then tested the hydrolytic activities of the Arabidopsis PFA-DSP homologues with all six "simple", synthetic $InsP_7$ isomers and with the two enantiomeric $InsP_8$ isomers 1,5-$InsP_8$ and 3,5-$InsP_8$ in the presence of Mg^{2+}. Of note, *myo*-inositol is a meso compound with a mirror plane dissecting the C2 and C5 positions. Derivatives differentially (pyro)phosphorylated at the C1 and C3 positions, as well as at the C4 and C6 positions are enantiomeric forms that can only be distinguished in the presence of appropriate chiral selectors (Irvine and Schell, 2001; Blüher *et al.*, 2017). Yeast Siw14 and all Arabidopsis PFA-DSPs with the exception of PFA-DSP5, displayed robust activity with a high specificity toward 5-$InsP_7$ (Figure II-1C), confirming earlier reports that 5-$InsP_7$ is a preferred substrate for yeast Siw14 compared to 1-$InsP_7$ (Steidle *et al.*, 2016; Wang *et al.*, 2018). PFA-DSP1–4 and Siw14 also displayed partial hydrolytic activities against the enantiomers 4-$InsP_7$ and 6-$InsP_7$, as well as very weak hydrolytic activities against enantiomeric 1-$InsP_7$ and 3-$InsP_7$ (Figure II-1C). The latter activities were more pronounced in PFA-DSP1 and PFA-DSP3 compared to Siw14 and PFA-DSP2. As for 5-$InsP_7$, the reaction products with the other $InsP_7$ isomers had the mass and the migration behavior of the $InsP_6$ isomer phytic acid, as deduced from CE-ESI-MS analyses (Figure II-1D and Figure II-S2). Notably, PFA-DSP5 only showed very weak activities at the 0.4 µM concentration tested in our assay. However, when the reaction time was extended from 1 h to 2 h and the enzyme concentration was increased to 2 µM, PFA-DSP5 displayed robust activity with a substrate specificity similar to PFA-DSP1-4 and yeast Siw14, with a high selectivity for 5-$InsP_7$ and only weak hydrolytic activities against 4-$InsP_7$ and 6-$InsP_7$ (Figure II-1E).

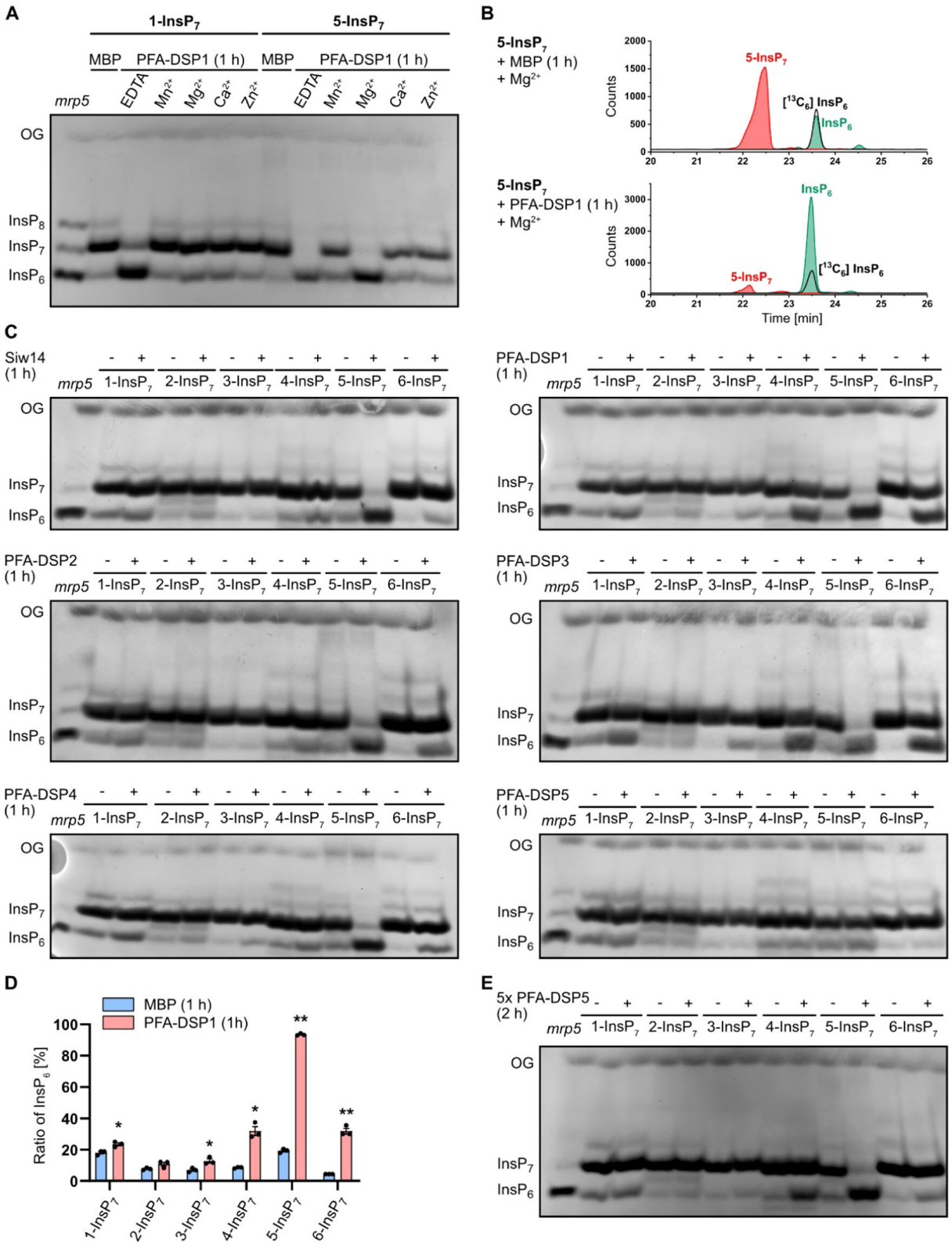

Figure II-1: *In vitro*, Arabidopsis PFA-DSPs display Mg^{2+}-dependent PP-InsP pyrophosphatase activity with high specificity for 5-$InsP_7$. Recombinant His-MBP-PFA-DSPs and His-MBP-Siw14 (indicated with the plus symbol in (C) and (E)) were incubated with 0.33 mM $InsP_7$ at 22 °C. His-MBP served as a negative control (as indicated with the minus symbol in (C) and (E)). (A) 0.4 µM His-MBP-PFA-DSP1 was incubated for 1 h with 1-$InsP_7$ or 5-$InsP_7$, and 1 mM EDTA, $MnCl_2$, $MgCl_2$, $CaCl_2$, or $ZnCl_2$ as indicated. The reaction products were then separated by 33 % PAGE and visualized by toluidine blue. (B–D) The $InsP_7$ pyrophosphatase activity of

~0.4 µM His-MBP-PFA-DSPs and His-MBP-Siw14 was analyzed in the presence of 1 mM $MgCl_2$. After 1 h, the reaction products were then (B, D) spiked with isotopic standards mixture ([$^{13}C_6$] 1,5-$InsP_8$, [$^{13}C_6$] 5-$InsP_7$, [$^{13}C_6$] 1-$InsP_7$, [$^{13}C_6$] $InsP_6$, [$^{13}C_6$] 2-OH $InsP_5$) and subjected to CE-ESI-MS analyses or (C) separated by 33 % PAGE and visualized by toluidine blue/DAPI staining. (D) Data represent mean ± SEM (n = 3). Representative extracted-ion electropherograms are shown in Figure II-S2. Asterisks indicate values that are significantly different from the MBP control reactions (according to Student's t test, $P < 0.05$ (*); $P < 0.01$ (**)). (E) Recombinant His-MBP-PFA-DSP5 (2 µM) was incubated with 0.33 mM $InsP_7$ isomers for 2 h. The reaction product was separated by 33 % PAGE and visualized with toluidine blue. (A, C, E) Identity of bands was determined by migration compared to TiO_2-purified *mrp5* seed extract.

Notably, the meso $InsP_7$ isomer 2-$InsP_7$ was completely resistant to Siw14 or any of the Arabidopsis PFA-DSP proteins under the assay conditions. This was also the case in the absence of divalent cations (i.e., in buffer not supplemented with divalent cations but instead supplemented with EDTA), where Siw14 and Arabidopsis PFA-DSP1-4 failed to hydrolyze 2-$InsP_7$ to a significant extent while all other $InsP_7$ isomers were at least partially converted to an InsP isomer with the mobility of phytic acid (Figure II-S3 and Figure II-S4). Even after a 24 h-long incubation with Arabidopsis PFA-DSP1, 2-$InsP_7$ remained largely resistant to hydrolysis. In contrast, all other PP-$InsP_7$ isomers were hydrolyzed to $InsP_6$ under these conditions, as revealed by PAGE and CE-ESI-MS analyses (Figure II-2A, B, and Figure II-S5). Corresponding control reactions that were supplemented with 5-$InsP_7$ after 23 h validated the activity of Arabidopsis PFA-DSP1 after such long incubation times (Figure II-2A and Figure II-S6). These spiking experiments also rule out the possibility that 2-$InsP_7$ contained a contaminant that inhibits PFA-DSP-dependent hydrolysis, as 5-$InsP_7$ was still efficiently hydrolyzed in the presence of 2-$InsP_7$.

Finally, we tested whether the enantiomeric $InsP_8$ isomers 1,5-$InsP_8$ and 3,5-$InsP_8$ serve as substrates for PFA-DSPs. As reported earlier for Siw14 (Wang *et al.*, 2018), PFA-DSP1–4 hydrolyzed 1,5-$InsP_8$ to an $InsP_7$ isomer based on the mobility of the reaction product in PAGE analyses (Figure II-3A). Also the enantiomeric 3,5-$InsP_8$ was efficiently hydrolyzed by Siw14 and PFA-DSP1–4 (Figure II-3A), and CE-ESI-MS analysis of the reaction products showed the migration behavior and the mass of 1/3-$InsP_7$ (Figure II-3B, C, and Figure II-S7).

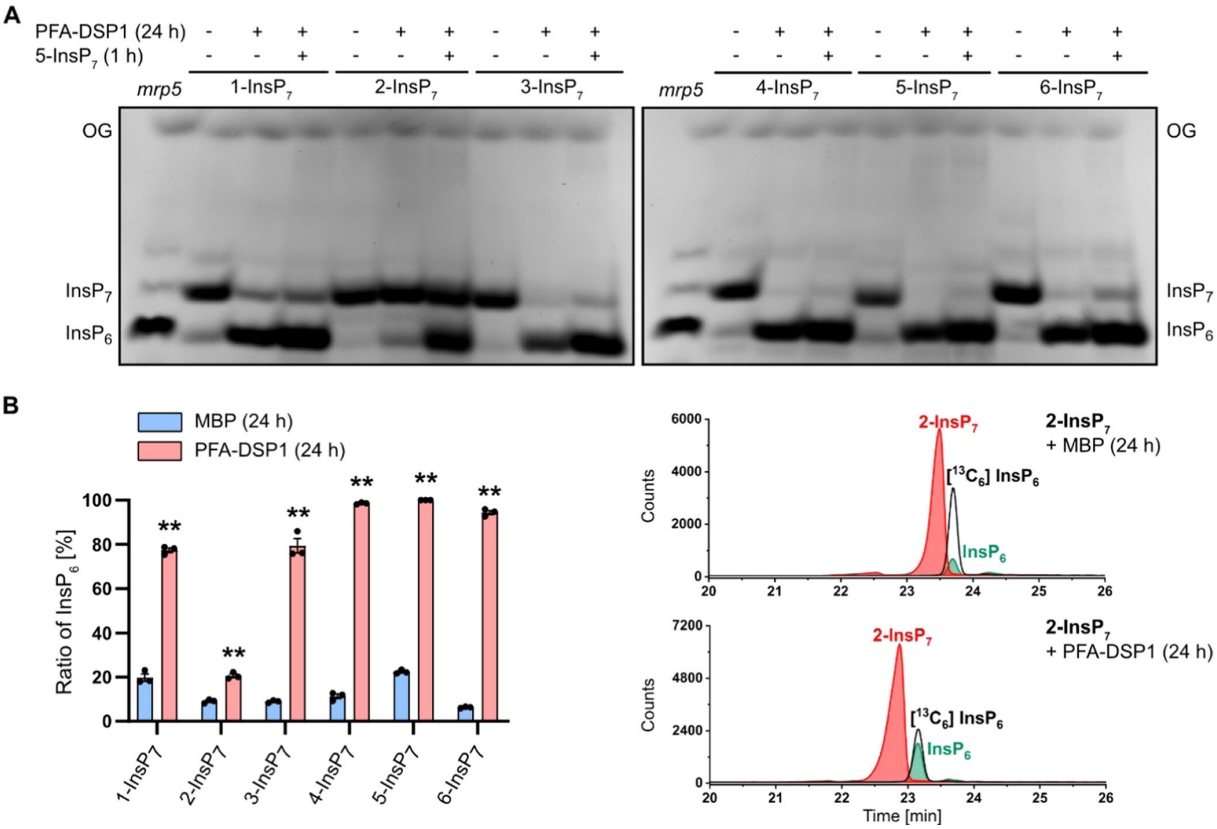

Figure II-2: Under prolonged incubation time Arabidopsis PFA-DSP1 hydrolyzes various $InsP_7$ isomers *in vitro*, except for 2-$InsP_7$. Recombinant His-MBP-PFA-DSP1 (0.4 µM) (indicated with the plus symbol in the first line of (A)) was incubated with 0.33 mM $InsP_7$ and 1 mM $MgCl_2$ for 24 h at 22 °C. To ensure that PFA-DSP1 is active during the whole incubation time, after 23 h, 0.33 mM 5-$InsP_7$ was added to a replicate and incubated for another 1 h (indicated with the plus symbol in the second line of (A)). His-MBP served as a negative control (as indicated with the minus symbol in (A)). (A) An aliquot of the reaction product was separated by 33 % PAGE and visualized with toluidine blue. The identity of bands was determined by migration compared to TiO_2-purified *mrp5* seed extract. (B) Another reaction was spiked with an isotopic standards mixture ([$^{13}C_6$] 1,5-$InsP_8$, [$^{13}C_6$] 5-$InsP_7$, [$^{13}C_6$] 1-$InsP_7$, [$^{13}C_6$] $InsP_6$, [$^{13}C_6$] 2-OH $InsP_5$) and subjected to CE-ESI-MS analyses. Data represent mean ± SEM (n = 3). Asterisks indicate values that are significantly different from the MBP control reactions (according to Student's t test, $P < 0.05$ (*); $P < 0.01$ (**)). Representative extracted-ion electropherograms are shown in Figure Figure II-S5.

Altogether, these findings reveal that Arabidopsis PFA-DSP proteins and yeast Siw14 have a high specificity for the 5-β-phosphate of 5-$InsP_7$, 1,5-$InsP_8$, and 3,5-$InsP_8$, and a weak activity against the β-phosphates of 4-$InsP_7$ and 6-$InsP_7$, respectively. In contrast, $InsP_6$ and 2-$InsP_7$ are resistant to PFA-DSP-catalyzed hydrolysis (summarized in Table II-S1).

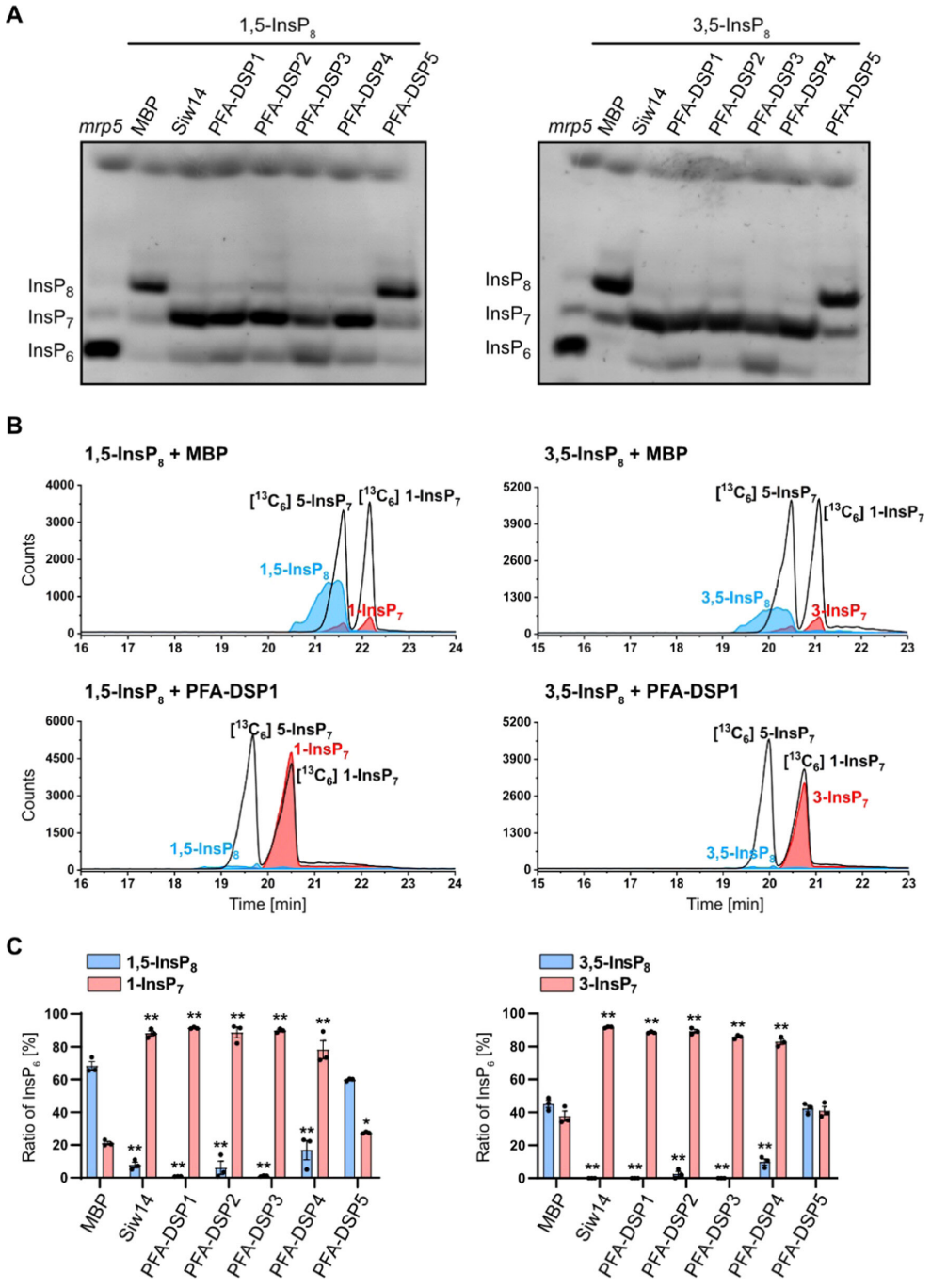

Figure II-3: Arabidopsis PFA-DSPs display robust 1/3,5-$InsP_8$ pyrophosphatase activity *in vitro*. (A) Approximately 0.4 µM His-MBP-PFA-DSPs and His-MBP-Siw14 were incubated with 0.33 mM 1,5-$InsP_8$ or 3,5-$InsP_8$ for 1 h, in the presence of 1 mM $MgCl_2$, and analyzed by PAGE and subsequent toluidine blue staining. The identity of bands was determined by migration compared to TiO_2-purified *mrp5* seed extract. (B, C) Second and third reactions were spiked with isotopic standards mixture ([$^{13}C_6$] 1,5-$InsP_8$, [$^{13}C_6$] 5-$InsP_7$, [$^{13}C_6$] 1-$InsP_7$, [$^{13}C_6$] $InsP_6$, [$^{13}C_6$] 2-OH $InsP_5$) and subjected to CE-ESI-MS analyses. (C) Data represent mean ± SEM (n = 3). Asterisks indicate values that are significantly different from the MBP control reactions (according to Student's t test, $P < 0.05$ (*); $P < 0.01$ (**)). Representative extracted-ion electropherograms are shown in Figure II-S7.

Heterologous expression of Arabidopsis PFA-DSP homologues complement yeast *siw14Δ* defects

To investigate the physiological consequences of Arabidopsis PFA-DSP activities *in vivo*, we carried out heterologous expression experiments in baker's yeast. To this end, we investigated the sensitivity of our *siw14Δ* yeast strain under conditions where phenotypes for *siw14Δ* strains and other yeast mutants defective in PP-InsP homeostasis have been reported previously (Brown *et al.*, 2006; Osada *et al.*, 2011; Laha *et al.*, 2015; Laha *et al.*, 2019; Steidle *et al.*, 2020) and selected the fungal toxin wortmannin (Arcaro and Wymann, 1993) that caused a severe *siw14Δ*-associated growth defect. Previous observations that *kcs1Δ* yeast cells are resistant to wortmannin (Saiardi *et al.*, 2005) suggest that wortmannin sensitivity of *siw14Δ* yeast might be related to Kcs1-dependent PP-InsPs. The *siw14Δ*-associated growth defect was fully complemented by heterologous expression of either of the five Arabidopsis *PFA-DSP* homologues or of yeast *SIW14* from episomal plasmids under control of a *PMA1* promoter fragment (Figure II-4A). Immunoblot analyses taking advantage of a C-terminal V5-tag revealed that all PFA-DSP homologues were expressed in yeast with PFA-DSP1 and PFA-DSP4 showing the highest protein abundance (Figure II-S8). Reduced growth of *siw14Δ* transformants expressing PFA-DSP4 on media supplemented with wortmannin is therefore likely not caused by inefficient expression of this homologue in yeast but might rather be a consequence of excess protein activity in this heterologous expression system. To investigate the contribution of PFA-DSPs in InsP metabolism, we monitored InsP profiles using SAX-HPLC analyses of various [^{3}H]-*myo*-inositol labeled yeast transformants. Of note, conventional SAX-HPLC analyses as employed here do not allow the discrimination of different $InsP_7$ or $InsP_8$ isomers (Blüher *et al.*, 2017; Riemer *et al.*, 2021). Heterologous expression of PFA-DSPs in *siw14Δ* restored $InsP_7$/$InsP_6$ ratios to wild-type (WT) levels, indicating that Arabidopsis PFA-DSP proteins are functionally similar to Siw14 (Figure II-4B).

Notably, the $InsP_7$ signal was the only one consistently affected by the loss of *SIW14* and heterologous expression of any *PFA-DSP* gene (Figure II-S9). We generated variants of Siw14 or PFA-DSP1, in which the catalytic cysteine was replaced by a serine resulting in a C214S and a C150S substitution in Siw14 and PFA-DSP1, respectively, and observed that complementation of *siw14Δ*-associated growth defects of respective transformants requires the catalytic activity of these proteins (Figure II-S10A, B). The inability of catalytic dead mutants to complement *siw14Δ*-associated growth defects was not caused by compromised expression or protein stability of these variants, as confirmed by immunoblot analyses (Figure II-S10C).

In agreement with the growth complementation assays, the catalytically inactive versions of Siw14 and PFA-DSP1 also failed to restore WT $InsP_7$ levels in *siw14Δ* transformants (Figure II-S10D, E). These experiments suggest that Arabidopsis PFA-DSPs can substitute for endogenous Siw14 in yeast with respect to wortmannin tolerance and $InsP_7$ homeostasis and that complementation of the *siw14Δ*-associated defects depends on the catalytic activity of these proteins

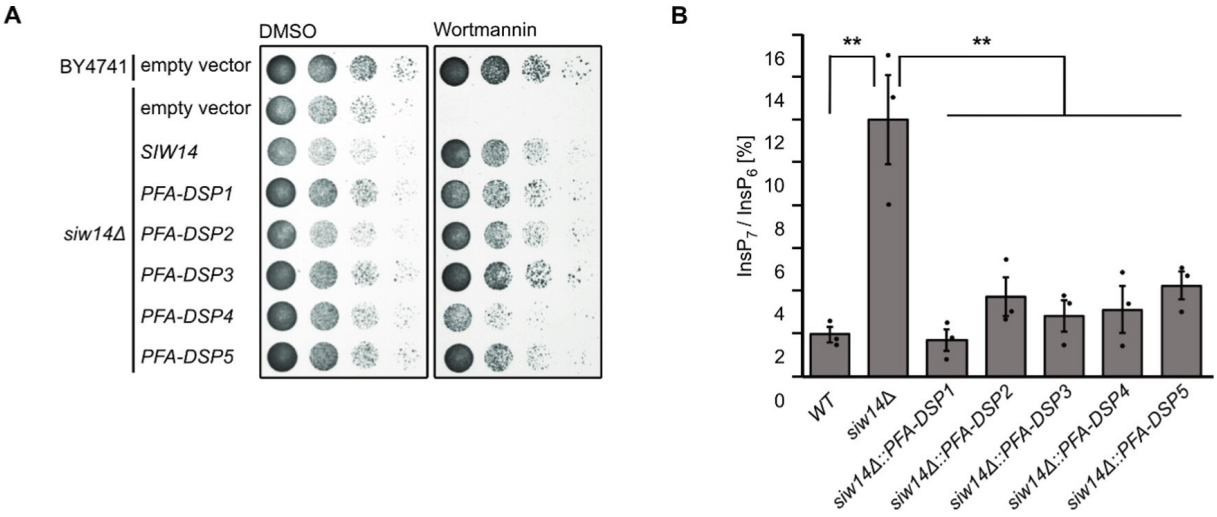

Figure II-4: Heterologous expression of Arabidopsis PFA-DSPs complements *siw14Δ*-associated wortmannin sensitivity in yeast. (A) Growth complementation assays of a *siw14Δ* yeast strain. WT yeast (BY4741) and an isogenic *siw14Δ* yeast mutant were transformed with either the empty episomal pDRf1-GW plasmid or different pDRf1-GW plasmids carrying the respective *PFA-DSP* gene or *SIW14*. Yeast transformants were then spotted in 8-fold serial dilutions (starting from OD_{600} 1.0) onto selective media supplemented with either wortmannin or DMSO as control. Plates were incubated at 26 °C for 2 days before photographing. The yeast growth assay was repeated twice ($n = 3$) with similar results. (B) Relative amounts of $InsP_7$ of WT yeast, *siw14Δ* and *siw14Δ* transformed with pDRf1-GW carrying the *PFA-DSP* genes are shown as $InsP_7/InsP_6$ ratios. $InsP_6$ and $InsP_7$ levels were determined by analysis of SAX-HPLC profiles using OriginPro 8. Data represent mean ± SEM ($n = 3$). Asterisks indicate values that are significantly different from *siw14Δ* (according to Student's *t* test, $P < 0.05$ (*); $P < 0.01$ (**)).

Growth defects of *siw14Δ* yeast on wortmannin require Kcs1-dependent 5-InsP$_7$ synthesis

For a deeper understanding of the wortmannin phenotype of *siw14Δ* yeast, we investigated genetic interactions between Siw14 and different InsP kinases. We generated different double mutants with defects in Siw14 and the PP-InsP synthases Kcs1 and Vip1, and tested their performance on wortmannin-containing media (Figure II-5A). Again, *siw14Δ* cells did not survive on media supplemented with 3 μM wortmannin, a defect that was fully complemented by the expression of *SIW14* under control of the endogenous promoter from a *CEN*-based single-copy plasmid (Figure II-5A). The growth of *vip1Δ* cells was comparable to WT yeast. In contrast, the *vip1Δ siw14Δ* double mutant showed a severe growth defect on media supplemented with wortmannin similar to single *siw14Δ* cells (Figure II-5A). Like the *vip1Δ* yeast strain, a *kcs1Δ* strain did not show growth defects on media supplemented with wortmannin compared to control media. In contrast, at increased concentrations, we observed *kcs1Δ*-associated wortmannin resistance (Figure II-5B), as reported earlier (Saiardi *et al.*, 2005). Importantly, deletion of *KCS1* in *siw14Δ* cells rescued *siw14Δ*-associated wortmannin sensitivity since the resulting *kcs1Δ siw14Δ* double-mutant yeast strain, despite growing overall weaker than the *kcs1Δ* single-mutant strain, showed no increased sensitivity to wortmannin (Figure II-5A). These findings indicate that the presence of Kcs1 is critical for the growth defects displayed by *siw14Δ* single-mutant cells on wortmannin. We then investigated whether the presence of Kcs1 itself or of Kcs1-dependent PP-InsPs such as 5-InsP$_7$ are relevant for *siw14Δ*-associated wortmannin sensitivity. To this end, we examined the phenotypes of *ipk2Δ* and of *ipk2Δ siw14Δ* yeast transformants. Both mutants lack IPK2, an inositol polyphosphate multikinase that sequentially phosphorylates Ins(1,4,5)P$_3$ to Ins(1,3,4,5,6)P$_5$ and is hence required for InsP$_6$ and subsequent Kcs1-dependent 5-InsP$_7$ or PP-InsP$_4$ synthesis (Estevez *et al.*, 1994; Saiardi *et al.*, 2005). Neither of the strains showed growth defects on media supplemented with wortmannin compared to the isogenic WT yeast strain, suggesting that also the loss of *IPK2* rescues *siw14Δ*-associated wortmannin sensitivity (Figure II-5A). We further tested wortmannin sensitivity of *kcs1Δ* and *kcs1Δ siw14Δ* yeast transformants in a different genetic background and observed similar results (Figure II-5B, C). Taken together, these results provide a causal link between Kcs1 (but not Vip1)-dependent PP-InsPs and *siw14Δ*-associated wortmannin sensitivity with Kcs1 and Siw14/PFA-DSPs playing antagonistic roles in regulating this sensitivity.

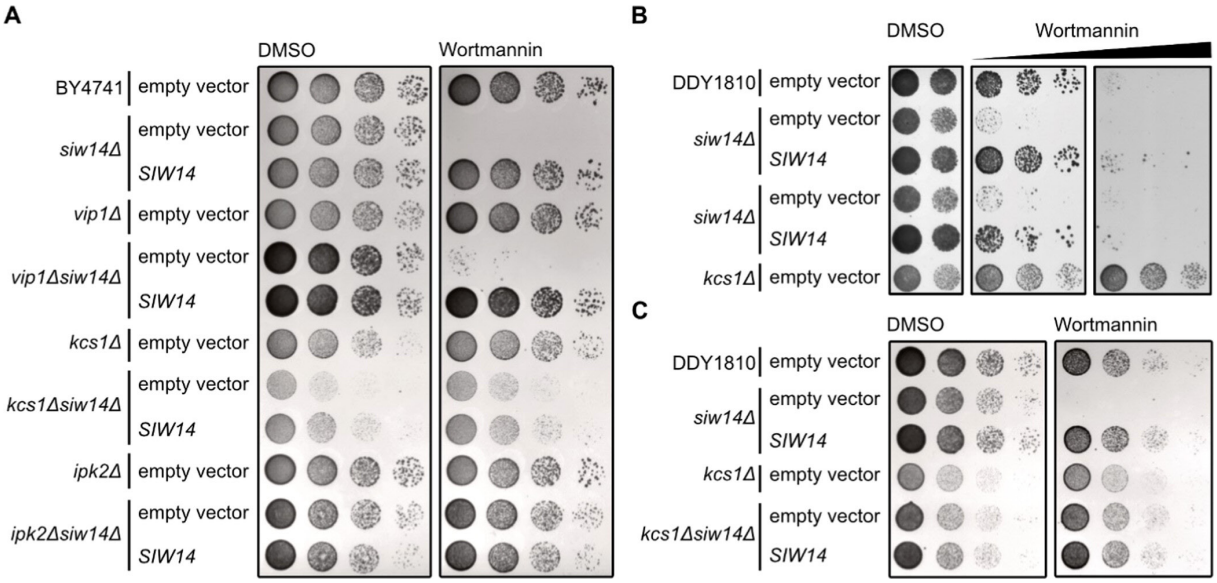

Figure II-5: Yeast *siw14Δ*-associated wortmannin sensitivity requires Kcs1-dependent 5-InsP$_7$. (A) WT yeast (BY4741), *siw14Δ*, *vip1Δ*, *kcs1Δ, ipk2Δ*, *vip1Δ siw14Δ, kcs1Δ siw14Δ*, and *ipk2Δ siw14Δ* double-mutant yeast strains were transformed with either an empty (*CEN*-based) YCplac33 vector or a YCplac33 vector carrying a genomic fragment of *SIW14* including a 653 bp promoter and 5′UTR and a 289 bp terminator region. Yeast transformants were then spotted in 8-fold serial dilutions (starting from OD_{600} 1.0) onto selective media supplemented with either wortmannin or DMSO as control. Plates were incubated at 26 °C for 2 days before photographing. (B, C) WT yeast (DDY1810), *siw14Δ*, *kcs1Δ*, and (C) *kcs1Δ siw14Δ* double-mutant yeast strains were transformed with either an empty YCplac33 vector or a YCplac33 vector carrying the genomic fragment of *SIW14*. The growth assay was performed as described for (A). All yeast growth assays (A–C) were repeated twice (n = 3) with similar results.

Increased *PFA-DSP1* expression coincides with decreased InsP$_7$ levels *in planta*

To gain insight into PFA-DSP functions *in planta*, we searched for Arabidopsis T-DNA insertion lines of *PFA-DSP1* and were able to identify three lines, *pfa-dsp1-3* and *pfa-dsp1-6* in the Col-0 background and *pfa-dsp1-4* in the Ler-0 background, for which homozygous progeny could be obtained. None of these lines displayed an obvious growth phenotype under our standard growth conditions. SAX-HPLC profiles of extracts of 20-day-old [^{3}H]-*myo*-inositol labeled *pfa-dsp1-3* and *pfa-dsp1-4* seedlings did not reveal a significant difference compared to the respective WTs (Figure II-S11A, B). However, SAX-HPLC analyses of the *pfa-dsp1-6* line revealed a significant average reduction (around 36 %) of the InsP$_7$/InsP$_6$ ratio compared to Col-0 (Figure II-6B). The levels of other InsP species remained largely unaffected (Figure II-6A, B). The available sequencing data for this line, as well as our analysis, indicated that the insertion of the T-DNA is 18 bp upstream of the start codon, suggesting that the full-length

transcript and PFA-DSP1 protein might be expressed in this line. We therefore conducted qPCR analyses of *pfa-dsp1-6* seedlings that were grown under identical conditions as the seedlings for SAX-HPLC analyses and detected ca. 6-fold increased expression of *PFA-DSP1* in *pfa-dsp1-6* in comparison to Col-0 seedlings (Figure II-6C).

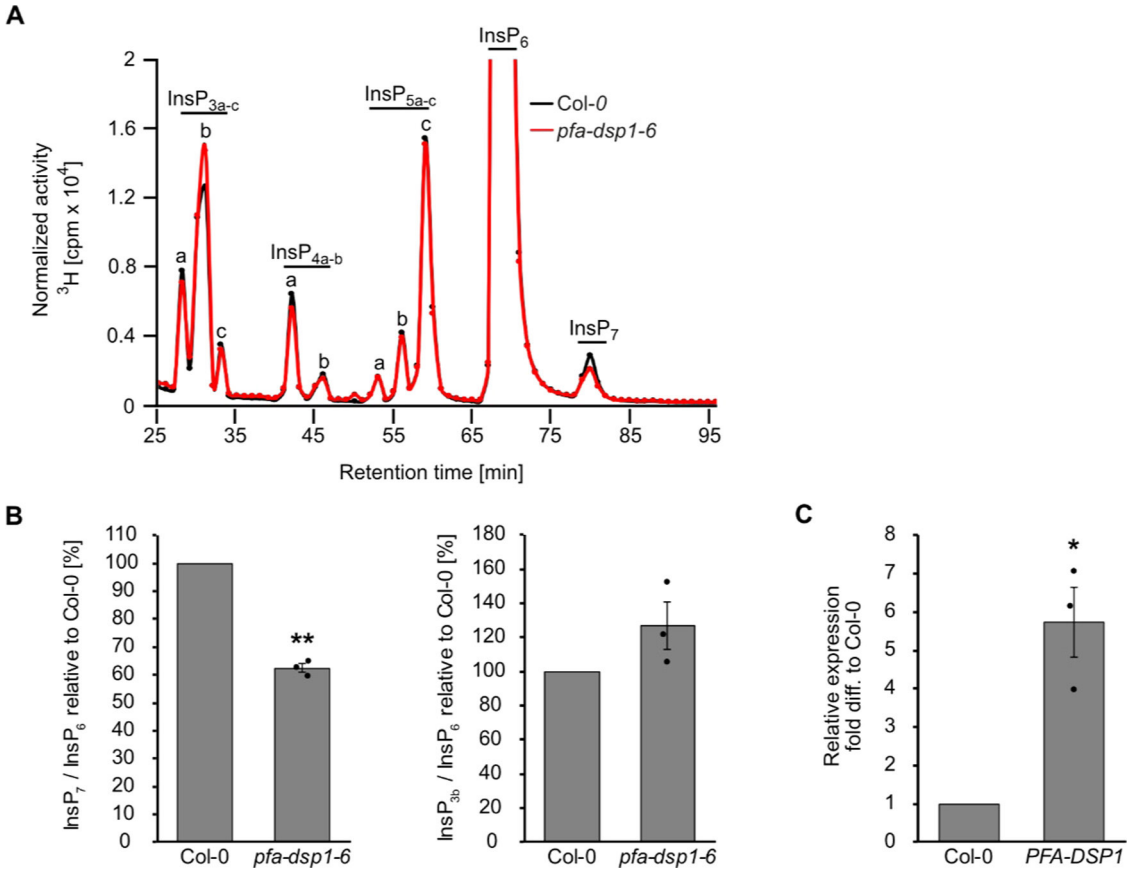

Figure II-6: Increased expression of *PFA-DSP1* in Arabidopsis decreases $InsP_7$ levels. (A) Representative SAX-HPLC profile of 20-day-old WT (Col-0) and *pfa-dsp1-6* Arabidopsis seedlings radiolabeled with [^{3}H]-*myo*-inositol. All visible peaks are highlighted and assigned to the corresponding InsP species. Based on published chromatographic mobilities (Stevenson-Paulik *et al.*, 2005; Kuo *et al.*, 2018), $InsP_{4a}$ likely represents Ins(1,4,5,6)P_4 or Ins(3,4,5,6)P_4, $InsP_{5a}$ likely represents $InsP_5$ [2-OH], $InsP_{5b}$ likely represents $InsP_5$ [4-OH] or its enantiomeric form $InsP_5$ [6-OH], and $InsP_{5c}$ likely represents $InsP_5$ [1-OH] or its enantiomeric form $InsP_5$ [3-OH]. The isomeric natures of $InsP_{3a-c}$, $InsP_{4b}$, $InsP_7$, and $InsP_8$ are unknown. (B) $InsP_7$/$InsP_6$ and $InsP_{3b}$/$InsP_6$ ratio of *pfa-dsp1-6* relative to Col-0 determined by the analysis of SAX-HPLC profiles using OriginPro 8. (C) Relative expression of *PFA-DSP1* in plants grown under identical conditions as for SAX-HPLC analyses, presented as fold difference compared to Col-0. (B, C) Data represent mean ± SEM (n = 3). Asterisks indicate values that are significantly different from the Col-0 control (according to Student's t test, $P < 0.05$ (*); $P < 0.01$ (**)).

Since the analyses of the *pfa-dsp1-6* line indicated that the T-DNA insertion causes an overexpression of *PFA-DSP1*, resulting in decreased $InsP_7$ levels, we investigated whether PP-InsP pyrophosphatase activity is also observed in a heterologous plant expression system. To this end, we transiently expressed a translational fusion of PFA-DSP1 with a C-terminal EYFP under control of the strong viral CaMV 35S promoter in *N. benthamiana* using agrobacterium-mediated transfection. The respective catalytically inactive PFA-DSP1^{C150S}-EYFP fusion protein was also expressed and InsPs were then extracted from *N. benthamiana* leaves and purified by TiO_2 pulldown 5 days after infiltration. PAGE analyses showed that transient expression of PFA-DSP1 or expression of its catalytic inactive version did not alter $InsP_6$ levels (Figure II-7A). In contrast, $InsP_7$ levels were reduced by the transient expression of PFA-DSP1 but not by the expression of its catalytic inactive version (Figure II-7A). These findings were strengthened by subsequent CE-ESI-MS analyses that revealed no changes in the ratios of 1/3-$InsP_7$/$InsP_6$ or 4/6-$InsP_7$/$InsP_6$ compared to control leaves infiltrated with agrobacteria carrying the silencing inhibitor *P19* alone (Figure II-7B). In contrast, the 5-$InsP_7$/$InsP_6$ ratio was significantly reduced in plants expressing *PFA-DSP1* compared to plants expressing the inactive version of *PFA-DSP1* or *P19* alone (Figure II-7C). The $InsP_8$/$InsP_6$ ratio, in turn, was strongly reduced by the expression of *PFA-DSP1* (Figure II-7D) in agreement with a partial hydrolytic activity of PFA-DSP proteins against $InsP_8$ isomers (Figure II-3 and Figure II-S7) and in agreement with the finding that 5-$InsP_7$, a substrate hydrolyzed by PFA-DSP1, represents the major precursor for $InsP_8$ synthesis (Riemer *et al.*, 2021). In summary, these results demonstrate that ectopic expression of Arabidopsis *PFA-DSP1* results in a specific decrease of 5-$InsP_7$ and $InsP_8$ *in planta*.

Conclusions

Recent studies elucidating the identity and substrate specificity of $InsP_6$/PP-InsP kinases have allowed us to establish important functions of PP-InsPs in nutrient sensing, hormone signaling, and plant immunity (Desai *et al.*, 2014; Laha *et al.*, 2015; Couso *et al.*, 2016; Laha *et al.*, 2016; Wild *et al.*, 2016; Dong *et al.*, 2019; Zhu *et al.*, 2019; Gulabani *et al.*, 2021; Ried *et al.*, 2021; Riemer *et al.*, 2021; Laha *et al.*, 2022). In contrast, information on enzymatic activities removing PP-InsPs to switch off their signaling functions in plants is sparse. Intriguingly, the first robust detection of PP-InsP messengers in mammalian cells was made possible by blocking mammalian PP-InsP phosphohydrolases with fluoride (Menniti *et al.*, 1993). While substantial

progress in elucidating the role of various PP-InsP phosphohydrolases in regulating these messengers in yeast and mammalian cells has been made (Safrany, 1998; Lonetti *et al.*, 2011; Kilari *et al.*, 2013; Steidle *et al.*, 2016), we are unaware of any study about PP-InsP degrading enzymes in plants at the onset of this study. Here, we provide evidence that the Arabidopsis PFA-DSP proteins are functional homologues of yeast Siw14 with high pyrophosphatase specificity for the 5-β-phosphate of various PP-InsPs.

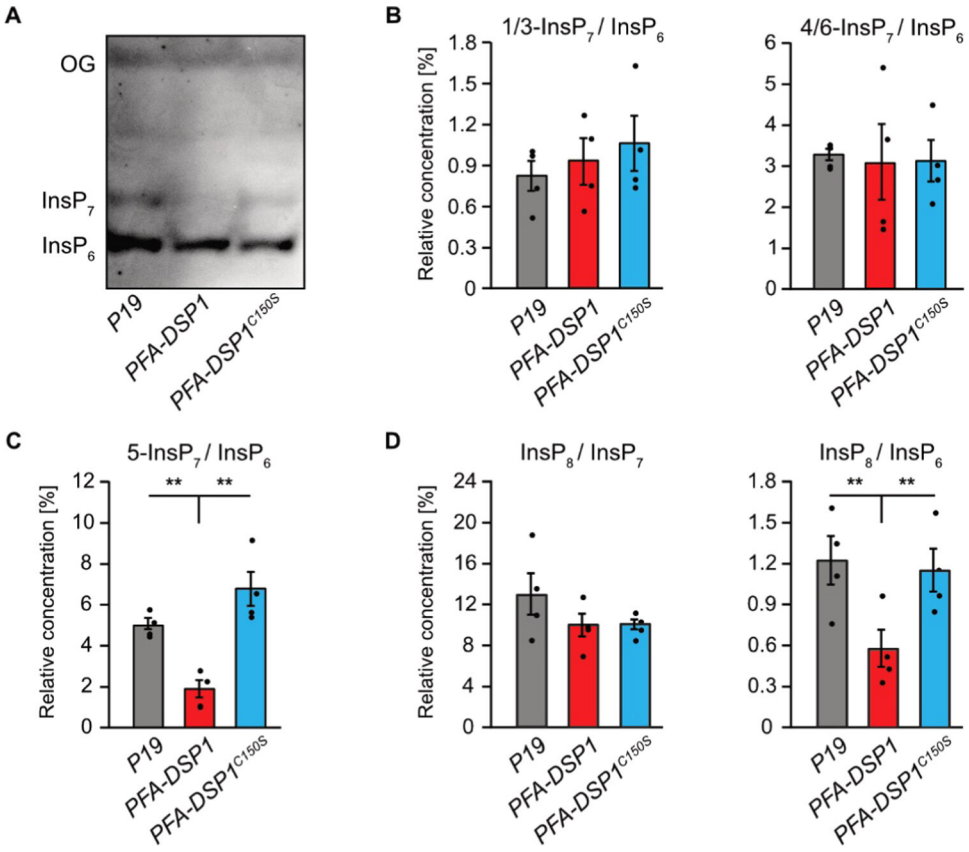

Figure II-7: Transient expression of *PFA-DSP1* in *N. benthamiana* leaves specifically decreases 5-$InsP_7$ and $InsP_8$. InsPs from infiltrated *N. benthamiana* leaves, transiently expressing the silencing inhibitor *P19* alone or together with *PFA-DSP1-EYFP* or *PFA-DSP1^{C150S}-EFYP*, were purified with TiO_2 pulldown and analyzed using CE-ESI-MS. Detected peaks were assigned to specific InsP isomers and quantified by comparing them with ^{13}C InsP standards that were spiked into the purified samples. (A) Representative PAGE gel of a sample set used for CE-ESI-MS analysis. (B–D) Relative amounts of PP-InsPs compared to $InsP_6$ or of $InsP_8$ compared to all $InsP_7$ isomers as indicated. Data represent mean ± SEM ($n = 4$). Asterisks indicate values that are significantly different from WT (according to Student's *t* test, $P < 0.05$ (*); $P < 0.01$ (**)). Note that 4- or 6-$InsP_7$, as well as 1- or 3-$InsP_7$ represent enantiomeric forms that cannot be distinguished by CE-ESI-MS analyses.

The striking biochemical similarities between Arabidopsis *PFA-DSPs* as deduced from *in vitro* assays and heterologous expressions analyses in yeast might well explain redundancies of these enzymes and consequently a lack of obvious phenotypes in single *pfa-dsp* loss-of-function lines in Arabidopsis. A search in transcriptome studies revealed that *PFA-DSP1*, *2*, and *4* are strongly induced by P_i deficiency (Figure II-S12). Such P_i-dependent regulation is in line with the disappearance of PP-InsPs in tissues of P_i-starved plants (Dong *et al.*, 2019; Riemer *et al.*, 2021) but future studies are required to establish the involvement of PFA-DSPs in the removal of messengers controlling P_i signaling. The high specificity of PFA-DSPs observed in this study establishes these enzymes as ideal tools to investigate the physiological roles of 5-β-phosphate containing PP-InsPs in plant development, plant immunity, nutrient perception, and abiotic stress tolerance. This is particularly important because of potentially confounding effects caused by the recently discovered plant 4/6-$InsP_7$ (Riemer *et al.*, 2021) and also because higher-order mutants involved in the synthesis of 5-β-phosphate containing PP-InsPs such as *itpk1 itpk2* and *vih1 vih2* display severe developmental defects or die at the young seedling stage (Zhu *et al.*, 2019; Riemer *et al.*, 2021). With the availability of a variety of promoters with tight spatial and temporal regulation, ectopic expression of *PFA-DSPs* in a tissue and developmentally controlled manner will provide helpful insights to unravel the roles of 5-$InsP_7$ and 1/3, 5-$InsP_8$ in plant development and plant physiology.

Material and Methods

Plant materials and growth conditions

Seeds of *A. thaliana* T-DNA insertion lines *pfa-dsp1-3* (WiscDsLox_473_B10, Col-0), *pfa-dsp1-4* (CSHL_GT1415, Ler-0), *pfa-dsp1-6* (SAIL_116_C12, Col-0) and *mrp5* (GK-068B10) were obtained from "The European Arabidopsis Stock Centre" (http://arabidopsis.info/). To identify homozygous lines, F2 and F3 plants were genotyped by PCR using the primers indicated in Table II-S2.

For sterile cultures, Arabidopsis seeds were surface sterilized in 1.2 % (v/v) $NaHClO_4$ and 0.05 % (v/v) Triton X-100 for 3 min, in 70 % (v/v) ethanol and 0.05 % (v/v) Triton X-100 for 3 min and in 100 % (v/v) ethanol before transferring onto sterile filter paper. Sterilized seeds were sown onto half-strength Murashige and Skoog (MS) medium (Gruber *et al.*, 2013) containing 1 % sucrose, pH 5.7 and solidified with 0.7 % (w/v) Phytagel (Sigma-Aldrich). After

2 days of stratification at 4 °C, the plates were transferred to a growth incubator and the seedlings were grown under short-day conditions with the following regime: 8/16 h light/dark; light intensity 120 µmol m^{-2} s^{-1}; temperature 22 °C/20 °C.

Constructs

The following full-length ORFs were amplified by PCR from an Arabidopsis whole seedling cDNA preparation: *PFA-DSP1* (At1g05000), *PFA-DSP2* (At2g32960), *PFA-DSP3* (At3g02800) *PFA-DSP4* (At4g03960), and *PFA-DSP5* (At5g16480). Likewise, the *SIW14* ORF sequence was amplified from yeast genomic DNA. Primers used for amplification are listed in Table II-S2. The reverse primers contained a *V5* sequence (underlined) allowing a translational fusion of the resulting gene products with a C-terminal V5 epitope tag. Amplification products were cloned into pDONR221 (Invitrogen) via BP clonase II (Invitrogen) reaction following the manufacturer's instructions. The ORFs were then swapped into the episomal yeast expression vector pDRf1-GW (Loqué *et al.*, 2007) by the LR clonase II (Invitrogen) reaction following the manufacturer's instructions. For expression of *SIW14* under control of the endogenous promoter from a *CEN*-based plasmid, the *SIW14* gDNA was amplified from purified yeast gDNA using the primers listed in Table II-S2. The *SIW14* gDNA was inserted into YCplac33 (ATCC #87586) using the restriction enzymes *Pst*I and *Eco*RI.

For protein expression, *PFA-DSP1–5* were amplified as described before but with a reverse primer containing a stop codon. Amplified products were cloned into pDONR221 (Invitrogen), then swapped by LR clonase II (Invitrogen) into the bacterial expression vector pDEST566 (Addgene plasmid # 11517), which contains a sequence encoding an N-terminal His_6-MBP epitope tag. Free His-tagged MBP protein was expressed from a modified pET28 vector carrying an N-terminal sequence encoding a His_8-MBP epitope tag (Laha *et al.*, 2015).

For transient expression in *Nicotiana benthamiana*, the ORF of *PFA-DSP1* (WT sequence and with a mutated sequence encoding the C150S substitution) was swapped by LR clonase II (Invitrogen) from pDONR221 into the plant expression vector pGWB641 (Nakamura *et al.*, 2010), which harbors a viral CaMV 35S promoter to allow gene expression and a sequence encoding a C-terminal EYFP tag. Site-directed mutagenesis was performed on the respective plasmids with the primers listed in Table II-S2.

N. benthamiana infiltration

A single colony of transformed Agrobacteria was inoculated in 2 mL of LB media containing the appropriate antibiotics and cultivated overnight at 26 °C in a spinning wheel. On the next morning, 1 mL of overnight culture was added to 5 mL of fresh LB with antibiotics and grown for another 4 h at 26 °C. Afterward, the cultures were harvested by centrifugation at 4 °C with 3000*g* for 20 min. The pellet was then resuspended in 3 mL of infiltration solution containing 10 mM $MgCl_2$, 10 mM MES-KOH (pH 5.6), and 150 µM acetosyringone. OD_{600} was determined using a 1:10 dilution and adjusted to 0.8 in infiltration solution. Then, the working solution was prepared by pooling equal amounts of cultures (e.g., *P19* + *PFA-DSP*1), which were then co-infiltrated in the abaxial surface of the leaf using a 1 mL syringe without a needle. Afterward, the plants were placed in a dark incubator at 26 °C for ~1 day before keeping them for another 4 days on the workbench. The leaves were then harvested and frozen in liquid nitrogen before continuing with the extraction of inositol phosphates.

Yeast strains

Different strains of the budding yeast *Saccharomyces cerevisiae* were used. The BY4741 WT (MATa *his3Δ leu2Δ met15Δ ura3Δ*), *siw14Δ* (*YNL032w::kanMX4*), *vip1Δ* (*YLR410w::kanMX4*) (Laha *et al.*, 2015), *kcs1Δ* (*YDR017c::kanMX*4), and *ipk2Δ* (*YDR*173*c::kanMX*4) were obtained from Euroscarf. *vip1Δ siw14Δ*, *kcs1Δ siw14Δ*, *ipk2Δ siw14Δ* were generated using *loxP*/Cre gene disruption and the *ble* resistance marker, which confers phleomycine/Zeocin (Invitrogen) resistance (Gueldener, 2002) using the primers listed in Table II-S2. In addition, the following mutants in the DDY1810 background (MATa; *leu2Δ ura3-52 trp1Δ; prb1-1122 pep4-3 pre1-451*) (Onnebo and Saiardi, 2009) were used: *kcs1Δ* and *kcs1Δ ddp1Δ*. *kcs1Δ siw14Δ*, *kcs1Δ ddp1Δ siw14Δ*, and *siw14Δ* were generated in this background as described before. For all assays, the yeast cells were transformed by the Li-acetate method (Gietz *et al.*, 1995) and cultured in either 2 × YPD + CSM medium or selective synthetic deficiency (SD) medium.

Yeast growth complementation assay

Yeast transformants were inoculated in selective SD medium and grown overnight at 28 °C while shaking (200 rpm). Then, OD_{600} was measured, adjusted to 1.0, and an 8-fold dilution series was prepared in a 96-well plate. Subsequently, 10 µL of each dilution were spotted on

selective solid media as described earlier (Zonneveld, 1986) and incubated at 26 °C for 2–4 days. To prepare selective solid media supplemented with wortmannin, autoclaved media was cooled down to 60 °C, wortmannin was added from a 10 mM stock in DMSO (Sigma-Aldrich) to a final concentration of 1–3 µM. Since the activity of wortmannin changed by age and by the number of freezing/thawing cycles, aliquots were kept at −20 °C and were not thawed more than five times. In addition, several concentrations were employed for the spotting assays to be able to identify the activity at which growth differences between *siw14Δ*, *kcs1Δ*, and their isogenic WT transformants became most obvious. Pictures were taken with a Bio-Rad ChemiDoc MP imager using white backlight.

Protein preparation

His_6-MBP-PFA-DSP protein fusions or free His_8-MBP were expressed in *Escherichia coli* BL21 CodonPlus (DE3)-RIL cells (Stratagene). Overnight bacterial cultures were inoculated 1:1000 into fresh 2YT medium (1.6 % tryptone, 1 % yeast extract, 0.5 % NaCl) with 100 mg/L ampicillin (pDEST566) or 50 mg/L kanamycin (pET28) and 25 mg/L chloramphenicol. Cells were grown at 37 °C while shaking (200 rpm) for 4 h (∼0.6 OD_{600}), and protein expression was induced at 16 °C overnight with 0.1 mM isopropyl-d-1-thiogalactopyranoside. The cells were lysed as described (Schaaf *et al.*, 2006) using the following lysis buffer: 50 mM Tris-Cl, pH 7.5, 100 mM NaCl, 25 mM imidazole, 10 % (v/v) glycerol, 0.1 % (v/v) Tween 20, 5 mM β-mercaptoethanol, and EDTA-free complete ULTRA protease inhibitor cocktail (Roche). Proteins were batch-purified using Ni-NTA agarose resin (Macherey-Nagel) and eluted using the above-mentioned lysis buffer with increased imidazole concentration (250 mM). Three elutions were combined and dialyzed using Slide-A-Lyzer Dialysis Cassettes (Thermo Scientific) following the manufacturer's instructions and a buffer containing 50 mM Tris-Cl, pH 7.5 and 100 mM NaCl. The concentrated protein preparations were then stored at −20 °C. Purified proteins were analyzed using SDS-PAGE followed by Coomassie blue staining. Proteins were compared with PageRuler plus prestained protein ladder (Thermo Fisher) and with designated amounts of a BSA standard to estimate target protein concentrations.

In vitro PP-InsP pyrophosphatase assay

The pyrophosphatase assay was carried out in a 15 µL reaction mixture containing 0.35–2 µM recombinant PFA-DSP or Siw14 protein, 50 mM HEPES (pH 7.0), 10 mM NaCl, 5 % (v/v) glycerol, 0.1 % (v/v) β-mercaptoethanol, and 0.33 mM of various $InsP_7$ and $InsP_8$ isomers as indicated, and was incubated for 1, 2, or 24 h at 22 °C. The PP-InsP isomers were synthesized as described previously (Capolicchio *et al.*, 2013; Capolicchio *et al.*, 2014). Reactions were separated by 33 % PAGE and visualized by toluidine blue or DAPI staining.

Titanium dioxide bead extraction and PAGE/CE-ESI-MS

Purification of inositol polyphosphates using TiO_2 beads and analysis via PAGE was performed as described previously (Riemer *et al.*, 2021). CE-ESI-MS analyses of *in vitro*, yeast and plant samples were performed as described previously (Qiu *et al.*, 2020; Riemer *et al.*, 2021).

Inositol polyphosphate extraction from yeast cells and seedlings and HPLC analyses

For inositol polyphosphate analyses from yeast, transformants were inoculated into a selective SD medium and grown overnight at 28 °C while shaking (200 rpm). They were then diluted 1:200 in 2 mL of fresh medium supplemented with 6 µCi mL^{-1} [^{3}H]-*myo*-inositol (30–80 Ci $mmol^{-1}$; Biotrend; ART-0261-5) and grown overnight at 28 °C in a spinning wheel. After centrifugation and washing of the cell pellet, inositol polyphosphates were extracted and analyzed as described before (Azevedo and Saiardi, 2006; Laha *et al.*, 2015; Gaugler *et al.*, 2020).

Extraction of [^{3}H]-*myo*-inositol polyphosphates from Arabidopsis seedlings and subsequent SAX-HPLC analyses were performed as described previously (Gaugler *et al.*, 2020).

RNA isolation and quantitative real-time PCR

Fifteen-day-old seedlings were transferred from solid half-strength MS plates to liquid half-strength MS media (supplemented with 1 % sucrose) for 5 days before harvest and immediately frozen in liquid N_2. Total RNA was extracted with NucleoSpin RNA Plant and Fungi kit (Macherey-Nagel). cDNA was synthesized using RevertAid RT reverse transcription

kit (Thermo Fisher). Quantitative PCR reactions were conducted with the CFX384 real-time system (Bio-Rad) and the SsoAdvanced Universal SYBR Green Supermix (Bio-Rad) using the primers listed in Table II-S2. *TIP41-like* and *PP2AA3* were used as reference genes to normalize relative expression levels of all tested genes. Relative expression was calculated using the CFX Maestro software (Bio-Rad).

Yeast protein extraction and immunodetection

Multiple transformants were inoculated into 4 mL of YPD (with 3 % glucose) or selective SD media and grown for up to 24 h at 28 °C. On the following day, the yeast was reinoculated into 4 mL of fresh media and grown for another day. Afterward, the cells were harvested and resuspended in 500 µL of extraction buffer (300 mM sorbitol, 150 mM NaCl, 50 mM Na_2HPO_4, 1 mM EDTA, pH 7.5), supplemented with 100 mM β-mercaptoethanol and a 1:50 dilution of protease inhibitor cocktail for fungal extracts (Sigma-Aldrich). The cells were lysed with bead beating using 150–200 µL of glass beads (ø 0.5 mm). The lysate was spun down and the supernatant boiled for 10 min after the addition of sample buffer. The protein extracts were then resolved by SDS-PAGE. Target proteins were detected by immunoblot. As the primary antibody, a mouse anti-V5 (Invitrogen, R960-25, 1:2000 dilution) antibody was used, followed by either an Alexa fluor plus 800 goat anti-mouse antibody (Invitrogen, 1:20 000 dilution) or a goat anti-mouse HRP antibody (Bio-Rad, 1:10 000 dilution). As a loading control, Gal4 was detected using a rabbit polyclonal anti-Gal4 antibody (Santa Cruz, 1:1000 dilution), followed by a goat anti-rabbit StarBright Blue 700 antibody (Bio-Rad, 1:2500 dilution). The signal was detected using the multi-plex function of the ChemiDoc MP imager (Bio-Rad). Alternatively, for blots where a secondary antibody coupled to HRP was used, the chemiluminescence signal of the ECL reagent was detected, followed by Ponceau staining as loading control.

Author Contributions

P.G. and R.S. contributed equally to this manuscript. D.L., G.S., and P.G. conceived the study. P.G., D.L., G.S., H.J.J., and R.F.H.G. designed experiments. P.G., R.S., D.L., G.L. D.Q., J.W., M.H., N.J., K.R., J.S., N.F.-R., and R.F.H.G. performed experiments. P.G. generated yeast mutants and performed all yeast experiments, generated constructs, isolated T-DNA insertion lines, performed HPLC analyses of plants, performed qPCR analyses, performed plant

infiltration and TiO_2 pulldowns, and analyzed most of the experiments. R.S. purified recombinant proteins and carried out and analyzed *in vitro* kinase assays. G.L. and D.Q. performed CE-ESI-MS/MS analysis and isomer identification. J.W. and J.S. generated constructs and established the expression and purification of recombinant proteins. N.J., M.H., and K.R. synthesized $InsP_7$ and $InsP_8$ isomers. N.F.-R. isolated T-DNA insertion lines, performed HPLC analyses of plants, generated constructs, and performed qPCR analyses. R.F.H.G. generated plant samples for CE-ESI-MS analysis and did transcriptome analysis. M.N.T. synthesized ^{13}C-InsP standards. V.G. analyzed and quantified HPLC analyses. P.G., G.S., D.L., H.J.J., and D.F. supervised the experimental work. P.G., G.S., R.S., D.L., and R.Y. wrote the manuscript with input from all authors.

Funding

This work was funded by grants from the Deutsche Forschungsgemeinschaft (SCHA 1274/4-1, SCHA 1274/5-1, Research Training Group GRK 2064 and under Germany's Excellence Strategy, EXC-2070-390732324, PhenoRob to G.S.; JE 572/4-1 and under Germany's Excellence Strategy, CIBSS-EXC-2189–Project ID 390939984 to H.J.J.; and HE 8362/1-1, DFG Eigene Stelle, to R.F.H.G.). D.L. acknowledges the Department of Biotechnology (DBT) for HGK-IYBA award (BT/13/IYBA/2020/04) and a DBT Indian Institute of Science Partnership Program. H.J.J. acknowledges funding from the Volkswagen Foundation (Momentum Grant 2021).

Notes

The authors declare no competing financial interest.

During the revision of this manuscript, a study by Wang and colleagues (2022) reported high-resolution crystal structures of Arabidopsis PFA-DSP1 in complex with 5-$InsP_7$, 6-$InsP_7$, and 5-$InsP_7$ analogues and provided evidence for efficient *in vitro* phosphatase activity of this enzyme against 5-$InsP_7$ as well as weaker *in vitro* activities against 4-$InsP_7$ and 6-$InsP_7$ in agreement with our findings.

Acknowledgments

The authors thank Li Schlüter and Brigitte Ueberbach (Department of Plant Nutrition, Institute of Crop Science and Resource Conservation, University of Bonn) for excellent technical assistance and Marília Kamleitner (Department of Plant Nutrition, Institute of Crop Science and Resource Conservation, University of Bonn) for critically reading this manuscript. They also thank Priyanshi Rana (Department of Biochemistry, Indian Institute of Science) for her inputs during the revision of the manuscript.

Supporting Information

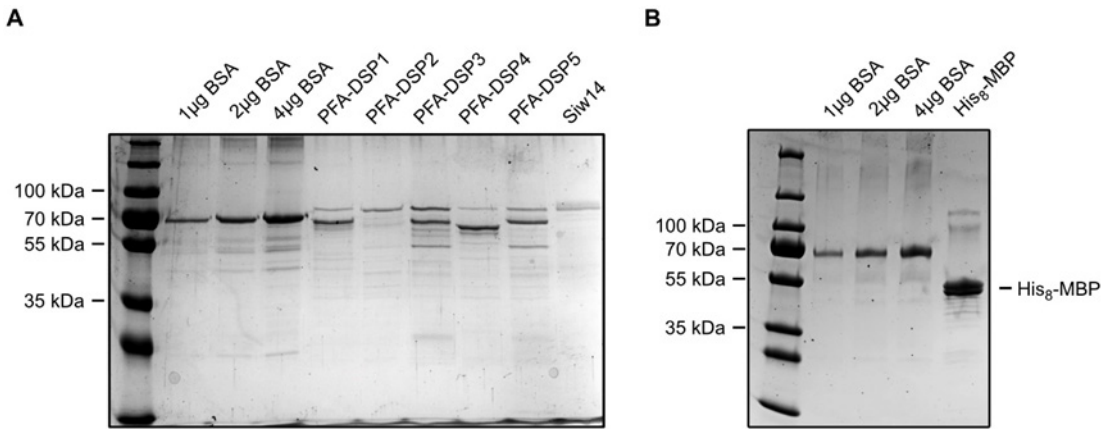

Figure II-S1: Purification of PFA-DSP proteins. (A, B) Recombinant His-MBP-PFA-DSPs or His-MBP-Siw14 were expressed in *E. coli* and purified with Ni-NTA resin as described in methods. Dialyzed proteins were denatured and separated by SDS-PAGE in parallel with BSA standards to determine protein concentrations by staining with Coomassie blue.

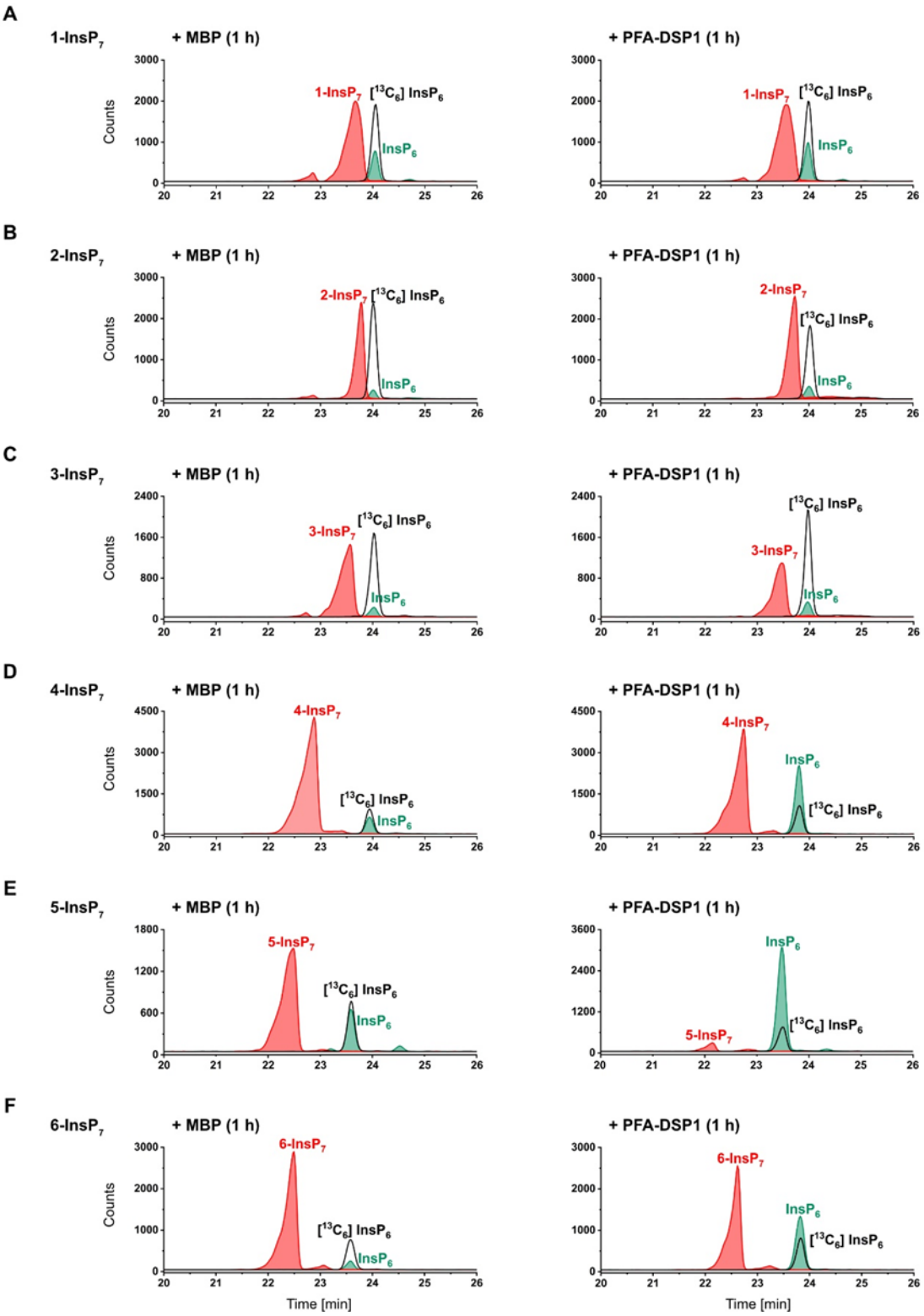

Figure II-S2: *In vitro*, Arabidopsis PFA-DSP1 displays robust PP-InsP pyrophosphatase activity against 5-$InsP_7$ and partial pyrophosphatase activity against 4-$InsP_7$ and 6-$InsP_7$, respectively. (A – F) 0.4 µM PFA-DSP1 was incubated with 0.33 mM $InsP_7$ and 1 mM $MgCl_2$ for 1 h. The reaction product was spiked with an isotopic standards mixture ([$^{13}C_6$] 1,5-$InsP_8$, [$^{13}C_6$] 5-$InsP_7$, [$^{13}C_6$] 1-$InsP_7$, [$^{13}C_6$] $InsP_6$, [$^{13}C_6$] 2-OH $InsP_5$) and subjected to CE-ESI-MS analyses. Representative extracted-ion electropherograms of samples shown in Figure II-1.

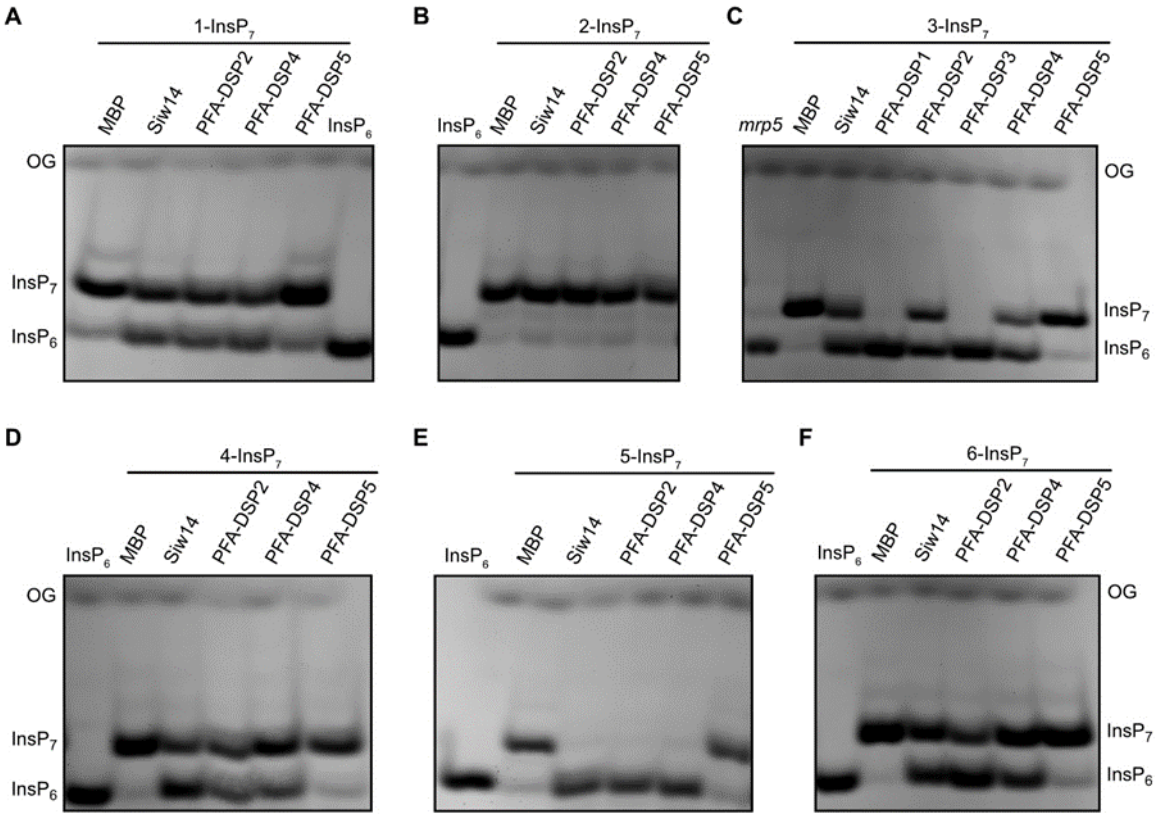

Figure II-S3: In the absence of divalent cations, all $InsP_7$ isomers with the exception of 2-$InsP_7$ become substrates for selected Arabidopsis PFA-DSPs *in vitro*. (A – F) Approximately 0.4 µM His-MBP-PFA-DSPs and His-MBP were incubated with 1 mM EDTA and 0.33 mM $InsP_7$ for 1 h at 22 °C. His-MBP served as a negative control. The reaction products were separated by 33 % PAGE and visualized with toluidine blue. The identity of bands was determined by migration compared to $InsP_6$ or (C) compared to TiO_2-purified *mrp5* seed extract.

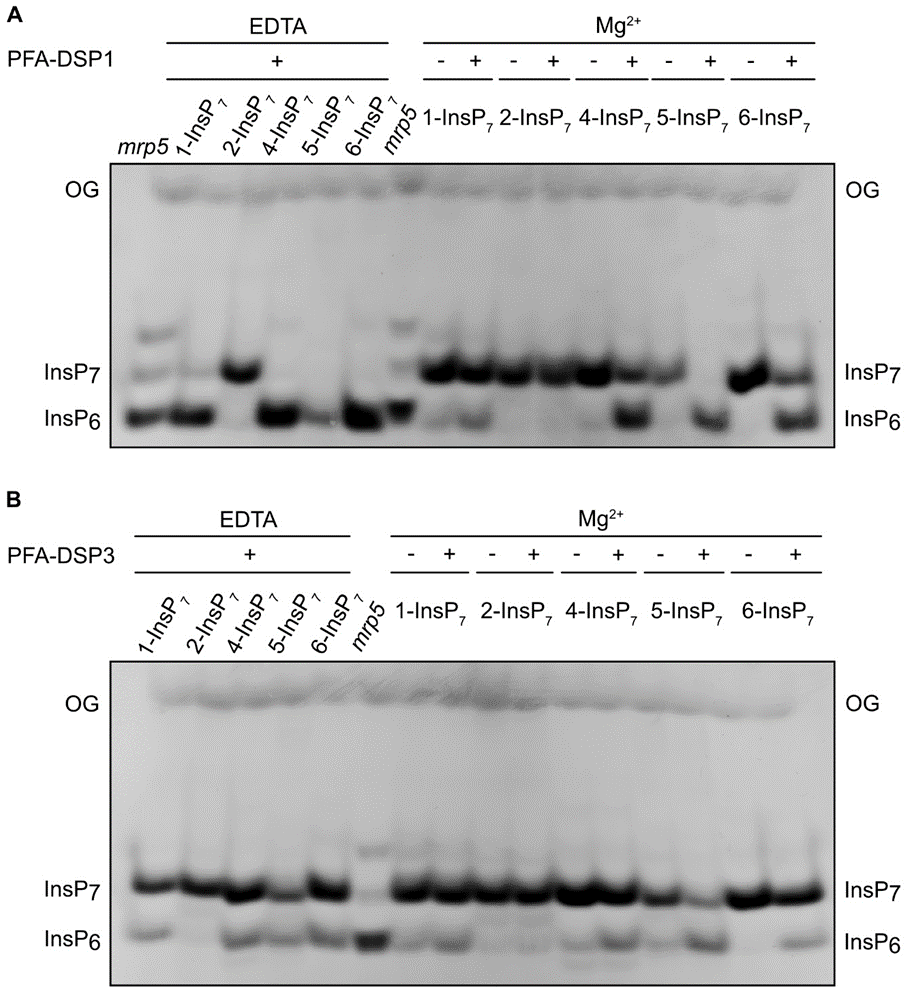

Figure II-S4: In the presence of Mg^{2+}, PFA-DSP1 and PFA-DSP3 display robust *in vitro* $InsP_7$ pyrophosphatase activity with high specificity for the 5-β-phosphate. (A – B) Approximately 0.4 µM His-MBP-PFA-DSP1 and His-MBP-PFA-DSP3 were incubated with 0.33 mM $InsP_7$ and 1 mM EDTA or 1 mM $MgCl_2$ for 1 h at 22 °C. His-MBP served as a negative control. The reaction products were separated by 33 % PAGE and visualized with toluidine blue. The identity of bands was determined by migration compared to TiO_2-purified *mrp5* seed extract.

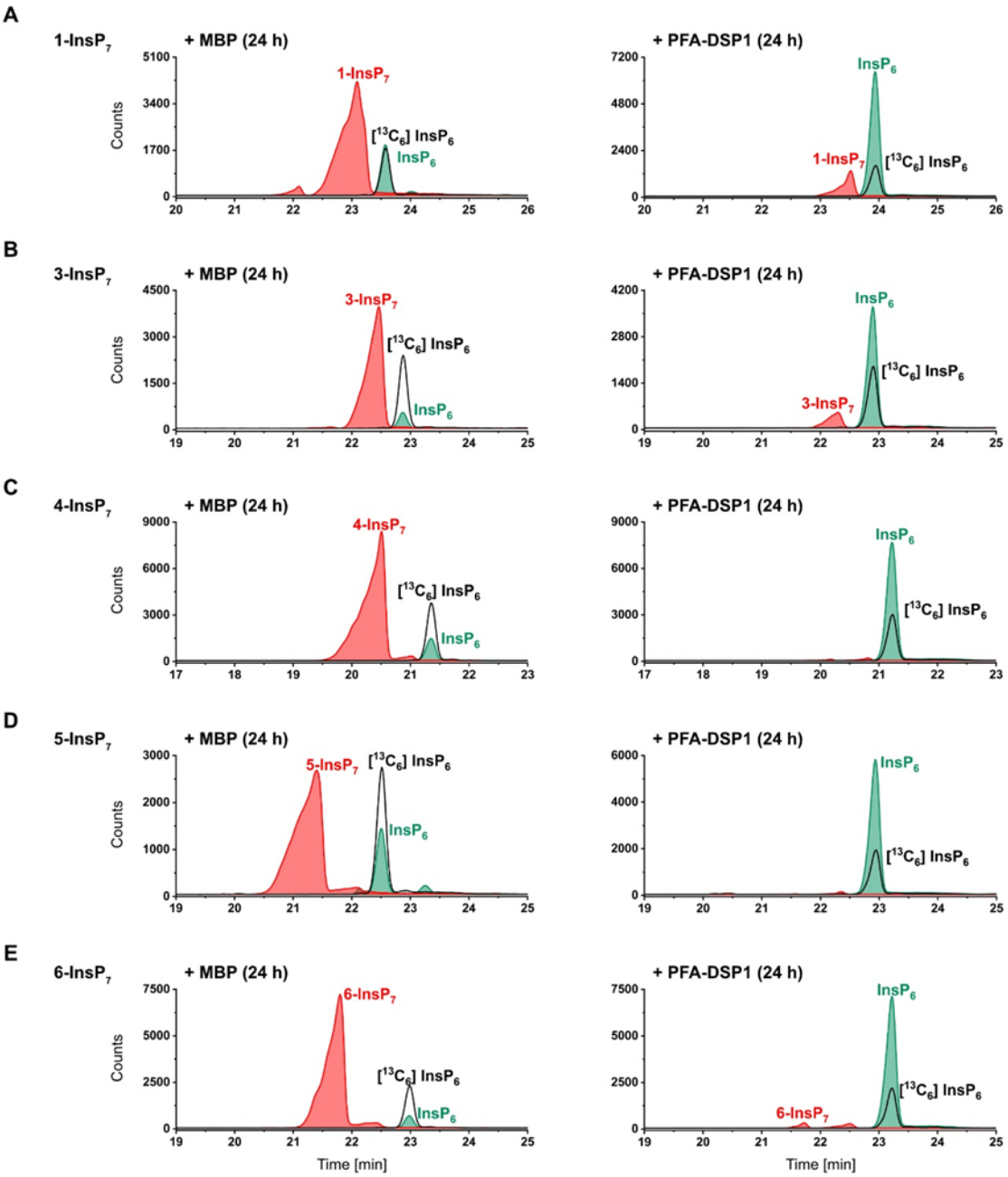

Figure II-S5: Under prolonged incubation time, Arabidopsis PFA-DSP1 efficiently hydrolyzes 5-$InsP_7$, 4-$InsP_7$ and 6-$InsP_7$ but only displays partial activities against 1-$InsP_7$ and 3-$InsP_7$. (A – E) 0.4 µM PFA-DSP1 was incubated with 0.33 mM $InsP_7$ and 1 mM $MgCl_2$ for 24 h. The reaction product was spiked with an isotopic standards mixture ([$^{13}C_6$] 1,5-$InsP_8$, [$^{13}C_6$] 5-$InsP_7$, [$^{13}C_6$] 1-$InsP_7$, [$^{13}C_6$] $InsP_6$, [$^{13}C_6$] 2-OH $InsP_5$) and subjected to CE-ESI-MS analyses. Representative extracted-ion electropherograms of samples shown in Figure II-2.

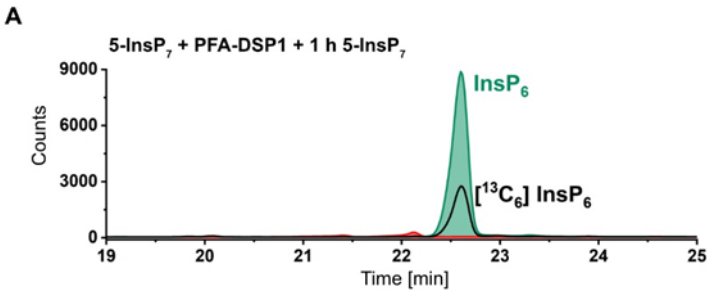

Figure II-S6: Arabidopsis PFA-DSP1 maintains 5-$InsP_7$ pyrophosphatase activity during prolonged incubation time *in vitro*. (A) 0.4 µM PFA-DSP1 was incubated with 0.33 mM 5-$InsP_7$ and 1 mM $MgCl_2$ for 24 h. To ensure that PFA-DSP1 is active during the whole incubation time, 0.33 mM 5-$InsP_7$ was added after 23 h and incubated for another 1 h. The reaction product was spiked with an isotopic standards mixture ([$^{13}C_6$] 1,5-$InsP_8$, [$^{13}C_6$] 5-$InsP_7$, [$^{13}C_6$] 1-$InsP_7$, [$^{13}C_6$] $InsP_6$, [$^{13}C_6$] 2-OH $InsP_5$) and subjected to CE-ESI-MS analyses.

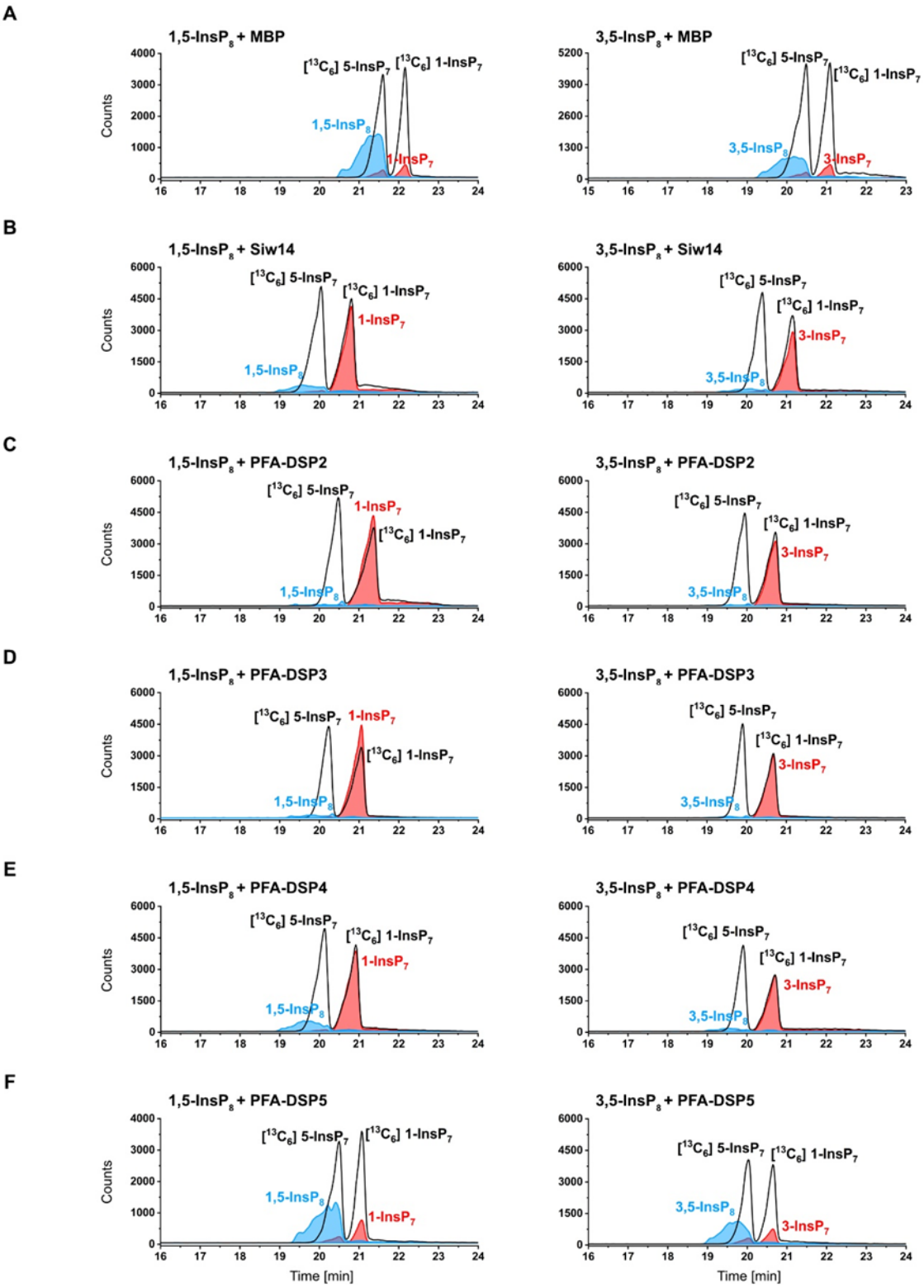

Figure II-S7: *In vitro*, Arabidopsis PFA-DSPs display robust 1/3,5-$InsP_8$ pyrophosphatase activity. (A - F) Approximately 0.4 µM His-MBP-PFA-DSPs and His-MBP-Siw14 were incubated with 0.33 mM 1,5-$InsP_8$ or 3,5-$InsP_8$ and 1 mM $MgCl_2$ for 1 h. The reaction products were spiked with isotopic standards mixture ([$^{13}C_6$] 1,5-$InsP_8$, [$^{13}C_6$] 5-$InsP_7$, [$^{13}C_6$] 1-$InsP_7$, [$^{13}C_6$] $InsP_6$, [$^{13}C_6$] 2-OH $InsP_5$) and subjected to CE-ESI-MS analyses. Representative extracted-ion electropherograms of samples shown in Figure II-3C.

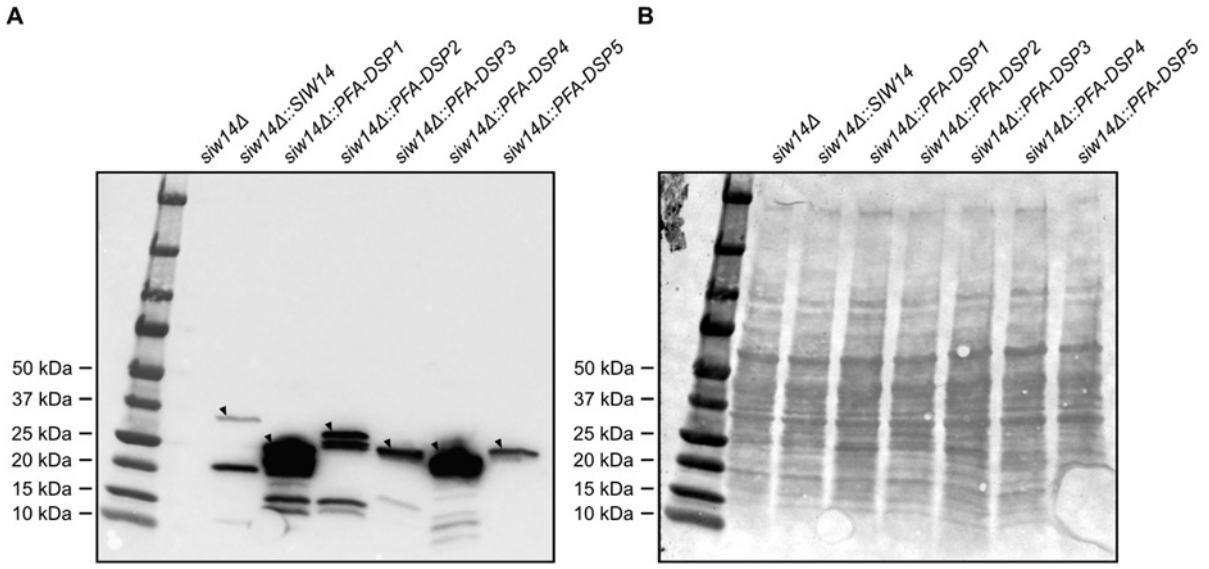

Figure II-S8: All five PFA-DSP homologs are stably expressed in the *siw14Δ* yeast strain. Immunoblot analyses of protein extracts from *siw14Δ* yeast transformed with either empty pDRf1-GW plasmid or pDRf1-GW carrying *SIW14* or *PFA-DSP1–5* encoding translational fusions with a C-terminal *V5*-tag. (A) For detection of V5-tagged proteins, an anti-V5 tag primary antibody (Invitrogen; 1:2000 dilution) and an anti-mouse secondary antibody coupled with HRP (Bio-Rad; goat; 1:10000 dilution) were used. The chemiluminescence signal of the ECL substrate (Bio-Rad) was detected using the ChemiDoc MP imager (Bio-Rad). Black arrows indicate the specific protein bands based on the calculated molecular weight. (B) Ponceau staining of the same blot.

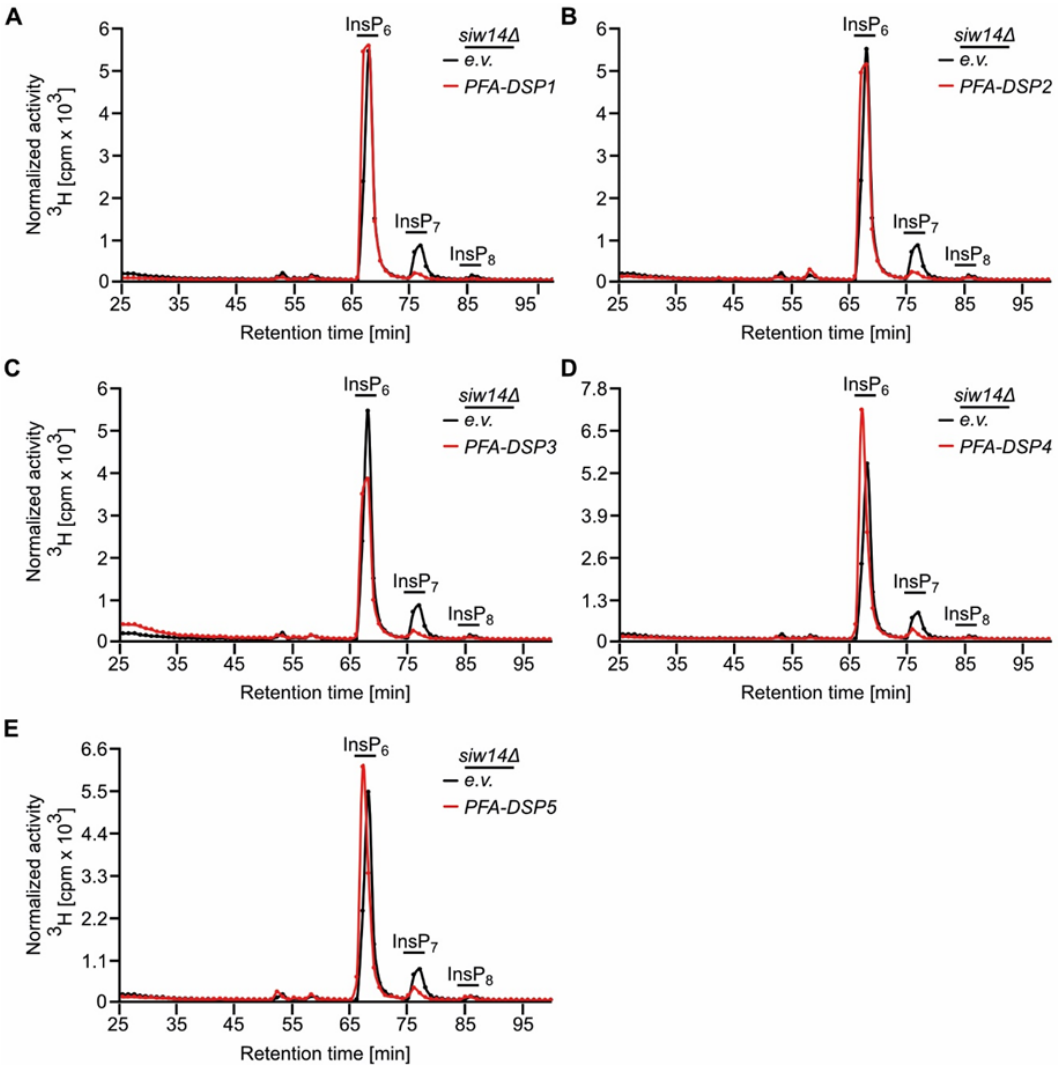

Figure II-S9: Heterologous expression of Arabidopsis PFA-DSPs complements *siw14Δ*-associated defects in $InsP_7/InsP_6$ ratios in yeast. (A - E) SAX-HPLC profiles of radiolabeled *siw14Δ* yeast transformed with either empty pDRf1-GW plasmid (e.v.) or pDRf1-GW carrying *PFA-DSP1-5*. Depicted is a representative analysis of each *PFA-DSP* transformant, with the same analysis of a representative empty vector transformant shown in the same profile in each graph. The experiment was repeated twice ($n = 3$) with similar results (combined data shown in Figure II-4B).

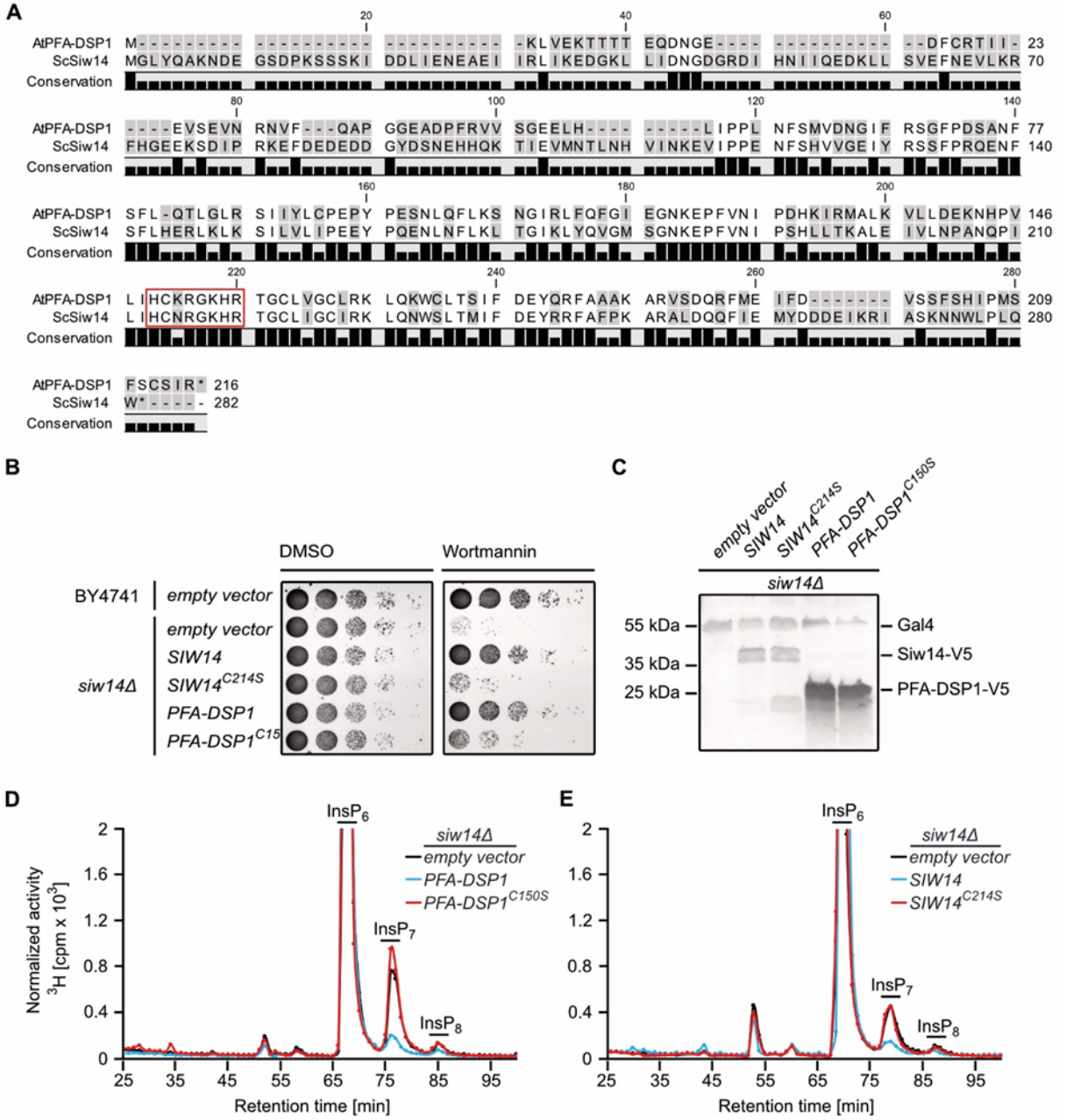

Figure II-S10: Complementation of *siw14Δ*-associated growth defects depends on catalytic activity. (A) Protein alignment of Siw14 from yeast and its homolog PFA-DSP1 from *Arabidopsis thaliana*. Identical amino acids are shown in black, different residues are highlighted with grey boxes. The conserved PTP signature motif HC(X)5R is highlighted with the red box. The alignment was generated via the Multiple Alignments function of CLC Main Workbench 8 (QIAGEN). (B) Growth complementation assay with *siw14Δ*. WT yeast (BY4741) and the *siw14Δ* yeast mutant were transformed with pDRf1-GW plasmids carrying either *SIW14* or its catalytic mutant C214S or carrying *PFA-DSP1* or its catalytic mutant C150S. Yeast strains transformed with empty pDRf1-GW vector as indicated served as controls. Transformants were then spotted in 8-fold serial dilutions (starting from OD_{600} 1.0) onto selective media containing wortmannin solved in DMSO or DMSO alone as control. Plates were incubated at 26 °C for 2 days before photographing. (C) Immunoblotting of Siw14, $Siw14^{C214S}$, PFA-DSP1 and $PFA\text{-}DSP1^{C150S}$. For detection of V5-tagged proteins an anti-V5 tag primary antibody (Invitrogen; 1:2000 dilution) and an anti-mouse secondary antibody coupled with Alexa Fluor plus 800 (Invitrogen; goat; 1:20000 dilution)

were used. As loading control, Gal4 protein levels were detected simultaneously using a polyclonal anti-Gal4 antibody (Santa Cruz; 1:1000 dilution) and an anti-rabbit StarBright Blue 700 antibody (Bio-Rad, goat; 1:2500 dilution). The signal was detected using the multiplex function of the ChemiDoc MP imager (Bio-Rad). (D) SAX-HPLC profiles of extracts of radiolabeled *siw14Δ* yeast transformed with either empty pDRf1-GW plasmid (empty vector) or pDRf1-GW carrying either *SIW14* or *SIW14*^{C214S}. (E) SAX-HPLC profiles of radiolabeled *siw14Δ* yeast transformed with either empty pDRf1-GW plasmid (e.v.) or pDRf1-GW carrying either *PFA-DSP1* or *PFA-DSP1*^{C150S}. (B – E) The experiments were repeated independently with similar results.

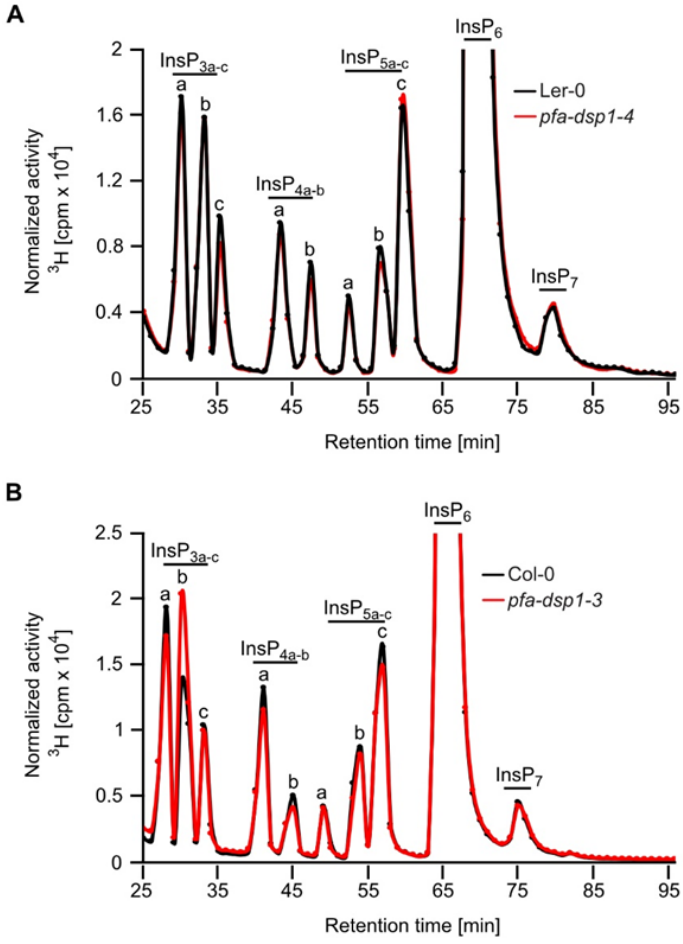

Figure II-S11: Single mutant Arabidopsis *pfa-dsp1* loss-of-function lines do not display InsP/PP-InsP defects. Representative SAX-HPLC profiles of 20-days-old WT Ler-0 and *pfa-dsp1-4* Arabidopsis seedlings (A) and of Col-0 and *pfa-dsp1-3* Arabidopsis seedlings (B) radiolabeled with [^{3}H]-*myo*-inositol. All visible peaks are highlighted and assigned to the corresponding InsP species. Based on published chromatographic mobilities (Stevenson-Paulik *et al.*, 2005; Kuo *et al.*, 2018), $InsP_{4a}$ likely represents Ins(1,4,5,6)P_4 or Ins(3,4,5,6)P_4, $InsP_{5a}$ likely represents $InsP_5$ [2-OH], $InsP_{5b}$ likely represents $InsP_5$ [4-OH] or its enantiomeric form $InsP_5$ [6-OH], and $InsP_{5c}$ likely represents $InsP_5$ [1-OH] or its enantiomeric form $InsP_5$ [3-OH]. The isomeric natures of $InsP_{3a-c}$, $InsP_{4b}$, $InsP_7$, and $InsP_8$ are unknown.

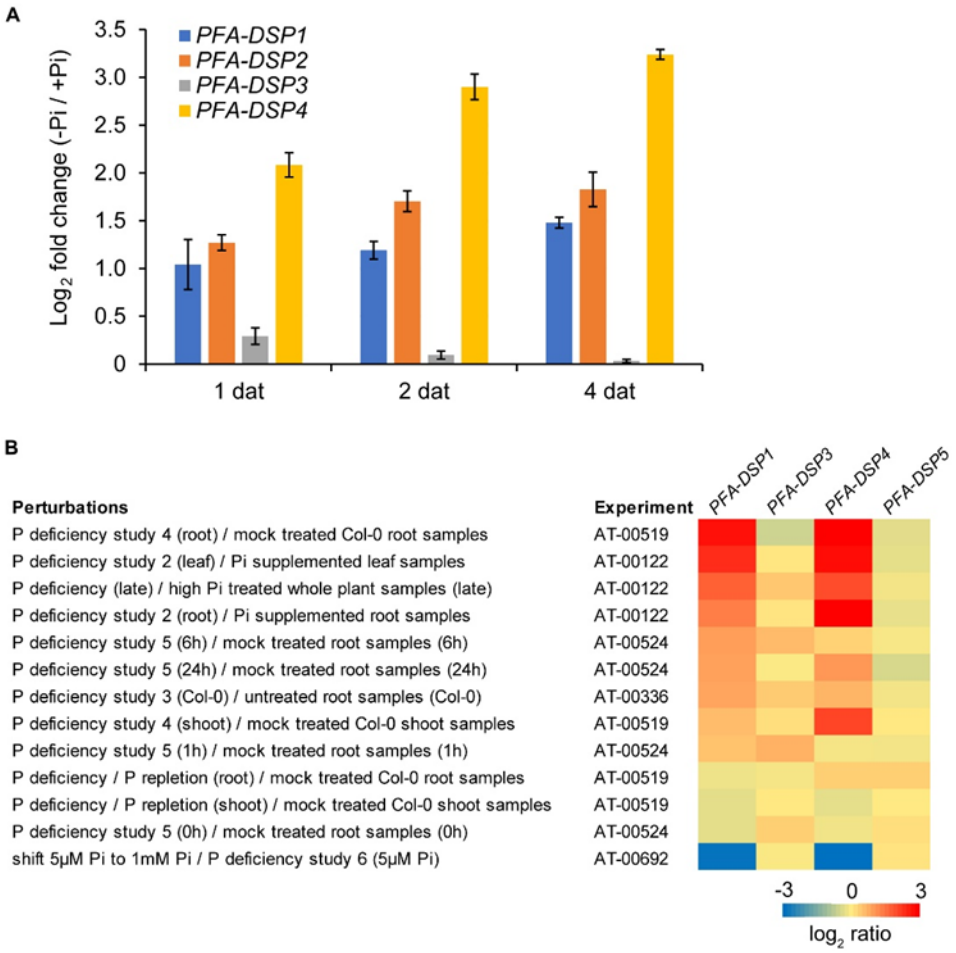

Figure II-S12: Arabidopsis *PFA-DSP1*, *2* and *4* are strongly induced by P_i deficiency. (A) Expression of the indicated *PFA-DSPs* in roots of *Aradidopsis thaliana* (accession Col-0) plants according to a transcriptome experiment with Agilent microarrays (Bhosale *et al.*, 2018); data deposited on e!DAL repository under the accession code https://doi.org/10.5447/IPK/2018/4. No probe for *PFA-DSP5* was present in the microarray chips. Seven-day-old plants pre-cultured on sufficient P_i supply were transferred to fresh solid media containing 625 µM P_i (+P_i) or 100 µM P_i (-P_i). Whole roots were collected at the indicated time points after transfer. Data represent means ± SD (n = 3). (B) Heatmap analysis of *PFA-DSPs* genes in response to the indicated P_i treatments. No data are presented for *PFA-DSP2* as no probe for this gene is present in Affimetrix chips. Transcriptional data were retrieved and analyzed with Genevestigator (http://www.genevestigator.ethz.ch).

Table II-S1: Overview of Arabidopsis PFA-DSP substrate specificities in presence of Mg^{2+} showing a robust PP-InsP pyrophosphatase activity against 5-$InsP_7$, 1,5-$InsP_8$ and 3,5-$InsP_8$, *in vitro*. The table summarizes the *in vitro* results of Figure II-1, Figure II-3, Figure II-S2, and Figure II-S7. (-) indicates no substrate, (+) poor substrate, (++) good substrate and n.d. no data.

Mg^{2+}	1-$InsP_7$	2-$InsP_7$	3-$InsP_7$	4-$InsP_7$	5-$InsP_7$	6-$InsP_7$	1,5-$InsP_8$	3,5-$InsP_8$
Siw14	(-)	(-)	(-)	(+)	(++)	(+)	(++)	(++)
PFA-DSP1	(+)	(-)	(+)	(+)	(++)	(+)	(++)	(++)
PFA-DSP2	(-)	(-)	(-)	(+)	(++)	(+)	(++)	(++)
PFA-DSP3	(+)	(-)	(+)	(+)	(++)	(+)	(++)	(++)
PFA-DSP4	(+)	(-)	(+)	(+)	(++)	(+)	(++)	(++)
PFA-DSP5	(-)	(-)	(-)	(-)	(-)	(-)	(-)	(-)
PFA-DSP5 *	(-)	(-)	(-)	(+)	(++)	(+)	n.d.	n.d.

* tested with a higher PFA-DSP5 concentration and increased incubation time

Table II-S2: Oligonucleotide sequences.

Primer name	**Sequence**
attB1 adapter	GGGGACAAGTTTGTACAAAAAAGCAGGCTTC
attB2 adapter	GGGGACCACTTTGTACAAGAAAGCTGGGTC
attB2+V5 adapter	GGGGACCACTTTGTACAAGAAAGCTGGGTCTTACGTAGAATCGAGAC CGAGGAGAGGGTTAGGGATAGGCTTACCTCCTCCAGATCC
attB1_ScSIW14	AAAAAGCAGGCTTCATGGGTTTATATCAAGCAAAG
attB2_ScSIW14s	AAAAAGCAGGCTTCATGGGTTTATATCAAGCAAAG
attB2_ScSIW14V5	CTTACCTCCTCCAGATCCCCATTGTAGAGGCAACCAG
attB1_AtPFA-DSP1	AAAAAGCAGGCTTCATGAAGCTTGTGGAGAAGAC
attB2_AtPFA-DSP1ns	AGAAAGCTGGGTCCCTGATGGAACAAGAGAATG
attB2_AtPFA-DSP1s	AGAAAGCTGGGTCTTACCTGATGGAACAAGAG
attB2_AtPFA-DSP1V5	ACCTCCTCCAGATCCCCTGATGGAACAAGAGAATG
attB1_AtPFA-DSP2	AAAAAGCAGGCTTCATGAAACTGATTGAGAAGACG
attB2_AtPFA-DSP2s	AGAAAGCTGGGTCTTACCTATTGGAGCAAGAAAAAG
attB2_AtPFA-DSP2V5	ACCTCCTCCAGATCCCCTATTGGAGCAAGAAAAAGAC
attB1_AtPFA-DSP3	AAAAAGCAGGCTTCATGTGTTTGATTATGGAAACGG
attB2_AtPFA-DSP3s	AGAAAGCTGGGTCTTAAACTCTAGCAGCCTGCG
attB2_AtPFA-DSP3V5	ACCTCCTCCAGATCCAACTCTAGCAGCCTGCGG
attB1_AtPFA-DSP4	AAAAAGCAGGCTTCATGACGTTAGAGAGTTACGCCG
attB2_AtPFA-DSP4s	AGAAAGCTGGGTCTCAGTAATCAATAGTATTAGTATACCTCTTGG

attB2_AtPFA-DSP4V5	ACCTCCTCCAGATCCGTAATCAATAGTATTAGTATACCTCTTGG
attB1_AtPFA-DSP5	AAAAAGCAGGCTTCATGGGCTTAATTGTGGATGATG
attB2_AtPFA-DSP5s	AGAAAGCTGGGTCTTATCCTTTGGTGGCTTGAGG
attB2_AtPFA-DSP5V5	ACCTCCTCCAGATCCTCCTTTGGTGGCTTGAGG
ScSIW14_C214S_F	TCAACCGATACTGATACATTCTAATAGAGGCAAACATAGAAC
ScSIW14_C214S_R	GTTCTATGTTTGCCTCTATTAGAATGTATCAGTATCGGTTGA
AtPFA-DSP1_C150S_F	GTTCTGATTCATAGTAAGCGAGGC
AtPFA-DSP1_C150S_R	GCCTCGCTTACTATGAATCAGAACA
ScSIW14pgt_PstI_F	AGCCTGCAGGATGGAGCTGCTCCTGGCTG
ScSIW14pgt_EcoRI_R	GAATTCAATATAAAGCGGGAATTTTTTTTTTTC
AtPFA-DSP1_267_F	ATACTTGTGCCCGGAGCCCT
AtPFA-DSP1_373_R	TCACAAATGGCTCCTTGTTGCCT
AtTIP41-like_F	TGGTTGGAAGCAGGAAGGGCT
AtTIP41-like_R	TGCTGAGACGGCTTGCTCCTGA
AtPP2AA3_F_qPCR	TGGTGCTCAGATGAGGGAGA
AtPP2AA3_R_qPCR	TAGCACATCTGGGGCACTTG
ScSIW14_pUG_F	CTCTTCTGGATCAATTTTTCTTTTTCATCTAAAGTTTAAAAGGAGCAGC TGAAGCTTCGTACGC
ScSIW14_pUG_R	CATCATTTTCGAAGAGACTAGTTACGTAAAGGTAATCACTGTCTACAT AGCATAGGCCACTAGTGGATCTG
WiscDsLox_473B10_LP	TTGTTTTGCAAAACTGCAAAG
WiscDsLox_473B10_RP	TTGCCTTCAATACCAAACTGG
P745_WiscDsLox_F	AACGTCCGCAATGTGTTATTAAGTTGTC
GT1415_F	CGACTCTCCTCACCTAAAGATTCA
GT1415_R	GTTGCCTTCAATACCAAACTGG
DS3-1	ACCCGACCGGATCGTATCGGT
SAIL_116_C12_LP	TTGTTTTGCAAAACTGCAAAG
SAIL_116_C12_RP	TTGCCTTCAATACCAAACTGG
LB1_SAIL_F	GCCTTTTCAGAAATGGATAAATAGCCTTGCTTCC

References

Aceti, D. J., Bitto, E., Yakunin, A. F., Proudfoot, M., Bingman, C. A., Frederick, R. O., Sreenath, H. K., Vojtik, F. C., Wrobel, R. L., Fox, B. G., Markley, J. L. and Phillips, G. N. (2008). Structural and functional characterization of a novel phosphatase from the *Arabidopsis thaliana* gene locus At1g05000. Proteins: Structure, Function, and Bioinformatics. 10.1002/prot.22041.

Adepoju, O., Williams, S. P., Craige, B., Cridland, C. A., Sharpe, A. K., Brown, A. M., Land, E., Perera, I. Y., Mena, D., Sobrado, P. and Gillaspy, G. E. (2019). Inositol Trisphosphate Kinase and Diphosphoinositol Pentakisphosphate Kinase Enzymes Constitute the Inositol Pyrophosphate Synthesis Pathway in Plants. Cold Spring Harbor Laboratory.

Andreeva, N., Ledova, L., Ryazanova, L., Tomashevsky, A., Kulakovskaya, T. and Eldarov, M. (2019). Ppn2 endopolyphosphatase overexpressed in *Saccharomyces cerevisiae*: Comparison with Ppn1, Ppx1, and Ddp1 polyphosphatases. Biochimie. 10.1016/j.biochi.2019.06.001.

Arcaro, A. and Wymann, M. P. (1993). Wortmannin is a potent phosphatidylinositol 3-kinase inhibitor: the role of phosphatidylinositol 3,4,5-trisphosphate in neutrophil responses. Biochemical Journal. 10.1042/bj2960297.

Azevedo, C. and Saiardi, A. (2006). Extraction and analysis of soluble inositol polyphosphates from yeast. Nature Protocols. 10.1038/nprot.2006.337.

Bhosale, R., Giri, J., Pandey, B. K., Giehl, R. F. H., Hartmann, A., Traini, R., Truskina, J., Leftley, N., Hanlon, M., Swarup, K., Rashed, A., Voß, U., Alonso, J., Stepanova, A., Yun, J., Ljung, K., Brown, K. M., Lynch, J. P., Dolan, L., Vernoux, T., Bishopp, A., Wells, D., von Wirén, N., Bennett, M. J. and Swarup, R. (2018). A mechanistic framework for auxin dependent Arabidopsis root hair elongation to low external phosphate. Nature Communications. Advanced Access published April 12, 2018: 10.1038/s41467-018-03851-3.

Blüher, D., Laha, D., Thieme, S., Hofer, A., Eschen-Lippold, L., Masch, A., Balcke, G., Pavlovic, I., Nagel, O., Schonsky, A., Hinkelmann, R., Wörner, J., Parvin, N., Greiner, R., Weber, S., Tissier, A., Schutkowski, M., Lee, J., Jessen, H., Schaaf, G. and Bonas, U. (2017). A 1-phytase type III effector interferes with plant hormone signaling. Nature Communications. 10.1038/s41467-017-02195-8.

Brown, J. A., Sherlock, G., Myers, C. L., Burrows, N. M., Deng, C., Wu, H. I., McCann, K. E., Troyanskaya, O. G. and Brown, J. M. (2006). Global analysis of gene function in yeast by quantitative phenotypic profiling. Molecular Systems Biology. 10.1038/msb4100043.

Bustos, R., Castrillo, G., Linhares, F., Puga, M. I., Rubio, V., Pérez-Pérez, J., Solano, R., Leyva, A. and Paz-Ares, J. (2010). A Central Regulatory System Largely Controls Transcriptional Activation and Repression Responses to Phosphate Starvation in Arabidopsis. PLoS Genetics. 10.1371/journal.pgen.1001102.

Caffrey, J. J., Hidaka, K., Matsuda, M., Hirata, M. and Shears, S. B. (1999). The human and rat forms of multiple inositol polyphosphate phosphatase: functional homology with a histidine acid phosphatase up-regulated during endochondral ossification. FEBS Letters. 10.1016/s0014-5793(98)01636-6.

Capolicchio, S., Thakor, D. T., Linden, A. and Jessen, H. J. (2013). Synthesis of Unsymmetric Diphospho-Inositol Polyphosphates. Angewandte Chemie International Edition. 10.1002/anie.201301092.

Capolicchio, S., Wang, H., Thakor, D. T., Shears, S. B. and Jessen, H. J. (2014). Synthesis of Densely Phosphorylated Bis-1,5-Diphospho-*myo*-Inositol Tetrakisphosphate and its Enantiomer by Bidirectional P-Anhydride Formation. Angewandte Chemie International Edition. 10.1002/anie.201404398.

Couso, I., Evans, B. S., Li, J., Liu, Y., Ma, F., Diamond, S., Allen, D. K. and Umen, J. G. (2016). Synergism between Inositol Polyphosphates and TOR Kinase Signaling in Nutrient Sensing, Growth Control, and Lipid Metabolism in Chlamydomonas. The Plant Cell. 10.1105/tpc.16.00351.

Desai, M., Rangarajan, P., Donahue, J. L., Williams, S. P., Land, E. S., Mandal, M. K., Phillippy, B. Q., Perera, I. Y., Raboy, V. and Gillaspy, G. E. (2014). Two inositol hexakisphosphate kinases drive inositol pyrophosphate synthesis in plants. The Plant Journal. 10.1111/tpj.12669.

Dong, J., Ma, G., Sui, L., Wei, M., Satheesh, V., Zhang, R., Ge, S., Li, J., Zhang, T.-E., Wittwer, C., Jessen, H. J., Zhang, H., An, G.-Y., Chao, D.-Y., Liu, D. and Lei, M. (2019). Inositol Pyrophosphate $InsP_8$ Acts as an Intracellular Phosphate Signal in Arabidopsis. Molecular Plant. 10.1016/j.molp.2019.08.002.

Estevez, F., Pulford, D., Stark, M. J., Carter, A. N. and Downes, C. P. (1994). Inositol trisphosphate metabolism in *Saccharomyces cerevisiae*: identification, purification and properties of inositol 1,4,5-trisphosphate 6-kinase. Biochemical Journal. 10.1042/bj3020709.

Flores, S. and Smart, C. C. (2000). Abscisic acid-induced changes in inositol metabolism in *Spirodela polyrrhiza*. Planta. 10.1007/s004250000348.

Fridy, P. C., Otto, J. C., Dollins, D. E. and York, J. D. (2007). Cloning and Characterization of Two Human VIP1-like Inositol Hexakisphosphate and Diphosphoinositol Pentakisphosphate Kinases. Journal of Biological Chemistry. 10.1074/jbc.m704656200.

Gaugler, P., Gaugler, V., Kamleitner, M. and Schaaf, G. (2020). Extraction and Quantification of Soluble, Radiolabeled Inositol Polyphosphates from Different Plant Species using SAX-HPLC. Journal of Visualized Experiments. 10.3791/61495.

Gerasimaite, R., Pavlovic, I., Capolicchio, S., Hofer, A., Schmidt, A., Jessen, H. J. and Mayer, A. (2017). Inositol Pyrophosphate Specificity of the SPX-Dependent Polyphosphate Polymerase VTC. ACS Chemical Biology. 10.1021/acschembio.7b00026.

Gietz, R. D., Schiestl, R. H., Willems, A. R. and Woods, R. A. (1995). Studies on the transformation of intact yeast cells by the LiAc/SS-DNA/PEG procedure. Yeast. 10.1002/yea.320110408.

Gruber, B. D., Giehl, R. F., Friedel, S. and von Wirén, N. (2013). Plasticity of the Arabidopsis Root System under Nutrient Deficiencies. Plant Physiology. 10.1104/pp.113.218453.

Gueldener, U. (2002). A second set of loxP marker cassettes for Cre-mediated multiple gene knockouts in budding yeast. Nucleic Acids Research. 10.1093/nar/30.6.e23.

Gulabani, H., Goswami, K., Walia, Y., Roy, A., Noor, J. J., Ingole, K. D., Kasera, M., Laha, D., Giehl, R. F. H., Schaaf, G. and Bhattacharjee, S. (2021). Arabidopsis inositol polyphosphate kinases IPK1 and ITPK1 modulate crosstalk between SA-dependent immunity and phosphate-starvation responses. Plant Cell Reports. 10.1007/s00299-021-02812-3.

Irvine, R. F. and Schell, M. J. (2001). Back in the water: the return of the inositol phosphates. Nature Reviews Molecular Cell Biology. 10.1038/35073015.

Kilari, R. S., Weaver, J. D., Shears, S. B. and Safrany, S. T. (2013). Understanding inositol pyrophosphate metabolism and function: Kinetic characterization of the DIPPs. FEBS Letters. 10.1016/j.febslet.2013.08.035.

Kuo, H.-F., Hsu, Y.-Y., Lin, W.-C., Chen, K.-Y., Munnik, T., Brearley, C. A. and Chiou, T.-J. (2018). Arabidopsis inositol phosphate kinases IPK1 and ITPK1 constitute a metabolic pathway in maintaining phosphate homeostasis. The Plant Journal. 10.1111/tpj.13974.

Laha, D., Johnen, P., Azevedo, C., Dynowski, M., Weiß, M., Capolicchio, S., Mao, H., Iven, T., Steenbergen, M., Freyer, M., Gaugler, P., Campos, M. K. de**, Zheng, N., Feussner, I., Jessen, H. J., van Wees, S. C., Saiardi, A. and Schaaf, G.** (2015). VIH2 Regulates the Synthesis of Inositol Pyrophosphate $InsP_8$ and Jasmonate-Dependent Defenses in Arabidopsis. The Plant Cell. 10.1105/tpc.114.135160.

Laha, D., Kamleitner, M., Johnen, P. and Schaaf, G. (2021). Analyses of Inositol Phosphates and Phosphoinositides by Strong Anion Exchange (SAX)-HPLC. Springer US.

Laha, D., Parvin, N., Dynowski, M., Johnen, P., Mao, H., Bitters, S. T., Zheng, N. and Schaaf, G. (2016). Inositol Polyphosphate Binding Specificity of the Jasmonate Receptor Complex. Plant Physiology. 10.1104/pp.16.00694.

Laha, D., Parvin, N., Hofer, A., Giehl, R. F. H., Fernandez-Rebollo, N., von Wirén, N., Saiardi, A., Jessen, H. J. and Schaaf, G. (2019). Arabidopsis ITPK1 and ITPK2 Have an Evolutionarily Conserved Phytic Acid Kinase Activity. ACS Chemical Biology. 10.1021/acschembio.9b00423.

Laha, N. P., Giehl, R. F. H., Riemer, E., Qiu, D., Pullagurla, N. J., Schneider, R., Dhir, Y. W., Yadav, R., Mihiret, Y. E., Gaugler, P., Gaugler, V., Mao, H., Zheng, N., von Wirén, N., Saiardi, A., Bhattacharjee, S., Jessen, H. J., Laha, D. and Schaaf, G. (2022). INOSITOL (1,3,4) TRIPHOSPHATE 5/6 KINASE1-dependent inositol polyphosphates regulate auxin responses in Arabidopsis. Plant Physiology. 10.1093/plphys/kiac425.

Lemtiri-Chlieh, F., MacRobbie, E. A. C. and Brearley, C. A. (2000). Inositol hexakisphosphate is a physiological signal regulating the K^+-inward rectifying conductance in guard cells. Proceedings of the National Academy of Sciences. 10.1073/pnas.140217497.

Lin, H., Fridy, P. C., Ribeiro, A. A., Choi, J. H., Barma, D. K., Vogel, G., Falck, J. R., Shears, S. B., York, J. D. and Mayr, G. W. (2009). Structural Analysis and Detection of Biological Inositol Pyrophosphates Reveal That the Family of VIP/Diphosphoinositol Pentakisphosphate Kinases Are 1/3-Kinases. Journal of Biological Chemistry. 10.1074/jbc.m805686200.

Lonetti, A., Szijgyarto, Z., Bosch, D., Loss, O., Azevedo, C. and Saiardi, A. (2011). Identification of an Evolutionarily Conserved Family of Inorganic Polyphosphate Endopolyphosphatases. Journal of Biological Chemistry. 10.1074/jbc.m111.266320.

Loqué, D., Lalonde, S., Looger, L. L., von Wirén, N. and Frommer, W. B. (2007). A cytosolic trans-activation domain essential for ammonium uptake. Nature. 10.1038/nature05579.

Menniti, F. S., Miller, R. N., Putney, J. W. and Shears, S. B. (1993). Turnover of inositol polyphosphate pyrophosphates in pancreatoma cells. Journal of Biological Chemistry. 10.1016/s0021-9258(18)53551-1.

Mulugu, S., Bai, W., Fridy, P. C., Bastidas, R. J., Otto, J. C., Dollins, D. E., Haystead, T. A., Ribeiro, A. A. and York, J. D. (2007). A Conserved Family of Enzymes That Phosphorylate Inositol Hexakisphosphate. Science. 10.1126/science.1139099.

Nagy, R., Grob, H., Weder, B., Green, P., Klein, M., Frelet-Barrand, A., Schjoerring, J. K., Brearley, C. and Martinoia, E. (2009). The Arabidopsis ATP-binding Cassette Protein AtMRP5/AtABCC5 Is a High Affinity Inositol Hexakisphosphate Transporter Involved in Guard Cell Signaling and Phytate Storage. Journal of Biological Chemistry. 10.1074/jbc.m109.030247.

Nakamura, S., Mano, S., Tanaka, Y., Ohnishi, M., Nakamori, C., Araki, M., Niwa, T., Nishimura, M., Kaminaka, H., Nakagawa, T., Sato, Y. and Ishiguro, S. (2010). Gateway Binary Vectors with the Bialaphos Resistance Gene, *bar*, as a Selection Marker for Plant Transformation. Bioscience, Biotechnology, and Biochemistry. 10.1271/bbb.100184.

Onnebo, S. M. N. and Saiardi, A. (2009). Inositol pyrophosphates modulate hydrogen peroxide signalling. Biochemical Journal. 10.1042/bj20090241.

Osada, S., Kageyama, K., Ohnishi, Y., Nishikawa, J., Nishihara, T. and Imagawa, M. (2011). Inositol phosphate kinase Vip1p interacts with histone chaperone Asf1p in *Saccharomyces cerevisiae*. Molecular Biology Reports. 10.1007/s11033-011-1295-z.

Pascual-Ortiz, M., Saiardi, A., Walla, E., Jakopec, V., Künzel, N. A., Span, I., Vangala, A. and Fleig, U. (2018). Asp1 Bifunctional Activity Modulates Spindle Function via Controlling Cellular Inositol Pyrophosphate Levels in *Schizosaccharomyces pombe*. Molecular and Cellular Biology. 10.1128/mcb.00047-18.

Puga, M. I., Mateos, I., Charukesi, R., Wang, Z., Franco-Zorrilla, J. M., Lorenzo, L. de**, Irigoyen, M. L., Masiero, S., Bustos, R., Rodríguez, J., Leyva, A., Rubio, V., Sommer, H. and Paz-Ares, J.** (2014). SPX1 is a phosphate-dependent inhibitor of PHOSPHATE STARVATION RESPONSE 1 in Arabidopsis. Proceedings of the National Academy of Sciences. 10.1073/pnas.1404654111.

Qiu, D., Eisenbeis, V. B., Saiardi, A. and Jessen, H. J. (2021). Absolute Quantitation of Inositol Pyrophosphates by Capillary Electrophoresis Electrospray Ionization Mass Spectrometry. Journal of Visualized Experiments. 10.3791/62847.

Qiu, D., Wilson, M. S., Eisenbeis, V. B., Harmel, R. K., Riemer, E., Haas, T. M., Wittwer, C., Jork, N., Gu, C., Shears, S. B., Schaaf, G., Kammerer, B., Fiedler, D., Saiardi, A. and Jessen, H. J. (2020). Analysis of inositol phosphate metabolism by capillary electrophoresis electrospray ionization mass spectrometry. Nature Communications. 10.1038/s41467-020-19928-x.

Ried, M. K., Wild, R., Zhu, J., Pipercevic, J., Sturm, K., Broger, L., Harmel, R. K., Abriata, L. A., Hothorn, L. A., Fiedler, D., Hiller, S. and Hothorn, M. (2021). Inositol pyrophosphates promote the interaction of SPX domains with the coiled-coil motif of PHR transcription factors to regulate plant phosphate homeostasis. Nature Communications. 10.1038/s41467-020-20681-4.

Riemer, E., Qiu, D., Laha, D., Harmel, R. K., Gaugler, P., Gaugler, V., Frei, M., Hajirezaei, M.-R., Laha, N. P., Krusenbaum, L., Schneider, R., Saiardi, A., Fiedler, D., Jessen, H. J., Schaaf, G. and Giehl, R. F. (2021). ITPK1 is an $InsP_6$/ADP phosphotransferase that controls phosphate signaling in Arabidopsis. Molecular Plant. 10.1016/j.molp.2021.07.011.

Romá-Mateo, C., Ríos, P., Tabernero, L., Attwood, T. K. and Pulido, R. (2007). A Novel Phosphatase Family, Structurally Related to Dual-specificity Phosphatases, that Displays Unique Amino Acid Sequence and Substrate Specificity. Journal of Molecular Biology. 10.1016/j.jmb.2007.10.008.

Romá-Mateo, C., Sacristán-Reviriego, A., Beresford, N. J., Caparrós-Martín, J. A., Culiáñez-Macià, F. A., Martín, H., Molina, M., Tabernero, L. and Pulido, R. (2011). Phylogenetic and genetic linkage between novel atypical dual-specificity phosphatases from non-metazoan organisms. Molecular Genetics and Genomics. 10.1007/s00438-011-0611-6.

Rubio, V., Linhares, F., Solano, R., Martín, A. C., Iglesias, J., Leyva, A. and Paz-Ares, J. (2001). A conserved MYB transcription factor involved in phosphate starvation signaling both in vascular plants and in unicellular algae. Genes & Development. 10.1101/gad.204401.

Safrany, S. T. (1998). A novel context for the `MutT´ module, a guardian of cell integrity, in a diphosphoinositol polyphosphate phosphohydrolase. The EMBO Journal. 10.1093/emboj/17.22.6599.

Safrany, S. T., Ingram, S. W., Cartwright, J. L., Falck, J. R., McLennan, A. G., Barnes, L. D. and Shears, S. B. (1999). The Diadenosine Hexaphosphate Hydrolases from *Schizosaccharomyces pombe* and *Saccharomyces cerevisiae* Are Homologues of the Human Diphosphoinositol Polyphosphate Phosphohydrolase. Journal of Biological Chemistry. 10.1074/jbc.274.31.21735.

Saiardi, A., Erdjument-Bromage, H., Snowman, A. M., Tempst, P. and Snyder, S. H. (1999). Synthesis of diphosphoinositol pentakisphosphate by a newly identified family of higher inositol polyphosphate kinases. Current Biology. 10.1016/s0960-9822(00)80055-x.

Saiardi, A., Resnick, A. C., Snowman, A. M., Wendland, B. and Snyder, S. H. (2005). Inositol pyrophosphates regulate cell death and telomere length through phosphoinositide 3-kinase-related protein kinases. Proceedings of the National Academy of Sciences. 10.1073/pnas.0409322102.

Schaaf, G., Betts, L., Garrett, T. A., Raetz, C. R. H. and Bankaitis, V. A. (2006). Crystallization and preliminary X-ray diffraction analysis of phospholipid-bound Sfh1p, a member of the *Saccharomyces cerevisiae* Sec14p-like phosphatidylinositol transfer protein family. Acta Crystallographica Section F Structural Biology and Crystallization Communications. 10.1107/s1744309106041728.

Shears, S. B. (2017). Intimate connections: Inositol pyrophosphates at the interface of metabolic regulation and cell signaling. Journal of Cellular Physiology. 10.1002/jcp.26017.

Steidle, E. A., Chong, L. S., Wu, M., Crooke, E., Fiedler, D., Resnick, A. C. and Rolfes, R. J. (2016). A Novel Inositol Pyrophosphate Phosphatase in *Saccharomyces cerevisiae*. Journal of Biological Chemistry. 10.1074/jbc.m116.714907.

Steidle, E. A., Morrissette, V. A., Fujimaki, K., Chong, L., Resnick, A. C., Capaldi, A. P. and Rolfes, R. J. (2020). The $InsP_7$ phosphatase Siw14 regulates inositol pyrophosphate levels to control localization of the general stress response transcription factor Msn2. Journal of Biological Chemistry. 10.1074/jbc.ra119.012148.

Stephens, L., Radenberg, T., Thiel, U., Vogel, G., Khoo, K. H., Dell, A., Jackson, T. R., Hawkins, P. T. and Mayr, G. W. (1993). The detection, purification, structural characterization, and metabolism of diphosphoinositol pentakisphosphate(s) and bisdiphosphoinositol tetrakisphosphate(s). Journal of Biological Chemistry. 10.1016/s0021-9258(18)53571-7.

Stevenson-Paulik, J., Bastidas, R. J., Chiou, S.-T., Frye, R. A. and York, J. D. (2005). Generation of phytate-free seeds in Arabidopsis through disruption of inositol polyphosphate kinases. Proceedings of the National Academy of Sciences. 10.1073/pnas.0504172102.

Thota, S. G. and Bhandari, R. (2015). The emerging roles of inositol pyrophosphates in eukaryotic cell physiology. Journal of Biosciences. 10.1007/s12038-015-9549-x.

Wang, H., Falck, J. R., Hall, T. M. T. and Shears, S. B. (2011). Structural basis for an inositol pyrophosphate kinase surmounting phosphate crowding. Nature Chemical Biology. 10.1038/nchembio.733.

Wang, H., Gu, C., Rolfes, R. J., Jessen, H. J. and Shears, S. B. (2018). Structural and biochemical characterization of Siw14: A protein-tyrosine phosphatase fold that metabolizes inositol pyrophosphates. Journal of Biological Chemistry. 10.1074/jbc.ra117.001670.

Wang, H., Nair, V. S., Holland, A. A., Capolicchio, S., Jessen, H. J., Johnson, M. K. and Shears, S. B. (2015). Asp1 from *Schizosaccharomyces pombe* Binds a $[2Fe\text{-}2S]^{2+}$ Cluster Which Inhibits Inositol Pyrophosphate 1-Phosphatase Activity. Biochemistry. 10.1021/acs.biochem.5b00532.

Wang, H., Perera, L., Jork, N., Zong, G., Riley, A. M., Potter, B. V. L., Jessen, H. J. and Shears, S. B. (2022). A structural exposé of noncanonical molecular reactivity within the protein tyrosine phosphatase WPD loop. Nature Communications. 10.1038/s41467-022-29673-y.

Wang, Z., Kuo, H.-F. and Chiou, T.-J. (2021). Intracellular phosphate sensing and regulation of phosphate transport systems in plants. Plant Physiology. 10.1093/plphys/kiab343.

Whitfield, H., White, G., Sprigg, C., Riley, A. M., Potter, B. V., Hemmings, A. M. and Brearley, C. A. (2020). An ATP-responsive metabolic cassette comprised of inositol tris/tetrakisphosphate kinase 1 (ITPK1) and inositol pentakisphosphate 2-kinase (IPK1) buffers diphosphosphoinositol phosphate levels. Biochemical Journal. 10.1042/bcj20200423.

Wild, R., Gerasimaite, R., Jung, J.-Y., Truffault, V., Pavlovic, I., Schmidt, A., Saiardi, A., Jessen, H. J., Poirier, Y., Hothorn, M. and Mayer, A. (2016). Control of eukaryotic phosphate homeostasis by inositol polyphosphate sensor domains. Science. 10.1126/science.aad9858.

Zhou, J., Hu, Q., Xiao, X., Yao, D., Ge, S., Ye, J., Li, H., Cai, R., Liu, R., Meng, F., Wang, C., Zhu, J.-K., Lei, M. and Xing, W. (2021). Mechanism of phosphate sensing and signaling revealed by rice SPX1-PHR2 complex structure. Nature Communications. 10.1038/s41467-021-27391-5.

Zhu, J., Lau, K., Puschmann, R., Harmel, R. K., Zhang, Y., Pries, V., Gaugler, P., Broger, L., Dutta, A. K., Jessen, H. J., Schaaf, G., Fernie, A. R., Hothorn, L. A., Fiedler, D. and Hothorn, M. (2019). Two bifunctional inositol pyrophosphate kinases/phosphatases control plant phosphate homeostasis. eLife. 10.7554/elife.43582.

Zonneveld, B. J. (1986). Cheap and simple yeast media. Journal of Microbiological Methods. 10.1016/0167-7012(86)90040-0.

Chapter III

The objective of chapter III is to determine whether the seven *Arabidopsis thaliana* NUDT hydrolases NUDT4, NUDT12, NUDT13, NUDT16, NUDT17, NUDT18, and NUDT21 are PP-InsP pyrophosphatases and whether they are involved in PP-InsP synthesis and P_i homeostasis in plants. This chapter is adapted from the preprint article Schneider *et al.* (2024), which is currently under review.

Schneider, R.*, Lami, K.*, Prucker, I.*, Stolze, S. C., Strauß, A., Langenbach, K., Kamleitner, M., Belay, Y. Z., Ritter, K., Furkert, D., Gaugler, P., Lange, E., Faiß, N., Schmidt, J. M., Harings, M., Krusenbaum, L., Wege, S., Kriescher, S., Schoof, H., Fiedler, D., Nakagami, H., Giehl, R. F. H., Lahaye, T., Jessen, H. J., Gaugler, V. and Schaaf, G. (2024). NUDIX Hydrolases Target Specific Inositol Pyrophosphates and Regulate Phosphate and Iron Homeostasis, and the Expression of Defense Genes in Arabidopsis.

*R.S., Kl.L. and I.P. contributed equally to this manuscript

Own contribution: I conceived the study with V.G. and G.S. I designed the experiments with V.G., Kl.L, G.S., T.L., R.F.H.G., H.J.J., H.N., and Do.F. I generated constructs, isolated T-DNA insertion lines, purified recombinant proteins, carried out and analyzed most of the *in vitro* pyrophosphatase assays and generated high order mutants with CRISPR/Cas9. I prepared the figures with Kl.L., I.P., M.K., L.K., V.G., and G.S. I wrote the manuscript with Kl.L., I.P., S.C.S, A.S., P.G., M.K., L.K., H.S., H.N., R.F.H.G., V.G. and G.S. with input from all authors.

NUDIX Hydrolases target specific inositol pyrophosphates and regulate phosphate and iron homeostasis, and the expression of defense genes in Arabidopsis

Abstract

Inositol pyrophosphates (PP-InsPs) are important signaling molecules that regulate diverse cellular processes in eukaryotes, including energy homeostasis and phosphate (P_i) signaling. Yet, in plants, the enzymes responsible for their turnover remain largely unknown. Using a non-hydrolysable PP-InsP analog in a pull-down approach, we identified a family of Arabidopsis NUDIX hydrolases (NUDTs) that group into two closely related subclades. Through *in vitro* assays, heterologous expression systems, and higher-order gene-edited mutants, we explored the substrate specificities and physiological roles of these hydrolases. Using a combination of strong anion exchange (SAX)-HPLC, PAGE, and capillary electrophoresis electrospray ionization mass spectrometry (CE-ESI-MS), we found that their PP-InsP pyrophosphatase activity is enantiomer-selective and Mg^{2+}-dependent. Specifically, subclade I NUDTs preferentially hydrolyze 4-$InsP_7$, while subclade II NUDTs target 3-$InsP_7$, with minor activity against other PP-InsPs, including 5-$InsP_7$. In higher-order mutants of subclade II NUDTs, we observed defects in both P_i and iron homeostasis, accompanied by increased levels of 1/3-$InsP_7$ and 5-$InsP_7$, with a markedly larger increase in 1/3-$InsP_7$. Ectopic expression of NUDTs from both subclades induced local P_i starvation responses (PSRs), while RNA-seq analysis comparing WT and *nudt12/13/16* loss-of-function plants indicates additional PSR-independent roles, potentially involving 1/3-$InsP_7$ in the regulation of plant defense. Expanding beyond subclade II NUDTs, we demonstrated susceptibility of the 3PP-position of PP-InsPs to enzymatic activities unrelated to NUDTs, and found that such activities are conserved across plants and humans. Additionally, we found that NUDT effectors from pathogenic ascomycete fungi exhibit a substrate specificity similar to subclade I NUDTs. Collectively, our study provides new insights into the roles of NUDTs in regulating PP-InsP signaling pathways in plants and highlights cross-kingdom conservation of enzymes involved in PP-InsP metabolism.

Introduction

Inositol pyrophosphates (PP-InsPs) are small signaling molecules consisting of a phosphorylated *myo*-inositol ring and one or several pyrophosphate groups, which regulate a wide range of cellular processes in eukaryotes. In metazoans, these messengers control DNA repair, insulin signaling, blood clotting, ribosome biogenesis, spermiogenesis, and telomere length maintenance (Stephens *et al.*, 1993; Menniti *et al.*, 1993; Shears, 2015; Thota and Bhandari, 2015; Shears, 2017). In plants, PP-InsPs regulate jasmonate and auxin signaling, as well as a nutrient status-dependent accumulation of storage lipids (Laha *et al.*, 2015; Couso *et al.*, 2016; Laha *et al.*, 2016; Laha *et al.*, 2022). An emerging and somewhat unifying role of these messengers in fungi, metazoans and plants is their critical involvement in energy homeostasis and phosphate (P_i) signaling (Lee *et al.*, 2007; Szijgyarto *et al.*, 2011; Wild *et al.*, 2016; Dong *et al.*, 2019; Wilson *et al.*, 2019; Zhu *et al.*, 2019; Li *et al.*, 2020; Gulabani *et al.*, 2021; Ried *et al.*, 2021; Riemer *et al.*, 2021; Wang *et al.*, 2021; Chabert *et al.*, 2023; Qin *et al.*, 2023). Phosphorus (P) is an essential macronutrient and a key determinant of agricultural yield (Tilman *et al.*, 2002; MacDonald *et al.*, 2011; Hawkesford *et al.*, 2023). Plants have evolved complex sensing and signaling mechanisms to adjust the plant's P demand with external P_i availability. In Arabidopsis, the MYB transcription factors PHR1 and PHL1 regulate the expression of P_i starvation-induced (PSI) genes (Rubio *et al.*, 2001; Bustos *et al.*, 2010). Under P_i deficiency, PHR1 activates PSI genes by binding to cognate binding elements (P1BS) in their promoter region. Under P_i sufficiency, stand-alone SPX proteins negatively regulate PHR transcription factors, as shown in various plant species (Liu *et al.*, 2010; Lv *et al.*, 2014; Puga *et al.*, 2014; Shi *et al.*, 2014; Wang *et al.*, 2014; Qi *et al.*, 2017; Zhong *et al.*, 2018; Osorio *et al.*, 2019; Ried *et al.*, 2021). Intriguingly, SPX proteins function as cellular receptors for certain PP-InsPs such as 5-$InsP_7$ and $InsP_8$ (Wild *et al.*, 2016; Gerasimaite *et al.*, 2017; Dong *et al.*, 2019; Zhu *et al.*, 2019; Li *et al.*, 2020; Pipercevic *et al.*, 2023; Yan *et al.*, 2024). When bound to $InsP_8$, SPX proteins interact with the unique coiled-coil motif of PHR1, interfering with its oligomerization and promoter-binding activity (Ried *et al.*, 2021). Consequently, mutants defective in these PP-InsPs display constitutively up-regulated P_i starvation responses (PSRs) both locally and systemically, suggesting that plants are largely unable to sense P_i directly but sense certain PP-InsPs as a proxy for P_i (Dong *et al.*, 2019; Zhu *et al.*, 2019; Riemer *et al.*, 2021). However, the regulation of these PSRs and the precise mechanisms and regulation of P_i sensing in plants still remains poorly understood.

Inositol polyphosphates (InsPs) and PP-InsPs (molecules) possess a high charge density and, in the case of many isomers, are present at low abundance in cells, making them particularly challenging to analyze. Additionally, many methods cannot separate PP-InsP isomers of identical molecular mass. Therefore, it was a major breakthrough when the development of capillary electrophoresis electrospray ionization mass spectrometry (CE-ESI-MS) (Qiu *et al.*, 2020), allowed the identification of three major $InsP_7$ (sometimes referred to as PP-$InsP_5$) isomers in plant extracts: 1-$InsP_7$ (carrying the PP-moiety at the 1-position) and/or 3-$InsP_7$ (hereafter referred to as 1/3-$InsP_7$), 4-$InsP_7$ and/or 6-$InsP_7$ (hereafter referred to as 4/6-$InsP_7$), and 5-$InsP_7$ (Riemer *et al.*, 2021). Because $InsP_6$, like *myo*-inositol, is a *meso* compound with a plane of symmetry dissecting the 2 and 5 positions, the 1/3 and 4/6 phosphates are enantiomeric and cannot be distinguished in the absence of chiral selectors (Blüher *et al.*, 2017; Ritter *et al.*, 2023) (Figure III-S1). In addition, CE-ESI-MS allowed identification of a novel PP-$InsP_4$ isomer of unknown isomer identity in Arabidopsis roots (Riemer *et al.*, 2021).

The biosynthetic pathways of PP-InsPs are only partially resolved. All eukaryotes appear to possess 5-$InsP_7$, but its synthesis from phytate ($InsP_6$) is mediated by distinct, sequence-unrelated enzyme families. In plants, 5-$InsP_7$ synthesis is catalyzed by inositol (1,3,4) trisphosphate 5/6-kinases (ITPKs), as shown *in vitro* and in yeast for various Arabidopsis and rice ITPKs (Laha *et al.*, 2019; Whitfield *et al.*, 2020), and as shown *in planta* for AtITPK1 and AtITPK2 (Riemer *et al.*, 2021; Laha *et al.*, 2022).

The synthesis of $InsP_8$ from 5-$InsP_7$ appears to be largely conserved in eukaryotes and is catalyzed by members of a protein family distinct from the above mentioned $InsP_6$ kinases (Mulugu *et al.*, 2007). In Arabidopsis, the synthesis of $InsP_8$ is catalyzed by two PPIP5K isoforms, namely AtVIH1 and AtVIH2 (Desai *et al.*, 2014; Laha *et al.*, 2015; Dong *et al.*, 2019; Zhu *et al.*, 2019). With the exception of the budding yeast PPIP5K Vip1 and the human PPIP5K2, both of which specifically generate 1-$InsP_7$ and 1,5-$InsP_8$ (Fridy *et al.*, 2007; Mulugu *et al.*, 2007; Dollins *et al.*, 2020), it remains unclear whether other PPIP5K isoforms catalyze the formation of the phosphoanhydride bond at the 1 or the 3 position of the fully phosphorylated *myo*-inositol ring. Therefore, the enantiomer identities of 1/3-$InsP_7$ and 1/3,5-$InsP_8$ in mammals and plants are still unknown. Besides, our knowledge about PP-InsP turnover in plants remains incomplete. Similar to yeast and mammalian PPIP5Ks, AtVIH1 and AtVIH2 are bifunctional enzymes, harboring an N-terminal ATP-grasp kinase domain and a C-terminal phosphatase-like domain (Fridy *et al.*, 2007; Mulugu *et al.*, 2007; Wang *et al.*, 2011; Laha *et al.*, 2015; Zhu *et al.*, 2019). *In vitro*, the latter has been shown to hydrolyze 1-$InsP_7$,

and 5-$InsP_7$ to $InsP_6$ for Arabidopsis VIH2, and 1-$InsP_7$ and 1,5-$InsP_8$ to $InsP_6$ and 5-$InsP_7$, respectively, for the fission yeast PPIP5K homolog Asp1 and for yeast Vip1 (Wang *et al.*, 2015; Pascual-Ortiz *et al.*, 2018; Zhu *et al.*, 2019; Dollins *et al.*, 2020). At low adenylate energy charge, AtITPK1 can catalyze a reverse reaction, transferring the β-phosphate from 5-$InsP_7$ to ADP to generate $InsP_6$ and ATP, presumably as a quick and energy-saving mechanism to shut down phosphate starvation responses (Whitfield *et al.*, 2020; Riemer *et al.*, 2021). Recently, also specific inositol pyrophosphatases, namely the *Arabidopsis thaliana* Plant and Fungi Atypical Dual Specificity Phosphatases (PFA-DSP1-5), were identified in plants. Similarly to the activity of the budding yeast homologue Siw14 (Steidle *et al.*, 2016; Wang *et al.*, 2018), all five PFA-DSP isoforms displayed robust and highly specific pyrophosphatase activities towards the 5-β-phosphates of 5-$InsP_7$ and 1/3,5-$InsP_8$ (Gaugler *et al.*, 2022; Wang *et al.*, 2022). However, the enzymes involved in the hydrolysis of other $InsP_7$ isomers, such as 1-$InsP_7$ and/or 3-$InsP_7$, as well as 4-$InsP_7$ and/or 6-$InsP_7$, remain unknown in plants. The identification of the respective PP-InsP pyrophosphatases will therefore provide a helpful tool to identify the physiological roles of these messengers.

To this end, we took advantage of a non-hydrolysable $InsP_7$ analog, 5PCP-$InsP_5$ (Wu *et al.*, 2016), in which the oxygen of a phosphoanhydride bond is substituted by a carbon, to carry out affinity pull-down experiments and identified Arabidopsis NUDIX proteins as potential interactors of $InsP_7$. NUDIX is an acronym for 'NUcleoside DIphosphate linked to some other moiety X,' reflecting the diverse nucleoside diphosphate substrates targeted by NUDIX-type (NUDT) hydrolases. The budding yeast ScDdp1 (Safrany *et al.*, 1999; Lonetti *et al.*, 2011; Andreeva *et al.*, 2019) and the five human hsDIPP proteins (DIPP1, 2α, 2β, 3α and 3β) (Kilari *et al.*, 2013) are members of the NUDIX family and were shown to hydrolyze preferentially the β-phosphate of 1-$InsP_7$. We provide evidence that members of two different subclades of these phosphohydrolases display distinct and highly specific PP-InsP pyrophosphatase activities. Subclade I members NUDT4, NUDT17, NUDT18 and NUDT21 show a preference for the 4-pyrophosphate moiety and subclade II members NUDT12, NUDT13 and NUDT16 show a preference for the 3-pyrophosphate moiety of PP-InsPs. We demonstrate that subclade II members play a role in P_i and iron (Fe) homeostasis, regulate defense gene expression, and that the 3PP-position of PP-InsPs is a preferred substrate for conserved enzymatic activities unrelated to NUDTs.

Results

Pull-down of *Arabidopsis thaliana* NUDT hydrolases with a non-hydrolysable $InsP_7$ analog

In an attempt to identify potential PP-InsP interactors, we performed an affinity pull-down assay using 5PCP-$InsP_5$ beads, a reagent consisting of a non-hydrolysable $InsP_7$ analog coupled to a solid phase resin (Wu *et al.*, 2016; Furkert *et al.*, 2021), which were incubated with Arabidopsis shoot or root extracts. Bound proteins were eluted with a high molar excess of $InsP_6$, and both beads and eluates were trypsinized and resulting peptides analyzed separately for eluate and on-bead fractions by liquid chromatography–mass spectrometry (LC-MS/MS) to identify proteins interacting with $InsP_7$. The peptide analysis revealed known proteins involved in InsP/PP-InsP metabolism such as MIPS3 (Luo *et al.*, 2011), IPK2α and IPK2β (Stevenson-Paulik *et al.*, 2002; Xia *et al.*, 2003; Stevenson-Paulik *et al.*, 2005), ITPK3 (Sweetman *et al.*, 2007), VIH1, VIH2, $InsP_6$/PP-InsP-binding proteins such as the jasmonate co-receptor F-box protein COI1, various TIR1/COI1 homologs (AFB1, AFB2, AFB3), components of the TIR1/COI1-dependent SKP1-CUL1-F-box protein (SCF) ubiquitin E3 ligase complex (ASK1, ASK2, CUL1, CUL2), as well as the presumed $InsP_8$ binding protein SPX2 (Ried *et al.*, 2021) (Table III-S1). Besides these known $InsP_6$/PP-InsP binding proteins or enzymes involved in InsP/PP-InsP metabolism, peptides of five different NUDT hydrolases were identified in shoot and root extracts. Three of these, NUDT4, NUDT17 and NUDT21 were present in eluates or beads incubated with Arabidopsis shoot extracts, while two, NUDT16 and NUDT18, were detected in root extracts (Table III-S1). The identified NUDT hydrolases are closely related and can be grouped into a clade in the phylogenetic tree of the 29 Arabidopsis NUDT hydrolases, in which two additional members, namely NUDT12 and -13, are also included (Figure III-1A). The clade can be divided into two subclades, with NUDT4, -17, -18, and -21 designated as subclade I and NUDT12, -13, and -16 designated as subclade II. The physiological role of these hydrolases and their substrates *in planta* remain unknown. We therefore decided to investigate all seven NUDT hydrolases of the clade for their possible involvement in inositol pyrophosphate metabolism, including those that were not isolated with the affinity pull-down assay.

Heterologous expression of Arabidopsis subclade I and II NUDTs partially complement yeast *ddp1Δ* defects

Considering that NUDTs share homology with yeast Ddp1 and mammalian DIPP proteins, all of which display pyrophosphatase activity against 1-$InsP_7$, we investigated whether the heterologous expression of subclade I and II NUDTs rescues the metabolic defects of the yeast *ddp1Δ* mutant. This yeast mutant strongly accumulates 1-$InsP_7$ as compared to its isogenic wild-type (WT) strain (Lonetti *et al.*, 2011) (Figure III-1B, C). As revealed by SAX-HPLC analyses of extracts from [^{3}H]-*myo*-inositol-labeled yeast transformants, we observed that, with the exception of NUDT4 and NUDT18, expression of all subclade I and II NUDTs partially rescued the *ddp1Δ*-associated defects in $InsP_7$ degradation (Figure III-1B and C). Because plants likely possess at least one form of 4/6-$InsP_7$ and one form of 1/3-$InsP_7$, although the respective enantiomer identities remain unresolved, and since yeast lacks 4/6-$InsP_7$ and 3-$InsP_7$, we resorted to *in vitro* assays to further investigate the substrate specificities of subclade I and II NUDTs.

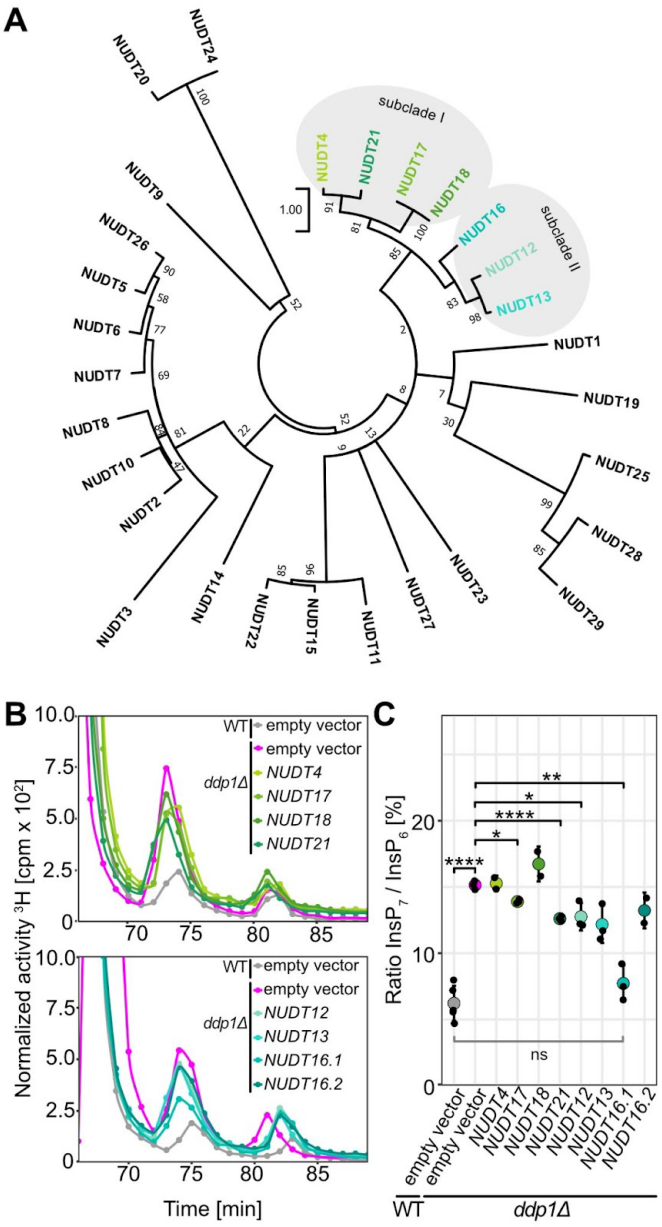

Figure III-1: Identified Arabidopsis NUDT hydrolases group in two subclades and heterologous expression partially complements *ddp1Δ*-associated defects in $InsP_7$ levels in yeast. Phylogenetic tree of 29 Arabidopsis NUDT hydrolases (A). The tree was created with MEGA11 and the Jones-Taylor-Thornton method with 500 bootstrap replications. Arabidopsis NUDT4, -17, -18, and -21 can be grouped as a subclade of the phylogenetic tree (subclade I). NUDT12, -13, and -16 can also be grouped as a subclade (subclade II) and together with subclade I as one clade in the phylogenetic tree. (B) SAX-HPLC profiles of radiolabeled *ddp1Δ* yeast transformed with either empty vector (pAG425GPD-*ccdB*), or pAG425GPD carrying the respective *NUDT* gene. Depicted are representative SAX-HPLC runs of one experiment. The experiment was repeated with similar results ($n = 3$ or 4, except for NUDT4, NUDT18, NUDT16.2, $n = 2$). Combined data are shown in (C). (C) Relative amounts of $InsP_7$ of WT and *ddp1Δ* yeast transformed with empty vector, and *ddp1Δ* transformed with pAG425GPD carrying the *NUDT* genes are shown as $InsP_7/InsP_6$ ratios. $InsP_6$ and $InsP_7$ levels were determined by SAX-HPLC analyses and data were processed with R. Data represents mean ± SD. Asterisks indicate values that are significantly different from *ddp1Δ* according to Student's *t* test ($P < 0.05$ (*); $P < 0.01$ (**); $P < 0.001$ (***); $P < 0.0001$ (****)).

In vitro biochemical analyses reveal distinct and highly specific PP-InsP pyrophosphatase activities for Arabidopsis subclade I and II NUDT proteins

We took advantage of chemically synthesized enantiomerically pure $InsP_7$ and $InsP_8$ isomers for thorough biochemical analyses (Capolicchio *et al.*, 2013; Capolicchio *et al.*, 2014). To this end, we generated recombinant NUDTs, N-terminally fused with a hexahistidine (His_6) maltose-binding protein (MBP) tag. A His-tag-MBP protein served as a negative control. *In vitro* reactions with $InsP_6$ or different $InsP_7$ isomers were performed in the presence of Mg^{2+}. By separating the reaction via PAGE, we observed nearly complete hydrolysis of 4-$InsP_7$ in presence of subclade I hydrolases (NUDT4, NUDT17, NUDT18 or NUDT21) (Figure III-2A). The hydrolysis product showed the same mobility as $InsP_6$ on PAGE (Figure III-2A), and CE-ESI-MS measurements of reactions spiked with [$^{13}C_6$] $InsP_6$ standards also confirmed that the product had the same migration time and mass as $InsP_6$ (Figure III-S3). Consequently, a significant increase of $InsP_6$ from 4-$InsP_7$ was observed in reactions with subclade I NUDT hydrolases compared to the negative control, as determined by CE-ESI-MS analyses (Figure III-2B). Notably, there was also a robust hydrolysis of 6-$InsP_7$ in the presence of NUDT18 (Figure III-2A and B) with minor activities of NUDT4 against 1-$InsP_7$ and of NUDT21 against 3-$InsP_7$ (Figure III-2A and B). In contrast, under these conditions, none of the subclade I NUDTs was able to hydrolyze $InsP_6$ or 5-$InsP_7$ *in vitro* (Figure III-2A, B and Figure III-S2).

We also tested whether subclade I NUDTs can catalyze the hydrolysis of 4-$InsP_7$ in the presence of alternative divalent cations, such as Ca^{2+}, Zn^{2+}, Mn^{2+} or in the absence of any divalent cations by using the metal chelator EDTA. In all reactions where Mg^{2+} was absent and either alternative cofactors or EDTA were present, no 4-$InsP_7$ hydrolysis was observed, revealing the critical role of Mg^{2+} as a cofactor for NUDT subclade I-dependent 4-$InsP_7$ hydrolysis (Figure III-2C).

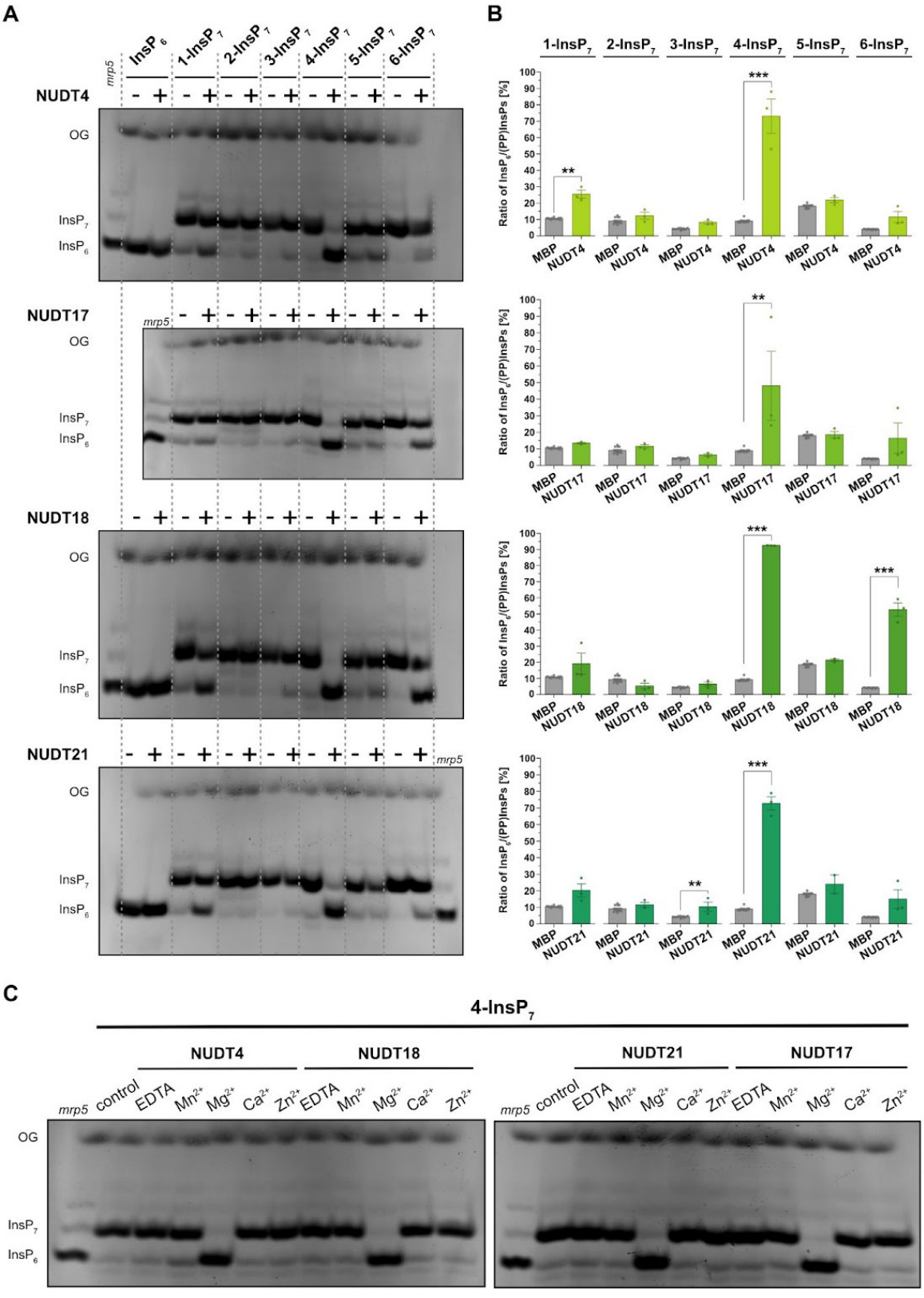

Figure III-2: Subclade I NUDTs display Mg^{2+}-dependent PP-InsP phosphatase activity with high specificity for 4-$InsP_7$ *in vitro*. Recombinant His_6-MBP-tagged NUDT4, NUDT17, NUDT18 or NUDT21 was incubated with 0.33 mM $InsP_7$ and (A and B) 1 mM $MgCl_2$ or (C) either 1 mM EDTA, $MnCl_2$, $MgCl_2$, $CaCl_2$, or $ZnCl_2$ at 28 °C (indicated with the plus symbol). His_8-MBP served as a negative control (indicated with the minus symbol). After 1 h, the reaction products were (A and C) separated by 33 % PAGE, and visualized by toluidine blue. A

TiO_2-purified Arabidopsis *mrp5* seed extract was used as a marker for $InsP_6$, $InsP_7$ and $InsP_8$. (B) For CE-ESI-MS analyses, samples were spiked with an isotopic standards mixture ([$^{13}C_6$] 1,5-$InsP_8$, [$^{13}C_6$] 5-$InsP_7$, [$^{13}C_6$] 1-$InsP_7$, [$^{13}C_6$] $InsP_6$, [$^{13}C_6$] 2-OH $InsP_5$). Data are presented as relative ratios of $InsP_6$ to all measured InsP/PP-InsPs and represent mean ± SEM ($n \geq 11$ for MBP and $n = 3$ for NUDT samples, with the exception of sample NUDT21 + 5-$InsP_7$, where only 2 samples were available due to CE-ESI-MS measurement issues). Representative extracted-ion electropherograms are shown in Figure III-S3. Asterisks indicate values that are significantly different determined by a Dunnett's test against MBP with Šidák correction k = 4 ($P \leq 0.05$ (*); $P \leq 0.01$ (**); $P \leq 0.001$ (***)). OG: orange G.

In contrast to subclade I NUDTs, the four hydrolases of subclade II (NUDT12, NUDT13, NUDT16.1 and NUDT16.2) displayed a strong preference for 3-$InsP_7$, with the reaction product showing the same mobility as $InsP_6$ by PAGE analysis (Figure III-3A), which was confirmed by CE-ESI-MS analysis (Figure III-3B). However, the *in vitro* activity of NUDT16.2 was comparatively low (Figure III-S4), requiring a 26-fold higher protein concentration than NUDT16.1 to achieve a similar activity level. Activities against other PP-InsPs were minor or not observed, as confirmed by CE-ESI-MS analyses. Specifically, NUDT12 showed minor pyrophosphatase activity against all PP-InsPs except 5-$InsP_7$. NUDT13 and NUDT16.1 showed minor pyrophosphatase activity against 1-$InsP_7$, 4-$InsP_7$ and 6-$InsP_7$, while NUDT16.2 showed minor activities against 1-$InsP_7$ and 6-$InsP_7$ (Figure III-3A and B). Similarly, to subclade I NUDTs, all subclade II NUDTs required Mg^{2+} as a cofactor to hydrolyze 3-$InsP_7$ to $InsP_6$, and no *in vitro* activity was observed in presence of other divalent cofactors, such as Ca^{2+}, Zn^{2+} and Mn^{2+} or in absence of any divalent cation (EDTA) (Figure III-3C).

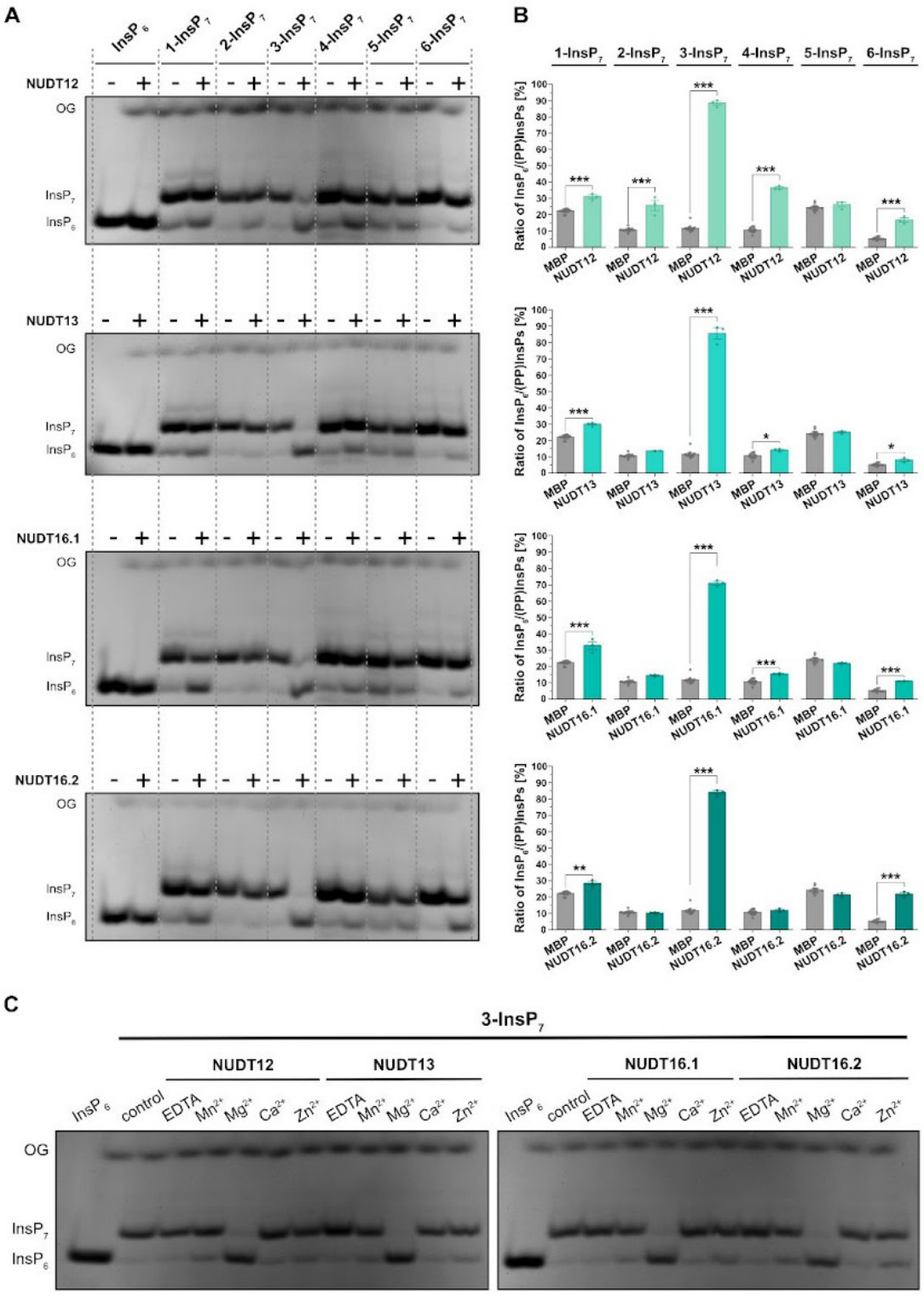

Figure III-3: Subclade II NUDTs display Mg^{2+}-dependent PP-InsP phosphatase activity with high specificity for 3-$InsP_7$ *in vitro.* Recombinant His_6-MBP-tagged NUDT12, NUDT13, NUDT16.1 or NUDT16.2 was incubated with 0.33 mM $InsP_7$ and (A and B) 1 mM $MgCl_2$ or (C) either 1 mM EDTA, $MnCl_2$, $MgCl_2$, $CaCl_2$, or $ZnCl_2$ at 28 °C (indicated with the plus symbol). His_8-MBP served as a negative control (indicated with the minus symbol). After 1 h, the reaction products were (A and C) separated by 33 % PAGE and visualized by toluidine blue or (B) spiked with isotopic standards mixture ([$^{13}C_6$] 1,5-$InsP_8$, [$^{13}C_6$] 5-$InsP_7$, [$^{13}C_6$] 1-$InsP_7$, [$^{13}C_6$] $InsP_6$, [$^{13}C_6$] 2-OH $InsP_5$) for CE-ESI-MS analyses. Data represent mean ± SEM (n = 12 for MBP and n = 3 for

NUDT samples). Representative extracted-ion electropherograms are shown in Figure III-S5. Asterisks indicate values that are significantly different determined by a Dunnett's test against MBP with Šidák correction k = 4 ($P \leq 0.05$ (*); $P \leq 0.01$ (**); $P \leq 0.001$ (***)). OG: orange G. Note that NUDT16.2 had a 16-times higher concentration (16 μM) than NUDT16.1 (0.6 μM).

Subclade II NUDT hydrolases display β-phosphate specificity also with 1,5-InsP$_8$ and 3,5-InsP$_8$, *in vitro*

We then tested whether subclade I and II NUDTs can also hydrolyze the enantiomers of InsP$_8$ 1,5-InsP$_8$ and 3,5-InsP$_8$ in the presence of Mg^{2+}. Subclade I NUDTs, which specifically hydrolyze the 4-β-phosphate of InsP$_7$, showed only weak or no hydrolysis of both InsP$_8$ isomers *in vitro* (Figure III-4A and B). Only NUDT4 and NUDT21 displayed minor hydrolytic activities against 1,5-InsP$_8$ (Figure III-4A) or, in the case of NUDT4, against 3,5-InsP$_8$ (Figure III-4B). In contrast, subclade II hydrolases NUDT12, NUDT13 and NUDT16 displayed robust hydrolytic activities against the 3-β-phosphate of 3,5-InsP$_8$ (Figure III-4D). This activity was enantiomer-specific for NUDT12 and NUDT13, while (the two splice forms of) NUDT16 also hydrolyzed 1,5-InsP$_8$ to 5-InsP$_7$ to some extent (Figure III-4C).

At high protein concentrations, NUDT hydrolases lose some of their substrate specificity

We next investigated whether increasing protein concentration and doubling the incubation time of our *in vitro* assays would result in a loss of substrate specificity. When carrying out the reactions at these altered conditions, substrate specificities remained largely as described above (Figure III-S4 and Figure III-S8). However, we observed additional hydrolytic activities. For instance, all subclade I NUDTs showed partial pyrophosphatase activities against 5-InsP$_7$, as well as 1,5- and 3,5-InsP$_8$ (Figure III-S8).

Likewise, subclade II NUDT12, NUDT13 and NUDT16.1 did not only display robust activities against 3-InsP$_7$ and minor activities against InsP$_7$ isomers carrying the PP-bond at positions 1, 2, 4 and 6, respectively, but also displayed a minor 5-InsP$_7$ pyrophosphatase activity (Figure III-S4). In these assays, we also included the more distantly related NUDT7, previously shown to harbor ADP-ribose/NADH phosphohydrolase activity (Ogawa *et al.*, 2005). Even at a high protein concentration (~7 μM), no PP-InsP hydrolytic activity was observed for NUDT7 (Figure III-S4).

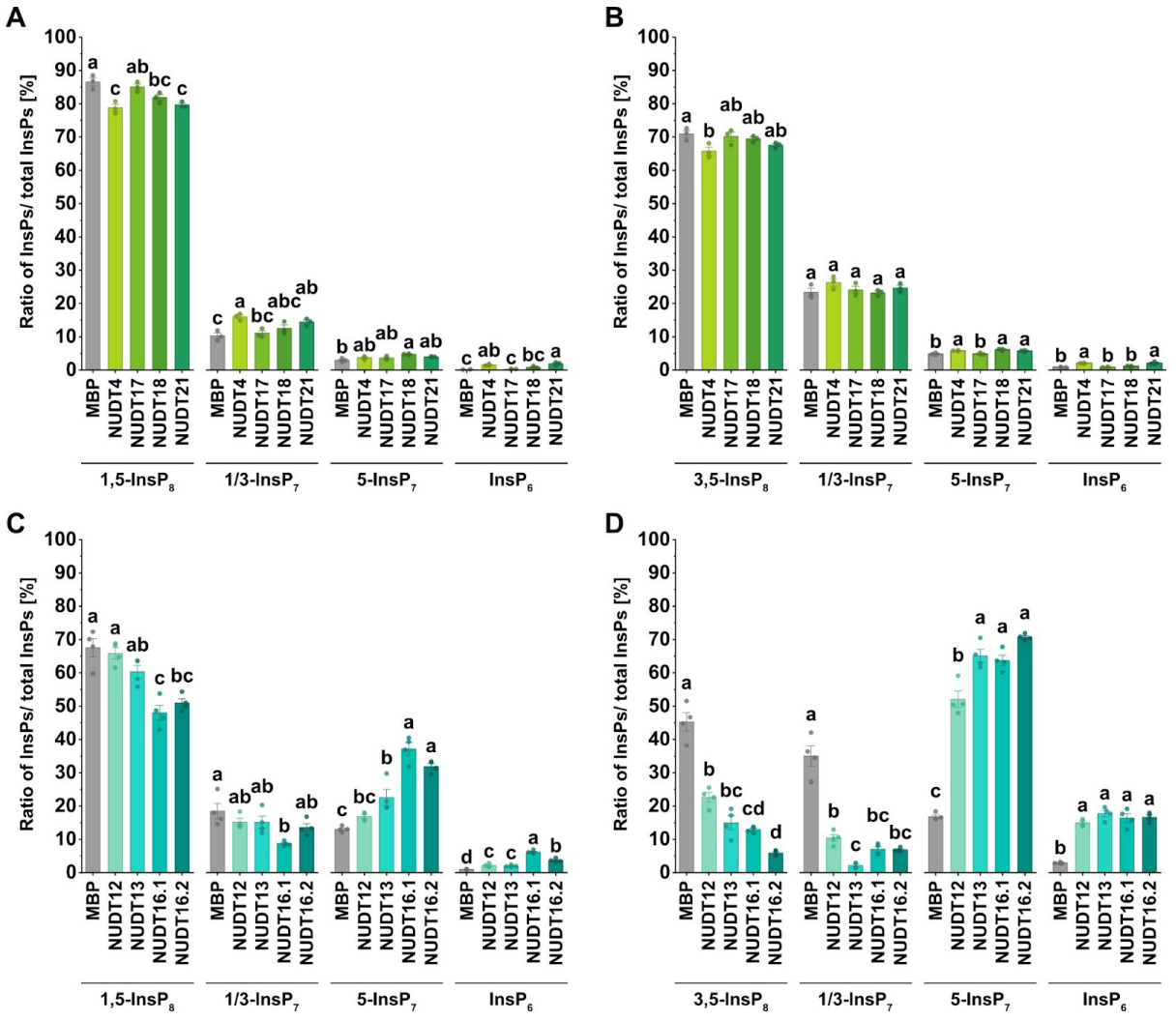

Figure III-4: Arabidopsis NUDT hydrolases display differential hydrolytic activities against 1,5-$InsP_8$ and 3,5-$InsP_8$ *in vitro*. Recombinant His_6-MBP-tagged (A and B) NUDT4, NUDT17, NUDT18, NUDT21, (C and D) NUDT12, NUDT13, NUDT16.1 or NUDT16.2 protein was incubated with 0.33 mM (A and C) 1,5-$InsP_8$ or (B and D) 3,5-$InsP_8$ and 1 mM $MgCl_2$ at 28 °C. His_8-MBP served as a negative control. After 1 h, the reaction products were spiked with isotopic standards mixture ([$^{13}C_6$] 1,5-$InsP_8$, [$^{13}C_6$] 5-$InsP_7$, [$^{13}C_6$] 1-$InsP_7$, [$^{13}C_6$] $InsP_6$, [$^{13}C_6$] 2-OH $InsP_5$) and subjected to CE-ESI-MS analyses. Data represent mean ± SEM with (A and B) $n = 3$ and (C and D) $n = 4$. Representative extracted-ion electropherograms are shown in Figure III-S6 and Figure III-S7. Different letters indicate values that are significantly different determined with one-way ANOVA followed by Dunn-Šidák test with a significance level of 0.05. The peak area of 1/2/3-$InsP_7$ and of 4/5/6-$InsP_7$ was not further resolved but, since 1,5-$InsP_8$ and 3,5-$InsP_8$ isomers were used in that reaction, we conclude that the 1/2/3-$InsP_7$ peak area represents 1/3-$InsP_7$ and the 4/5/6-$InsP_7$ peak area represents 5-$InsP_7$, respectively.

Higher order mutants of subclade II NUDTs display an increase in 1/3-$InsP_7$ and 5-$InsP_7$

To investigate the physiological role of subclade I and II NUDT hydrolases *in planta*, we established single and higher order loss-of-function mutants in *Arabidopsis thaliana.* The single

T-DNA insertion lines *nudt17-1* and *nudt18-1*, as well as two independent T-DNA insertion lines of *nudt4* (*nudt4-1* and *nudt4-2*) and *nudt21* (*nudt21-1* and *nudt21-2*) showed no significant difference in the PP-InsP levels in comparison to the WT when grown hydroponically under optimal P conditions (Figure III-S9). We also generated a double mutant *nudt21-1 nudt4-1*, but also in this case we did not observe a significant effect on PP-InsP levels (Figure III-S9).

In order to overcome a possible functional redundancy of NUDT hydrolases, we generated higher order mutants by targeting *NUDT4*, *NUDT17*, *NUDT18* and *NUDT21*, or *NUDT12*, *NUDT13* and *NUDT16* at two different positions via CRISPR/Cas9. Each guideRNA (gRNA) was designed to target the gene at the beginning of the coding region, and upstream or within the conserved 23 amino acid region typical for NUDT hydrolases (Figure III-S10A and Figure III-S11A). The resulting higher order mutants *nudt4/17/18/21* and *nudt12/13/16* harbor mutations in all four and three targeted NUDT hydrolases, respectively (Figure III-S10B and Figure III-S11B). As depicted in Figure III-S10C, the resulting mutations in *nudt4/17/18/21* lead to a frameshift in all targeted open reading frames, except for line 1, where an in-frame deletion resulted in a truncated NUDT21 lacking residues 32-74. Most of the frameshifts were caused by a single base pair mutation or larger deletions (Figure III-S10C). The mutations in the triple mutant *nudt12/13/16* lead to a frameshift and premature stop codon in NUDT13 and NUDT16 or, in the case of NUDT12, the start codon is already mutated (Figure III-S11C). None of the higher order subclade I or II *nudt* lines displayed any obvious developmental phenotype under standard growth conditions (Figure III-5A). We first carried out SAX-HPLC analyses of cell extracts from [^{3}H]-*myo*-inositol-labeled WT and the higher order mutants, *nudt4/17/18/21* and *nudt12/13/16*, respectively. For *nudt4/17/18/21* (line 2) plants, we did not observe any significant differences in any InsP or PP-InsP species (Figure III-5B). In contrast, *nudt12/13/16* plants displayed a significant increase in $InsP_7$ (Figure III-5C). Because SAX-HPLC analyses cannot resolve between different $InsP_7$ isomers and rely on plants grown under sterile conditions, we employed CE-ESI-MS analyses of Nb_2O_5-purified InsPs from plants grown on a P-sufficient peat-based substrate. Under our standard growth conditions, we did not observe changes in any inositol pyrophosphate species that would be consistent in all three independent subclade I *nudt4/17/18/21* lines (Figure III-5D, left panel). In contrast, subclade II *nudt12/13/16* lines showed a robust ~2.5-fold increase in 1/3-$InsP_7$ (Figure III-5D, right panel), indicating that the *in vitro* hydrolytic activity against the 1/3-PP bond is of physiological relevance *in planta*. Additionally, we observed an ~1.5-fold increase in 5-$InsP_7$ and a minor but significant reduction in $InsP_6$ (Figure III-5D, right panel).

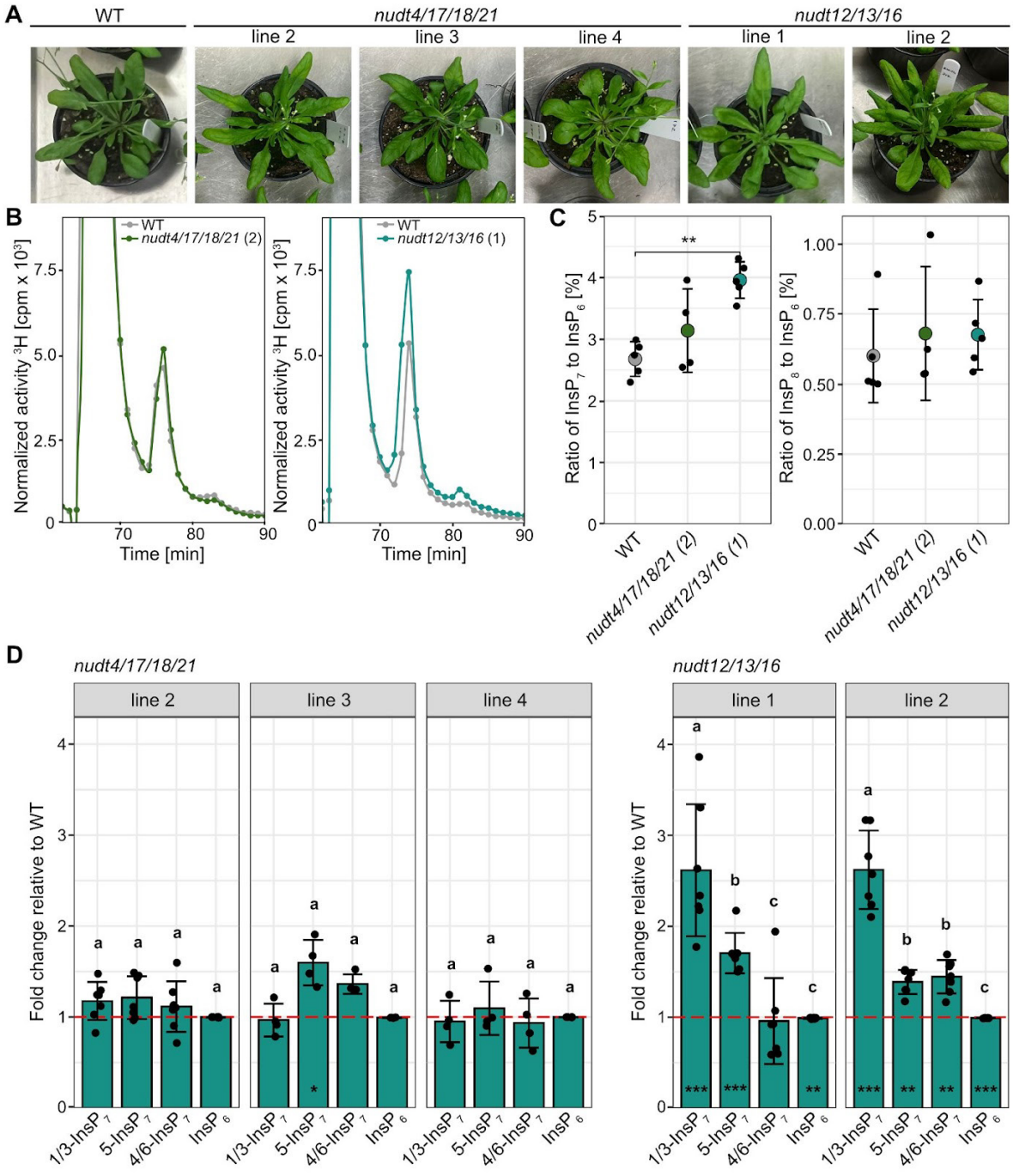

Figure III-5: Higher order subclade II *nudt* mutant lines display increased 1/3-$InsP_7$ and 5-$InsP_7$ levels. (A) Photographs of 5-6-weeks old WT and independent higher order subclade I and subclade II *nudt* mutant lines grown on peat-based substrate. (B) SAX-HPLC profiles of 2- weeks old WT and subclade I and subclade II *nudt* mutant lines. Lines were grown in liquid ½ MS medium supplemented with sucrose. Labeling with [^{3}H]-*myo*-inositol was done for 5 days. Depicted are representative SAX-HPLC runs of one line for each subclade. The experiment was repeated with similar results (n = 4 or 5). Combined data are shown in (C). (C) Relative amounts of $InsP_7$ and $InsP_8$ of WT, subclade I and subclade II NUDT mutant lines are shown as $InsP_7$/$InsP_6$ or $InsP_8$/$InsP_6$ ratios. $InsP_6$, $InsP_7$ and $InsP_8$ levels were determined by SAX-HPLC analyses and data were processed with R. Asterisks indicate significantly different $InsP_7$/$InsP_6$ or $InsP_8$/$InsP_6$ ratios compared to WT determined with Wilcoxon test for unpaired samples ($P \leq 0.01$ (**)). (D) Fold changes of various $InsP_7$ isomers and $InsP_6$ to total

quantified InsPs in subclade I and subclade II NUDT mutant lines relative to WT as indicated. In this experiment, plants were grown on ½ MS agar plates supplemented with sucrose for 2 weeks. Asterisks indicate fold-changes to WT that are significantly different from 1 based on a Wilcoxon test for unpaired samples ($P \leq 0.05$ (*); $P \leq 0.01$ (**); $P \leq 0.001$ (***)). Compact letters display is based on a pairwise Wilcoxon test for paired samples. Fold changes of different InsPs sharing the same letter are not significantly different at $\alpha = 0.05$. The very low abundant $InsP_8$ was below or close to the detection limit in some plants and was therefore excluded from the analysis.

Transient expression of subclade I NUDT hydrolases in *Nicotiana benthamiana* reveals PP-InsP pyrophosphatase activity and regulation of phosphate starvation responses *in vivo*

Since the *nudt4/17/18/21* lines did not show significant differences in inositol pyrophosphates, possibly due to redundancy with other enzymatic activities, we investigated the potential PP-InsP pyrophosphatase activity of NUDTs by heterologous transient expression in *N. benthamiana* leaves. To this end, we generated constructs encoding translational fusions of NUDTs from both subclades with a C-terminal 4xMyc epitope tag, driven by the strong viral CaMV 35S promoter. In agreement with our *in vitro* data (Figure III-2), ectopic expression of *NUDT17*, *-18*, and *-21* significantly reduced 4/6-$InsP_7$ in *N. benthamiana* leaves, as revealed by CE-ESI-MS analyses (Figure III-6A). In addition, expression of all subclade I *NUDTs* also resulted in reduced 5-$InsP_7$ levels, which is consistent with our findings that *in vitro*, all subclade I NUDTs also act as 5-$InsP_7$ pyrophosphatases at increased protein concentration (Figure III-6B and Figure III-S8). Similarly, expression of subclade II *NUDTs*, with the exception of *NUDT13*, led to reduced levels of 4/6-$InsP_7$ and 5-$InsP_7$ in *N. benthamiana* (Figure III-6A, B). Quantification of $InsP_8$ and 1/3-$InsP_7$ species was not possible in samples from this transient expression system as concentrations were close to or below the detection limit of CE-ESI-MS measurements.

Experimental data extracted from the ePlant browser platform indicate that *NUDT21* and *NUDT17* are induced locally and transiently by wounding (Kilian *et al.*, 2007). Because of the role of 5-$InsP_7$ in PSR, we investigated whether transient expression of subclade I and II NUDTs could also induce local PSR. To this end, we co-expressed a *RUBY* reporter (He *et al.*, 2020) under transcriptional control of a *Solanum lycopersicum SPX2* promoter fragment with NUDT hydrolases in *N. benthamiana* leaves (Figure III-6C). Heterologous expression of Arabidopsis *PFA-DSP1*, which encodes a *bona fide* 5PP-InsP pyrophosphatase hydrolysing the

5-β-phosphate of 5-$InsP_7$, as well as 1,5-$InsP_8$ and 3,5-$InsP_8$ (Gaugler *et al.*, 2022), served as a positive control (Figure III-6D).

The induction of the PSR was dependent on the catalytic activity of PFA-DSP1 since the construct encoding the catalytically inactive variant, PFA-DSP1^{C150S} (Gaugler *et al.*, 2022), failed to induce PSR (Figure III-6D). Notably, heterologous expression of all subclade I *NUDTs* caused robust red staining reporting local activation of PSR (Figure III-6D). Likewise, expression of *NUDT12* and the active splice variant 1 of *NUDT16* also resulted in red staining, albeit generally at lower intensity (Figure III-6D). In contrast, expression of *NUDT13* or the less active splice variant 2 of *NUDT16* failed to activate PSR as compared to the empty vector or PFA-DSP1^{C150S} negative controls (Figure III-6D).

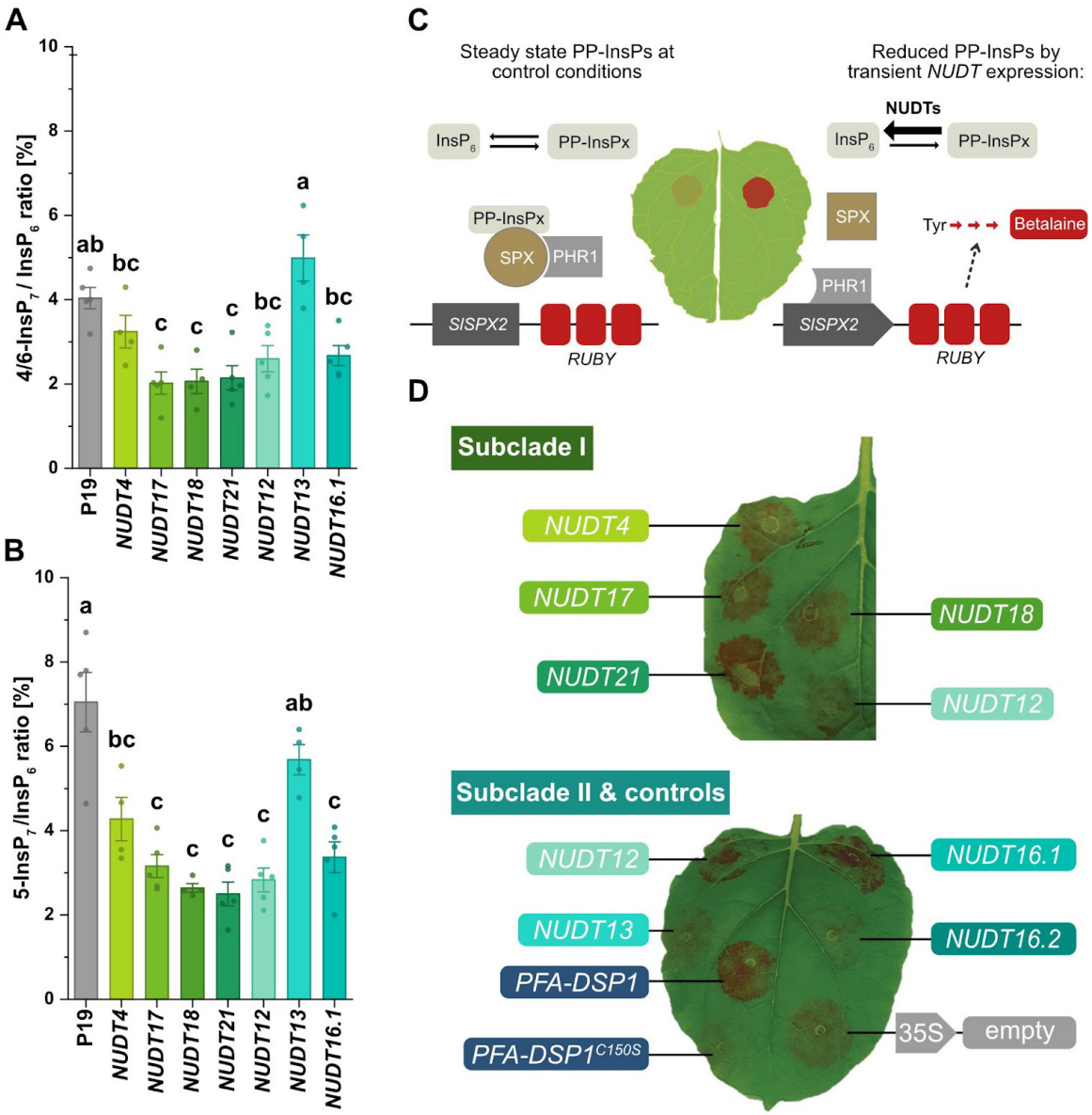

Figure III-6: Transient expression of NUDTs in *N. benthamiana* reveals PP-InsP activity and regulation of phosphate starvation responses. (A and B) Heterologous expression of subclade I and II NUDTs results in 4/6-PP-InsP$_7$ and 5-PP-InsP$_7$ turnover *in planta* and induces local PSR. The silencing inhibitor *P19* alone or together with NUDT*s* were transiently expressed in 6-weeks old *N. benthamiana* leaves. 2-3 days post infiltration (dpi) (PP-)InsPs were purified with Nb_2O_5 beads, spiked with isotopic standards mixture ([$^{13}C_6$] 1,5-InsP$_8$, [$^{13}C_6$] 5-InsP$_7$, [$^{18}O_2$] 4-InsP$_7$, [$^{13}C_6$] 1-InsP$_7$, [$^{13}C_6$] InsP$_6$, [$^{13}C_6$] 2-OH InsP$_5$) and subjected to CE-ESI-MS analyses. Data represent mean ± SEM ($n \geq 4$). Different letters indicate values that are significantly different determined with one-way ANOVA followed by Dunn-Šidák test with a significance level of 0.05. Representative extracted-ion electropherograms are shown in Figure III-S12. (C) Schematic representation of PSR reporter assay in *N. benthamiana* leaves, in which a reduced PP-InsP concentration enables PHR1 to bind a P1BS binding site in the *SlSPX2* promoter (Solyc12g009480; LOC101257836) driving the expression (dotted arrow) of a *RUBY* reporter cassette (encoding three different proteins CYP76AD1, DODA and a glycosyltransferase) that catalyze the stepwise synthesis (red arrows) of a red betalain pigment. (D) Transient co-expression of the *RUBY* reporter with subclade I or subclade II *NUDT* hydrolase genes under the transcriptional control of the viral CaMV

35S promoter. Co-expression with *PFA-DSP1* served as a positive control while co-expression with *PFA-DSP1*^{C150S} encoding the catalytic inactive protein or an empty vector served as negative controls. The picture was taken 2 dpi (upper leaf) or 3 dpi (bottom leaf). Note that subclade I *NUDT12* was expressed in both leaves for comparison. Three independent replicates are shown in Figure III-S13.

Subclade II NUDTs are involved in P- and Fe-homeostasis

We then investigated the consequences of increased 1/3-InsP$_7$ and 5-InsP$_7$ in *nudt12/13/16* lines. Under standard growth conditions, none of the higher order subclade I or II *nudt* lines displayed any obvious developmental phenotype (Figure III-5A). Since 5-InsP$_7$ has been shown to bind and activate SPX domains (Wild *et al.*, 2016) and is suggested to partially compensate for the loss of InsP$_8$ in suppressing PSR in Arabidopsis (Riemer *et al.*, 2021), we performed a mineral element analysis of WT and two independent *nudt12/13/16* lines grown under P$_i$-sufficient conditions on a peat-based substrate. In agreement with a role of 5-InsP$_7$ in suppressing PSR, we indeed observed decreased shoot P accumulation in both lines, as determined by ICP-OES analysis (Figure III-7A). No consistent changes (i.e., changes in both independent lines) were observed for other macronutrients (Figure III-7A). However, among the micronutrients, shoot iron (Fe) concentration was decreased by 53 % in *nudt12/13/16* plants (Figure III-7B). To raise further evidence for the role of subclade II NUDTs in PSR regulation, we checked whether they are transcriptionally responsive to the plant's P status. For this purpose, we grew plants in hydroponic culture and subjected them to sufficient or deficient P$_i$ conditions, or deficient P$_i$ followed by P$_i$ resupply, as reported previously (Riemer *et al.*, 2021). Notably, transcripts of all subclade II NUDTs increased under P$_i$-deficient conditions in shoots (Figure III-7C). Additionally, elevated levels of *NUDT13* and *NUDT16* transcripts were also observed in roots of Arabidopsis WT plants grown under P$_i$-deficient conditions (Figure III-7C). When P$_i$-deficient plants were resupplied with P$_i$ for 12 hours, the expression levels of all *NUDTs* were comparable or even below the levels observed in plants grown under sufficient P$_i$ (Figure III-7C).

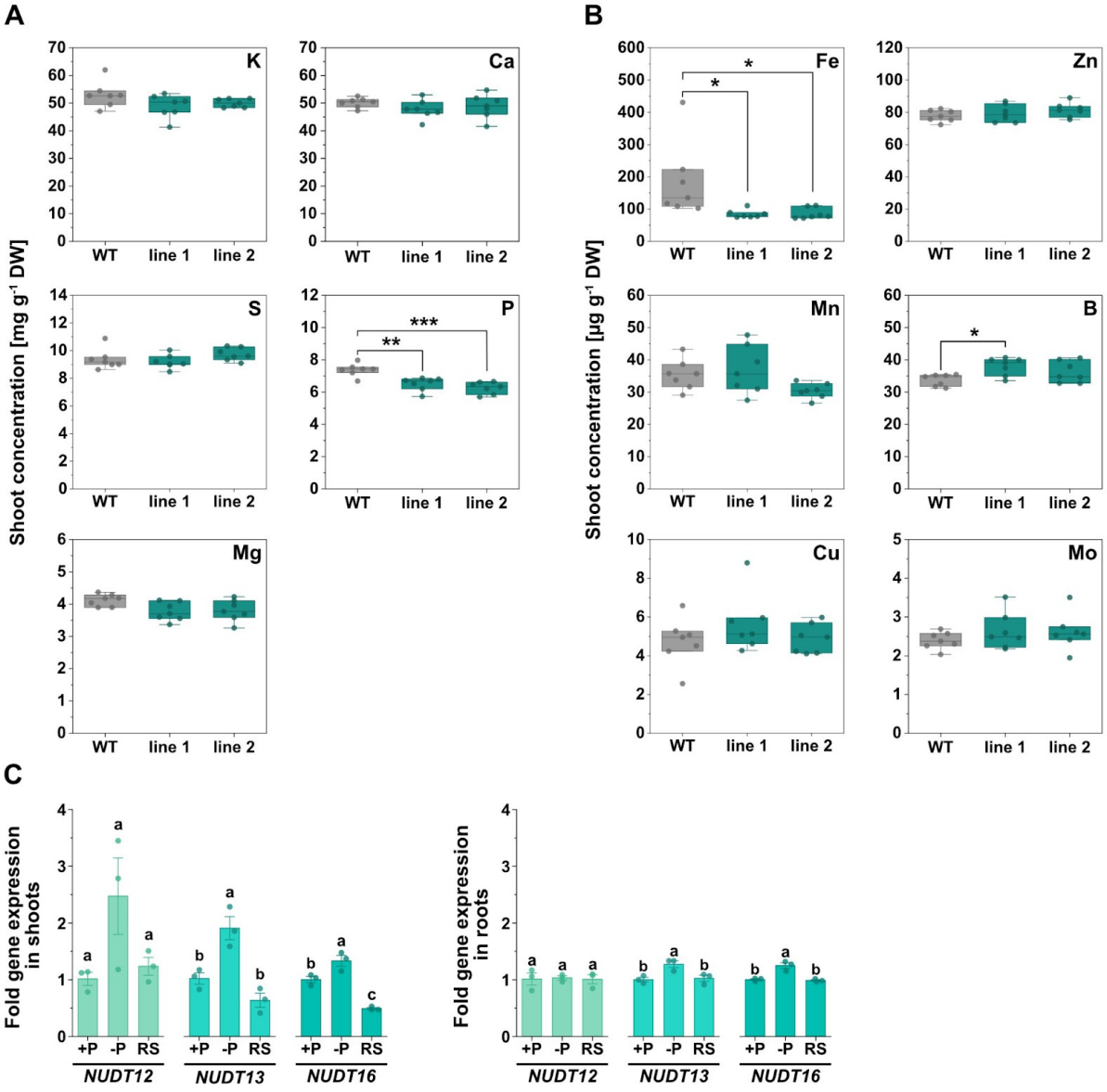

Figure III-7: Subclade II NUDTs are involved in P and Fe homeostasis and are upregulated by P-deficiency. (A and B) Shoot concentration of the indicated mineral (A) macronutrients and (B) micronutrients. Each line is represented by seven biological replicates (n = 7). Asterisks indicate values that are significantly different determined with one-way ANOVA followed by Dunn-Šidák test ($P \leq 0.05$ (*); $P \leq 0.01$ (**); $P \leq 0.001$ (***)). Plants were grown for 4-5 weeks on a peat-based substrate. (C) Arabidopsis WT plants were grown under sufficient P (indicated with +P), under deficient conditions (indicated with -P) or grown under deficient conditions and resupplied with P_i for 12 h (indicated with RS). Gene expression of *NUDT12*, *NUDT13* and *NUDT16* represent means ± SEM (n = 3). Different letters indicate values that are significantly different determined with one-way ANOVA followed by Dunn-Šidák test with a significance level of 0.05.

Transcriptome analyses suggests subclade II NUDT-dependent PP-InsPs act primarily as negative regulators of gene expression and also modulate PSR-independent functions

To gain more insights into subclade II NUDTs and, thus, potentially 1/3-InsP$_7$-related processes, we conducted RNA-seq experiments using shoots of two *nudt12/13/16* triple mutants and the corresponding WT, grown on P$_i$-sufficient peat-based substrate. We identified 256 differentially expressed genes (DEGs) common to both mutant lines, compared to WT plants (Figure III-8). Of these, the majority represent downregulated genes (206), while 50 genes were upregulated. We observed a number of PSR-related genes, the purple acid phosphatase *PAP1*, *ATL80* and *ZAT6*, all of which were downregulated (Table III-S2 and Table III-S3). In addition, we observed a number of Fe-related genes to be differentially regulated (Table III-S3 and Table III-S4). PSR genes only represented a minor subset of DEGs in *nudt12/13/16* triple mutants. Gene Ontology (GO) enrichment analysis revealed an overrepresentation of terms related to defense and associated processes, such as reactive oxygen species (ROS), wounding, systemic acquired resistance, and responses to chitin and insects, in both independent lines (Figure III-9 and Figure III-S14). Additionally, transcripts encoding proteins involved in responses to hypoxia, oxidative stress, ozone, and anaerobic respiration—terms also associated with ROS—were similarly enriched (Figure III-9 and Figure III-S14).

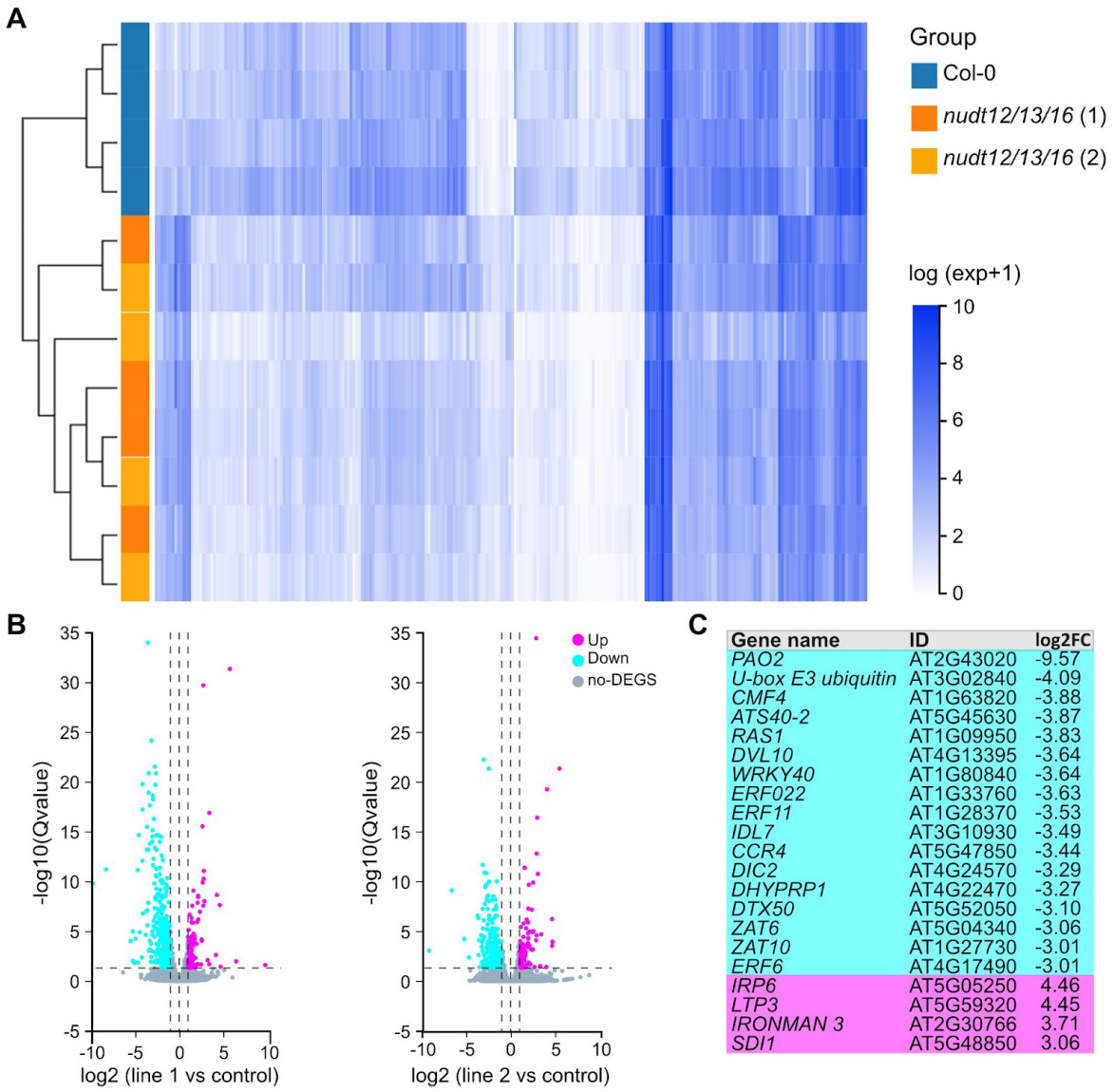

Gene name	ID	log2FC
PAO2	AT2G43020	-9.57
U-box E3 ubiquitin	AT3G02840	-4.09
CMF4	AT1G63820	-3.88
ATS40-2	AT5G45630	-3.87
RAS1	AT1G09950	-3.83
DVL10	AT4G13395	-3.64
WRKY40	AT1G80840	-3.64
ERF022	AT1G33760	-3.63
ERF11	AT1G28370	-3.53
IDL7	AT3G10930	-3.49
CCR4	AT5G47850	-3.44
DIC2	AT4G24570	-3.29
DHYPRP1	AT4G22470	-3.27
DTX50	AT5G52050	-3.10
ZAT6	AT5G04340	-3.06
ZAT10	AT1G27730	-3.01
ERF6	AT4G17490	-3.01
IRP6	AT5G05250	4.46
LTP3	AT5G59320	4.45
IRONMAN 3	AT2G30766	3.71
SDI1	AT5G48850	3.06

Figure III-8: Shoot transcriptome analyses of *nudt12/13/16* triple mutants suggest subclade II NUDT-dependent PP-InsPs act primarily as negative regulators of gene expression. (A) Clustered Heatmap of differentially expressed genes (DEGs) filtered by Q < 0.05 and log2 fold change (|log2FC| > 1). The horizontal axis represents the log2 (expression value + 1) for the samples based on TPM (Transcripts per million) expression value, while the vertical axis represents genes. In the default color scheme, dark blue indicates higher expression levels and white indicates lower expression levels. Mutant lines are represented in orange and light orange, and are clustered together, while the control is depicted in blue. Each line is represented by four biological replicates (n = 4). (B) Volcano plot comparing triple mutant line 1 and 2 to WT. The X-axis represents the log2FC values, and the Y-axis shows -log10-transformed significance values. Magenta dots indicate upregulated DEGs, cyan dots indicate downregulated DEGs, and gray dots indicate non-DEGs. (C) The table displays genes that showed strongest differential expression (|log2FC| > 3) of only downregulated and upregulated genes with known annotations. A complete list with all genes in this category of strongest differential expression is shown in Table III-S3. All plants used in these analyses, including wildtype controls, were grown on a peat-based substrate for 2-3 weeks.

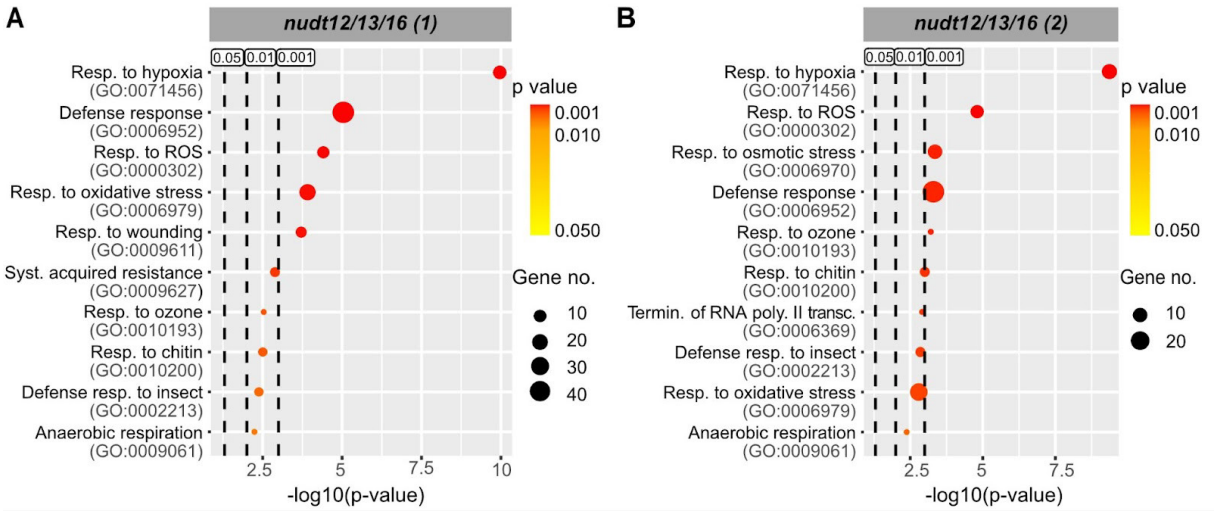

Figure III-9: Gene Ontology (GO) enrichment analysis suggests subclade II NUDT-dependent PP-InsPs regulate PSR-unrelated processes with numerous genes involved in plant defense and related GO terms. Shown is a GO enrichment analysis of DEGs with Q < 0.05 and (|log2FC| > 1), based on Biological Processes (BP) for *nudt12/13/16* triple mutant lines 1 and 2. The X-axis represents the statistical significance of these GO terms in -log10 (p-value), while the Y-axis lists the GO terms with their respective ID. Bubble size indicates the number of DEGs annotated to each GO term, and the graph highlights three significance thresholds: 0.05, 0.01, and 0.001. The color of the bubbles corresponds to the p-value, with red indicating more significant enrichment (Resp.: response, ROS: reactive oxygen species, syst.: systematic, termin.: termination, poly.: polymerase, transc.: transcription).

The 3PP- position of PP-InsPs is also vulnerable to enzymatic activities unrelated to subclade II NUDTs

Because RNA-seq data of *nudt12/13/16* lines indicated misregulation of gene expression unrelated to PSR, we speculated whether increased PP-InsPs other than 5-InsP$_7$ might be responsible for these transcriptional phenotypes and could be substrates of known enzymes involved in PP-InsP metabolism. Recent work by Whitfield and colleagues (2024) demonstrated that both potato and Arabidopsis ITPK1 can phosphorylate 1-InsP$_7$ and 3-InsP$_7$ to 1,5 InsP$_8$ and 3,5-InsP$_8$, respectively. To address this intriguing activity of ITPK1 further, we tested all six synthetic InsP$_7$ isomers and, in agreement with these findings, observed a robust phosphorylation of 3-InsP$_7$, presumably resulting in the generation of 3,5-InsP$_8$ (Figure III-10A). Besides, we detected a minor activity with 1-InsP$_7$ and no detectable activity against any other InsP$_7$ isomer, suggesting a highly specific 3-InsP$_7$ kinase activity of ITPK1 (Figure III-10A). Likewise, human ITPK1, for which we had previously identified InsP$_6$ kinase activity (Laha *et al.*, 2019), also phosphorylated 3-InsP$_7$, suggesting a high degree of evolutionary

conservation of this activity (Figure III-10B). We also investigated whether ITPK1 catalyzes a 3,5-$InsP_8$/ADP phosphotransferase activity leading to the production of ATP and 3-$InsP_7$, as reported earlier by Whitfield and colleagues (2024). Notably, we observed a robust generation of $InsP_7$ (presumably 3-$InsP_7$) when incubating 3,5-$InsP_8$ and ADP in presence of human ITPK1. While we did not observe significant 3,5-$InsP_8$/ADP phosphotransferase activity of Arabidopsis ITPK1 under our experimental conditions, we detected phosphotransferase activity of the recombinant Arabidopsis VIH2 kinase domain, presumably resulting in the generation of ATP and 5-$InsP_7$ (Figure III-10B). In summary, our findings and those by Whitfield and colleagues (2024) suggest that 3PP-InsP species represent preferred products and substrates of various plant enzymes and that some of their activities appear to be evolutionarily conserved.

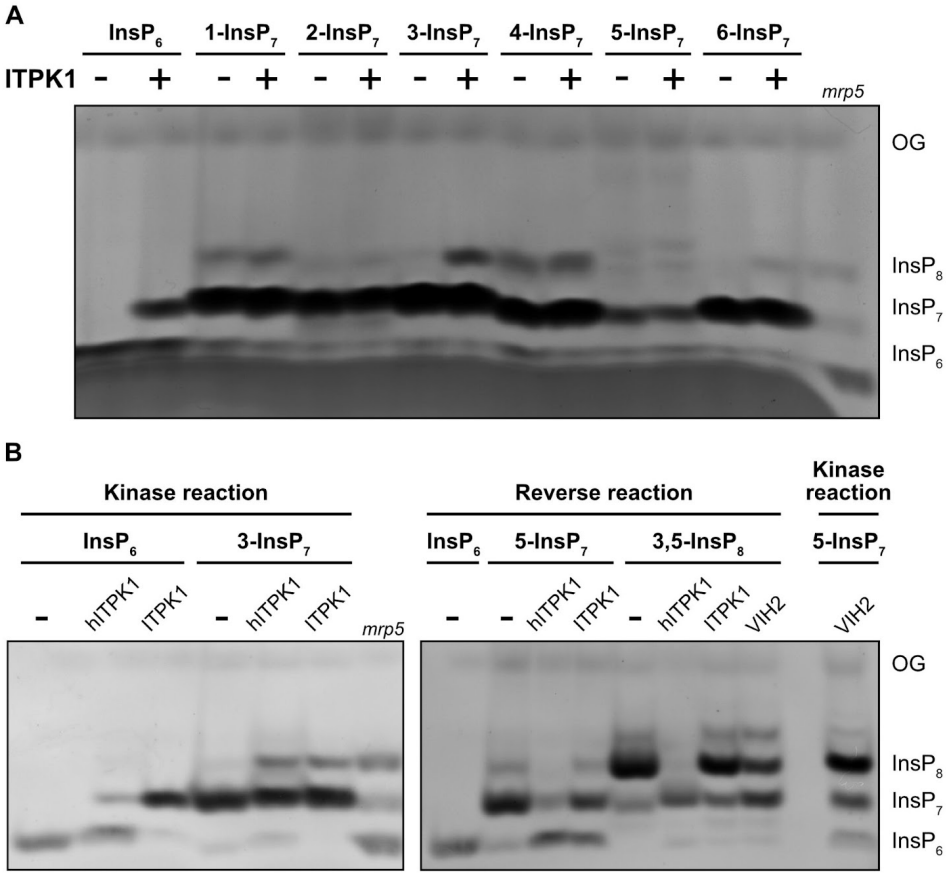

Figure III-10: 3PP-InsP species are preferred substrates for evolutionary conserved kinase and ADP phosphotransfer reactions. (A) Kinase assay with recombinant His_8-MBP-ITPK1 and $InsP_6$ or $InsP_7$ species as indicated. (B) Kinase assay (kinase reaction) and PP-InsP/ADP phosphotransfer assay (reverse reaction) with recombinant His_8-MBP-ITPK1, His_8-MBP-VIH2 and His_8-MBP-hsITPK1 and 1 mM of the indicated (PP)-InsP species. (A, B) After 6 h at 25°C, the reaction products were separated by 33 % PAGE, and visualized by toluidine blue staining. His_8-MBP served as a negative control (indicated with the minus symbol). KD: kinase domain, OG: orange G.

NUDT effectors of pathogenic ascomycete fungi display a substrate specificity reminiscent of subclade I NUDTs

Because the RNA-seq data of *nudt12/13/16* lines revealed a large portion of DEGs involved in plant defense (Figure III-9A, B), we speculated whether plant pathogens might be able to directly interfere in PP-InsP homeostasis. Notably, recent work by McCombe and colleagues (2023) showed that NUDT hydrolase-type effectors of plant pathogenic fungi contribute to fungal virulence. The authors proposed that a 5-$InsP_7$ pyrophosphatase activity and the local induction of PSR at the infection site might be responsible for this phenotype (McCombe *et al.*, 2023). To further investigate the substrate specificity of fungal NUDT effectors, we generated His_6-tagged recombinant proteins for NUDTs from *Magnaporthe oryzae* (the causal agent of rice blast), *Colletotrichum graminicola* (which causes anthracnose leaf blight in maize and wheat), *Colletotrichum higginsianum* (a fungus that infects many species of the Brassicaceae, including *Arabidopsis thaliana*) and *Colletotrichum tofieldiae* (a root endophyte infecting *Arabidopsis thaliana*). In line with their potential role in inducing phosphate starvation responses, we observed robust activity against 5-$InsP_7$ under our *in vitro* conditions, corroborating the findings of McCombe and colleagues (2023). Furthermore, we noted substrate specificities reminiscent of subclade I NUDTs: while 2-$InsP_7$ and 3-$InsP_7$ were largely resistant to these NUDT effectors, all four enzymes displayed robust 4-$InsP_7$ and 6-$InsP_7$ pyrophosphatase activities, alongside partial pyrophosphatase activity against 1-$InsP_7$ (Figure III-11).

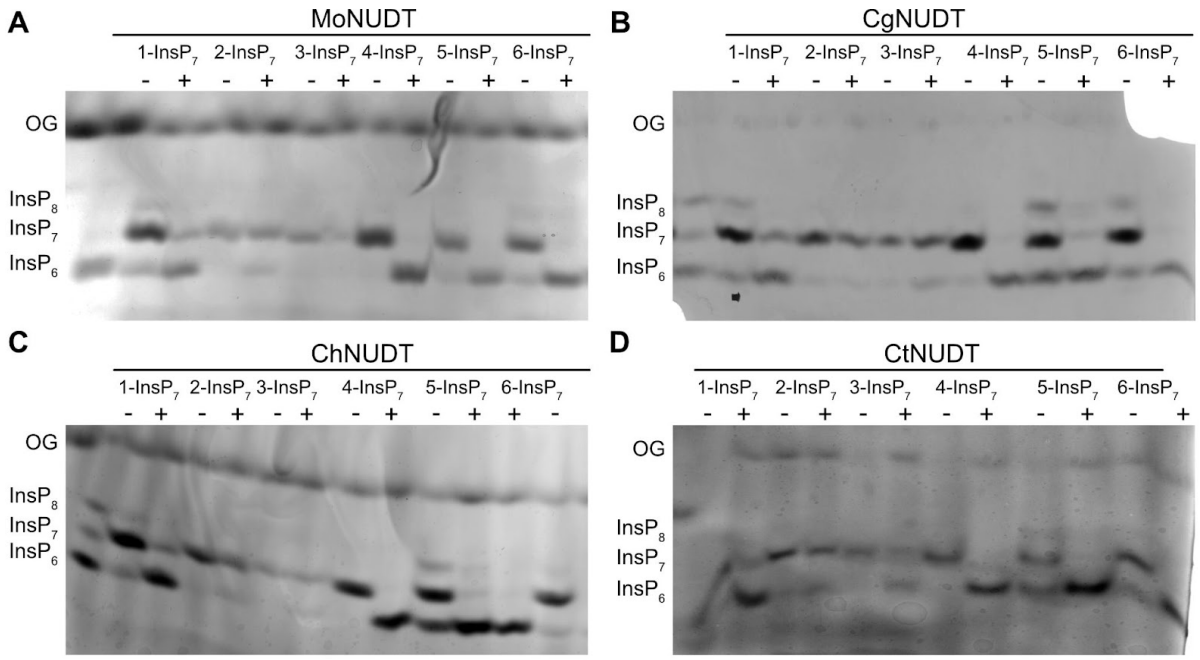

Figure III-11: Fungal NUDT effectors show similar substrate specificities as NUDTs of clade I. Recombinant His_6-tagged MoNUDT (A), CgNUDT (B), ChNUDT(C) or CtNUDT (D) were incubated with 0.25 mM $InsP_7$. Columns with a minus symbol show control reactions where no protein was added. After 45 min, the reaction products were separated by 33 % PAGE, and visualized by toluidine blue staining. A TiO_2-purified Arabidopsis *mrp5* seed extract was used as a marker for $InsP_6$, $InsP_7$ and $InsP_8$. OG: orange G.

Discussion

PP-InsPs were detected for the first time in mammalian cells more than 30 years ago by treating pancreatic rat tumor AR4-2J cells with high doses of sodium fluoride (NaF), (Menniti *et al.*, 1993). The authors used NaF, supposedly inhibiting mammalian PP-InsP pyrophosphatases, to show a massive turnover of these messengers, suggesting that, in mammalian cells, about 50 % of the $InsP_6$ pool (comprising about 50-100 µM) is converted to a low abundant pool of PP-InsPs (0.1 - 2 µM) within one hour. In yeast, recent ^{18}O-water labeling experiments demonstrated rapid incorporation of label into 1,5-$InsP_8$ and 5-$InsP_7$ reaching equilibrium within 15-20 min, suggesting a high turnover of these messengers (Kim *et al.*, 2024), as in mammalian cells. In plants, despite important functions of PP-InsPs in defense, auxin-perception and regulation of PSR, little is known about the turnover of these metabolites. While PFA-DSP-type hydrolases have been shown to execute *in vitro* pyrophosphatase activity with a high specificity against the 5PP-moiety of PP-InsPs (Gaugler *et al.*, 2022; Wang *et al.*, 2022), a physiological role in 5-$InsP_7$ or 1,5-$InsP_8$ turnover *in planta* still remains unresolved. Hydrolases involved in the turnover of 4-$InsP_7$, 6-$InsP_7$ or 3-$InsP_7$ have not yet been presented

until now. Using an affinity pull-down assay with stable 5PCP-$InsP_5$ beads, we isolated previously proposed PP-InsP-interacting proteins, including AtVIH1/AtVIH2 (Laha *et al.*, 2015; Zhu *et al.*, 2019), AtSPX2 (Ried *et al.*, 2021), and AtCOI1 (Laha *et al.*, 2015; Laha *et al.*, 2016) from Arabidopsis extracts. We also isolated AtIPK2α and AtIPK2β, which have been shown to be involved in the synthesis of lower InsP species and so far not been linked to PP-InsP binding or synthesis *in planta* (Stevenson-Paulik *et al.*, 2002; Stevenson-Paulik *et al.*, 2005). However, recent findings show that Arabidopsis IPK2α synthesizes 4/6-$InsP_7$ from $InsP_6$ *in vitro* and may regulate 4/6-$InsP_7$ *in vivo* (Yadav *et al.*, 2023). In addition to those targets, the assay also revealed five *Arabidopsis thaliana* NUDT hydrolases with previously unknown functions as novel interaction partners of 5PCP-$InsP_5$: NUDT4, -16, -17, -18, and -21 (Table III-S1). We identified distinct substrate specificities of NUDTs investigated in this study, with a preference of subclade I NUDTs for 4-$InsP_7$ and a preference of subclade II for 3-$InsP_7$ (Figure III-2 and Figure III-3, respectively). Considering that subclade II NUDTs only display a minor activity against 1-$InsP_7$ and that higher order mutants of this subclade show a robust 2.5-fold increase in 1/3-$InsP_7$, our findings suggest that Arabidopsis might synthesize 3-$InsP_7$ - possibly in addition to its canonical enantiomeric isomer 1-$InsP_7$ also found in yeast and mammals (Mulugu *et al.*, 2007; Fridy *et al.*, 2007; Dollins *et al.*, 2020). In favor of this idea are observations by Whitfield and colleagues (2024) and presented in this manuscript that 3-$InsP_7$ is also the preferred $InsP_7$ substrate recognized by the $InsP_6$ kinases ITPK1 (Figure III-10A), a specificity that appears to be conserved from plants to humans (Figure III-10B). However, conclusions regarding isomer identity are indirect, and we propose that the enantiomer selectivity of these different subclade I and II NUDTs might be used as tools to address the enantiomer identities of plant 4/6-$InsP_7$ and 1/3-$InsP_7$ directly by *in vitro* digests of plant-purified PP-InsPs and the help of synthetic [$^{13}C_6$]-labeled $InsP_7$ standards spiked into these reactions. As 4/6-$InsP_7$ has recently also been identified in mammalian tissues (Qiu *et al.*, 2023) and 1/3-$InsP_7$ awaits clarification in animals as well, there might be a wider interest for such tools. Interestingly, human DIPP1 (alternative name NUDT3), the NUDT hydrolase which is most closely related to yeast Ddp1 and also subclade I and II Arabidopsis NUDTs, showed robust hydrolytic activity towards 1-$InsP_7$ and 3-$InsP_7$ *in vitro* (Dollins *et al.*, 2020).

Initially, we were surprised by a minor yet significant increase in 5-$InsP_7$ levels in the independent triple mutants of subclade II NUDTs (Figure III-5D), given the poor activity of these NUDTs against 5-$InsP_7$ *in vitro* (Figure III-3A, B). However, transient expression of NUDT12 or NUDT16.1 in *N. benthamiana* resulted in a decrease in 5-$InsP_7$, suggesting activity

against this isomer (Figure III-6B). Moreover, when using higher protein concentrations, we detected 5-InsP$_7$ pyrophosphatase activity in all subclade II NUDTs, but not in the more distantly related NUDT7 (Figure III-S4). Collectively, these findings suggest that NUDTs exhibit direct pyrophosphatase activity also toward 5-InsP$_7$. We hypothesize that this "side activity" has physiological significance, as the concomitant decrease in shoot P levels observed in both independent subclade II *nudt12/13/16* lines (Figure III-7A) aligns with the role of 5-InsP$_7$ in suppressing PSR in yeast and plants (Wild *et al.*, 2016; Riemer *et al.*, 2021). Importantly, in both independent subclade II *nudt12/13/16* lines, we observed a robust increase in 1/3-InsP$_7$, in addition to the minor increase in 5-InsP$_7$ (Figure III-5D).

Our RNA-seq experiment with two independent *nudt12/13/16* triple mutants revealed that downregulated genes represented by far the larger fraction, consistent with the concept that PP-InsPs, such as 5-InsP$_7$ and InsP$_8$, act as negative regulators of gene expression (Dong *et al.*, 2019; Zhu *et al.*, 2019; Ried *et al.*, 2021; Riemer *et al.*, 2021). We observed a number of DEGs involved in PSR (Table III-S2) that might explain the decreased P-content in shoots (Figure III-7A). Additionally, genes showing the highest degree of downregulation or upregulation (log2FC < -3 or > +3, Figure III-8B and Table III-S3) revealed potential PSR-independent roles of PP-InsPs in plants. Many downregulated genes were related to ethylene signaling and senescence (e.g., *ATS40-2*, *ERF022*, *ERF11*, *ERF6*), while another set, in agreement with the GO enrichment results, was defense-related (e.g., *WRKY40*, *PAO2*, *IDL7*, *DHYPRP1*) (Table III-S3). Future research will need to explore the functional relevance of these transcriptional changes. Infection assays with pathogenic bacteria, necrotrophic and biotrophic fungi, as well as insect herbivore experiments, could provide valuable insights. Such work would build on existing studies that have established a causal link between PP-InsPs and plant defense (Laha *et al.*, 2015; Laha *et al.*, 2016; Gulabani *et al.*, 2021). Particularly noteworthy is the recent discovery that fungal effector proteins exhibit 5-InsP$_7$ pyrophosphatase activity (McCombe *et al.*, 2023), along with activities described here against 4-InsP$_7$, 6-InsP$_7$, and partially 1-InsP$_7$, but not 3-InsP$_7$ (Figure III-11). As proposed by McCombe and colleagues (2023), these effectors might simply be employed to induce PSR at the expense of plant defense. Alternatively, a change in 4/6-InsP$_7$ may also play a direct role in suppressing plant defenses, a topic deserving further investigation.

We also observed differential expression of a number of Fe-regulated genes in the mutant lines (Table III-S4). For instance *IRONMAN3*, which encodes a peptide that activates iron deficiency response genes, as well as the gene encoding the Iron-Responsive Protein 6 *IRP6* (Grillet *et al.*,

2018; Hirayama *et al.*, 2018) were both strongly upregulated. This response might have been triggered by cytoplasmic chelation of iron by 1/3-InsP$_7$ or 5-InsP$_7$, leading to increased expression of both Fe-deficiency-induced genes. Supporting this hypothesis, we found a downregulation of *ZAT6* and *ZAT10*, which encode zinc finger transcription factors that activate phytochelatin synthesis. Phytochelatins are small, cysteine-rich peptides localised in the cytosolthat primarily function to chelate and detoxify heavy metals. If Fe (and other di- or trivalent metals) are chelated by increased cytosolic PP-InsPs, it is conceivable that phytochelatin expression would decrease, as the need for metal detoxification might be reduced. In addition, *FER1*, encoding the Fe storage protein ferritin (Briat *et al.*, 2010), was downregulated as well, in agreement with a potentially reduced (cytosolic) availability of Fe and thus compromised Fe sensing (Table III-S4). This disturbance in iron homeostasis might also explain why subclade II *nudt12/13/16* plants display decreased shoot Fe content (Figure III-7B). Alternatively, disturbed Fe homeostasis might also be a consequence of altered PP-InsP signaling in these mutants, topics warranting further investigation in future studies.

Material and Methods

Plant materials and growth conditions

Seeds of *Arabidopsis thaliana* WT (Col-0) and T-DNA insertion lines *nudt4-1* (SALK_102051.27.90.x), *nudt4-2* (SAIL_1211_A06), *nudt17-1* (SAIL_500_D10), *nudt18-1* (SALKseq_117563.1), *nudt21-1* (SALK_031788.56.00.x), *nudt21-2* (SALKseq_132932.101) and *mrp5* (GK-068B10) were obtained from "The European Arabidopsis Stock" Centre (http://arabidopsis.info/). To identify homozygous mutant lines, the plants were genotyped by PCR using the primers indicated in Table III-S5.

For sterile growth, *Arabidopsis thaliana* seeds were surface sterilized by washing them three times with 70 % (v/v) ethanol mixed with 0.05 % (v/v) Triton X-100 and once with 100 % (v/v) ethanol. Sterilized seeds were sown onto ½ MS plates containing 0.5 % (w/v) sucrose and 0.7 % (w/v) Phytagel (Sigma-Aldrich), pH 5.7. The seeds were stratified for 2 days at 4 °C and afterwards transferred to a growth chamber with a 16 h/8 h day/night period, equipped with white LEDs (160 µmol^{-1} m^{-2}) ("True daylight", Polyklima) and a temperature of 22 °C/20 °C to amplify seeds.

For the affinity pull-down with the 5PCP-InsP$_5$ resin, the plants were grown for 3 weeks in a growth incubator (Percival) with an 8 h/16 h day/night period, equipped with fluorescent light bulbs (120 μmol^{-1} m^{-2}) and a temperature of 22 °C/20 °C. The roots and shoots of approximately 150 seedlings were collected and frozen in liquid nitrogen.

For the quantification of inositol pyrophosphate content by CE-ESI-MS, the control and mutant lines were grown on ½ MS plates, transferred to a growth chamber with a 16 h/8 h day/night period, light by white LEDs (160 μmol^{-1} m^{-2}) ("True daylight", Polyklima) and a temperature of 22 °C/20 °C. After 14 days, the shoots were collected and transferred to 2 mL centrifuge tubes and frozen in liquid nitrogen. The remaining plant material from the plates was transferred to pots containing peat substrate (Einheitserde Vermehrungserde) in block randomized design, and plants were grown for another week. 100 mg material was harvested and frozen in liquid nitrogen. The material was later grinded into powder and used for RNA extraction.

For nutrient content analyses, WT and triple mutant plants were grown for 4-5 weeks in pots containing peat-based substrate (Einheitserde Vermehrungserde) in block randomized design. The whole shoots were harvested and dried at 60 °C for 5 days, grinded into fine powder and the nutrient content was analyzed using ICP-OES.

To investigate the P$_i$-dependent regulation of inositol (pyro)phosphates, the Arabidopsis plants were hydroponically grown as described previously (Riemer *et al.*, 2021).

Constructs

The open reading frames (ORFs) of *NUDT4* (At1g18300), *NUDT7* (At4g12720), *NUDT12* (At1g12880), *NUDT13* (At3g26690), *NUDT16.1* (At3g12600.1), *NUDT16.2* (At3g12600.2), *NUDT17* (At2g01670), *NUDT18* (At1g14860), *NUDT21* (At1g73540) were amplified from *Arabidopsis thaliana* seedling cDNA by PCR, fused to Gateway compatible *attB1* and *attB2* sites with primers listed in Table III-S5 and cloned in pDONR221 (Invitrogen) with BP clonase II (Invitrogen) following the manufacturer's instructions. To express recombinant proteins fused N-terminally to a His$_6$-MBP epitope tag, the ORFs were recombined into the bacterial expression vector pDest-566 (Addgene plasmid #11517 was a gift from Dominic Esposito; http://n2t.net/addgene:11517; RRID:Addgene_11517) by LR clonase II (Invitrogen) following the manufacturer's instructions. His-tagged MBP used as control for the *in vitro* assays was expressed with a modified pET28b vector encoding a His$_8$-MBP protein (Laha *et al.*, 2015).

His_8-MBP-VIH2 and His_8-MBP-hsITPK were expressed with the previously mentioned modified pETB28b vector (Laha *et al.*, 2015; Laha *et al.*, 2019).

The fungal *NUDT* genes *MoNUDT*, *CgNUDT*, *ChNUDT* and *CtNUDT* were ordered in a pTWIST ENTR vector (Twist Biosciences, San Francisco, CA, USA). The ORFs were then recombined into the bacterial expression vector pDest-527 (Addgene plasmid #11518 was a gift from Dominic Esposito; http://n2t.net/addgene:11518; RRID:Addgene_11518) by LR clonase II (Invitrogen) following the manufacturer's instructions.

For the *RUBY*-reporter construct, 1 kb *SlSPX2* promoter fragment upstream of the *SlSPX* start codon including the 5'UTR was fused upstream of the *RUBY* reporter. The given *SlSPX2* promoter-*RUBY* fusion was placed in a LII α (4-5) plasmid backbone.

For yeast expression, NUDTs were expressed as translational fusion with a C-terminal V5 epitope tag (primers listed in Table III-S5). The amplified genes harboring the *V5* sequence were cloned with BP clonase II in pDONR221 and then recombined into the destination vector pAG425GPD-*ccdB* (Alberti *et al.*, 2007) (Addgene plasmid #14154 was a gift from Susan Lindquist; http://n2t.net/addgene:14154; RRID:Addgene_14154) with LR clonase II following the manufacturer's instructions.

Generation of high order NUDT mutants in plants with CRISPR/Cas9

CRISPR-Cas9 constructs were generated as described earlier (Ursache *et al.*, 2021), with sgRNAs listed in Table III-S6. For each of the *nudt4/nudt17/nudt18/nudt21* quadruple and the *nudt12/nudt13/nudt16* triple mutants, two constructs were generated: one with the *sgRNA-NUDT17.1*, *sgRNA-NUDT18.2*, *sgRNA-NUDT21.1* and *sgRNA-NUDT4.2* in the expression vector pRU295 (Addgene plasmid #167694 was a gift from Niko Geldner; http://n2t.net/addgene:167694; RRID:Addgene_167694), and one construct with *sgRNA-NUDT18.1*, *sgRNA-NUDT17.2*, *sgRNA-NUDT4.1* and *sgRNA-NUDT21.2* in the expression vector pRU294 (Addgene plasmid #16768 was a gift from Niko Geldner; http://n2t.net/addgene:167689; RRID:Addgene_167689). To generate the triple mutant, *sgRNA-NUDT12.1*, *sgRNA-NUDT13.2*, *sgRNA-NUDT16.1* and *sgRNA-NUDT16.2* were cloned in the expression vector pRU295 and sgRNA-*NUDT13.1* and *sgRNA-NUDT12.2* were cloned in the expression vector pRU294.

The triple *nudt12/nudt13/nudt16* and quadruple *nudt4/nudt17/nudt18/nudt21* mutants were then generated by co-transforming *Arabidopsis thaliana* WT plants with *Agrobacterium tumefaciens* strain GV3101 harboring the respective pRU294 or pRU295 constructs. By co-transforming the plants via floral dip, it was possible to insert CRISPR-Cas9 constructs targeting two specific sequences for each NUDT. Three days after the first infiltration, the plants were transformed again to increase the transformation efficiency.

The seeds were screened for a red and green fluorescence signal using a fluorescence stereomicroscope (OLYMPUS SZX16, Japan). The seeds were sterilized and germinated on ½ MS plates as described above. After two weeks, the seedlings were transferred to soil and plant gDNA was extracted from leaves with the Phire Plant Direct PCR kit (Thermo Fisher). The promoter and gene regions of the targeted genes were amplified with the primers listed in Table III-S5 and analyzed by Sanger Sequencing.

Yeast strains, transformation and growth

The BY4741 WT (MATa *his3Δ leu2Δ met15Δ ura3Δ*) and *ddp1Δ* (MATa *his3Δ leu2Δ met15Δ ura3Δ ddp1Δ::KanMX*) were obtained from Euroscarf. The yeast cells were transformed with the Li-acetate method and grown on 2x CSM-Leu plates for 3 days at 28 °C. Yeast transformants were grown in the respective media overnight at 28 °C in a rotating wheel before radioactive labeling with [^{3}H]-*myo*-inositol.

Affinity pull-down with 5PCP-InsP$_5$ resin

The plant material was powdered with mortar and pestle. 3 mL of lysis buffer (50 mM Tris pH 7.5, 100 mM NaCl, 5 mM ß-mercaptoethanol, 1 mM $MgCl_2$, 0.1 % Tween 20, 10 % glycerol and cOmplete™ ULTRA EDTA free protease inhibitor tablets (Roche, Basel, Switzerland)) was added to the ground shoots and 1 mL was added to the ground roots. The suspension was pelleted at 4 °C for 15 min at 19000 x g and the supernatant was transferred to a new tube and centrifuged again. The resulting extract was filtered through a 20 µm syringe filter to remove remaining particles.

A 200 µL suspension of 5PCP-InsP$_5$ beads or control beads was washed three times for 5 min in 50 mM Tris pH 7.5, 100 mM NaCl, 1 mM $MgCl_2$, 10 % glycerol (Wu *et al.*, 2016). After

equilibration, the beads were incubated with the prepared plant lysates for 2 h at 4 °C on an overhead shaker. The beads were then washed three times for 10 min with the equilibration buffer and then incubated overnight at 4 °C with 100 µL $InsP_6$-containing wash buffer (50 mM Tris, 100 mM NaCl, 1 mM $MgCl_2$, 20 mM $InsP_6$ (SiChem) on a rotating shaker. Subsequently, the beads were pelleted and washed again with wash buffer for 10 min. The beads were then further analyzed by LC-MS/MS.

$InsP_6$-washed beads were submitted to an on-bead digestion. In brief, dry beads were re-dissolved in 50 µL digestion buffer 1 (50 mM Tris, pH 7.5, 2 M urea, 1 mM DTT), trypsin (125 ng) was added and beads were incubated for 30 min at 30 °C in a thermal shaker with 400 rpm. Next, beads were pelleted and the supernatant was transferred to a fresh tube. Digestion buffer 2 (50 mM Tris, pH 7.5, 2 M urea, 5 mM CAA) was added to the beads and mixed, beads were pelleted and the supernatant was collected and combined with the previous one. The combined supernatants were then incubated overnight at 32 °C in a thermal shaker with 400 rpm. Samples were protected from light during incubation. The digestion was stopped by adding 1 µL TFA and desalted with C18 Empore disk membranes according to the StageTip protocol. The proteins that were eluted with an excess of $InsP_6$ were reduced with dithiothreitol (DTT), alkylated with chloroacetamide (CAA), and digested with trypsin. These digested samples were desalted using StageTips with C18 Empore disk membranes (3 M), dried in a vacuum evaporator, and dissolved in 2 % ACN, 0.1 % TFA (Rappsilber *et al.*, 2003).

Dried peptides were re-dissolved in 2 % ACN, 0.1 % TFA (10 µL) for analysis. Samples were analyzed using an EASY-nLC 1000 (Thermo Fisher) coupled to a Q Exactive mass spectrometer (Thermo Fisher). Peptides were separated on 16 cm frit-less silica emitters (New Objective, 0.75 µm inner diameter) and packed in-house with reversed-phase ReproSil-Pur C18 AQ 1.9 µm resin (Dr. Maisch). Peptides were loaded on the column and eluted for 115 min using a segmented linear gradient of 5 % to 95 % solvent B (0 min: 5 % B; 0 - 5 min -> 5 % B; 5 - 65 min -> 20 % B; 65 - 90 min ->35 % B; 90 - 100 min -> 55 % B; 100 - 105 min -> 95 % B, 105-115 min -> 95 % B) (solvent A 0 % ACN, 0.1 % FA; solvent B 80 % ACN, 0.1 % FA) at a flow rate of 300 nL/min. Mass spectra were acquired in data-dependent acquisition mode with a TOP15 method. MS spectra were acquired in the Orbitrap analyzer with a mass range of 300–1750 m/z at a resolution of 70,000 FWHM and a target value of 3×106 ions. Precursors were selected with an isolation window of 2.0 m/z. HCD fragmentation was performed at a normalized collision energy of 25. MS/MS spectra were acquired with a target value of 105 ions at a resolution of 17,500 FWHM, a maximum injection time (max.) of 55 ms and a fixed

first mass of m/z 100. Peptides with a charge of +1, greater than 6, or with unassigned charge state were excluded from fragmentation for MS2, dynamic exclusion for 30 s prevented repeated selection of precursors.

Raw data were processed using MaxQuant software (version 1.5.7.4, http://www.maxquant.org/) (Cox and Mann, 2008) with label-free quantification (LFQ) and iBAQ enabled (Tyanova *et al.*, 2016) and the match-between runs option disabled. MS/MS spectra were searched by the Andromeda search engine against a combined database containing the sequences from *A. thaliana* (TAIR10_pep_20101214; ftp://ftp.arabidopsis.org/home/tair/Proteins/TAIR10_protein_lists/) and sequences of 248 common contaminant proteins and decoy sequences. Trypsin specificity was required and a maximum of two missed cleavages allowed. Minimal peptide length was set to seven amino acids. Carbamidomethylation of cysteine residues was set as fixed, oxidation of methionine and protein N-terminal acetylation as variable modifications. Peptide-spectrum-matches and proteins were retained if they were below a false discovery rate of 1 %.

The MaxQuant output (msms.txt) was further processed using Skyline (https://skyline.ms) (MacLean *et al.*, 2010). Peaks were inspected and, if necessary, re-integrated manually. To identify potential binding candidates, proteins were filtered for two or more unique peptides and idot products with > 0.95 confidence. Subsequently, peptides were assessed individually for enrichment in the 5PCP-$InsP_5$ condition versus the control condition based on peak areas. Background binders were identified as proteins with equal abundance in both the 5PCP-$InsP_5$ and control conditions.

ICP-OES analyses

Shoots of 4-week-old plants were dried, ground to powder and 0.150 g were digested with 3 mL nitric acid (HNO_3, 65 %) in a microwave-accelerated reaction system (CEM, Matthews, NC, USA). Nutrient concentrations were measured using inductively coupled plasma optical emission spectroscopy (ICP-OES; iCAP Pro X ICP-OES Duo; Thermo Fisher Scientific, Waltham, MA, USA). To ensure precision and accuracy throughout the analyses standard materials (IPE100; Wageningen Evaluation Programs for Analytical Laboratories, WEPAL; Wageningen University, the Netherlands) were used.

Protein preparation

Recombinant NUDT proteins fused to His_6-MBP and free His_8-MBP protein were expressed in *Escherichia coli* BL21-CodonPlus(DE3)-RIL cells (Stratagene). The bacterial cultures were grown overnight and fresh 2YT medium (16 g/L tryptone, 10 g/L yeast extract, 5 g/L NaCl) with respective antibiotics was inoculated 1:500 with the overnight culture. In the case of CgNUDT and ChNUDT LB medium (10 g/L tryptone, 5 g/L yeast extract, 10 g/L NaCl) and in the case of CtNUDT TB medium (12 g/L tryptone, 24 g/L yeast extract, 0.4 % v/v glycerol, 0.017 M KH_2PO_4, 0.072 K_2HPO_4) was used. The cultures were grown for 3 h at 37 °C while shaking (200 rpm) to reach an estimated OD_{600} of 0.6. Protein expression was induced by adding 0.1 mM (CgNUDT, ChNUDT, CtNUDT), 0.125 mM (NUDT7 and -12), 0.25 mM (NUDT4, -16, -17, -18, and -21) or 0.5 mM (NUDT13, MoNUDT) isopropyl-d-1-thiogalactopyranoside (IPTG). The cultures were grown for 24 h at 12 °C (NUDT4, and -18) or at 16 °C (NUDT7, -13, -16, -17, and -21, CgNUDT, ChNUDT) or for 3 h at 37 °C (NUDT12, MoNUDT, CtNUDT). Bacterial cells were lysed by vortexing the cells 8 times for 1 min with lysis buffer (20 mM Na_2HPO_4, 300 mM NaCl, 2 mM DTT, 0.05 mM EDTA and 1 % Triton X-100, pH 7.4) and glass beads (0.1 – 0.25 mm). NUDT4, -17, -18, and -21 were purified using a FPLC (ÄKTA pure^{TM}), while NUDT12, -13, -16, MoNUDT, CgNUDT, ChNUDT and CtNUDT were batch purified using Ni-NTA agarose resin (Macherey-Nagel). For both methods, the same binding buffer (20 mM Na_2HPO_4, 500 mM NaCl, 25 mM imidazol, pH 7.4) and elution buffer (20 mM Na_2HPO_4, 500 mM NaCl, 500 mM imidazol, pH 7.4) were used. The recombinant proteins were concentrated and imidazole was diluted by using Vivaspin 20 (50 kDa, Merck) for FPLC-purified proteins or Amicon Ultra 0.5 mL Centrifugal Filters (50 kDa, Merck) for the batch-purified proteins and the elution buffer without imidazole. The purified proteins were mixed with 20 % glycerol and stored at -20 °C. Recombinant Arabidopsis and human ITPK1 and VIH2 proteins fused to His_8-MBP were expressed and purified as described before (Laha *et al.*, 2015; Laha *et al.*, 2019). Concentrations were estimated by using SDS-PAGE followed by Coomassie blue staining and comparing the proteins with designated amounts of a BSA standard.

***In vitro* (PP-)InsP assays**

The (PP-)InsP pyrophosphatase assays were performed with recombinant His_6-MBP-NUDT proteins or His_8-MBP proteins as control and 50 mM HEPES (pH 7.0), 10 mM NaCl, 5 % (v/v)

glycerol, 0.1 % (v/v) β-mercaptoethanol, either 1 mM EDTA, $MnCl_2$, $MgCl_2$, $CaCl_2$, or $ZnCl_2$ and 0.33 mM of various $InsP_7$ or $InsP_8$ isomers as indicated. The recombinant protein concentrations were: ~4.9 µM His_6-MBP-NUDT4, ~3.7 µM His_6-MBP-NUDT12, ~1.9 µM His_6-MBP-NUDT13, ~0.6 µM His_6-MBP-NUDT16.1, ~15.8 µM His_6-MBP-NUDT16.2, ~2.0 µM His_6-MBP-NUDT17, ~5.1 µM His_6-MBP-NUDT18 and ~5.0 µM His_6-MBP-NUDT21. For the assays with His_6-MBP-MoNUDT, His_6-MBP-CgNUDT, His_6-MBP-ChNUDT and His_6-MBP-CtNUDT 0.25 mM of the various $InsP_7$ isomers and 0.13 µg/µL protein was used.

PP-InsP pyrophosphatase assays with higher subclade II protein concentrations were performed with ~7 µM His_6-MBP-NUDT7, ~7.5 µM His_6-MBP-NUDT12 or His_6-MBP-NUDT13, and ~8 µM His_6-MBP-NUDT16.1 or His_6-MBP-NUDT16.2. The pyrophosphatase assays with a higher subclade I protein concentration were performed in a reaction buffer as described previously (Riemer *et al.*, 2021) with 0.33 mM of various $InsP_7$ or $InsP_8$ isomers as indicated. The recombinant protein concentrations were ~9 µM His_6-MBP-NUDT4, ~6 µM His_6-MBP-NUDT17, ~6 µM His_6-MBP-NUDT18 and ~8 µM His_6-MBP-NUDT21. $InsP_7$ and $InsP_8$ isomers were chemically synthesized as described previously (Capolicchio *et al.*, 2013; Capolicchio *et al.*, 2014). The reactions were incubated for 1 h at 28 °C or 2 h at 22 °C and either separated by 33 % PAGE and visualized by toluidine blue staining or analyzed by CE-ESI-MS as described previously (Qiu *et al.*, 2020; Riemer *et al.*, 2021). Kinase assays were performed as described previously (Riemer *et al.*, 2021) with 0.2 µg/µl of protein.

Inositol phosphate extraction and purification

The extraction and purification of InsPs of *A. thaliana* T-DNA insertion lines were performed using TiO_2 (titanium(IV) oxide rutile, Sigma Aldrich) beads as previously described (Riemer *et al.*, 2021). Inositol phosphate from the triple mutant *nudt12/13/16*, quadruple mutant *nudt4/17/18/21* and *N. benthamiana* were extracted with Nb_2O_5 beads (Niobium (V) pentoxide, Sigma Aldrich) with the following method: The beads were weighed for each sample and washed once in water (300 µL) and once in 1 M perchloric acid (300 µL) (PA). Liquid N_2-frozen plant material was homogenized using a pestle and immediately resuspended in 800 µL ice-cold PA (1 M). Samples were kept on ice for 10 min with short intermediate vortexing and then centrifuged for 10 min at 18000 g at 4 °C. The supernatants were transferred into fresh 1.5-mL tubes and centrifuged again for 10 min at 18000 g at 4 °C. To bind InsPs onto the beads, the

supernatants were resuspended in the prewashed Nb_2O_5 beads and rotated at 4 °C for 45 min. Afterwards, the tubes were centrifuged at 11000 g for 1 min at 4 °C and washed twice in 500 µL ice-cold PA (1 M) and once with 500 µL PA (0.1 M). To elute inositol polyphosphates, beads were resuspended in 200 µL 10 % ammonium hydroxide and then rotated for 5 min at room temperature. After centrifuging, the supernatants were transferred into fresh 1.5-mL tubes. The elution process was repeated and the second supernatants were added to the first. Eluted samples were vacuum evaporated at 45 °C to dry completely.

PAGE, CE-ESI-MS and HPLC analyses

Arabidopsis plants and yeast transformants were radioactively labeled with [^{3}H]-*myo*-inositol (ARC), extracted and analyzed via SAX-HPLC as described before (Azevedo and Saiardi, 2006; Laha *et al.*, 2015; Gaugler *et al.*, 2020). *In vitro* biochemical assays were analyzed by PAGE and CE-ESI-MS, and purified inositol phosphates of *A. thaliana* mutant lines or *N. benthamiana* leaves were analyzed by CE-ESI-MS as described in (Qiu *et al.*, 2020; Riemer *et al.*, 2021; Qiu *et al.*, 2023).

RNA extraction and quantitative real-time PCR

Total RNA was extracted from homogenized root or shoot samples using the NucleoSpin RNA Mini Kit (Machery-Nagel), followed by on-column DNase treatment (QIAGEN), according to the manufacturers' protocols. cDNA was synthesized from 0.5-1 µg RNA by reverse transcription using the RevertAid First Strand cDNA synthesis Kit (Thermo Fisher Scientific) and oligo(dT) primer. A ten- or twenty-times diluted cDNA sample was then used for quantitative real-time (RT) PCR analysis with the CFX384 Touch Real-Time PCR Detection System (Bio-Rad Laboratories) and the iQ SYBR Green Supermix (Bio-Rad Laboratories). All reactions were repeated in two technical and three biological replicates. Recorded C_t values were exported from the Bio-Rad CFX Manager Software (Version 3.1, Bio-Rad Laboratories) and used for the calculation of relative expression values according to ΔΔCT method and using *UBQ2* (*At2g36170*) or *ACTIN2* (*At3g18780*) as the reference gene. The reactions were carried out using the primers listed in Table III-S5.

Total RNA for transcriptome analysis was extracted from shoot samples using the QIAGEN Kit followed by on-column DNase treatment (QIAGEN), according to the manufacturers' protocols.

RNA sequencing, bioinformatic analysis and data visualization

For RNA-seq analysis, total RNA was extracted as described above. Library construction and sequencing were performed at BGI Genomics (Poland). mRNA enrichment was performed on total RNA using oligo(dT)-attached magnetic beads. The enriched mRNA with poly(A) tails was fragmented using a fragmentation buffer, followed by reverse transcription using random N6 primers to synthesize cDNA double strands. The synthesized double-stranded DNA was then end-repaired and 5'-phosphorylated, with a protruding 'A' at the 3' end forming a blunt end, followed by ligation of a bubble-shaped adapter with a protruding 'T' at the 3' end. The ligation products were PCR amplified using specific primers. The PCR products were denatured to single strands, and then single-stranded circular DNA libraries were generated using abridged primer. The constructed libraries were quality-checked and sequenced after passing the quality control. Sequencing was performed on the DNBSEQ platform using paired-end 150 bp reads (PE150). The raw data obtained from sequencing was filtered using SOAPnuke (Chen *et al.*, 2018) to remove adapters, reads containing ploy-N and low-quality reads, and the filtered data (clean reads) was aligned to the Arabidopsis genome (TAIR10) using HISAT2 (https://daehwankimlab.github.io/hisat2/) based on Burrows-Wheeler transform and Ferragina-Manzini (FM) index. Clean data was aligned to the reference gene set using Bowtie2 (v2.3.4.3). Gene expression quantification was performed using RSEM (v1.3.1) software, and gene expression clustering heatmaps across different samples were generated using pheatmap (v1.0.8) (10.32614/CRAN.package.pheatmap). DESeq2 (v1.4.5) (Love *et al.*, 2014) or DEGseq (Wang *et al.*, 2010) or PoissonDis (Audic and Claverie, 1997) was employed for differential gene (DEGs) detection, with criteria set as Q (http://bioconductor.org/packages/qvalue/) value < 0.05 or FDR ≤ 0.001 and ($|\log2FC| > 1$). The subsequent analysis and data mining were performed on Dr. Tom Multi-omics Data mining system (https://biosys.bgi.com).

For the GO terms (http://www.geneontology.org/), the base mean expression for each gene was calculated as the average expression of mutant and control samples (base mean = (avg. Exp. of Mutant + avg. Exp of Control) / 2). Genes with a base mean greater than 20 were selected to form the background set. From this background, an interest set was defined by selecting genes

with a log2 fold change (|log2FC| > 1), and Q-values < 0.05. GO enrichment analysis was performed using the topGO **(**https://bioconductor.org/packages/release/bioc/html/topGO.html) package for all three gene ontology categories: biological process (BP), cellular component (CC), and molecular function (MF). The weigh01 algorithm and Fisher's exact test were employed as parameters, and the results were filtered to include the top 200 GO terms (nodes). The significance of each GO term was determined by the associated *p*-value, and the top 10 GO terms were plotted in the order of the *p*-values. Data analysis and visualization was done using R software (https://www.r-project.org/, R Core Team, 2023). GO enrichment analysis was conducted using the hypergeometric test, implemented via the Phyper function in R, with a significance threshold of $Q \leq 0.05$.

Tobacco growth conditions and infiltration procedure

Nicotiana benthamiana seeds were germinated in a growth chamber with a 16 h/8 h day/night period equipped with fluorescence light bulbs and a temperature of 22 °C/20 °C for 5-6 weeks prior to infiltration.

A single colony of transformed *Agrobacterium tumefaciens* strain GV3101 containing T-DNA vectors was inoculated in 2 mL of YEB media containing the respective antibiotics and cultivated overnight at 28 °C while shaking. On the following day, 500 µL of overnight culture was added to 5 mL of fresh YEB with respective antibiotics and grown for another 4-6 h at 28 °C. Cultures were harvested by centrifugation at room temperature with 4000 g for 10 min. The pellet was resuspended in 250 µL infiltration medium containing 10 mM $MgCl_2$, 10 mM MES (pH 5.8) and 150 µM of freshly added acetosyringone. OD_{600} was determined using a 1:10 dilution and adjusted to OD_{600} = 0.8 in infiltration medium. The working solution for the RUBY assay was prepared by adding equal amounts of RUBY-reporter and NUDTs strains, and adding *P19* (OD_{600} = 0.05). The NUDT overexpression experiment in the absence of the RUBY-reporter was done in a similar way. The mixtures were then infiltrated into the abaxial surface of 5–6-week-old *N. benthamiana* leaves using a 1 mL syringe without a needle. After infiltration, the plants were kept under previous growth conditions for 2-3 days before analyzing RUBY staining or extracting and purifying the inositol phosphates.

Data Availability

The mass spectrometry proteomics data have been deposited to the ProteomeXchange Consortium via the PRIDE (Perez-Riverol et al., 2022) partner repository with the dataset identifier PXD056943. RNA-seq clean data is available on the preprint server bioRxiv (Schneider *et al.*, 2024).

Author Contributions

R.S., V.G., and G.S. conceived the study. R.S., V.G., Kl.L, G.S., T.L., R.F.H.G., H.J.J., H.N., Do.F. designed experiments; R.S., Kl.L., I.P., V.G., A.S., S.C.S, Ke.L, E.L., J.M.S., K.R., Da.F., N.F.; S.W., Y.Z.B., S.K., M.H., P.G., and R.F.H.G. performed experiments; R.S., Kl.L., I.P., V.G., S.C.S, A.S., H.S., L.K., P.G., M.K., H.N., and R.F.H.G., R.S., G.S. wrote the manuscript with input from all authors.

Funding

The author(s) declare that financial support was received for the research, authorship, and/or publication of this article. This work was funded by grants from the Deutsche Forschungsgemeinschaft (SCHA 1274/4-1, SCHA 1274/5-1, and under Germany's Excellence Strategy, EXC-2070-390732324, PhenoRob to G.S.; JE 572/4-1 and under Germany's Excellence Strategy, CIBSS-EXC-2189–Project ID 390939984 to H.J.J.; LA 1338/18-1 to T.L.) and through funds from the Marie Skłodowska-Curie Action Grant agreement ID 101108767 to S.W.

Acknowledgments

The authors thank Brigitte Ueberbach, Li Schlüter, Nur Gömec (Department of Plant Nutrition, Institute of Crop Science and Resource Conservation, University of Bonn), Jacqueline Fuge (Department of Physiology & Cell Biology, Leibniz-Institute of Plant Genetics and Crop Plant Research) and Anne Harzen (Plant Proteomics and Mass Spectronomy Group, Max Planck Institute for Plant Breeding Research) for excellent technical assistance.

Supporting Information

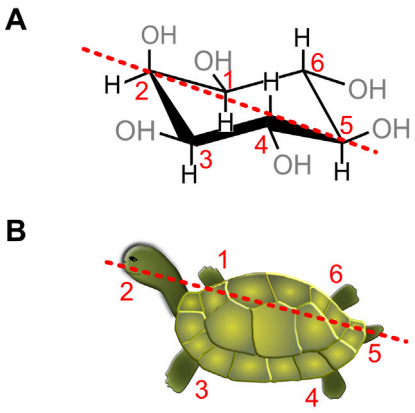

Figure III-S1: Structure of *myo*-inositol. (A) Spatial representation as chair conformation. (B) Schematic representation based on Agranoff´s turtle.

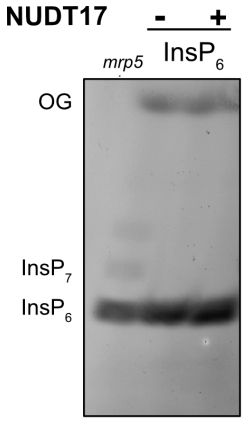

Figure III-S2: NUDT17 does not hydrolyze $InsP_6$ *in vitro*. Recombinant His_6-MBP-NUDT17 was incubated with 0.33 mM $InsP_6$ and 1 mM $MgCl_2$ at 28 °C. Recombinant His_8-MBP served as a negative control (indicated with the minus). After 1 h, the reactions were analyzed by 33 % PAGE and visualized by toluidine blue staining. OG: orange G.

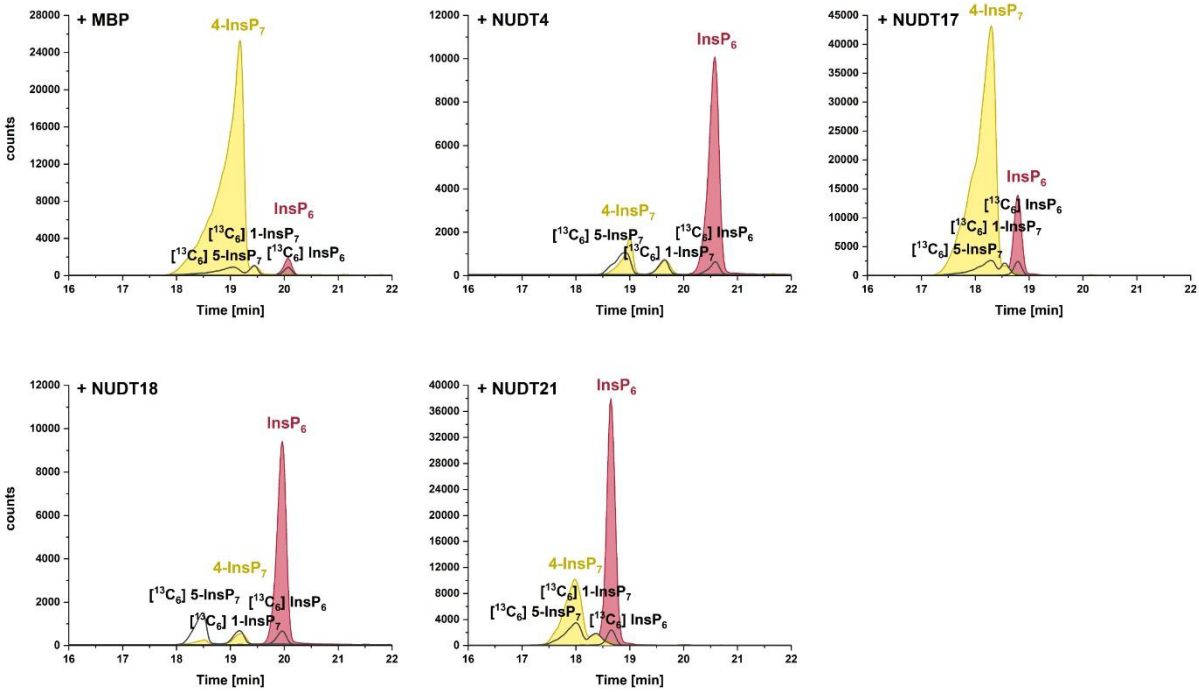

Figure III-S3: Arabidopsis NUDT hydrolases of subclade I display a 4-InsP$_7$ pyrophosphatase activity *in vitro*. Recombinant His$_6$-MBP-NUDT proteins were incubated with 0.33 mM 4-InsP$_7$ and 1 mM $MgCl_2$ at 28 °C. His$_8$-MBP served as a negative control. His$_6$-MBP-NUDT4, -17, -18, or -21 were incubated with 4-InsP$_7$. After 1 h, the reaction products were spiked with isotopic standards mixture ([$^{13}C_6$] 1,5-InsP$_8$, [$^{13}C_6$] 5-InsP$_7$, [$^{13}C_6$] 1-InsP$_7$, [$^{13}C_6$] InsP$_6$, [$^{13}C_6$] 2-OH InsP$_5$) and subjected to CE-ESI-MS analyses.

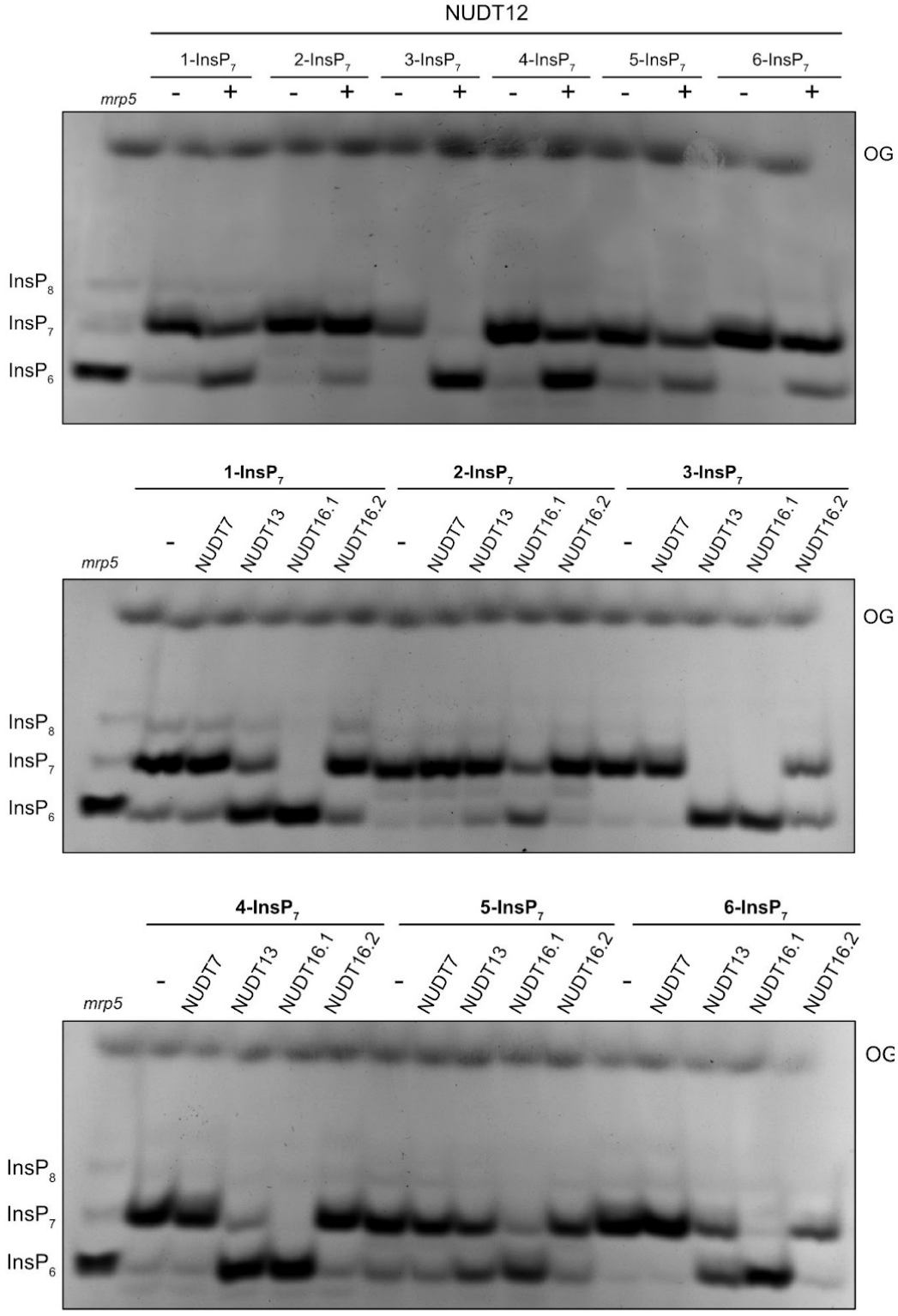

Figure III-S4: Subclade II NUDT hydrolases lose substrate specificity at higher concentrations *in vitro*. Recombinant His_6-MBP-tagged NUDT7 (~7 µM), NUDT12 (~7.5 µM), NUDT13 (~7.5 µM), NUDT16.1 (~8 µM) or NUDT16.2 (~8 µM) was incubated with 0.33 mM $InsP_7$ and 1 mM $MgCl_2$ at 28 °C (indicated with the plus symbol). His_8-MBP served as a negative control (indicated with the minus symbol). After 1 h, the reaction products were separated by 33 % PAGE and visualized by toluidine blue. OG: orange G.

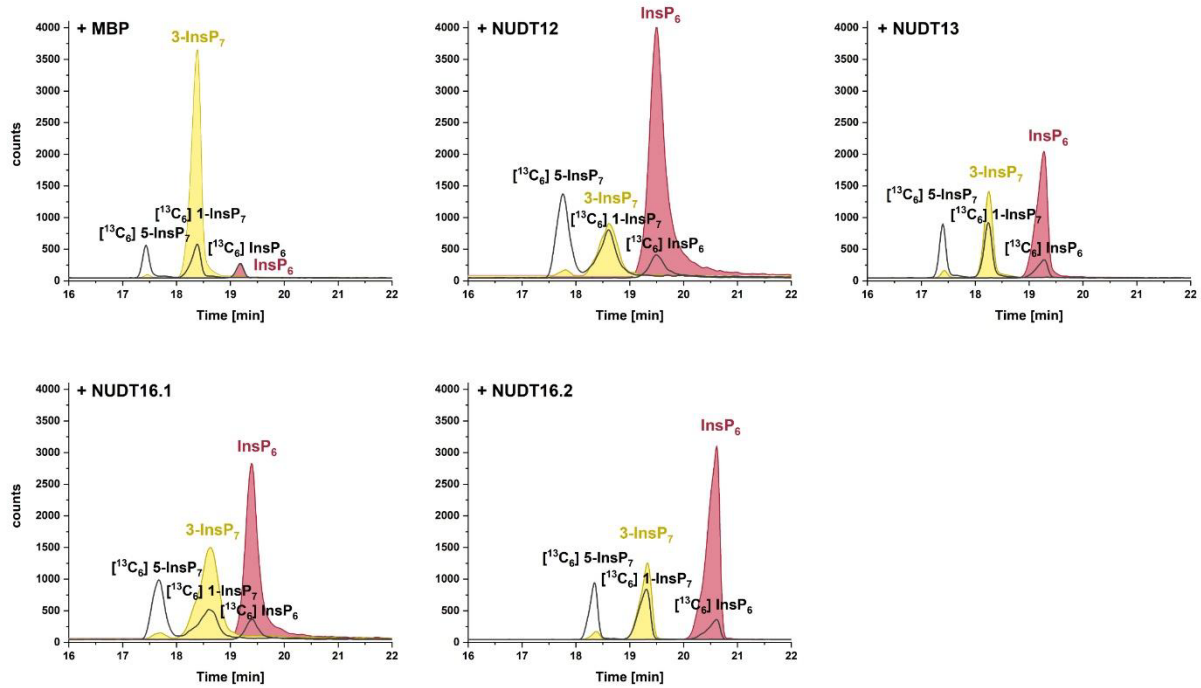

Figure III-S5: Arabidopsis NUDT hydrolases of subclade II display a 3-$InsP_7$ pyrophosphatase activity *in vitro*. Recombinant His_6-MBP-NUDT proteins were incubated with 0.33 mM 3-$InsP_7$ and 1 mM $MgCl_2$ at 28 °C. His_8-MBP served as a negative control. His_6-MBP-NUDT12, -13, -16.1, or -16.2 were incubated with 3-$InsP_7$. After 1 h, the reaction products were spiked with isotopic standards mixture ([$^{13}C_6$] 1,5-$InsP_8$, [$^{13}C_6$] 5-$InsP_7$, [$^{13}C_6$] 1-$InsP_7$, [$^{13}C_6$] $InsP_6$, [$^{13}C_6$] 2-OH $InsP_5$) and subjected to CE-ESI-MS analyses.

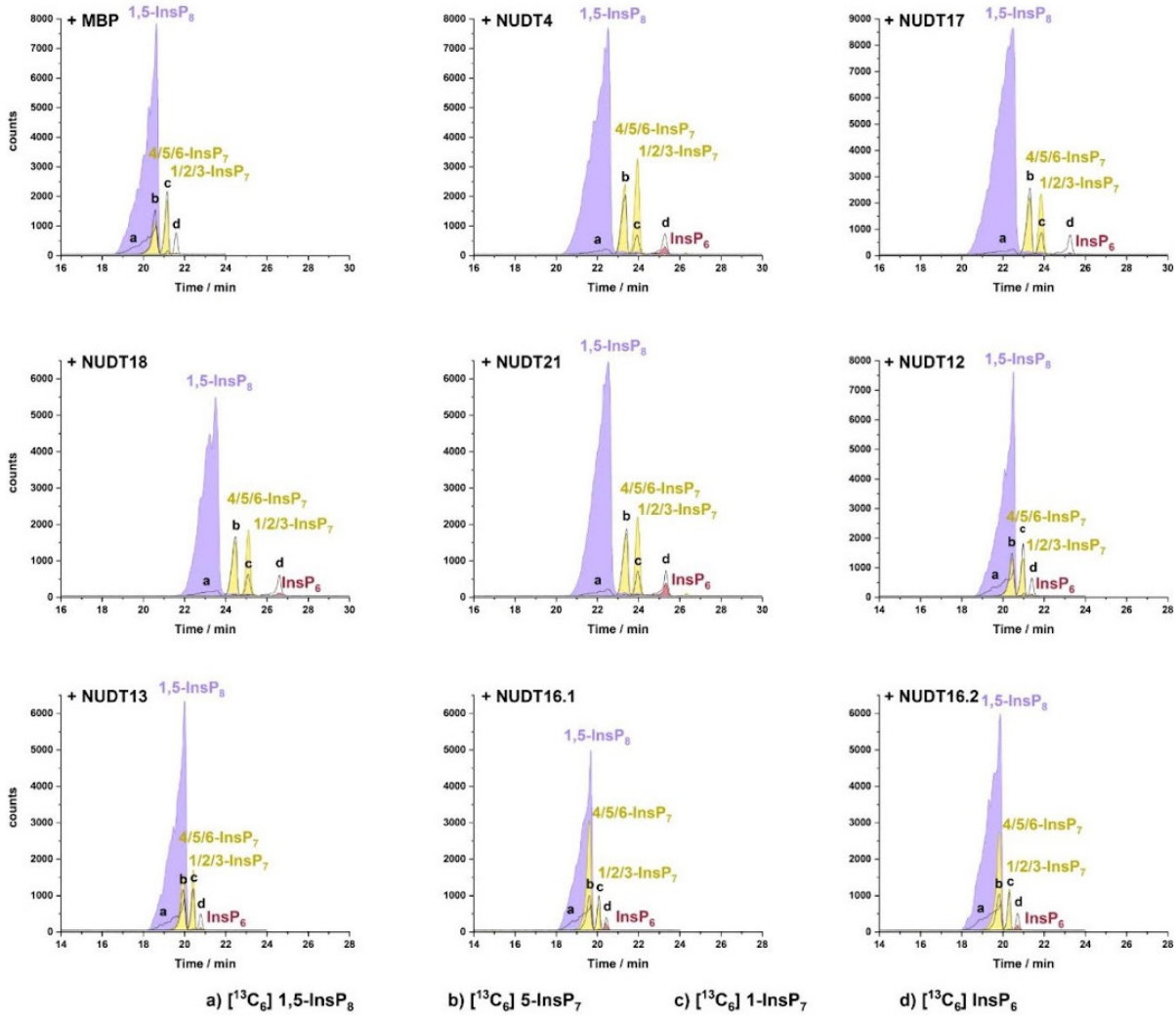

Figure III-S6: Arabidopsis NUDT hydrolases show a weak hydrolysis activity towards 1,5-$InsP_8$ *in vitro*. Recombinant His_6-MBP-NUDT proteins were incubated with 0.33 mM 1,5-$InsP_8$ and 1 mM $MgCl_2$ at 28 °C. His_8-MBP served as a negative control. After 1 h, the reaction products were spiked with isotopic standards mixture ([$^{13}C_6$] 1,5-$InsP_8$, [$^{13}C_6$] 5-$InsP_7$, [$^{13}C_6$] 1-$InsP_7$, [$^{13}C_6$] $InsP_6$, [$^{13}C_6$] 2-OH $InsP_5$) and subjected to CE-ESI-MS analyses.

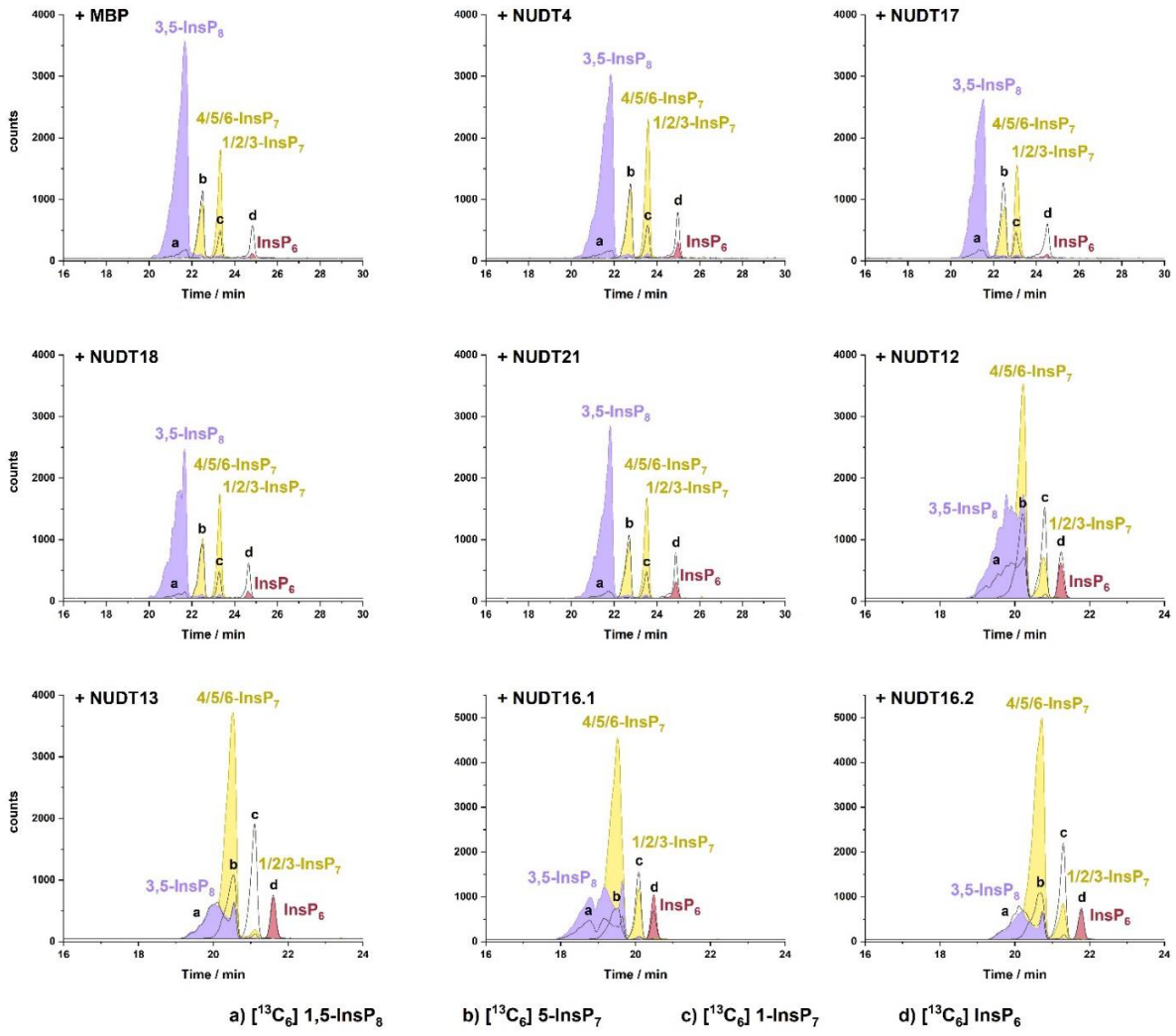

Figure III-S7: Arabidopsis NUDT hydrolases display differential hydrolysis activity towards and 3,5-$InsP_8$ *in vitro*. Recombinant His_6-MBP-NUDT proteins were incubated with 0.33 mM 3,5-$InsP_8$ and 1 mM $MgCl_2$ at 28 °C. His_8-MBP served as a negative control. After 1 h, the reaction products were spiked with isotopic standards mixture ([$^{13}C_6$] 1,5-$InsP_8$, [$^{13}C_6$] 5-$InsP_7$, [$^{13}C_6$] 1-$InsP_7$, [$^{13}C_6$] $InsP_6$, [$^{13}C_6$] 2-OH $InsP_5$) and subjected to CE-ESI-MS analyses.

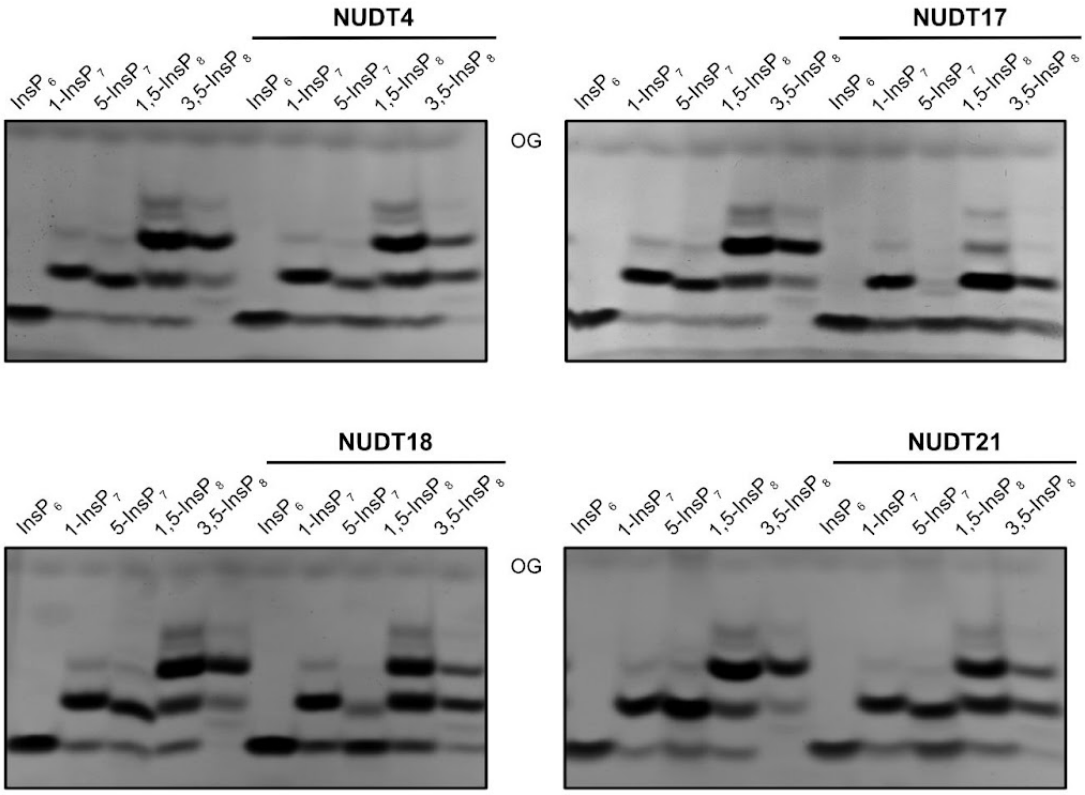

Figure III-S8: Subclade I NUDT hydrolases lose substrate specificity at higher concentrations *in vitro*. Recombinant His_6-MBP-tagged NUDT4 (~9 µM), NUDT17 (~6 µM), NUDT18 (~6 µM) or NUDT21 (~8 µM) was incubated with 0.33 mM $InsP_7$ and 1 mM $MgCl_2$ at 22 °C. His_8-MBP served as a negative control (placed at the left side of each gel). After 2 h, the reaction products were separated by 33 % PAGE and visualized by toluidine blue. OG: orange G.

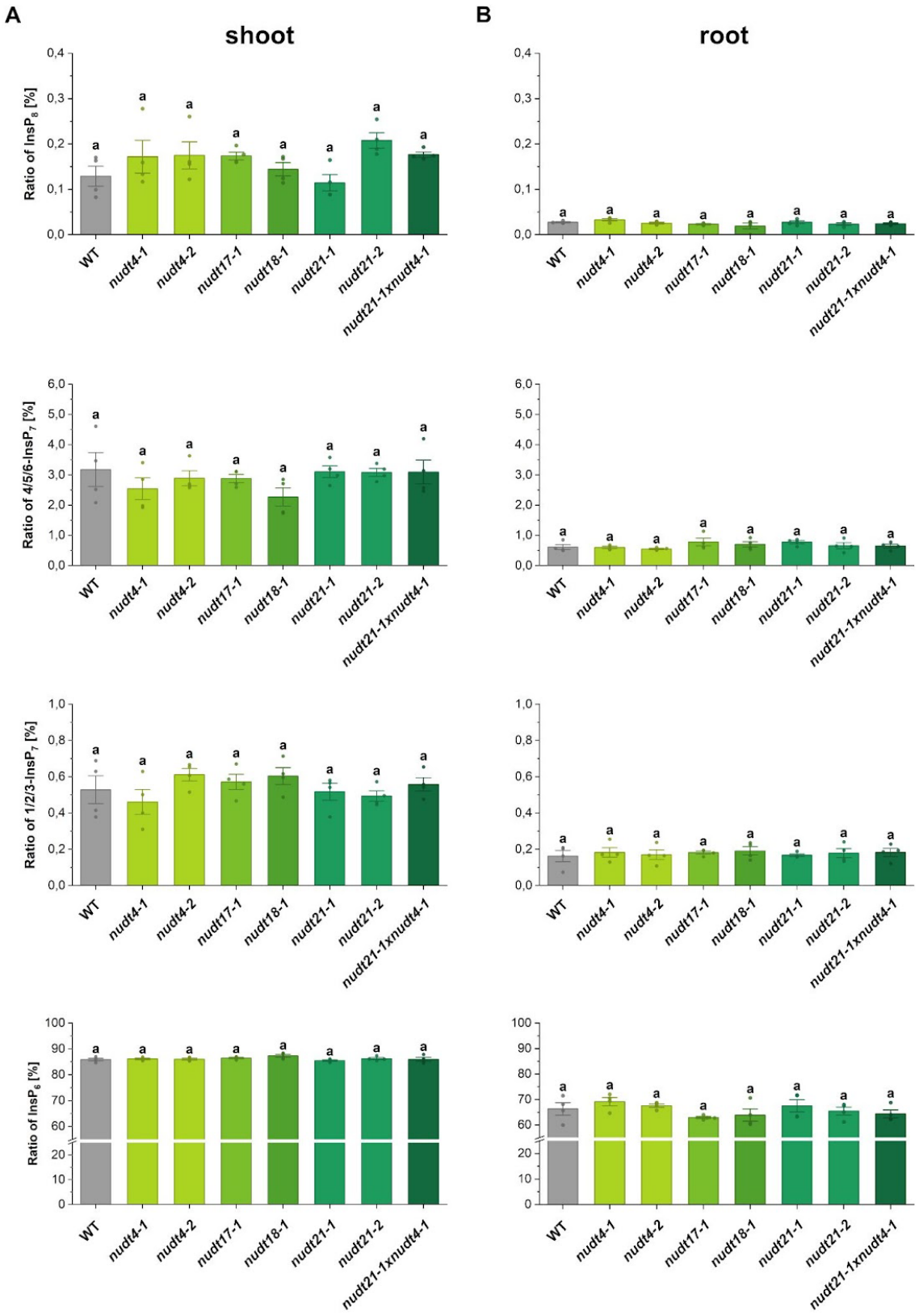

Figure III-S9: *S*ingle and double knockout mutants do not show a significant (PP-)InsP increase. *Arabidopsis thaliana* T-DNA insertion lines were grown hydroponically for 5 weeks. (PP-)InsPs were purified with TiO_2, spiked with isotopic standards mixture ([$^{13}C_6$] 1,5-$InsP_8$, [$^{13}C_6$] 5-$InsP_7$, [$^{13}C_6$] 1-$InsP_7$, [$^{13}C_6$] $InsP_6$, [$^{13}C_6$] 2-OH $InsP_5$) and subjected to CE-ESI-MS analyses. Different letters indicate values that are significantly different determined with one-way ANOVA followed by Dunn-Šidák test with a significance level of 0.05.

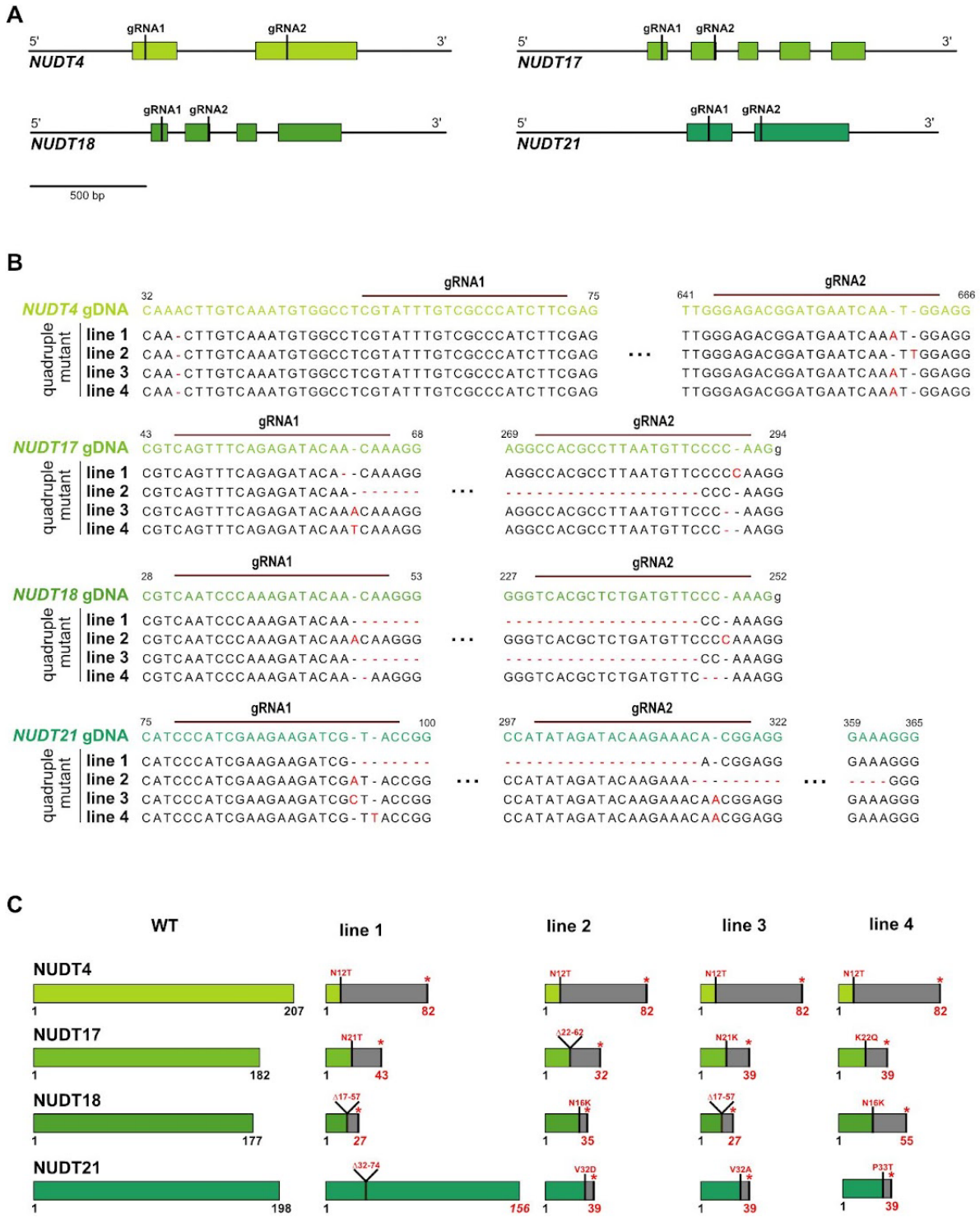

Figure III-S10: Schematic representation of the mutations in four subclade I *nudt4/17/18/21* mutants. (A) gRNA1 was designed to target the beginning of the open reading frame (ORF), while gRNA2 was designed to target in front or directly the sequence encoding the NUDT motif ($GX_5EX_7REUXEEXGU$, where U represents a hydrophobic amino acid such as leucine, isoleucine or valine and X represents any amino acid). (B) Observed deletions, insertions and point mutations in four *nudt4/17/18/21* mutants. (C) Predicted amino acids changes.

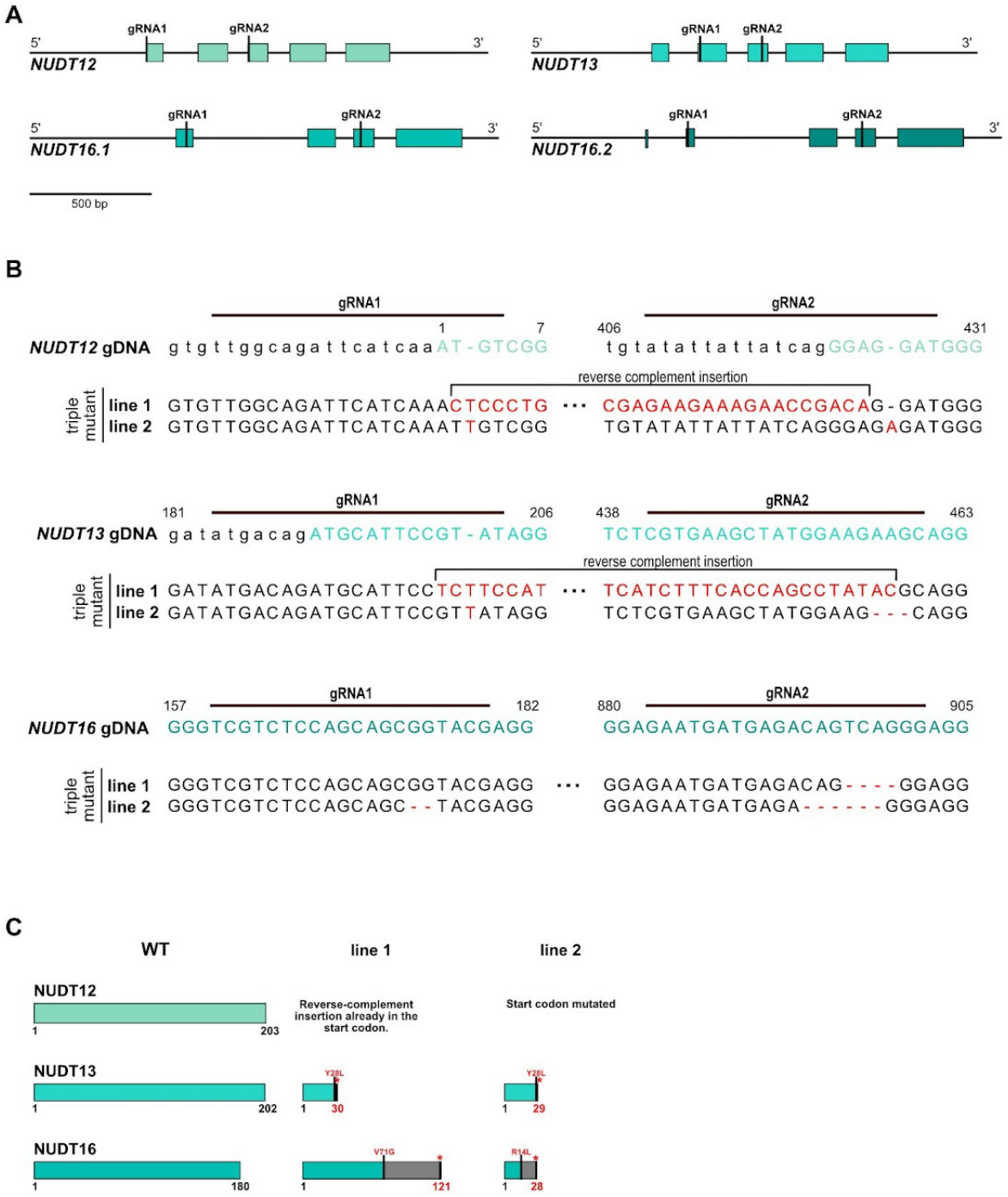

Figure III-S11: Schematic representation of the mutations in four subclade II *nudt12/13/16* mutants. (A) gRNA1 was designed to target the beginning of the open reading frame (ORF), while gRNA2 was designed to target in front or directly the sequence encoding the NUDT motif ($GX_5EX_7REUXEEXGU$, where U represents a hydrophobic amino acid such as leucine, isoleucine or valine and X represents any amino acid). (B) Observed deletions, insertions and point mutations in two *nudt12/13/16* mutants. (C) Predicted amino acids changes.

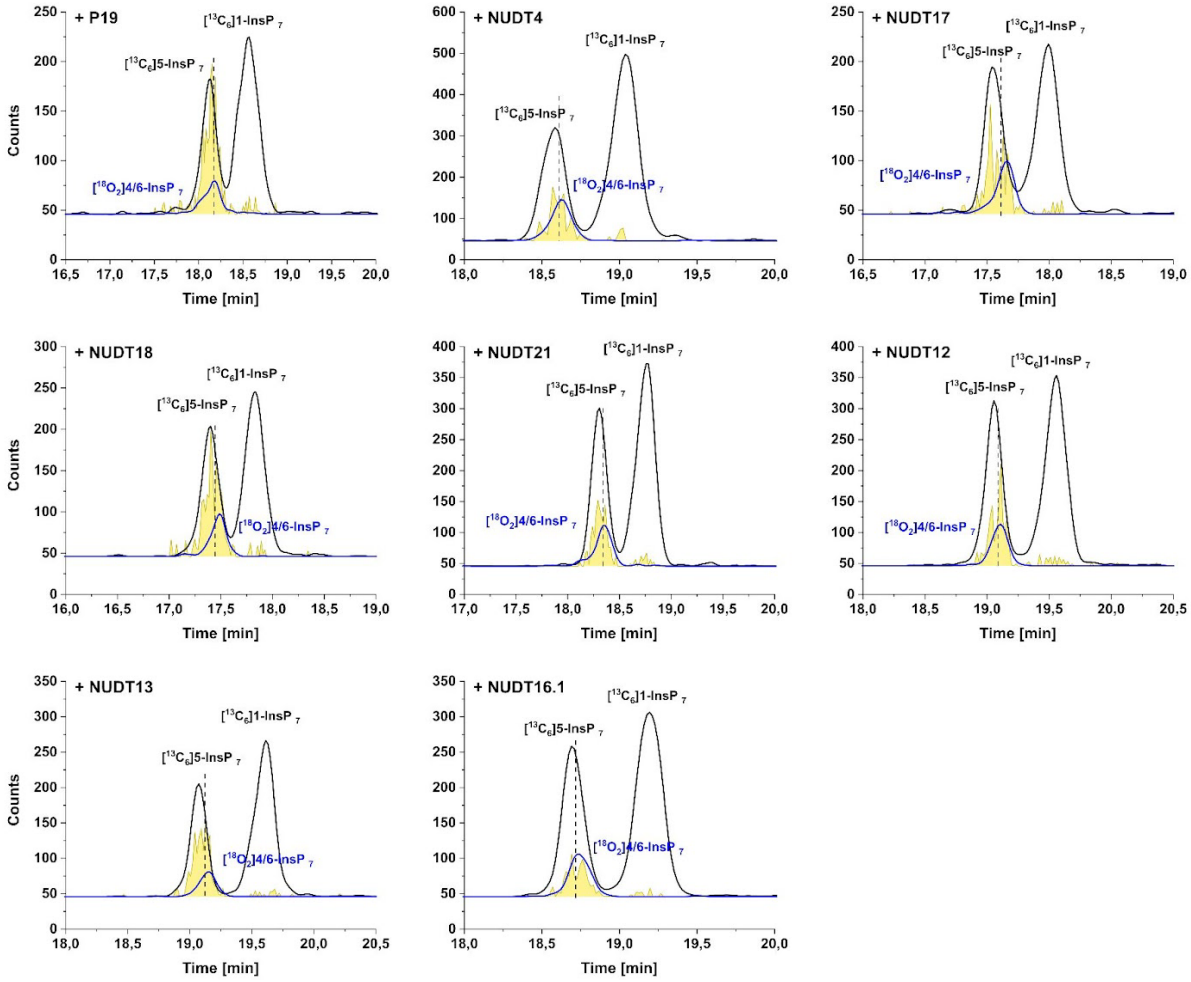

Figure III-S12: Transient expression of NUDTs in *N. benthamiana* reveals PP-InsP activity. Heterologous expression of subclade I and II NUDTs results in 4/6-PP-InsP$_7$ and 5-PP-InsP$_7$ turnover *in planta*. The silencing inhibitor *P19* alone or together with NUDTs were transiently expressed in *N. benthamiana* leaves. 2-3 days post infiltration (dpi) (PP-)InsPs were purified with Nb_2O_5 beads, spiked with isotopic standards mixture ([$^{13}C_6$] 1,5-InsP$_8$, [$^{13}C_6$] 5-InsP$_7$, [$^{18}O_2$] 4-InsP$_7$, [$^{13}C_6$] 1-InsP$_7$, [$^{13}C_6$] InsP$_6$, [$^{13}C_6$] 2-OH InsP$_5$) and subjected to CE-ESI-MS analyses.

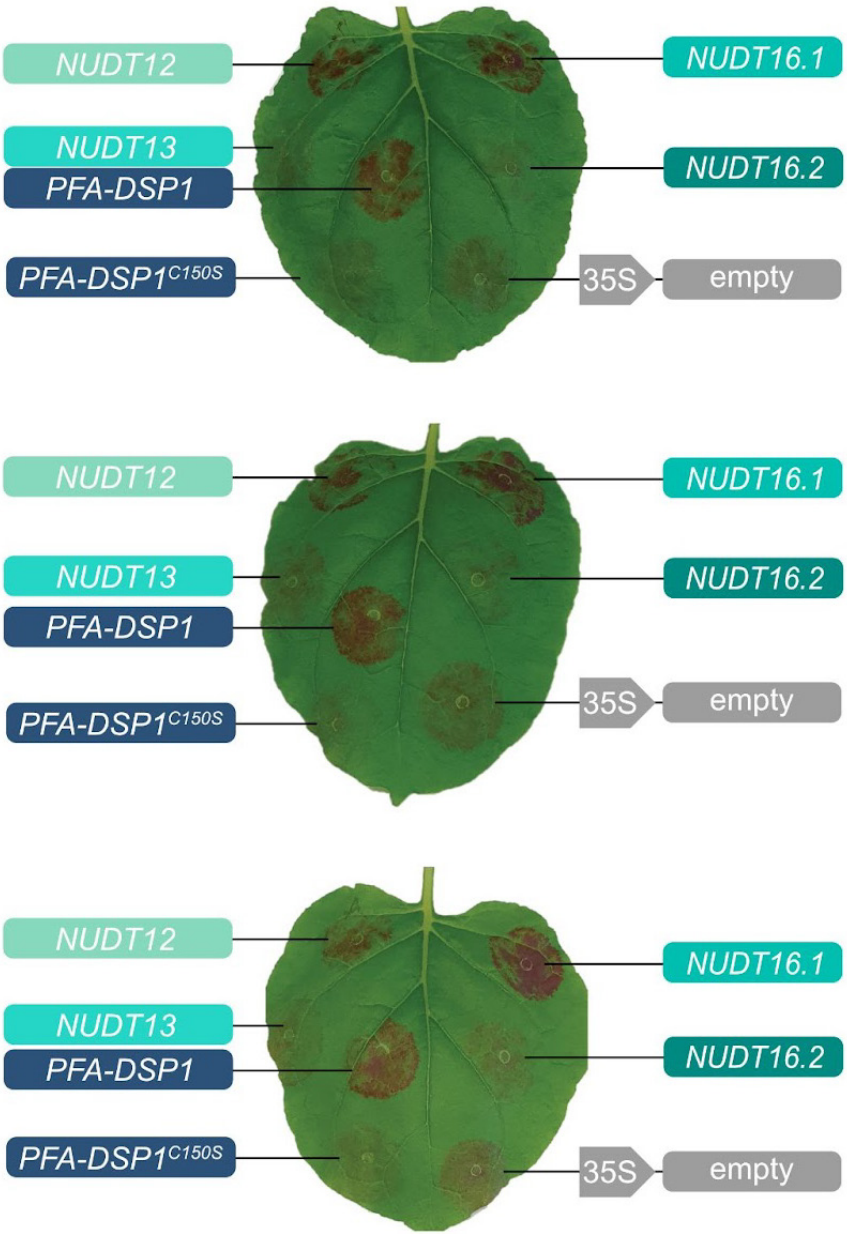

Figure III-S13: Transient co-expression of the *RUBY* reporter with subclade II *NUDT* hydrolase genes under the transcriptional control of the viral CaMV 35S promoter. Co-expression with *PFA-DSP1* served as a positive control, while co-expression with the catalytic inactive *PFA-DSP1*^{C150S} encoding the catalytic inactive protein or an empty vector served as negative controls. The picture was taken 3 dpi.

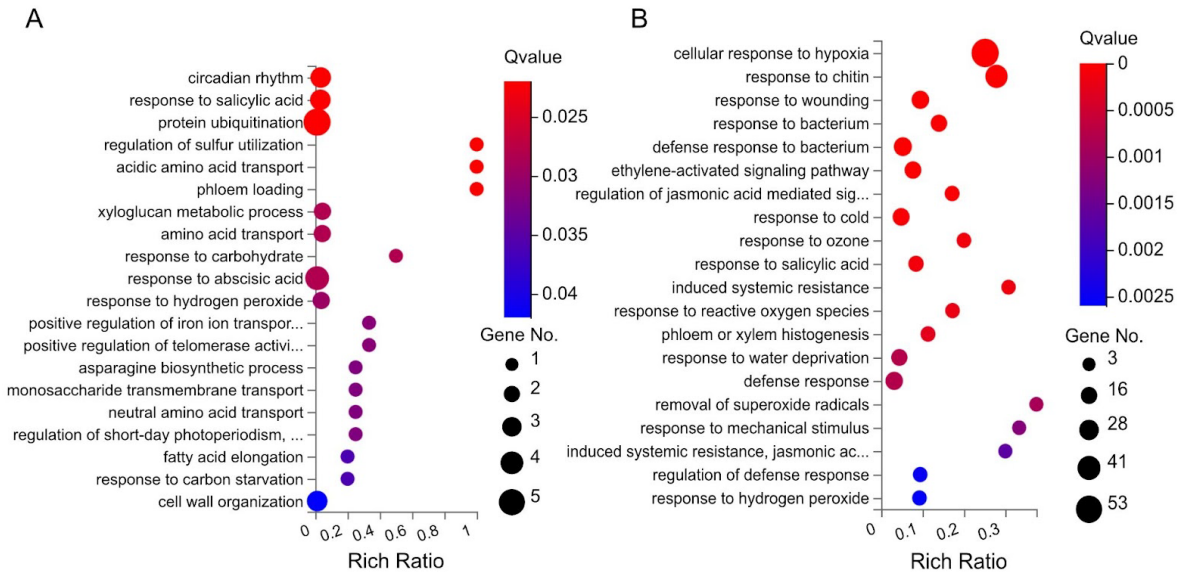

Figure III-S14: GO Enrichment bubble chart of DEGs for (A) upregulated and (B) downregulated genes with $Q < 0.05$ and ($|\log2FC| > 1$), based on Biological Processes (BP) for triple mutant lines. The X-axis represents the enrichment ratio of genes, and the Y-axis represents the GO Term. The size of the bubble represents the number of differential genes annotated to a certain GO Term. The color represents the significance value of enrichment (Q-value), where red indicates smaller significance values.

Table III-S1: List of known and putative Arabidopsis PP-InsP interactors and NUDT hydrolases identified via 5PCP-InsP$_5$ affinity pull-down. Numbers indicate identified peptides.

		Shoot		Root	
Gene Name	**Accession Number**	**Beads**	**Eluate**	**Beads**	**Eluate**
AFB1	AT4G03190.1	8	20	9	20
AFB2	AT3G26810.1	5	3	1	2
AFB3	AT1G12820.1	6	3	1	1
ASK1	AT1G75950.1	5	9	4	10
ASK2	AT5G42190.1	0	7	0	7
COI1	AT2G39940.1	6	10	1	3
CUL1	AT4G02570.4/ AT4G02570.3/ AT4G02570.2/ AT4G02570.1	4	1	1	0
CUL2	AT1G43140.1	2	0	1	0
IPK2α	AT5G07370.4/ AT5G07370.3/ AT5G07370.2/ AT5G07370.1	0	0	3	5
IPK2β	AT5G61760.1	0	2	4	3
ITPK3	AT4G08170.3	0	0	1	0
MIPS3/ MIPS1	AT5G10170.1/ AT4G39800.1	1	0	0	0
NUDT16	AT3G12600.1	0	0	1	0
NUDT17	AT2G01670.1	2	4	0	0
NUDT18	AT1G14860.1	0	1	0	0
NUDT21/ NUDT4	AT1G73540.1/ AT1G18300.1	5	7	0	0
SPX1	AT5G20150.1	1	0	0	0
SPX2	AT2G26660.1	0	0	2	0
VIH1/VIH2	AT5G15070.1/ AT5G15070.2/ AT3G01310.1/ AT3G01310.2	4	4	13	7

Table III-S2: List of DEGs and no-DEGs related to P. Upregulated and downregulated genes have a |log2FC| > 1 and Q-values < 0.05. Non-significant genes have Q-values > 0.05.

	Gene name	Gene ID	log2FC
Upregulated	*SDI1*	AT4G14070	3.07
	AAE15	AT3G47340	2.80
	ASN1	AT2G18700	2.17
	TPS9	AT5G48850	1.67
	TPS11	AT1G23870	1.64
	SDI2	AT1G04770	1.11
Downregulated	*DIC2*	AT5G04340	-3.30
	ZAT6	AT4G24570	-3.06
	GLTP	AT4G39670	-2.98
	TIR-NBS9	AT1G72920	-2.37
		AT4G36010	-2.03
	ACS6	AT4G11280	-1.99
	CaLB1	AT4G34150	-1.85
	DIC1	AT2G22500	-1.84
	PR5	AT1G75040	-1.68
	MYB62	AT1G68320	-1.62
	PAP1	AT2G01180	-1.48
	ATL80	AT1G20823	-1.4
	CaLB domain	AT3G16510	-1.38
	SOT17	AT1G18590	-1.28
	GPAT6	AT2G38110	-1.21
Non-significant	*SPX1*	AT5G20150	
	BAH1	AT1G02860	
	WRKY6	AT1G62300	
	VPT3	AT4G22990	
	PHB	AT2G34710	
	PHT4;5	AT5G20380	
	LPR1	AT1G23010	
	BAK1	AT4G33430	
	PHR2	AT2G47590	
	PAP10	AT2G16430	
	SPX3	AT2G45130	
	STOP1	AT1G34370	
	SIZ1	AT5G60410	
	PHL4	AT2G20400	
	SPX2	AT2G26660	
	PHR1	AT4G28610	
	PEPR2	AT1G17750	
	PBL12	AT2G26290	
	PHO2	AT2G33770	
	VPT1	AT1G63010	
	MYB62	AT1G68320	
	CERK1	AT3G21630	

PHT1;4	AT2G38940
GLP1	AT1G72610
bHLH050	AT1G73830
VIH2	AT3G01310
EAL1	AT4G37650
PHT3;1	AT5G14040
ALS3	AT2G37330
MRP5	AT1G04120
ALMT1	AT1G08430
CLV2	AT1G65380
LPR2	AT1G71040
PAP12	AT2G27190
PHT5	AT2G32830
MOR1	AT2G35630
SPDT	AT3G15990
RALF23	AT3G16570
PHO1	AT3G23430
PHL2	AT3G24120
PHT2;1	AT3G26570
PHL3	AT4G13640
ITPK2	AT4G33770
IPS2	AT5G03545
WRKY75	AT5G13080
VIH1	AT5G15070
SPX4	AT5G15330
ITPK1	AT5G16760
SEC12	AT2G01470
PDR2	AT5G23630

Table III-S3: Most highly downregulated and upregulated genes, defined as |log2FC| > 3.

	Gene name	Gene ID	log2FC
Downregulated	*PAO2*	AT2G43020	-9,57
	U-box E3 ubiquitin	AT3G02840	-4,09
	CMF4	AT1G63820	-3,88
	ATS40-2	AT5G45630	-3,87
	RAS1	AT1G09950	-3,83
	WRKY40	AT1G80840	-3,64
	DVL10	AT4G13395	-3,64
	ERF022	AT1G33760	-3,63
	ERF11	AT1G28370	-3,53
		AT4G29780	-3,52
	IDL7	AT3G10930	-3,49
	CCR4	AT5G47850	-3,44
	DIC2	AT4G24570	-3,29
	DHYPRP1	AT4G22470	-3,27
	DTX50	AT5G52050	-3,10
		AT5G16200	-3,07
	ZAT6	AT5G04340	-3,06
	ZAT10	AT1G27730	-3,01
	ERF6	AT4G17490	-3,01
Upregulated	*SDI1*	AT5G48850	3,06
	IRONMAN 3	AT2G30766	3,71
		AT2G05540	3,78
	LTP3	AT5G59320	4,45
	IRP6	AT5G05250	4,46
		AT5G35935	5,64

Table III-S4: List of DEGs and no-DEGs related to Fe. Upregulated and downregulated genes have a |log2FC| > 1 and Q-values < 0.05. Non-significant genes have Q-values > 0.05.

	Gene name	Gene ID	log2FC
Upregulated	*IRP6*	AT5G05250	4.46
	IRONMAN 3	AT2G30766	3.72
Downregulated	*ZAT12*	AT5G35735	-2.66
	FER1	AT5G01600	-2.02
	HYP1	AT5G59820	-1.30
Non- significant	*NRAMP2*	AT1G47240	
	NAS1	AT5G04950	
	NRAMP1	AT1G80830	
	DEG18	AT4G12980	
	CRR	AT3G25290	
	YSL6	AT3G27020	
	BHLH115	AT1G51070	
	AHA2	AT4G30190	
	BTS	AT3G18290	
	AHA8	AT3G42640	
	BHLH38	AT3G56970	
	YSL2	AT5G24380	
	AHA10	AT1G17260	
	LPR1	AT1G23010	
	IRT3	AT1G60960	
	AIR12	AT3G07390	
	COSY	AT1G28680	
	VTL1	AT1G21140	
	MYB10	AT3G12820	
	BHLH34	AT3G23210	
	CIPK11	AT2G30360	
	AHA1	AT2G18960	
	VTL2	AT1G76800	
	YSL5	AT3G17650	
	CYBDOMs	AT5G54830	
	YSL3	AT5G53550	
	NAS4	AT1G56430	
	AHA3	AT5G57350	
	IRONMAN 2	AT1G47395	
	BHLH121	AT3G19860	
	BHLH29	AT2G28160	
	BHLH105	AT5G54680	
	PYE	AT3G47640	
	AHA4	AT3G47950	
	BHLH100	AT2G41240	
	CYBDOMs	AT5G47530	
	YSL4	AT5G41000	
	YSL1	AT4G24120	

AHA5	AT2G24520
AHA9	AT1G80660
AHA11	AT5G62670
YSL8	AT1G48370
YSL7	AT1G65730
IRONMAN 1	AT1G47400
NRAMP6	AT1G15960
BHLH39	AT3G56980
NAS3	AT1G09240
BTSL2	AT1G18910
LPR2	AT1G71040
BTSL1	AT1G74770
NRAMP3	AT2G23150
CYBDOMs	AT3G07570
FRD3	AT3G08040
F6'H1	AT3G13610
VTL5	AT3G25190
PDR9	AT3G53480
MTP8	AT3G58060
CYBDOMs	AT3G59070
AHA7	AT3G60330
BHLH104	AT4G14410
CYBDOMs	AT4G17280
NRAMP5	AT4G18790
IRT1	AT4G19690
BHLH101	AT5G04150
ZIF1	AT5G13740
NRAMP4	AT5G67330

Table III-S5: List of primers used in this study.

Target gene	Objective	Primer sequence 5'-3'
NUDT4	attb1 cDNA	AAAAAGCAGGCTTC ATGACAGGGTTCTCTGTGTC
	attb1 promoter	AAAAAGCAGGCTTCGTCCGACTTTAAAGAGAAATTGAGG
	attb2 stop	AGAAAGCTGGGTCTCAGTTCCCACTTTCATCATCG
	attb2 no stop	AGAAAGCTGGGTCGTTCCCACTTTCATCATCGTC
	attb2 no stop V5	ACCTCCTCCAGATCCGTTCCCACTTTCATCATCGTC
	genotyping	F: AAAAAGCAGGCTTCGTCCGACTTTAAAGAGAAATTGAGG R: AGAAAGCTGGGTC GTTCCCACTTTCATCATCGTC Seq: ACTCTTTCTCTCTTGTTCTG
NUDT17	attb1 cDNA	AAAAAGCAGGCTTCATGGGTGTTGAGAAAATGGTG
	attb1 promoter	AAAAAGCAGGCTTCGTCGTATTGTATGTTCCATGC
	attb2 stop	AGAAAGCTGGGTCTCAACACATTGTTTCAATAGAGATTG
	attb2 no stop	AGAAAGCTGGGTCACACATTGTTTCAATAGAGATTGAC
	attb2 no stop V5	ACCTCCTCCAGATCCACACATTGTTTCAATAGAGATTGAC
	genotyping	F: AAAAAGCAGGCTTC GTCGTATTGTATGTTCCATGC R: AGAAAGCTGGGTC TCAACACATTGTTTCAATAGAGATTG Seq: CATCAGACCCTTCTCTTCTC
NUDT18	attb1 cDNA	AAAAAGCAGGCTTC ATGGTGTGTTTGGTCTCCC
	attb1 promoter	AAAAAGCAGGCTTC GAGCTTCTTCTAGATCGAGCTG
	attb2 stop	AGAAAGCTGGGTC TCAGTAGATAGAGATCAGTGGAAG
	attb2 no stop	AGAAAGCTGGGTC GTAGATAGAGATCAGTGGAAGGTTC
	attb2 no stop V5	ACCTCCTCCAGATCCGTAGATAGAGATCAGTGGAAGGTTC
	genotyping	F: GGATAAGCCGCAAGGAGG R: TTTCCAAGTTGTCTCTGCACC Seq: CTCACCCCATCATAACTTC
NUDT21	attb1 cDNA	AAAAAGCAGGCTTCATGATTTCTCTATTCATCTCAAACTTTTC
	attb1 promoter	AAAAAGCAGGCTTCCTCCGTAAATACCGTGTTGG
	attb2 stop	AGAAAGCTGGGTCTTATTGGGTCTGGCATTTCC
	attb2 no stop	AGAAAGCTGGGTCTTGGGTCTGGCATTTCC
	attb2 no stop V5	ACCTCCTCCAGATCCTTGGGTCTGGCATTTCC
	genotyping	F: AAAAAGCAGGCTTC CTCCGTAAATACCGTGTTGG R: AGAAAGCTGGGTC TTATTGGGTCTGGCATTTCC Seq: ATAAAGACGCTCGCAAAC
NUDT12	attb1 cDNA	AAAAAGCAGGCTTCATGTCGGTTCTTTCTTCTCG
	attb1 promoter	AAAAAGCAGGCTTCCCCTTCTGTTTCGTACATGC
	attb2 stop	AGAAAGCTGGGTCCTAGTTAACTACAAAACAGTACCAAGG
	attb2 no stop	AGAAAGCTGGGTCGTTAACTACAAAACAGTACCAAGG
	attb2 no stop V5	ACCTCCTCCAGATCCGTTAACTACAAAACAGTACCAAGG
	qPCR	F: AACTCGAGGATTGGCCAGAGCGA
		R: CCGACAAAGCTCCAACGCTTCT
	genotyping	F: CCCTTCTGTTTCGTACATGC R: CTAGTTAACTACAAAACAGTACCAAGG Seq: CCCTGACTGTCTCATCATTC
NUDT13	attb1 cDNA	AAAAAGCAGGCTTCATGTCGAATCTTTCTGCAAG
	attb1 promoter	AAAAAGCAGGCTTCGGGGACATTTGTTCTACACAG
	attb2 stop	AGAAAGCTGGGTCTTAGACTACAAAGCAGTAGCG
	attb2 no stop	AGAAAGCTGGGTCGACTACAAAGCAGTAGCGAG

	attb2 no stop V5	ACCTCCTCCAGATCCGACTACAAAGCAGTAGCGAG
	qPCR	F: AGGCTGGTGAAAGATGAAGAAGA
		R: TCCCATCCTCCCTTTGGGAA
	genotyping	F: ATGTCGAATCTTTCTGCAAG R: TTAGACTACAAAGCAGTAGCG Seq: TTAGACTACAAAGCAGTAGCG
NUDT16 both	attb1 promoter	AAAAAGCAGGCTTCCAATTACCTGCGATCTCTCTCTG
	attb2 stop	AGAAAGCTGGGTCTCAATGTTCACCAGTTATCTCCTCTCC
	attb2 NS	AGAAAGCTGGGTCATGTTCACCAGTTATCTCCTCTCC
	attb2 NS V5	ACCTCCTCCAGATCCATGTTCACCAGTTATCTCCTCTCC
	qPCR	F: CGCCGGGTGTATTCCGTTTA
		R: AGGTCCACTAGACGAGCTGA
	genotyping	F: CAATTACCTGCGATCTCTCTCTG R: ATGTTCACCAGTTATCTCCTCTCC Seq: AGCTATAGACAGACACACCC
NUDT16.1	attb1 cDNA	AAAAAGCAGGCTTCATGTGTGATTTGGTCGCGCG
	qPCR	F: TGTCTCCAAGCTGGGTGTTT
		R: CGCGACCAAATCACACATGA
NUDT16.2	attb1 cDNA	AAAAAGCAGGCTTCATGGTAGAGCAGCGGTACGAG
General	attb1 adapter	GGGGACAAGTTTGTACAAAAAAGCAGGCTTC
	attb1 adapter	GGGGACCACTTTGTACAAGAAAGCTGGGTC
	attb2 V5 adapter	GGGGACCACTTTGTACAAGAAAGCTGGGTCTTAC GTAGAATCGAGACCGAGGAGAGGGTTAGGGATA GGCTTACCTCCTCCAGATCC
ACTIN2	qPCR	F: GACCAGCTCTTCCATCGAGAA
		R: CAAACGAGGGCTGGAACAAG
UBQ2	qPCR	F: AGACGAACGCAAAGATGCAG
		R: CCGGCGAAGATCAACCTCTG

Line/Plasmid	**Primer Sequence**
SALK_102051.27.90.x	F: CAACAACGTTTGGGCTTCTAG
	R: ATTGTGAATTTGAACAACGGC
SAIL_1211_A06	F: TTGGTGGTTTACGAGTTGACC
	R: TCAACACGTTATTCCAAATTGC
SAIL_500_D10	F: GAAAAATTGCTCCACACTTGC
	R: TGAAGAAGAACGTACCCAACG
SALKseq_117563.1	F: AAACCAAACCGAAATCCAAAC
	R: AGATCCTCCTTCCCTTTAGCC
SALK_031788.56.00.x	F: TCACCCACTTGCTTGCTACTC
	R: TGCTTTTGTATTGCCATTTCC
SALKseq_132932.101	F: AAATACCGTGTTGGCATGAAC
	R: TGCTTTTGTATTGCCATTTCC
oRU906	GAGTCTATGATCAAGTAATTATGC
oRU908	GCTTGCATGCCTGCAGGTCGACTCT
oRU385	CAACGCGTTGGGAGCTCTCCCATATG
LBa1 SALK	TGGTTCACGTAGTGGGCC
LB2 SAIL	GCTTCCTATTATATCTTCCCAAATTACCAATACA

Table III-S6: List of primers used to generate sgRNAs for the *NUDT* knockout mutants. Overhangs for oligo annealing are highlighted.

Target gene	gRNA	Primer
NUDT17	sgRNA1	F: **ATTG** CAGTTTCAGAGATACAACAA
		R: **AAAC** TTGTTGTATCTCTGAAACTG
NUDT17	sgRNA2	F: **GTCA** CCACGCCTTAATGTTCCCCA
		R: **AAAC** TGGGGAACATTAAGGCGTGG
NUDT18	sgRNA1	F: **ATTG** CAATCCCAAAGATACAACAA
		R: **AAAC** TTGTTGTATCTTTGGGATTG
NUDT18	sgRNA2	F: **GTCA** TCACGCTCTGATGTTCCCAA
		R: **AAAC** TTGGGAACATCAGAGCGTGA
NUDT21	sgRNA1	F: **ATTG** CCCATCGAAGAAGATCGTAC
		R: **AAAC** GTACGATCTTCTTCGATGGG
NUDT21	sgRNA2	F: **GTCA** TATAGATACAAGAAACACGG
		R: **AAAC** CCGTGTTTCTTGTATCTATA
NUDT4	sgRNA1	F: **ATTG** GAAGATGGGCGACAAATACG
		R: **AAAC** CGTATTTGTCGCCCATCTTC
NUDT4	sgRNA2	F: **GTCA** GGAGACGGATGAATCAATGG
		R: **AAAC** CCATTGATTCATCCGTCTCC
NUDT12	sgRNA1	F: **ATTG** TTGGCAGATTCATCAAATGT
		R: **AAAC** ACATTTGATGAATCTGCCAA
NUDT12	sgRNA2	F: **GTCA** ATATTATTATCAGGGAGGAT
		R: **AAAC** ATCCTCCCTGATAATAATAT
NUDT13	sgRNA1	F: **ATTG** ATGACAGATGCATTCCGTAT
		R: **AAAC** ATACGGAATGCATCTGTCAT
NUDT13	sgRNA2	F: **GTCA** CGTGAAGCTATGGAAGAAGC
		R: **AAAC** GCTTCTTCCATAGCTTCACG
NUDT16	sgRNA1	F: **ATTG** TCGTCTCCAGCAGCGGTACG
		R: **AAAC** CGTACCGCTGCTGGAGACGA
NUDT16	sgRNA2	F: **GTCA** GAATGATGAGACAGTCAGGG
		R: **AAAC** CCCTGACTGTCTCATCATTC

References

Alberti, S., Gitler, A. D. and Lindquist, S. (2007). A suite of Gateway cloning vectors for high-throughput genetic analysis in *Saccharomyces cerevisiae*. Yeast (Chichester, England). 10.1002/yea.1502.

Andreeva, N., Ledova, L., Ryazanova, L., Tomashevsky, A., Kulakovskaya, T. and Eldarov, M. (2019). Ppn2 endopolyphosphatase overexpressed in *Saccharomyces cerevisiae*: Comparison with Ppn1, Ppx1, and Ddp1 polyphosphatases. Biochimie. 10.1016/j.biochi.2019.06.001.

Audic, S. and Claverie, J. M. (1997). The significance of digital gene expression profiles. Genome research. 10.1101/gr.7.10.986.

Azevedo, C. and Saiardi, A. (2006). Extraction and analysis of soluble inositol polyphosphates from yeast. Nature Protocols. 10.1038/nprot.2006.337.

Blüher, D., Laha, D., Thieme, S., Hofer, A., Eschen-Lippold, L., Masch, A., Balcke, G., Pavlovic, I., Nagel, O., Schonsky, A., Hinkelmann, R., Wörner, J., Parvin, N., Greiner, R., Weber, S., Tissier, A., Schutkowski, M., Lee, J., Jessen, H., Schaaf, G. and Bonas, U. (2017). A 1-phytase type III effector interferes with plant hormone signaling. Nature Communications. 10.1038/s41467-017-02195-8.

Briat, J.-F., Duc, C., Ravet, K. and Gaymard, F. (2010). Ferritins and iron storage in plants. Biochimica et biophysica acta. Advanced Access published December 21, 2009: 10.1016/j.bbagen.2009.12.003.

Bustos, R., Castrillo, G., Linhares, F., Puga, M. I., Rubio, V., Pérez-Pérez, J., Solano, R., Leyva, A. and Paz-Ares, J. (2010). A Central Regulatory System Largely Controls Transcriptional Activation and Repression Responses to Phosphate Starvation in Arabidopsis. PLoS Genetics. 10.1371/journal.pgen.1001102.

Capolicchio, S., Thakor, D. T., Linden, A. and Jessen, H. J. (2013). Synthesis of Unsymmetric Diphospho-Inositol Polyphosphates. Angewandte Chemie International Edition. 10.1002/anie.201301092.

Capolicchio, S., Wang, H., Thakor, D. T., Shears, S. B. and Jessen, H. J. (2014). Synthesis of Densely Phosphorylated Bis-1,5-Diphospho-*myo*-Inositol Tetrakisphosphate and its Enantiomer by Bidirectional P-Anhydride Formation. Angewandte Chemie International Edition. 10.1002/anie.201404398.

Chabert, V., Kim, G.-D., Qiu, D., Liu, G., Michaillat Mayer, L., Jamsheer K, M., Jessen, H. J. and Mayer, A. (2023). Inositol pyrophosphate dynamics reveals control of the yeast phosphate starvation program through 1,5-IP_8 and the SPX domain of Pho81. eLife. 10.7554/eLife.87956.3.

Chen, Y., Chen, Y., Shi, C., Huang, Z., Zhang, Y., Li, S., Li, Y., Ye, J., Yu, C., Li, Z., Zhang, X., Wang, J., Yang, H., Fang, L. and Chen, Q. (2018). SOAPnuke: a MapReduce acceleration-supported software for integrated quality control and preprocessing of high-throughput sequencing data. GigaScience. 10.1093/gigascience/gix120.

Couso, I., Evans, B. S., Li, J., Liu, Y., Ma, F., Diamond, S., Allen, D. K. and Umen, J. G. (2016). Synergism between Inositol Polyphosphates and TOR Kinase Signaling in Nutrient Sensing, Growth Control, and Lipid Metabolism in Chlamydomonas. The Plant Cell. 10.1105/tpc.16.00351.

Cox, J. and Mann, M. (2008). MaxQuant enables high peptide identification rates, individualized p.p.b.-range mass accuracies and proteome-wide protein quantification. Nature biotechnology. Advanced Access published November 30, 2008: 10.1038/nbt.1511.

Desai, M., Rangarajan, P., Donahue, J. L., Williams, S. P., Land, E. S., Mandal, M. K., Phillippy, B. Q., Perera, I. Y., Raboy, V. and Gillaspy, G. E. (2014). Two inositol hexakisphosphate kinases drive inositol pyrophosphate synthesis in plants. The Plant Journal. 10.1111/tpj.12669.

Dollins, D. E., Bai, W., Fridy, P. C., Otto, J. C., Neubauer, J. L., Gattis, S. G., Mehta, K. P. M. and York, J. D. (2020). Vip1 is a kinase and pyrophosphatase switch that regulates inositol diphosphate signaling. Proceedings of the National Academy of Sciences. Advanced Access published April 17, 2020: 10.1073/pnas.1908875117.

Dong, J., Ma, G., Sui, L., Wei, M., Satheesh, V., Zhang, R., Ge, S., Li, J., Zhang, T.-E., Wittwer, C., Jessen, H. J., Zhang, H., An, G.-Y., Chao, D.-Y., Liu, D. and Lei, M. (2019). Inositol Pyrophosphate $InsP_8$ Acts as an Intracellular Phosphate Signal in Arabidopsis. Molecular Plant. 10.1016/j.molp.2019.08.002.

Fridy, P. C., Otto, J. C., Dollins, D. E. and York, J. D. (2007). Cloning and Characterization of Two Human VIP1-like Inositol Hexakisphosphate and Diphosphoinositol Pentakisphosphate Kinases. Journal of Biological Chemistry. 10.1074/jbc.m704656200.

Furkert, D., Nadler-Holly, M. and Fiedler, D. (2021). Affinity enrichment and identification of inositol poly- and pyrophosphate interactomes. STAR protocols. Advanced Access published January 14, 2021: 10.1016/j.xpro.2020.100277.

Gaugler, P., Gaugler, V., Kamleitner, M. and Schaaf, G. (2020). Extraction and Quantification of Soluble, Radiolabeled Inositol Polyphosphates from Different Plant Species using SAX-HPLC. Journal of Visualized Experiments. 10.3791/61495.

Gaugler, P., Schneider, R., Liu, G., Qiu, D., Weber, J., Schmid, J., Jork, N., Häner, M., Ritter, K., Fernández-Rebollo, N., Giehl, R. F. H., Trung, M. N., Yadav, R., Fiedler, D., Gaugler, V., Jessen, H. J., Schaaf, G. and Laha, D. (2022). Arabidopsis PFA-DSP-Type Phosphohydrolases Target Specific Inositol Pyrophosphate Messengers. Biochemistry. Advanced Access published May 31, 2022: 10.1021/acs.biochem.2c00145.

Gerasimaite, R., Pavlovic, I., Capolicchio, S., Hofer, A., Schmidt, A., Jessen, H. J. and Mayer, A. (2017). Inositol Pyrophosphate Specificity of the SPX-Dependent Polyphosphate Polymerase VTC. ACS Chemical Biology. 10.1021/acschembio.7b00026.

Grillet, L., Lan, P., Li, W., Mokkapati, G. and Schmidt, W. (2018). IRON MAN is a ubiquitous family of peptides that control iron transport in plants. Nature plants. Advanced Access published October 15, 2018: 10.1038/s41477-018-0266-y.

Gulabani, H., Goswami, K., Walia, Y., Roy, A., Noor, J. J., Ingole, K. D., Kasera, M., Laha, D., Giehl, R. F. H., Schaaf, G. and Bhattacharjee, S. (2021). Arabidopsis inositol polyphosphate kinases IPK1 and ITPK1 modulate crosstalk between SA-dependent immunity and phosphate-starvation responses. Plant Cell Reports. 10.1007/s00299-021-02812-3.

Hawkesford, M. J., Cakmak, I., Coskun, D., De Kok, L. J., Lambers, H., Schjoerring, J. K. and White, P. J. Chapter 6 - Functions of macronutrients. This chapter is a revision of the third edition chapter by M. Hawkesford, W. Horst, T. Kichey, H. Lambers, J. Schjoerring, I. Skrumsager Møller, and P. White, pp. 135–189. DOI: https://doi.org/10.1016/B978-0-12-384905-2.00006-6. © Elsevier Ltd. In Rengel, Z., Cakmak, I., White, P. (eds.), Marschner's Mineral Nutrition of Plants. San Diego: Academic Press, pp. 201–281.

He, Y., Zhang, T., Sun, H., Zhan, H. and Zhao, Y. (2020). A reporter for noninvasively monitoring gene expression and plant transformation. Horticulture research. Advanced Access published September 19, 2020: 10.1038/s41438-020-00390-1.

Hirayama, T., Lei, G. J., Yamaji, N., Nakagawa, N. and Ma, J. F. (2018). The Putative Peptide Gene FEP1 Regulates Iron Deficiency Response in Arabidopsis. Plant & cell physiology. 10.1093/pcp/pcy145.

Kilari, R. S., Weaver, J. D., Shears, S. B. and Safrany, S. T. (2013). Understanding inositol pyrophosphate metabolism and function: Kinetic characterization of the DIPPs. FEBS Letters. 10.1016/j.febslet.2013.08.035.

Kilian, J., Whitehead, D., Horak, J., Wanke, D., Weinl, S., Batistic, O., D'Angelo, C., Bornberg-Bauer, E., Kudla, J. and Harter, K. (2007). The AtGenExpress global stress expression data set: protocols, evaluation and model data analysis of UV-B light, drought and cold stress responses. The Plant journal: for cell and molecular biology. Advanced Access published March 21, 2007: 10.1111/j.1365-313X.2007.03052.x.

Kim, G., Liu, G., Qiu, D., Gopaldass, N., Leo, G. de**, Hermes, J., Timmer, J., Saiardi, A., Mayer, A. and Jessen, H. J.** (2024). Pools of independently cycling inositol phosphates revealed by pulse labeling with ^{18}O-water.

Laha, D., Johnen, P., Azevedo, C., Dynowski, M., Weiß, M., Capolicchio, S., Mao, H., Iven, T., Steenbergen, M., Freyer, M., Gaugler, P., Campos, M. K. de**, Zheng, N., Feussner, I., Jessen, H. J., van Wees, S. C., Saiardi, A. and Schaaf, G.** (2015). VIH2 Regulates the Synthesis of Inositol Pyrophosphate $InsP_8$ and Jasmonate-Dependent Defenses in Arabidopsis. The Plant Cell. 10.1105/tpc.114.135160.

Laha, D., Parvin, N., Dynowski, M., Johnen, P., Mao, H., Bitters, S. T., Zheng, N. and Schaaf, G. (2016). Inositol Polyphosphate Binding Specificity of the Jasmonate Receptor Complex. Plant Physiology. 10.1104/pp.16.00694.

Laha, D., Parvin, N., Hofer, A., Giehl, R. F. H., Fernandez-Rebollo, N., von Wirén, N., Saiardi, A., Jessen, H. J. and Schaaf, G. (2019). Arabidopsis ITPK1 and ITPK2 Have an Evolutionarily Conserved Phytic Acid Kinase Activity. ACS Chemical Biology. 10.1021/acschembio.9b00423.

Laha, N. P., Giehl, R. F. H., Riemer, E., Qiu, D., Pullagurla, N. J., Schneider, R., Dhir, Y. W., Yadav, R., Mihiret, Y. E., Gaugler, P., Gaugler, V., Mao, H., Zheng, N., von Wirén, N., Saiardi, A., Bhattacharjee, S., Jessen, H. J., Laha, D. and Schaaf, G. (2022). INOSITOL (1,3,4) TRIPHOSPHATE 5/6 KINASE1-dependent inositol polyphosphates regulate auxin responses in Arabidopsis. Plant Physiology. 10.1093/plphys/kiac425.

Lee, Y.-S., Mulugu, S., York, J. D. and O'Shea, E. K. (2007). Regulation of a cyclin-CDK-CDK inhibitor complex by inositol pyrophosphates. Science (New York, N.Y.). 10.1126/science.1139080.

Li, X., Gu, C., Hostachy, S., Sahu, S., Wittwer, C., Jessen, H. J., Fiedler, D., Wang, H. and Shears, S. B. (2020). Control of XPR1-dependent cellular phosphate efflux by $InsP_8$ is an exemplar for functionally-exclusive inositol pyrophosphate signaling. Proceedings of the National Academy of Sciences. Advanced Access published February 4, 2020: 10.1073/pnas.1908830117.

Liu, F., Wang, Z., Ren, H., Shen, C., Li, Y., Ling, H.-Q., Wu, C., Lian, X. and Wu, P. (2010). OsSPX1 suppresses the function of OsPHR2 in the regulation of expression of OsPT2 and phosphate homeostasis in shoots of rice. The Plant Journal. Advanced Access published February 9, 2010: 10.1111/j.1365-313X.2010.04170.x.

Lonetti, A., Szijgyarto, Z., Bosch, D., Loss, O., Azevedo, C. and Saiardi, A. (2011). Identification of an Evolutionarily Conserved Family of Inorganic Polyphosphate Endopolyphosphatases. Journal of Biological Chemistry. 10.1074/jbc.m111.266320.

Love, M. I., Huber, W. and Anders, S. (2014). Moderated estimation of fold change and dispersion for RNA-seq data with DESeq2. Genome biology. 10.1186/s13059-014-0550-8.

Luo, Y., Qin, G., Zhang, J., Liang, Y., Song, Y., Zhao, M., Tsuge, T., Aoyama, T., Liu, J., Gu, H. and Qu, L.-J. (2011). D-*myo*-inositol-3-phosphate affects phosphatidylinositol-mediated endomembrane function in Arabidopsis and is essential for auxin-regulated embryogenesis. The Plant Cell. Advanced Access published April 19, 2011: 10.1105/tpc.111.083337.

Lv, Q., Zhong, Y., Wang, Y., Wang, Z., Zhang, L., Shi, J., Wu, Z., Liu, Y., Mao, C., Yi, K. and Wu, P. (2014). SPX4 Negatively Regulates Phosphate Signaling and Homeostasis through Its Interaction with PHR2 in Rice. The Plant Cell. Advanced Access published April 1, 2014: 10.1105/tpc.114.123208.

MacDonald, G. K., Bennett, E. M., Potter, P. A. and Ramankutty, N. (2011). Agronomic phosphorus imbalances across the world's croplands. Proceedings of the National Academy of Sciences. Advanced Access published January 31, 2011: 10.1073/pnas.1010808108.

MacLean, B., Tomazela, D. M., Shulman, N., Chambers, M., Finney, G. L., Frewen, B., Kern, R., Tabb, D. L., Liebler, D. C. and MacCoss, M. J. (2010). Skyline: an open source document editor for creating and analyzing targeted proteomics experiments. Bioinformatics (Oxford, England). Advanced Access published February 9, 2010: 10.1093/bioinformatics/btq054.

McCombe, C. L., Wegner, A., Zamora, C. S., Casanova, F., Aditya, S., Greenwood, J. R., Wirtz, L., Paula, S. de**, England, E., Shang, S., Ericsson, D. J., Oliveira-Garcia, E., Williams, S. J. and Schaffrath, U.** (2023). Plant pathogenic fungi hijack phosphate starvation signaling with conserved enzymatic effectors.

Menniti, F. S., Miller, R. N., Putney, J. W. and Shears, S. B. (1993). Turnover of inositol polyphosphate pyrophosphates in pancreatoma cells. Journal of Biological Chemistry. 10.1016/s0021-9258(18)53551-1.

Mulugu, S., Bai, W., Fridy, P. C., Bastidas, R. J., Otto, J. C., Dollins, D. E., Haystead, T. A., Ribeiro, A. A. and York, J. D. (2007). A Conserved Family of Enzymes That Phosphorylate Inositol Hexakisphosphate. Science. 10.1126/science.1139099.

Ogawa, T., Ueda, Y., Yoshimura, K. and Shigeoka, S. (2005). Comprehensive analysis of cytosolic Nudix hydrolases in *Arabidopsis thaliana*. The Journal of biological chemistry. Advanced Access published May 5, 2005: 10.1074/jbc.M503536200.

Osorio, M. B., Ng, S., Berkowitz, O., Clercq, I. de**, Mao, C., Shou, H., Whelan, J. and Jost, R.** (2019). SPX4 Acts on PHR1-Dependent and -Independent Regulation of Shoot Phosphorus Status in Arabidopsis. Plant Physiology. Advanced Access published July 1, 2019: 10.1104/pp.18.00594.

Pascual-Ortiz, M., Saiardi, A., Walla, E., Jakopec, V., Künzel, N. A., Span, I., Vangala, A. and Fleig, U. (2018). Asp1 Bifunctional Activity Modulates Spindle Function via Controlling Cellular Inositol Pyrophosphate Levels in *Schizosaccharomyces pombe*. Molecular and Cellular Biology. 10.1128/mcb.00047-18.

Pipercevic, J., Kohl, B., Gerasimaite, R., Comte-Miserez, V., Hostachy, S., Müntener, T., Agustoni, E., Jessen, H. J., Fiedler, D., Mayer, A. and Hiller, S. (2023). Inositol pyrophosphates activate the vacuolar transport chaperone complex in yeast by disrupting a homotypic SPX domain interaction. Nature Communications. Advanced Access published May 8, 2023: 10.1038/s41467-023-38315-w.

Puga, M. I., Mateos, I., Charukesi, R., Wang, Z., Franco-Zorrilla, J. M., Lorenzo, L. de**, Irigoyen, M. L., Masiero, S., Bustos, R., Rodríguez, J., Leyva, A., Rubio, V., Sommer, H. and Paz-Ares, J.** (2014). SPX1 is a phosphate-dependent inhibitor of PHOSPHATE STARVATION RESPONSE 1 in Arabidopsis. Proceedings of the National Academy of Sciences. 10.1073/pnas.1404654111.

Qi, W., Manfield, I. W., Muench, S. P. and Baker, A. (2017). AtSPX1 affects the AtPHR1-DNA-binding equilibrium by binding monomeric AtPHR1 in solution. Biochemical Journal. Advanced Access published October 23, 2017: 10.1042/BCJ20170522.

Qin, N., Li, L., Ji, X., Pereira, R., Chen, Y., Yin, S., Li, C., Wan, X., Qiu, D., Jiang, J., Luo, H., Zhang, Y., Dong, G., Zhang, Y., Shi, S., Jessen, H. J., Xia, J., Chen, Y., Larsson, C., Tan, T., Liu, Z. and Nielsen, J. (2023). Flux regulation through glycolysis and respiration is balanced by inositol pyrophosphates in yeast. Cell. Advanced Access published February 8, 2023: 10.1016/j.cell.2023.01.014.

Qiu, D., Gu, C., Liu, G., Ritter, K., Eisenbeis, V. B., Bittner, T., Gruzdev, A., Seidel, L., Bengsch, B., Shears, S. B. and Jessen, H. J. (2023). Capillary electrophoresis mass spectrometry identifies new isomers of inositol pyrophosphates in mammalian tissues. Chemical science. Advanced Access published December 5, 2022: 10.1039/D2SC05147H.

Qiu, D., Wilson, M. S., Eisenbeis, V. B., Harmel, R. K., Riemer, E., Haas, T. M., Wittwer, C., Jork, N., Gu, C., Shears, S. B., Schaaf, G., Kammerer, B., Fiedler, D., Saiardi, A. and Jessen, H. J. (2020). Analysis of inositol phosphate metabolism by capillary electrophoresis electrospray ionization mass spectrometry. Nature Communications. 10.1038/s41467-020-19928-x.

Rappsilber, J., Ishihama, Y. and Mann, M. (2003). Stop and go extraction tips for matrix-assisted laser desorption/ionization, nanoelectrospray, and LC/MS sample pretreatment in proteomics. Analytical chemistry. 10.1021/ac026117i.

Ried, M. K., Wild, R., Zhu, J., Pipercevic, J., Sturm, K., Broger, L., Harmel, R. K., Abriata, L. A., Hothorn, L. A., Fiedler, D., Hiller, S. and Hothorn, M. (2021). Inositol pyrophosphates promote the interaction of SPX domains with the coiled-coil motif of PHR transcription factors to regulate plant phosphate homeostasis. Nature Communications. 10.1038/s41467-020-20681-4.

Riemer, E., Qiu, D., Laha, D., Harmel, R. K., Gaugler, P., Gaugler, V., Frei, M., Hajirezaei, M.-R., Laha, N. P., Krusenbaum, L., Schneider, R., Saiardi, A., Fiedler, D., Jessen, H. J., Schaaf, G. and Giehl, R. F. (2021). ITPK1 is an $InsP_6$/ADP phosphotransferase that controls phosphate signaling in Arabidopsis. Molecular Plant. 10.1016/j.molp.2021.07.011.

Ritter, K., Jork, N., Unmüßig, A.-S., Köhn, M. and Jessen, H. J. (2023). Assigning the Absolute Configuration of Inositol Poly- and Pyrophosphates by NMR Using a Single Chiral Solvating Agent. Biomolecules. Advanced Access published July 19, 2023: 10.3390/biom13071150.

Rubio, V., Linhares, F., Solano, R., Martín, A. C., Iglesias, J., Leyva, A. and Paz-Ares, J. (2001). A conserved MYB transcription factor involved in phosphate starvation signaling both in vascular plants and in unicellular algae. Genes & Development. 10.1101/gad.204401.

Safrany, S. T., Caffrey, J. J., Yang, X. and Shears, S. B. (1999). Diphosphoinositol polyphosphates: the final frontier for inositide research? Biological chemistry. 10.1515/BC.1999.117.

Schneider, R., Lami, K., Prucker, I., Stolze, S. C., Strauß, A., Langenbach, K., Kamleitner, M., Belay, Y. Z., Ritter, K., Furkert, D., Gaugler, P., Lange, E., Faiß, N., Schmidt, J. M., Harings, M., Krusenbaum, L., Wege, S., Kriescher, S., Schoof, H., Fiedler, D., Nakagami, H., Giehl, R. F. H., Lahaye, T., Jessen, H. J., Gaugler, V. and Schaaf, G. (2024). NUDIX Hydrolases Target Specific Inositol Pyrophosphates and Regulate Phosphate and Iron Homeostasis, and the Expression of Defense Genes in Arabidopsis.

Shears, S. B. (2015). Inositol pyrophosphates: why so many phosphates? Advances in biological regulation. Advanced Access published October 5, 2014: 10.1016/j.jbior.2014.09.015.

Shears, S. B. (2017). Intimate connections: Inositol pyrophosphates at the interface of metabolic regulation and cell signaling. Journal of Cellular Physiology. 10.1002/jcp.26017.

Shi, J., Hu, H., Zhang, K., Zhang, W., Yu, Y., Wu, Z. and Wu, P. (2014). The paralogous SPX3 and SPX5 genes redundantly modulate P_i homeostasis in rice. Journal of Experimental Botany. Advanced Access published December 24, 2013: 10.1093/jxb/ert424.

Steidle, E. A., Chong, L. S., Wu, M., Crooke, E., Fiedler, D., Resnick, A. C. and Rolfes, R. J. (2016). A Novel Inositol Pyrophosphate Phosphatase in *Saccharomyces cerevisiae*. Journal of Biological Chemistry. 10.1074/jbc.m116.714907.

Stephens, L., Radenberg, T., Thiel, U., Vogel, G., Khoo, K. H., Dell, A., Jackson, T. R., Hawkins, P. T. and Mayr, G. W. (1993). The detection, purification, structural characterization, and metabolism of diphosphoinositol pentakisphosphate(s) and bisdiphosphoinositol tetrakisphosphate(s). Journal of Biological Chemistry. 10.1016/s0021-9258(18)53571-7.

Stevenson-Paulik, J., Bastidas, R. J., Chiou, S.-T., Frye, R. A. and York, J. D. (2005). Generation of phytate-free seeds in Arabidopsis through disruption of inositol polyphosphate kinases. Proceedings of the National Academy of Sciences. 10.1073/pnas.0504172102.

Stevenson-Paulik, J., Odom, A. R. and York, J. D. (2002). Molecular and biochemical characterization of two plant inositol polyphosphate 6-/3-/5-kinases. Journal of Biological Chemistry. Advanced Access published September 10, 2002: 10.1074/jbc.M209112200.

Sweetman, D., Stavridou, I., Johnson, S., Green, P., Caddick, S. E. K. and Brearley, C. A. (2007). *Arabidopsis thaliana* inositol 1,3,4-trisphosphate 5/6-kinase 4 (AtITPK4) is an outlier to a family of ATP-grasp fold proteins from Arabidopsis. FEBS Letters. Advanced Access published July 30, 2007: 10.1016/j.febslet.2007.07.046.

Szijgyarto, Z., Garedew, A., Azevedo, C. and Saiardi, A. (2011). Influence of inositol pyrophosphates on cellular energy dynamics. Science (New York, N.Y.). 10.1126/science.1211908.

Thota, S. G. and Bhandari, R. (2015). The emerging roles of inositol pyrophosphates in eukaryotic cell physiology. Journal of Biosciences. 10.1007/s12038-015-9549-x.

Tilman, D., Cassman, K. G., Matson, P. A., Naylor, R. and Polasky, S. (2002). Agricultural sustainability and intensive production practices. Nature. 10.1038/nature01014.

Tyanova, S., Temu, T. and Cox, J. (2016). The MaxQuant computational platform for mass spectrometry-based shotgun proteomics. Nature Protocols. Advanced Access published October 27, 2016: 10.1038/nprot.2016.136.

Ursache, R., Fujita, S., Dénervaud Tendon, V. and Geldner, N. (2021). Combined fluorescent seed selection and multiplex CRISPR/Cas9 assembly for fast generation of multiple Arabidopsis mutants. Plant methods. Advanced Access published October 30, 2021: 10.1186/s13007-021-00811-9.

Wang, H., Falck, J. R., Hall, T. M. T. and Shears, S. B. (2011). Structural basis for an inositol pyrophosphate kinase surmounting phosphate crowding. Nature Chemical Biology. 10.1038/nchembio.733.

Wang, H., Gu, C., Rolfes, R. J., Jessen, H. J. and Shears, S. B. (2018). Structural and biochemical characterization of Siw14: A protein-tyrosine phosphatase fold that metabolizes inositol pyrophosphates. Journal of Biological Chemistry. 10.1074/jbc.ra117.001670.

Wang, H., Nair, V. S., Holland, A. A., Capolicchio, S., Jessen, H. J., Johnson, M. K. and Shears, S. B. (2015). Asp1 from *Schizosaccharomyces pombe* Binds a [2Fe-2S]$^{2+}$ Cluster Which Inhibits Inositol Pyrophosphate 1-Phosphatase Activity. Biochemistry. 10.1021/acs.biochem.5b00532.

Wang, H., Perera, L., Jork, N., Zong, G., Riley, A. M., Potter, B. V. L., Jessen, H. J. and Shears, S. B. (2022). A structural exposé of noncanonical molecular reactivity within the protein tyrosine phosphatase WPD loop. Nature Communications. 10.1038/s41467-022-29673-y.

Wang, L., Feng, Z., Wang, X., Wang, X. and Zhang, X. (2010). DEGseq: an R package for identifying differentially expressed genes from RNA-seq data. Bioinformatics (Oxford, England). Advanced Access published October 24, 2009: 10.1093/bioinformatics/btp612.

Wang, Z., Kuo, H.-F. and Chiou, T.-J. (2021). Intracellular phosphate sensing and regulation of phosphate transport systems in plants. Plant Physiology. 10.1093/plphys/kiab343.

Wang, Z., Ruan, W., Shi, J., Zhang, L., Xiang, D., Yang, C., Li, C., Wu, Z., Liu, Y., Yu, Y., Shou, H., Mo, X., Mao, C. and Wu, P. (2014). Rice SPX1 and SPX2 inhibit phosphate starvation responses through interacting with PHR2 in a phosphate-dependent manner. Proceedings of the National Academy of Sciences. Advanced Access published September 30, 2014: 10.1073/pnas.1404680111.

Whitfield, H., White, G., Sprigg, C., Riley, A. M., Potter, B. V., Hemmings, A. M. and Brearley, C. A. (2020). An ATP-responsive metabolic cassette comprised of inositol tris/tetrakisphosphate kinase 1 (ITPK1) and inositol pentakisphosphate 2-kinase (IPK1) buffers diphosphosphoinositol phosphate levels. Biochemical Journal. 10.1042/bcj20200423.

Whitfield, H. L., Rodriguez, R. F., Shipton, M. L., Li, A. W. H., Riley, A. M., Potter, B. V. L., Hemmings, A. M. and Brearley, C. A. (2024). Crystal Structure and Enzymology of *Solanum tuberosum* Inositol Tris/Tetrakisphosphate Kinase 1 (StITPK1). Biochemistry. Advanced Access published December 26, 2023: 10.1021/acs.biochem.3c00404.

Wild, R., Gerasimaite, R., Jung, J.-Y., Truffault, V., Pavlovic, I., Schmidt, A., Saiardi, A., Jessen, H. J., Poirier, Y., Hothorn, M. and Mayer, A. (2016). Control of eukaryotic phosphate homeostasis by inositol polyphosphate sensor domains. Science. 10.1126/science.aad9858.

Wilson, M. S., Jessen, H. J. and Saiardi, A. (2019). The inositol hexakisphosphate kinases IP6K1 and -2 regulate human cellular phosphate homeostasis, including XPR1-mediated phosphate export. The Journal of biological chemistry. Advanced Access published June 11, 2019: 10.1074/jbc.RA119.007848.

Wu, M., Chong, L. S., Perlman, D. H., Resnick, A. C. and Fiedler, D. (2016). Inositol polyphosphates intersect with signaling and metabolic networks via two distinct mechanisms. Proceedings of the National Academy of Sciences of the United States of America. Advanced Access published October 19, 2016: 10.1073/pnas.1606853113.

Xia, H.-J., Brearley, C., Elge, S., Kaplan, B., Fromm, H. and Mueller-Roeber, B. (2003). Arabidopsis inositol polyphosphate 6-/3-kinase is a nuclear protein that complements a yeast mutant lacking a functional ArgR-Mcm1 transcription complex. The Plant Cell. 10.1105/tpc.006676.

Yadav, R., Liu, G., Rana, P., Pullagurla, N. J., Qiu, D., Jessen, H. J. and Laha, D. (2023). Conservation of heat stress acclimation by the inositol polyphosphate multikinase, IPMK responsible for 4/6-$InsP_7$ production in land plants.

Yan, R., Chen, H., Liu, C., Zhao, J., Di Wu, Jiang, J., Gong, J. and Jiang, D. (2024). Human XPR1 structures reveal phosphate export mechanism. Nature. Advanced Access published August 21, 2024: 10.1038/s41586-024-07852-9.

Zhong, Y., Wang, Y., Guo, J., Zhu, X., Shi, J., He, Q., Liu, Y., Wu, Y., Zhang, L., Lv, Q. and Mao, C. (2018). Rice SPX6 negatively regulates the phosphate starvation response through suppression of the transcription factor PHR2. New Phytologist. Advanced Access published April 15, 2018: 10.1111/nph.15155.

Zhu, J., Lau, K., Puschmann, R., Harmel, R. K., Zhang, Y., Pries, V., Gaugler, P., Broger, L., Dutta, A. K., Jessen, H. J., Schaaf, G., Fernie, A. R., Hothorn, L. A., Fiedler, D. and Hothorn, M. (2019). Two bifunctional inositol pyrophosphate kinases/phosphatases control plant phosphate homeostasis. eLife. 10.7554/elife.43582.

Chapter IV

General Discussion, Outlook, and Conclusion

General Discussion and Outlook

In order to ensure food security for a growing world population while at the same time addressing environmental and economic concerns, it is crucial for the agricultural sector to gain a deeper understanding of nutrient homeostasis in plants. Especially of the macronutrient P_i, which plays a pivotal role in plant growth and development (Heuer *et al.*, 2017). The P_i-use efficiency of plants is notably low, with only 10% of the applied fertilizer effectively available for plants (Fageria, 2012). Moreover, the phosphate rock supply is a finite resource and the excessive use of P fertilizer can lead to environmental concerns, such as the pollution of open water bodies (Vance *et al.*, 2003; Gregory and Nortcliff, 2013; Baker *et al.*, 2015; Chen and Graedel, 2016). It is therefore important to gain a deeper understanding of the plant P_i homeostasis in order to enhance the P_i-use efficiency in crops. The discovery that the signaling molecules PP-InsPs act as a proxy of cellular P_i levels and are, therefore, involved in P_i homeostasis in plants (Dong *et al.*, 2019; Zhu *et al.*, 2019; Riemer *et al.*, 2021) has prompted a novel approach to improve P_i-use efficiency. Nevertheless, PP-InsP metabolism is not completely solved in plants. Although their biosynthesis is based on a balanced phosphorylation and dephosphorylation of InsPs/PP-InsPs, the research focus was mainly on the characterization of kinases involved in the phosphorylation of these signaling molecules. Consequently, the state of knowledge regarding PP-InsP dephosphorylation was notably limited. This thesis provides evidence for the regulation of the plants' PP-InsPs levels by pyrophosphatases belonging to two conserved phosphatase families, the PFA-DSPs and NUDT hydrolases.

PFA-DSPs are PP-InsP pyrophosphatases with a high specificity for the 5PP-moiety of $InsP_7$ and $InsP_8$

In a previous study, the phosphatase activity of Arabidopsis PFA-DSP1 was tested in the presence of various nucleotides. Although numerous potential substrates were identified in the analysis, no significant preference of PFA-DSP1 was observed (Aceti *et al.*, 2008). As PP-InsPs were not tested as potential substrates in the study (Aceti *et al.*, 2008), but the bakers' yeast homologue ScSiw14 was demonstrated to be a PP-InsP pyrophosphatase (Steidle *et al.*, 2016; Wang *et al.*, 2018), we investigated the potential PP-InsPs pyrophosphatase activity of Arabidopsis PFA-DSPs. The results presented in chapter II demonstrate that Arabidopsis PFA-DSPs are PP-InsP pyrophosphatases with a high specificity for the 5PP-moiety of $InsP_7$ and $InsP_8$ (Gaugler *et al.*, 2022). This specificity is confirmed by the findings of PFA-DSP

in vitro analysis of two independent research groups (Wang *et al.*, 2022; Laurent *et al.*, 2024). Consistent with our heterologous expression of *PFA-DSP1* in tobacco and overexpression in Arabidopsis (Figures II-6 and II-7), a recent study has demonstrated that the overexpression of *PFA-DSP2* in *Arabidopsis thaliana* also results in decreased 5-InsP$_7$ and 1,5-InsP$_8$ levels *in planta* (Laurent *et al.*, 2024). Moreover, the preference for the 5PP-moiety and, in particular, for 5-InsP$_7$ was also observed in *Marchantia polymorpha* with PFA-DSP1, as well as in the yeast *Schizosaccharomyces pombe* with the homologue Siw14 (Sanchez *et al.*, 2023; Laurent *et al.*, 2024). Taken together, the *in vitro* and *in vivo* experiments demonstrate a conserved PP-InsP pyrophosphatase activity of PFA-DSPs with a preference for 5-InsP$_7$.

Subclade I NUDT hydrolases display a PP-InsP pyrophosphatase activity with a preference for 4-InsP$_7$

The results presented in chapter III demonstrate the PP-InsP pyrophosphatase activity of seven NUDT hydrolases with distinct InsP$_7$ specificities (Schneider *et al.*, 2024). In contrast to the findings of a recent study, which identified 5-InsP$_7$ as the preferred substrate of NUDT17 (Laurent *et al.*, 2024), our experiments demonstrate that NUDT17, as well as the other members of subclade I (NUDT4, NUDT18, and NUDT21), are PP-InsP pyrophosphatases with a high specificity for 4-InsP$_7$ (Figure III-2A, B). Nevertheless, Laurent and colleagues (2024) concentrated their analysis on the NUDT17 activity in presence of 1-InsP$_7$, 5-InsP$_7$, and 1,5-InsP$_8$, and observed a notable lower activity of NUDT17 against 5-InsP$_7$ in comparison to the activity of PFA-DSP1 against 5-InsP$_7$. With our established protein concentration and *in vitro* assay conditions, we did not observe a hydrolytic activity of subclade I NUDTs against 5-InsP$_7$ (Figure III-2A, B). However, by increasing the protein concentration we also observed a partial 5-InsP$_7$, 1,5-InsP$_8$, and/or 3,5-InsP$_8$ pyrophosphatase activity (Figure III-S8). The heterologous expression of *NUDT17* and other subclade I members under a strong promoter in *N. benthamiana* resulted in a reduction of both 4/6-InsP$_7$ and 5-InsP$_7$ levels, indicating a potential dual function of those enzymes in hydrolyzing 4/6-InsP$_7$ and 5-InsP$_7$ in plants (Figure III-6A, B). These reductions were also recently demonstrated in an Arabidopsis *NUDT17* overexpressing line (Laurent *et al.*, 2024). Our findings demonstrated only a minor change in PP-InsP levels in the *nudt4/17/18/21* quadruple mutant (Figure III-5B, C, D), in alignment with results of Laurent and colleagues (2024), who observed a similar behavior in the *nudt17/18/21* mutant. Based on that, it is likely that these enzymes act redundantly with other pyrophosphatases and, therefore, it was not possible to clarify the physiological role of

4/6-InsP$_7$ in plants using our quadruple mutant *nudt4/17/18/21*. Nevertheless, the pyrophosphatase activity of subclade I NUDTs against 4-InsP$_7$ could be used in future research to investigate the enantiomer identities of plant 4/6-InsP$_7$ through *in vitro* digestions of plant-purified PP-InsPs and the help of synthetic [$^{13}C_6$] labeled InsP$_7$ standards spiked into these reactions.

A unique glycine rich extension was identified in subclade I and II NUDT hydrolases

In Arabidopsis, 29 genes were identified encoding NUDT proteins, which provide numerous opportunities for enzymatically redundant NUDT hydrolases (Yoshimura and Shigeoka, 2015). A bioinformatics analysis of the Arabidopsis NUDT family predicted that seven NUDT hydrolases may function as diphosphoinositol polyphosphate phosphohydrolases (DIPPs), namely the subclade I and II NUDT hydrolases (Gunawardana *et al.*, 2009). The elevated number of Arabidopsis DIPP NUDT hydrolases in comparison to human DIPPs was hypothesized to be the result of a potential segmental duplication event in plants (Gunawardana *et al.*, 2009). A unique characteristic of the seven NUDTs is the presence of a glycine rich ($GX_2GX_{6-7}G$) extension of the conserved NUDT motif (Yoshimura and Shigeoka, 2015). Notably, this extension is present in the human hsDIPP1, as well as in the bakers' yeast ScDdp1, and was shown to be essential for the PP-InsP and diadenosine hexaphosphate (Ap$_6$A) dual specificity, *in vitro* (Yang *et al.*, 1999). A mutation of one of these glycine residues in hsDIPP1 resulted in almost complete impaired PP-InsP and Ap$_6$A hydrolysis (Yang *et al.*, 1999). Moreover, proteins targeting diadenosine polyphosphates (Ap$_n$A), but not PP-InsPs, like hsAPAH1 and *Bartonella bacilliformis* IaIA, lack this glycine rich extension (Yang *et al.*, 1999). Although many NUDT hydrolases have been shown to have an Ap$_n$A pyrophosphatase activity (Yoshimura and Shigeoka, 2015), within subclade I and II NUDT hydrolases, only NUDT13 has been identified exhibiting an Ap$_5$A and Ap$_6$A pyrophosphatase activity (Olejnik *et al.*, 2007; Yoshimura and Shigeoka, 2015; Freed *et al.*, 2024). However, Ap$_5$A and Ap$_6$A have not been identified in plants so far and, therefore, the physiological relevance of this enzymatic activity remains unknown (Freed *et al.*, 2024). Given the presence of a glycine rich extension that is unique to subclade I and II NUDTs and essential for the PP-InsP pyrophosphatase activity, it is possible that the observed unaltered 4/6-InsP$_7$ level in *nudt4/17/18/21* mutants, in comparison to WT plants, is the result of the pyrophosphatase activity of subclade II NUDT hydrolases (Figure III-5D).

Subclade II NUDTs are PP-InsP pyrophosphatases with a preference for 3-InsP$_7$

Our experiments demonstrated that subclade II NUDTs (NUDT12, NUDT13, and NUDT16) display a PP-InsP pyrophosphatase activity with a high specificity for 3-InsP$_7$ (Figure III-3A, B). Minor pyrophosphatase activity was observed against other PP-InsPs indicating a potential redundancy with subclade I NUDTs (Figure III-3A, B). In contrast, a previous study demonstrated that NUDT13 was unable to hydrolyze InsP$_7$ under their specified *in vitro* assay conditions (Olejnik *et al.*, 2007). This was most likely observed due to the use of an InsP$_7$ isomer that is not, or only to a minor extent, hydrolyzed by NUDT13. Moreover, a second study identified a 1-InsP$_7$ and 5-InsP$_7$ pyrophosphatase activity of NUDT13 *in vitro*, while not analyzing the potential PP-InsP pyrophosphatase activity with other InsP$_7$ isomers (Laurent *et al.*, 2024). In line with the observed enzymatic activity of NUDT13, a recent study demonstrated a pyrophosphatase activity in the presence of InsP$_7$ and InsP$_8$, although the exact isomer identity was not specified (Freed *et al.*, 2024). Furthermore, the authors reported that the knockout or overexpression of *NUDT13* in Arabidopsis resulted in an increase or decrease of PP-InsP levels, respectively, but the InsP$_7$ and InsP$_8$ isomer identity remains unknown (Freed *et al.*, 2024). Given the possibility that subclade II NUDT hydrolases may have a potential enzymatic redundancy, we analyzed PP-InsPs levels in the triple knockout mutant *nudt12/13/16* and identified a robust increase in 1/3-InsP$_7$ (Figure III-5B, C, D). Based on the findings of our *in vitro* analyses, it is possible that the observed increase in 1/3-InsP$_7$ originates from 3-InsP$_7$ (Figure III-3A, B). A similar pyrophosphatase activity was recently identified with *M. polymorpha* NUDT/DDP1, displaying a PP-InsP pyrophosphatase activity *in vitro* and in yeast (Chalak *et al.*, 2024; Laurent *et al.*, 2024). Furthermore, the *in planta* analysis identified increased 1/3-InsP$_7$ and InsP$_8$ levels in *M. polymorpha* knockout plants, indicating a preference for the 1/3PP-moiety of InsP$_7$ and InsP$_8$ (Chalak *et al.*, 2024; Laurent *et al.*, 2024). These observations align with the known activity of the yeast and human NUDT family members, which have been shown to exhibit a preference for the β-phosphate of 1-InsP$_7$ (Safrany *et al.*, 1999; Lonetti *et al.*, 2011; Kilari *et al.*, 2013; Andreeva *et al.*, 2019). Interestingly, a recent study has demonstrated that, in addition to 1-InsP$_7$, hsDIPP1 is also able to hydrolyze 3-InsP$_7$ *in vitro* (Dollins *et al.*, 2020). In contrast to the observations in Marchantia, we observed a steady-state InsP$_8$ level in the Arabidopsis triple mutant *nudt12/13/16* compared to the WT (Figure III-5C), which could have various reasons such as a potential preference of subclade II NUDTs for InsP$_7$ *in planta*, the functional redundancy of other enzymes or the absence of 3,5-InsP$_8$ *in planta*, which was the preferred InsP$_8$ isomer *in vitro* (Figure III-4C, D). However,

these hypotheses remain speculative as long as it is unclear whether plants, in facts, synthesize 3-InsP$_7$, 1,5-InsP$_8$ or 3,5-InsP$_8$. Moreover, we observed a minor but significant increase in 5-InsP$_7$ levels in the *nudt12/13/16* triple mutants (Figure III-5D), which, along with the observed 5-InsP$_7$ decrease in *N. benthamiana* leaves expressing NUDT12 or NUDT16 and the observed 5-InsP$_7$ hydrolysis of subclade II NUDTs *in vitro*, indicates a 5-InsP$_7$ pyrophosphatase activity of subclade II NUDTs *in planta*.

Taken together, the presented results demonstrate a PP-InsP pyrophosphatase activity of subclade II NUDTs with a preference for 3-InsP$_7$. Although the presence of 3-InsP$_7$ remains to be clarified in plants, the specific *in vitro* preference for the 3PP-moiety of PP-InsPs can be used as tool to unravel the enantiomer identities of 1/3-InsP$_7$ in plants through *in vitro* digestions.

In vitro pyrophosphatase activity is dependent on the presence of Mg^{2+}

Our experiments showed that the *in vitro* PP-InsP pyrophosphatase activity of PFA-DSPs, subclade I NUDTs, and subclade II NUDTs are highly dependent on the presence of Mg^{2+} (Figures II-1A, III-2C, and III-3C). We demonstrated that in the absence of any divalent cations PFA-DSP1 hydrolyzes 1-InsP$_7$ and 5-InsP$_7$ (Figure II-1A). However, in presence of Mg^{2+} PFA-DSP1 displays a high preference for 5-InsP$_7$ (Figure II-1A), which was also observed with the homologue SpSiw14 (Sanchez *et al.*, 2023). In addition, the *in vitro* experiments with subclade I and II NUDTs indicate a pyrophosphatase activity against 4-InsP$_7$ and 3-InsP$_7$, respectively, only in presence of Mg^{2+}. These shifted pyrophosphatase activities could be explained by the phenomenon that metal cations can alter the conformational equilibrium of PP-InsPs, leading to the flip of five phosphoryl groups from the equatorial to the axial position (Kurz *et al.*, 2023). Furthermore, it was demonstrated that pH and temperature also alter the conformational equilibrium of PP-InsPs (Kurz *et al.*, 2023), which may provide an explanation for the observed discrepancy of subclade I NUDTs and their 5-InsP$_7$ activity *in vitro* and *in vivo*. Further research is required to investigate whether alteration to the conformational equilibrium of PP-InsPs, induced by changed metal cations, pH, and temperature, could affect the substrate specificity of PP-InsP pyrophosphatases.

PP-InsP pyrophosphatases as tool to increase the P_i-use efficiency of plants

Although two pyrophosphatase families were identified as being involved in PP-InsP biosynthesis, the question remains whether they can be used to increase the P_i-use efficiency of plants. Subclade I NUDT hydrolases showed *in vitro* a high specificity for 4-$InsP_7$ (Figure III-2A, B), which is supposed to be unrelated to P_i sensing in plants (Riemer *et al.*, 2021). However, the heterologous expression of subclade I NUDTs under a strong promoter in *N. benthamiana*, as well as the overexpression in *Arabidopsis thaliana* (Laurent *et al.*, 2024), decreased not only the 4/6-$InsP_7$ but also the 5-$InsP_7$ level (Figure III-6A, B). As important precursor for $InsP_8$, the 5-$InsP_7$ level is a key factor influencing the PSR activation in plants (Riemer *et al.*, 2021). An overexpression of a 5-$InsP_7$ pyrophosphatase, such as PFA-DSPs or subclade I NUDTs, has therefore the potential to reduce the $InsP_8$ level in plants. A reduction in $InsP_8$ results in a lower level of PHR1/PHL1 being bound to the $InsP_8$/SPX1 complex, thereby activating the expression of PSI genes and the P_i uptake of plants (Rubio *et al.*, 2001; Bustos *et al.*, 2010; Puga *et al.*, 2014; Ried *et al.*, 2021). Consequently, we observed the local activation of the PSR mechanism by co-expressing *PFA-DSP1* or subclade I NUDTs with a *RUBY* reporter transcriptional controlled by the *SlSPX2* promoter in *N. benthamiana* leaves (Figure III-6D). In addition, a recent study demonstrated that Arabidopsis *PFA-DSP2* and *NUDT17* overexpression plants accumulate P_i under sufficient growth conditions (Laurent *et al.*, 2024). However, as previously observed in plants with an activated PSR mechanism grown under sufficient P_i conditions, such as *itpk1 itpk2* and *vih1 vih2* double mutants, the *PFA-DSP1*, *PFA-DSP2* and *PFA-DSP4* overexpression lines showed severe growth defects (Dong *et al.*, 2019; Zhu *et al.*, 2019; Riemer *et al.*, 2021; Laurent *et al.*, 2024). It should be noted, though, that the weaker overexpression of *NUDT17* results only in reduced rosette areas (Laurent *et al.*, 2024).

By disrupting the expression of *NUDT12*, *NUDT13*, and *NUDT16*, we created an imbalance in the cellular P_i homeostasis, resulting in a decreased total P concentration in shoots and the downregulation of genes involved in PSR (Figure III-7A and Table III-S2). These changes were most likely observed due to the increased levels of 1/3-$InsP_7$ and 5-$InsP_7$ in the triple mutant *nudt12/13/16*, as well as the steady-state $InsP_8$ level that prevents PSR activation (Figure III-5C, D). Furthermore, a recent study has demonstrated the P_i overaccumulation, along with growth defects in Arabidopsis mutants that overexpress *NUDT13* or the yeast gene *ScDdp1*, as well as pennycress overexpressing *ScDdp1* (Freed *et al.*, 2024). The P_i overaccumulation is most likely the result of the observed $InsP_7$, probably 1/3-$InsP_7$, and $InsP_8$ decrease, which activates the PSR and P_i uptake (Freed *et al.*, 2024). Moreover, we have

previously demonstrated that ITPK1 plays an important role in the PSR of plants by phosphorylating $InsP_6$ to 5-$InsP_7$, the precursor of $InsP_8$ (Riemer *et al.*, 2021). However, a recent publication and our own data show that Arabidopsis ITPK1, as well as *Solanum tuberosum* ITPK1, phosphorylate 3-$InsP_7$ to $InsP_8$, *in vitro* (Figure III-10) (Whitfield *et al.*, 2024). These findings may suggest that plants synthesize 3-$InsP_7$, which could be together with 5-$InsP_7$ the precursor for 3,5-$InsP_8$, thus playing an important role in the PSR regulation. Nevertheless, this hypothesis remains speculative as long as it is unclear whether plants, in fact, synthesize 3-$InsP_7$.

Taken together, the overexpression of PFA-DSPs, subclade I NUDTs, and subclade II NUDTs reduces PP-InsP levels, thereby activating PSR in plants. However, the P_i overaccumulation in plants leads to severe growth defects, most likely caused by P_i toxicity. Therefore, the overexpression of these pyrophosphatases has the potential to enhance the P_i-use efficiency, although this may lead to toxic P_i levels in the plant. It can be concluded that the strong overexpression of these pyrophosphatases is not a useful tool for crop breeding. Nevertheless, a lower expression of these pyrophosphatases, as observed with NUDT17 (Laurent *et al.*, 2024), may avoid a toxic accumulation and at the same time enhance the P_i-use efficiency. An alternative strategy that could be investigated in further experiments is the local PSR activation in roots to enhance the P_i-use efficiency while preventing the P_i overaccumulation in shoots. As demonstrated in grafting experiments with Arabidopsis *itpk1* mutants, shoots accumulate significantly more P_i when *itpk1* shoots are grafted onto WT roots than the reciprocal graft (Riemer *et al.*, 2021). Given that *ITPK1* is expressed in shoots and roots (Kuo *et al.*, 2018), the results indicate the importance of ITPK1 in shoots to regulate the local P_i accumulation (Riemer *et al.*, 2021). In addition, a recent study demonstrated that *Lotus japonicus vih2-1* shoots grafted onto WT roots, as well as the reciprocal graft, resulted in significant increased arbuscular mycorrhizal (AM) colonization in comparison to *L. japonicus* WT shoots grafted onto WT roots (Raj *et al.*, 2024). These findings suggest that the inactivation of *LjVIH2* induces the PSR systemically and locally in *L. japonicus*, which in turn results in AM colonization even under high P_i growth conditions (Raj *et al.*, 2024). Furthermore, Raj and colleagues (2024) proposed that the ectopic expression of PP-InsP pyrophosphatases with a specificity for 5-β-phosphate, such as PFA-DSPs, in roots could be a useful tool to fine-tune the local PSR activation without affecting PP-InsP levels in shoots. In view of the findings that ectopically expressed subclade I and II NUDTs activated the PSR in *N. benthamiana* leaves as well (Figure III-6), it would be interesting to investigate whether these PP-InsP pyrophosphatases, in addition to PFA-DSPs,

are able to induce the PSR locally in *L. japonicus* roots. Therefore, the AM colonization of *L. japonicus* mutants expressing *PFA-DSP*s, subclade I *NUDT*s, or subclade II *NUDT*s under control of a root-specific promoter, such as *Agrobacterium rhizogens* rolD promoter, domain A CaMV 35S or the rice promoters rRSP1, rRSP3, or rRSP5 (Elmayan and Tepfer, 1995; Huang *et al.*, 2015), could be investigated. However, it has been shown that PHR1 regulates various PSRs, including the expression of P_i transporter, the release of acid phosphatases (APases), as well as the primary root and root hair growth (Bustos *et al.*, 2010; Guo *et al.*, 2015; Wang *et al.*, 2023). Therefore, the modification of PP-InsP levels in roots and, consequently, the PHR1 activity could affect several PSRs. It would be interesting to investigate whether the PP-InsP pyrophosphatase expression in specific root tissues, such as root meristem where a strong PSI APase activity of PAP12 and PAP26 was observed (Robinson *et al.*, 2012), or root epidermal and outer cortical cells, where the P_i transporter 1 (*PHT1*) family is mainly expressed (Mudge *et al.*, 2002; Karthikeyan *et al.*, 2002), might regulate the respective PSR. The promoters of genes such as *RCH1*, which has been shown to be expressed specifically in root meristem cells (Casamitjana-Martínez *et al.*, 2003; Dello Ioio *et al.*, 2007), and *WER*, which has been shown to be expressed specifically in epidermal cells (Bruex *et al.*, 2012; Marquès-Bueno *et al.*, 2016), could be considered for the root tissue-specific expression.

A more advanced approach would be to investigate the local PSR activation in cereal crops, such as rice, where a considerable potential exists to enhance the P fertilizer use efficiency (Yu *et al.*, 2021). In rice, *Oryza sativa*, a PSR regulatory mechanism similar to that in Arabidopsis has been observed, involving the PHR1 homologue, OsPHR2, and SPX proteins as repressors (Zhou *et al.*, 2008; Liu *et al.*, 2010; Lv *et al.*, 2014). Moreover, between 18 and 33 putative NUDT hydrolases and four putative PFA-DSPs have been identified in rice (Kraszewska, 2008; Liu *et al.*, 2012; Yoshimura and Shigeoka, 2015; Kondo *et al.*, 2022; Liu *et al.*, 2022). Of these putative rice NUDT and PFA-DSP hydrolases, seven NUDTs (LOC_Os02g32060, LOC_Os04g32740, LOC_Os11g32750, LOC_Os03g59580, LOC_Os07g11120, LOC_Os02g50130, LOC_Os06g14420) are closely related to Arabidopsis subclade I and II NUDT hydrolases (Liu *et al.*, 2022), and the four identified PFA-DSPs are closely related to Arabidopsis PFA-DSPs as well (Liu *et al.*, 2012). The initial step would be to investigate their PP-InsP pyrophosphatase activity and their involvement in P_i homeostasis *in vitro* and *in planta*, similar to the experiments presented in chapters II and III. In addition, expressing these rice NUDTs or PFA-DSPs with root-specific promoters, such as rRSP1, rRSP3, or rRSP5 (Huang *et al.*, 2015), enables the investigation of local PSR activation in roots and its effects on root growth, root exudates release, AM colonization and P_i uptake.

Taken together, the local expression of PFA-DSPs and NUDT hydrolases in roots may offer a potential approach to enhance the P_i-use efficiency of plants, if it is possible to activate the PSR locally in roots without significantly altering PP-InsP levels in shoots. However, further investigations are necessary to validate this hypothesis, such as the expression of the presented PP-InsP pyrophosphatases with root-specific and root tissue-specific promoters.

Phosphatases are housecleaning enzymes involved in nutrient homeostasis, abiotic and biotic stress responses

Phosphatases have been referred to as "housecleaning" enzymes based on their ability to hydrolyze metabolites, thereby preventing their accumulation at potentially harmful or toxic concentrations (Bessman *et al.*, 1996; McLennan, 2006). An accumulation of PP-InsPs could not only result in P_i deficiency due to the missing PSR activation, but can also have a broader influence on other cellular processes. Due to their high negative charge, PP-InsPs have the ability to chelate metals (Kurz *et al.*, 2023), and thereby the potential to detoxify cells from these. The triple mutant *nudt12/13/16* displayed not only increased 1/3-$InsP_7$ and 5-$InsP_7$ levels, but also a differential expression of genes related to Fe homeostasis (Table III-S4). For instance, we observed downregulation of transcription factors that are responsible for the activation of phytochelatin synthesis, which are involved in the chelation and detoxification of heavy metals in cells (Faizan *et al.*, 2024). This finding indicates the potential detoxification of heavy metals by PP-InsPs but also the importance of a balanced PP-InsPs synthesis to prevent the excessive chelation of essential metals in plant cells.

Furthermore, the disrupted PP-InsP pyrophosphatase activity in our triple mutant *nudt12/13/16* resulted in a significant reduction of the Fe concentration in shoots (Figure III-7B). It has been demonstrated that the P_i and Fe homeostasis in plants are closely related, as evidenced by the overaccumulation of Fe in plants grown under P_i deficient conditions (Hirsch *et al.*, 2006; Ward *et al.*, 2008; Thibaud *et al.*, 2010). In our triple mutant, we observed a downregulation of ferritin *FER1* (Table III-S4), a Fe storage protein, which has been demonstrated to be involved in the close interaction of P_i and Fe homeostasis in Arabidopsis (Hirsch *et al.*, 2006). Our findings are consistent with the observation that *FER1* is transcriptionally activated by PHR1/PHL1, which binds to the P1BS element in the *FER1* promoter region (Bournier *et al.*, 2013). As the triple mutant has been demonstrated to have an unaltered $InsP_8$ level (Figure III-5C), in comparison to WT plants, it can be hypothesized that PHR1/PHL1 is repressed by forming a complex with

SPX1 and $InsP_8$. Therefore, PHR1/PHL1 is unable to bind to the P1BS element of PSI genes and *FER1*, which results in a P_i and Fe deficiency in these mutants. Furthermore, there is known cross-talk between nitrate and P_i homeostasis (Medici *et al.*, 2015; Maeda *et al.*, 2018; Hu *et al.*, 2019; Medici *et al.*, 2019; Ueda *et al.*, 2020). It was demonstrated that PHR1/PHL1 controls NIGT1/HRS1, which is a transcription factor involved in the high-affinity nitrate transport (Kiba *et al.*, 2018; Maeda *et al.*, 2018; Safi *et al.*, 2018) and also represses the transcription of SPX proteins (Ueda *et al.*, 2020). Moreover, the rice PHR2 (homologue of Arabidopsis PHR1) was shown to activate a nitrate-induced MYB transcription factor, which directly activates PSI genes and competes with PHR2 for binding to SPX proteins (Zhang *et al.*, 2021). A recent study also demonstrated that the overexpression of *PFA-DSP2* and *NUDT17* results in decreased PP-InsP levels and an increased expression of nitrate transporters (Laurent *et al.*, 2024), which is consistent with previous observations regarding the closely linked P_i and nitrate homeostasis. These results demonstrate the critical role of PP-InsP pyrophosphatases in regulation the PP-InsP biosynthesis, which has a significant impact on nutrient homeostasis in plants.

Furthermore, PP-InsPs have been shown to play a role in the response to various abiotic and biotic stresses by interacting with phytohormones (Laha *et al.*, 2015; Laha *et al.*, 2016; Gulabani *et al.*, 2021; Laha *et al.*, 2022; Riemer *et al.*, 2022). For example, it was proposed that PP-InsPs regulate jasmonic acid signaling by binding and allosterically regulating the COI1-JAZ jasmonate coreceptor complex (Laha *et al.*, 2015). Based on the observation that PP-InsPs bind to the F-box protein COI1 *in vitro*, a potential binding of 5-$InsP_7$ to the F-box protein TIR1 was postulated to stabilize the formation of the TIR1-ASK1-IAA complex and, in turn, regulate auxin signaling in plants (Laha *et al.*, 2022). Moreover, it has been demonstrated that *myo*-inositol phosphate synthase (MIPS) plays a role in the ethylene response in Arabidopsis and wheat, thereby regulating growth and stress tolerance of plants (Sharma *et al.*, 2020a; Sharma *et al.*, 2020b). Although the direct involvement of PP-InsP in the ethylene signaling pathway remains elusive, our findings demonstrate that numerous genes related to ethylene signaling are downregulated in the triple mutant *nudt12/13/16* with increased 1/3-$InsP_7$ and 5-$InsP_7$ levels (Figure III-5D and Table III-S3). These findings suggest a potential interaction of $InsP_7$ and ethylene, which represents an important area for future research on the role of PP-InsPs in plant phytohormone signaling. Furthermore, ethylene has been demonstrated to play an important role in plant immune response (Adie *et al.*, 2007). The plant immune response is regulated by a number of different phytohormones and their interactions, including jasmonic acid, auxin, and salicylic acid, which have been shown to be linked with PP-InsPs (Ghanashyam and Jain, 2009; Laha *et al.*, 2015; Laha *et al.*, 2016; Djami-Tchatchou *et al.*, 2020; Gulabani *et*

al., 2021; Laha *et al.*, 2022). The role of 5-InsP$_7$ and InsP$_8$ in plant defense response were already investigated with *itpk1* and *vih2* knockout mutants (Gulabani *et al.*, 2021; Laha *et al.*, 2015). The triple mutant *nudt12/13/16*, which has been demonstrated to have increased 1/3-InsP$_7$ level and reduced expression of genes involved in defense mechanisms, could represent a tool to investigate the potential role of 1/3-InsP$_7$ in the plant immune response (Figure III-5D and Table III-S3). Nevertheless, 5-InsP$_7$ was also slightly increased, which could lead to confounding effects and challenges in investigating the role of 1/3-InsP$_7$ with certainty (Figure III-5D). Further research could investigate whether subclade II NUDT single knockout mutants or double knockout mutants display increased 1/3-InsP$_7$ levels and unaltered levels of other InsP$_7$ isomers, in order to identify the potential role of 1/3-InsP$_7$ in plant immune response. Taken together, the described plant defense response, along with other biotic or abiotic stress responses, indicate the importance of PP-InsP pyrophosphatases to enable a rapid conversion of PP-InsP, thereby ensuring dynamic adaptation to varying environmental challenges.

In addition to the previously mentioned allosteric binding of PP-InsPs to proteins, another potential role of PP-InsPs in plants has been proposed, namely the non-enzymatic protein pyrophosphorylation (Saiardi *et al.*, 2004; Bhandari *et al.*, 2007; Mihiret *et al.*, 2024). Although this post-translational modification has not yet been detected in plants (Mihiret *et al.*, 2024), a novel pyrophosphoproteomics approach revealed PP-InsP-dependent pyrophosphorylation of several proteins in human cell lines, providing a potential avenue for investigating this mechanism in plants (Morgan *et al.*, 2024). This would be particularly useful to unravel the physiological role of PP-InsPs as regulatory molecules in plants. As previously suggested by Mihiret and colleagues (2024), it would be interesting to investigate a potential substrate specificity of PP-InsP isomers. *In vitro* studies have demonstrated that 5-InsP$_7$ is able to pyrophosphorylate several mammalian and yeast proteins (Saiardi *et al.*, 2004; Bhandari *et al.*, 2007; Azevedo *et al.*, 2009; Lolla *et al.*, 2021; Chanduri *et al.*, 2016). Moreover, an *in vitro* study of Bhandari and colleagues (2007) has demonstrated that 1-InsP$_7$ (initially wrong annotated as 4/6-InsP$_7$ (Mihiret *et al.*, 2024)) and 1,5-InsP$_8$ show a similar protein phosphorylation pattern to that of 5-InsP$_7$ when incubated with protein extracts obtained from budding yeast. In order to investigate the involvement of 5-InsP$_7$ in protein pyrophosphorylation in plants, PFA-DSP mutants, either overexpression or knockout mutants, would provide helpful tools. Once further research has identified knockout combinations that affects the intended InsP$_7$ isomer without altering 5-InsP$_7$ levels, NUDT hydrolases could provide an additional tool to investigate the role of 1/3-InsP$_7$ and 4/6-InsP$_7$ in post-translational protein modification in plants.

Conclusion

Collectively, this thesis provides new insights into the roles of PFA-DSPs and NUDTs in regulating PP-InsP signaling pathways in plants (Figure IV-1). Despite the identification of pyrophosphatases with a 4-$InsP_7$ specificity, the physiological function of 4/6-$InsP_7$ remains unknown in plants due to the enzymatic redundancy of pyrophosphatases with subclade I NUDT hydrolases. Nevertheless, the identified substrate specificities of subclade I and II NUDT hydrolases provide a novel tool to investigate the enantiomer identities of 4/6-$InsP_7$ and 1/3-$InsP_7$, respectively, in plants. The findings discussed in this thesis demonstrated that the overexpression of the analyzed pyrophosphatases has the potential to activate the PSR and, consequently, the P_i uptake of plants. However, an overaccumulation of P_i has been linked to severe growth defects in plants, most likely caused by P_i toxicity. Therefore, the excessive overexpression of pyrophosphatases is an inappropriate approach to improve the P_i-use efficiency of crops. Future research could investigate whether a lower pyrophosphatase overexpression prevents the P_i toxicity, while at the same time enhances the P_i-use efficiency. A more promising approach would be to investigate whether PP-InsP pyrophosphatases could be used to induce the PSR locally in roots, without altering PP-InsP levels in shoots significantly and leading to a P_i toxicity. Nevertheless, it should be noted that PP-InsPs have been demonstrated to be involved in numerous processes, including nutrient homeostasis and phytohormone signaling, and the overexpression of PP-InsP may create an imbalance that affects not only PSR but also a variety of other signaling pathways in plants.

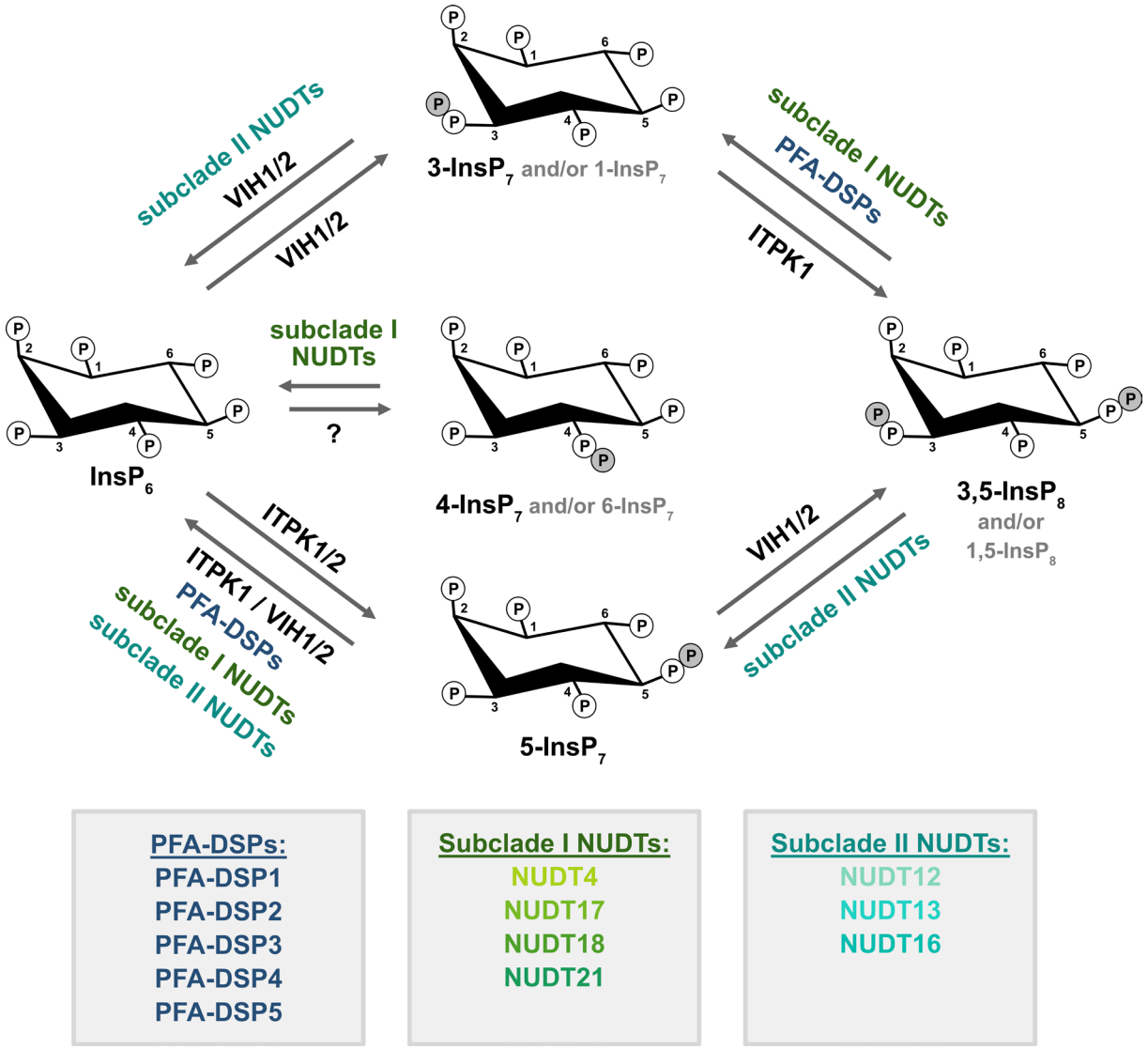

Figure IV-1: Current state of knowledge about PP-InsP biosynthesis in plants, complemented with the identified *in vitro*, *in vivo* and/or *in planta* pyrophosphatase activities of PFA-DSPs, subclade I and II NUDTs and the identified 3-InsP$_7$ kinase activity of ITPK1 *in vitro*.

References

Aceti, D. J., Bitto, E., Yakunin, A. F., Proudfoot, M., Bingman, C. A., Frederick, R. O., Sreenath, H. K., Vojtik, F. C., Wrobel, R. L., Fox, B. G., Markley, J. L. and Phillips, G. N. (2008). Structural and functional characterization of a novel phosphatase from the *Arabidopsis thaliana* gene locus At1g05000. Proteins: Structure, Function, and Bioinformatics. 10.1002/prot.22041.

Adie, B., Chico, J. M., Rubio-Somoza, I. and Solano, R. (2007). Modulation of Plant Defenses by Ethylene. Journal of Plant Growth Regulation. 10.1007/s00344-007-0012-6.

Andreeva, N., Ledova, L., Ryazanova, L., Tomashevsky, A., Kulakovskaya, T. and Eldarov, M. (2019). Ppn2 endopolyphosphatase overexpressed in *Saccharomyces cerevisiae*: Comparison with Ppn1, Ppx1, and Ddp1 polyphosphatases. Biochimie. 10.1016/j.biochi.2019.06.001.

Azevedo, C., Burton, A., Ruiz-Mateos, E., Marsh, M. and Saiardi, A. (2009). Inositol pyrophosphate mediated pyrophosphorylation of AP3B1 regulates HIV-1 Gag release. Proceedings of the National Academy of Sciences. Advanced Access published November 23, 2009: 10.1073/pnas.0909176106.

Baker, A., Ceasar, S. A., Palmer, A. J., Paterson, J. B., Qi, W., Muench, S. P. and Baldwin, S. A. (2015). Replace, reuse, recycle: improving the sustainable use of phosphorus by plants. Journal of Experimental Botany. Advanced Access published May 4, 2015: 10.1093/jxb/erv210.

Bessman, M. J., Frick, D. N. and O'Handley, S. F. (1996). The MutT proteins or "Nudix" hydrolases, a family of versatile, widely distributed, "housecleaning" enzymes. Journal of Biological Chemistry. 10.1074/jbc.271.41.25059.

Bhandari, R., Saiardi, A., Ahmadibeni, Y., Snowman, A. M., Resnick, A. C., Kristiansen, T. Z., Molina, H., Pandey, A., Werner, J. K., Juluri, K. R., Xu, Y., Prestwich, G. D., Parang, K. and Snyder, S. H. (2007). Protein pyrophosphorylation by inositol pyrophosphates is a posttranslational event. Proceedings of the National Academy of Sciences of the United States of America. Advanced Access published September 14, 2007: 10.1073/pnas.0707338104.

Bournier, M., Tissot, N., Mari, S., Boucherez, J., Lacombe, E., Briat, J.-F. and Gaymard, F. (2013). Arabidopsis ferritin 1 (AtFer1) gene regulation by the phosphate starvation response 1 (AtPHR1) transcription factor reveals a direct molecular link between iron and phosphate homeostasis. The Journal of biological chemistry. Advanced Access published June 20, 2013: 10.1074/jbc.M113.482281.

Bruex, A., Kainkaryam, R. M., Wieckowski, Y., Kang, Y. H., Bernhardt, C., Xia, Y., Zheng, X., Wang, J. Y., Lee, M. M., Benfey, P., Woolf, P. J. and Schiefelbein, J. (2012). A gene regulatory network for root epidermis cell differentiation in Arabidopsis. PLoS Genetics. Advanced Access published January 12, 2012: 10.1371/journal.pgen.1002446.

Bustos, R., Castrillo, G., Linhares, F., Puga, M. I., Rubio, V., Pérez-Pérez, J., Solano, R., Leyva, A. and Paz-Ares, J. (2010). A Central Regulatory System Largely Controls Transcriptional Activation and Repression Responses to Phosphate Starvation in Arabidopsis. PLoS Genetics. 10.1371/journal.pgen.1001102.

Casamitjana-Martínez, E., Hofhuis, H. F., Xu, J., Liu, C.-M., Heidstra, R. and Scheres, B. (2003). Root-specific *CLE19* overexpression and the sol1/2 suppressors implicate a CLV-like pathway in the control of Arabidopsis root meristem maintenance. Current Biology. 10.1016/s0960-9822(03)00533-5.

Chalak, K., Yadav, R., Liu, G., Rana, P., Jessen, H. J. and Laha, D. (2024). Functional Conservation of the DDP1-type Inositol Pyrophosphate Phosphohydrolases in Land Plant. Biochemistry. Advanced Access published October 15, 2024: 10.1021/acs.biochem.4c00458.

Chanduri, M., Rai, A., Malla, A. B., Wu, M., Fiedler, D., Mallik, R. and Bhandari, R. (2016). Inositol hexakisphosphate kinase 1 (IP6K1) activity is required for cytoplasmic dynein-driven transport. Biochemical Journal. Advanced Access published July 29, 2016: 10.1042/BCJ20160610.

Chen, M. and Graedel, T. E. (2016). A half-century of global phosphorus flows, stocks, production, consumption, recycling, and environmental impacts. Global Environmental Change. 10.1016/j.gloenvcha.2015.12.005.

Dello Ioio, R., Linhares, F. S., Scacchi, E., Casamitjana-Martinez, E., Heidstra, R., Costantino, P. and Sabatini, S. (2007). Cytokinins determine Arabidopsis root-meristem size by controlling cell differentiation. Current Biology. Advanced Access published March 15, 2007: 10.1016/j.cub.2007.02.047.

Djami-Tchatchou, A. T., Harrison, G. A., Harper, C. P., Wang, R., Prigge, M. J., Estelle, M. and Kunkel, B. N. (2020). Dual Role of Auxin in Regulating Plant Defense and Bacterial Virulence Gene Expression During *Pseudomonas syringae* PtoDC3000 Pathogenesis. Molecular plant-microbe interactions: MPMI. Advanced Access published June 29, 2020: 10.1094/MPMI-02-20-0047-R.

Dollins, D. E., Bai, W., Fridy, P. C., Otto, J. C., Neubauer, J. L., Gattis, S. G., Mehta, K. P. M. and York, J. D. (2020). Vip1 is a kinase and pyrophosphatase switch that regulates inositol diphosphate signaling. Proceedings of the National Academy of Sciences. Advanced Access published April 17, 2020: 10.1073/pnas.1908875117.

Dong, J., Ma, G., Sui, L., Wei, M., Satheesh, V., Zhang, R., Ge, S., Li, J., Zhang, T.-E., Wittwer, C., Jessen, H. J., Zhang, H., An, G.-Y., Chao, D.-Y., Liu, D. and Lei, M. (2019). Inositol Pyrophosphate $InsP_8$ Acts as an Intracellular Phosphate Signal in Arabidopsis. Molecular Plant. 10.1016/j.molp.2019.08.002.

Elmayan, T. and Tepfer, M. (1995). Evaluation in tobacco of the organ specificity and strength of the rolD promoter, domain A of the 35S promoter and the $35S^2$ promoter. Transgenic research. 10.1007/BF01973757.

Fageria, N. K. (2012). The Role of Plant Roots in Crop Production. CRC Press.

Faizan, M., Alam, P., Hussain, A., Karabulut, F., Tonny, S. H., Cheng, S. H., Yusuf, M., Adil, M. F., Sehar, S., Alomrani, S. O., Albalawi, T. and Hayat, S. (2024). Phytochelatins: Key regulator against heavy metal toxicity in plants. Plant Stress. 10.1016/j.stress.2024.100355.

Freed, C., Craige, B., Donahue, J., Cridland, C., Williams, S. P., Pereira, C., Kim, J., Blice, H., Owen, J. and Gillaspy, G. (2024). Using Native and Synthetic Genes to Disrupt Inositol Pyrophosphates and Phosphate Accumulation in Plants. Plant Physiology. Advanced Access published October 30, 2024: 10.1093/plphys/kiae582.

Gaugler, P., Schneider, R., Liu, G., Qiu, D., Weber, J., Schmid, J., Jork, N., Häner, M., Ritter, K., Fernández-Rebollo, N., Giehl, R. F. H., Trung, M. N., Yadav, R., Fiedler, D., Gaugler, V., Jessen, H. J., Schaaf, G. and Laha, D. (2022). Arabidopsis PFA-DSP-Type Phosphohydrolases Target Specific Inositol Pyrophosphate Messengers. Biochemistry. Advanced Access published May 31, 2022: 10.1021/acs.biochem.2c00145.

Ghanashyam, C. and Jain, M. (2009). Role of auxin-responsive genes in biotic stress responses. Plant signaling & behavior. Advanced Access published September 16, 2009: 10.4161/psb.4.9.9376.

Gregory, P. J. and Nortcliff, S. (eds.) (2013). Soil conditions and plant growth. Chichester: Wiley-Blackwell.

Gulabani, H., Goswami, K., Walia, Y., Roy, A., Noor, J. J., Ingole, K. D., Kasera, M., Laha, D., Giehl, R. F. H., Schaaf, G. and Bhattacharjee, S. (2021). Arabidopsis inositol polyphosphate kinases IPK1 and ITPK1 modulate crosstalk between SA-dependent immunity and phosphate-starvation responses. Plant Cell Reports. 10.1007/s00299-021-02812-3.

Gunawardana, D., Likic, V. A. and Gayler, K. R. (2009). A comprehensive bioinformatics analysis of the Nudix superfamily in *Arabidopsis thaliana*. Comparative and functional genomics. Advanced Access published July 2, 2009: 10.1155/2009/820381.

Guo, M., Ruan, W., Li, C., Huang, F., Zeng, M., Liu, Y., Yu, Y., Ding, X., Wu, Y., Wu, Z., Mao, C., Yi, K., Wu, P. and Mo, X. (2015). Integrative Comparison of the Role of the PHOSPHATE RESPONSE1 Subfamily in Phosphate Signaling and Homeostasis in Rice. Plant Physiology. Advanced Access published June 16, 2015: 10.1104/pp.15.00736.

Heuer, S., Gaxiola, R., Schilling, R., Herrera-Estrella, L., López-Arredondo, D., Wissuwa, M., Delhaize, E. and Rouached, H. (2017). Improving phosphorus use efficiency: a complex trait with emerging opportunities. The Plant Journal. Advanced Access published February 3, 2017: 10.1111/tpj.13423.

Hirsch, J., Marin, E., Floriani, M., Chiarenza, S., Richaud, P., Nussaume, L. and Thibaud, M. C. (2006). Phosphate deficiency promotes modification of iron distribution in Arabidopsis plants. Biochimie. Advanced Access published May 24, 2006: 10.1016/j.biochi.2006.05.007.

Hu, B., Jiang, Z., Wang, W., Qiu, Y., Zhang, Z., Liu, Y., Li, A., Gao, X., Liu, L., Qian, Y., Huang, X., Yu, F., Kang, S., Wang, Y., Xie, J., Cao, S., Zhang, L., Wang, Y., Xie, Q., Kopriva, S. and Chu, C. (2019). Nitrate-NRT1.1B-SPX4 cascade integrates nitrogen and phosphorus signalling networks in plants. Nature plants. Advanced Access published March 25, 2019: 10.1038/s41477-019-0384-1.

Huang, L., Zhang, F., Qin, Q., Wang, W., Zhang, T. and Fu, B. (2015). Identification and validation of root-specific promoters in rice. Journal of Integrative Agriculture. 10.1016/S2095-3119(14)60763-2.

Karthikeyan, A. S., Varadarajan, D. K., Mukatira, U. T., D'Urzo, M. P., Damsz, B. and Raghothama, K. G. (2002). Regulated expression of Arabidopsis phosphate transporters. Plant Physiology. 10.1104/pp.020007.

Kiba, T., Inaba, J., Kudo, T., Ueda, N., Konishi, M., Mitsuda, N., Takiguchi, Y., Kondou, Y., Yoshizumi, T., Ohme-Takagi, M., Matsui, M., Yano, K., Yanagisawa, S. and Sakakibara, H. (2018). Repression of Nitrogen Starvation Responses by Members of the Arabidopsis GARP-Type Transcription Factor NIGT1/HRS1 Subfamily. The Plant Cell. Advanced Access published April 5, 2018: 10.1105/tpc.17.00810.

Kilari, R. S., Weaver, J. D., Shears, S. B. and Safrany, S. T. (2013). Understanding inositol pyrophosphate metabolism and function: Kinetic characterization of the DIPPs. FEBS Letters. 10.1016/j.febslet.2013.08.035.

Kondo, Y., Rikiishi, K. and Sugimoto, M. (2022). Rice Nudix Hydrolase OsNUDX2 Sanitizes Oxidized Nucleotides. Antioxidants (Basel, Switzerland). Advanced Access published September 13, 2022: 10.3390/antiox11091805.

Kraszewska, E. (2008). The plant Nudix hydrolase family. Acta Biochimica Polonica. 10.18388/abp.2008_3025.

Kuo, H.-F., Hsu, Y.-Y., Lin, W.-C., Chen, K.-Y., Munnik, T., Brearley, C. A. and Chiou, T.-J. (2018). Arabidopsis inositol phosphate kinases IPK1 and ITPK1 constitute a metabolic pathway in maintaining phosphate homeostasis. The Plant Journal. 10.1111/tpj.13974.

Kurz, L., Schmieder, P., Veiga, N. and Fiedler, D. (2023). One Scaffold, Two Conformations: The Ring-Flip of the Messenger $InsP_8$ Occurs under Cytosolic Conditions. Biomolecules. Advanced Access published April 4, 2023: 10.3390/biom13040645.

Laha, D., Johnen, P., Azevedo, C., Dynowski, M., Weiß, M., Capolicchio, S., Mao, H., Iven, T., Steenbergen, M., Freyer, M., Gaugler, P., Campos, M. K. de**, Zheng, N., Feussner, I., Jessen, H. J., van Wees, S. C., Saiardi, A. and Schaaf, G.** (2015). VIH2 Regulates the Synthesis of Inositol Pyrophosphate $InsP_8$ and Jasmonate-Dependent Defenses in Arabidopsis. The Plant Cell. 10.1105/tpc.114.135160.

Laha, D., Parvin, N., Dynowski, M., Johnen, P., Mao, H., Bitters, S. T., Zheng, N. and Schaaf, G. (2016). Inositol Polyphosphate Binding Specificity of the Jasmonate Receptor Complex. Plant Physiology. 10.1104/pp.16.00694.

Laha, N. P., Giehl, R. F. H., Riemer, E., Qiu, D., Pullagurla, N. J., Schneider, R., Dhir, Y. W., Yadav, R., Mihiret, Y. E., Gaugler, P., Gaugler, V., Mao, H., Zheng, N., von Wirén, N., Saiardi, A., Bhattacharjee, S., Jessen, H. J., Laha, D. and Schaaf, G. (2022). INOSITOL (1,3,4) TRIPHOSPHATE 5/6 KINASE1-dependent inositol polyphosphates regulate auxin responses in Arabidopsis. Plant Physiology. 10.1093/plphys/kiac425.

Laurent, F., Bartsch, S. M., Shukla, A., Rico-Resendiz, F., Couto, D., Fuchs, C., Nicolet, J., Loubéry, S., Jessen, H. J., Fiedler, D. and Hothorn, M. (2024). Inositol pyrophosphate catabolism by three families of phosphatases regulates plant growth and development. PLoS Genetics. Advanced Access published November 12, 2024: 10.1371/journal.pgen.1011468.

Liu, B., Fan, J., Zhang, Y., Mu, P., Wang, P., Su, J., Lai, H., Li, S., Feng, D., Wang, J. and Wang, H. (2012). OsPFA-DSP1, a rice protein tyrosine phosphatase, negatively regulates drought stress responses in transgenic tobacco and rice plants. Plant Cell Reports. Advanced Access published January 5, 2012: 10.1007/s00299-011-1220-x.

Liu, F., Wang, Z., Ren, H., Shen, C., Li, Y., Ling, H.-Q., Wu, C., Lian, X. and Wu, P. (2010). OsSPX1 suppresses the function of OsPHR2 in the regulation of expression of OsPT2 and phosphate homeostasis in shoots of rice. The Plant Journal. Advanced Access published February 9, 2010: 10.1111/j.1365-313X.2010.04170.x.

Liu, Y., Zhang, W., Wang, Y., Xie, L., Zhang, Q., Zhang, J., Li, W., Wu, M., Cui, J., Wang, W. and Zhang, Z. (2022). Nudix hydrolase 14 influences plant development and grain chalkiness in rice. Frontiers in plant science. Advanced Access published December 8, 2022: 10.3389/fpls.2022.1054917.

Lolla, P., Shah, A., Unnikannan, C. P., Oddi, V. and Bhandari, R. (2021). Inositol pyrophosphates promote MYC polyubiquitination by FBW7 to regulate cell survival. Biochemical Journal. 10.1042/BCJ20210081.

Lonetti, A., Szijgyarto, Z., Bosch, D., Loss, O., Azevedo, C. and Saiardi, A. (2011). Identification of an Evolutionarily Conserved Family of Inorganic Polyphosphate Endopolyphosphatases. Journal of Biological Chemistry. 10.1074/jbc.m111.266320.

Lv, Q., Zhong, Y., Wang, Y., Wang, Z., Zhang, L., Shi, J., Wu, Z., Liu, Y., Mao, C., Yi, K. and Wu, P. (2014). SPX4 Negatively Regulates Phosphate Signaling and Homeostasis through Its Interaction with PHR2 in Rice. The Plant Cell. Advanced Access published April 1, 2014: 10.1105/tpc.114.123208.

Maeda, Y., Konishi, M., Kiba, T., Sakuraba, Y., Sawaki, N., Kurai, T., Ueda, Y., Sakakibara, H. and Yanagisawa, S. (2018). A NIGT1-centred transcriptional cascade regulates nitrate signalling and incorporates phosphorus starvation signals in Arabidopsis. Nature Communications. Advanced Access published April 10, 2018: 10.1038/s41467-018-03832-6.

Marquès-Bueno, M. M., Morao, A. K., Cayrel, A., Platre, M. P., Barberon, M., Caillieux, E., Colot, V., Jaillais, Y., Roudier, F. and Vert, G. (2016). A versatile Multisite Gateway-compatible promoter and transgenic line collection for cell type-specific functional genomics in Arabidopsis. The Plant Journal. 10.1111/tpj.13099.

McLennan, A. G. (2006). The Nudix hydrolase superfamily. Cellular and molecular life sciences: CMLS. 10.1007/s00018-005-5386-7.

Medici, A., Marshall-Colon, A., Ronzier, E., Szponarski, W., Wang, R., Gojon, A., Crawford, N. M., Ruffel, S., Coruzzi, G. M. and Krouk, G. (2015). AtNIGT1/HRS1 integrates nitrate and phosphate signals at the Arabidopsis root tip. Nature Communications. Advanced Access published February 27, 2015: 10.1038/ncomms7274.

Medici, A., Szponarski, W., Dangeville, P., Safi, A., Dissanayake, I. M., Saenchai, C., Emanuel, A., Rubio, V., Lacombe, B., Ruffel, S., Tanurdzic, M., Rouached, H. and Krouk, G. (2019). Identification of Molecular Integrators Shows that Nitrogen Actively Controls the Phosphate Starvation Response in Plants. The Plant Cell. Advanced Access published March 14, 2019: 10.1105/tpc.18.00656.

Mihiret, Y. E., Schaaf, G. and Kamleitner, M. (2024). Protein pyrophosphorylation by inositol phosphates: a novel post-translational modification in plants? Frontiers in plant science. Advanced Access published February 22, 2024: 10.3389/fpls.2024.1347922.

Morgan, J. A. M., Singh, A., Kurz, L., Nadler-Holly, M., Ruwolt, M., Ganguli, S., Sharma, S., Penkert, M., Krause, E., Liu, F., Bhandari, R. and Fiedler, D. (2024). Extensive protein pyrophosphorylation revealed in human cell lines. Nature Chemical Biology. Advanced Access published April 25, 2024: 10.1038/s41589-024-01613-5.

Mudge, S. R., Rae, A. L., Diatloff, E. and Smith, F. W. (2002). Expression analysis suggests novel roles for members of the Pht1 family of phosphate transporters in Arabidopsis. The Plant journal: for cell and molecular biology. 10.1046/j.1365-313x.2002.01356.x.

Olejnik, K., Murcha, M. W., Whelan, J. and Kraszewska, E. (2007). Cloning and characterization of AtNUDT13, a novel mitochondrial *Arabidopsis thaliana* Nudix hydrolase specific for long-chain diadenosine polyphosphates. The FEBS journal. 10.1111/j.1742-4658.2007.06009.x.

Puga, M. I., Mateos, I., Charukesi, R., Wang, Z., Franco-Zorrilla, J. M., Lorenzo, L. de**, Irigoyen, M. L., Masiero, S., Bustos, R., Rodríguez, J., Leyva, A., Rubio, V., Sommer, H. and Paz-Ares, J.** (2014). SPX1 is a phosphate-dependent inhibitor of PHOSPHATE STARVATION RESPONSE 1 in Arabidopsis. Proceedings of the National Academy of Sciences. 10.1073/pnas.1404654111.

Raj, K., Gaugler, V., Lu, M., Schaedel, M., Gaugler, P., Grothaus, C. M. M., Jochimsen, U. A., Liu, G., Harings, M., Jessen, H. J., Schaaf, G. and Ried-Lasi, M. K. (2024). Lotus japonicus VIH2 is an inositol pyrophosphate synthase that regulates arbuscular mycorrhiza.

Ried, M. K., Wild, R., Zhu, J., Pipercevic, J., Sturm, K., Broger, L., Harmel, R. K., Abriata, L. A., Hothorn, L. A., Fiedler, D., Hiller, S. and Hothorn, M. (2021). Inositol pyrophosphates promote the interaction of SPX domains with the coiled-coil motif of PHR transcription factors to regulate plant phosphate homeostasis. Nature Communications. 10.1038/s41467-020-20681-4.

Riemer, E., Pullagurla, N. J., Yadav, R., Rana, P., Jessen, H. J., Kamleitner, M., Schaaf, G. and Laha, D. (2022). Regulation of plant biotic interactions and abiotic stress responses by inositol polyphosphates. Frontiers in plant science. Advanced Access published August 11, 2022: 10.3389/fpls.2022.944515.

Riemer, E., Qiu, D., Laha, D., Harmel, R. K., Gaugler, P., Gaugler, V., Frei, M., Hajirezaei, M.-R., Laha, N. P., Krusenbaum, L., Schneider, R., Saiardi, A., Fiedler, D., Jessen, H. J., Schaaf, G. and Giehl, R. F. (2021). ITPK1 is an $InsP_6$/ADP phosphotransferase that controls phosphate signaling in Arabidopsis. Molecular Plant. 10.1016/j.molp.2021.07.011.

Robinson, W. D., Park, J., Tran, H. T., Del Vecchio, H. A., Ying, S., Zins, J. L., Patel, K., McKnight, T. D. and Plaxton, W. C. (2012). The secreted purple acid phosphatase isozymes AtPAP12 and AtPAP26 play a pivotal role in extracellular phosphate-scavenging by *Arabidopsis thaliana*. Journal of Experimental Botany. Advanced Access published November 3, 2012: 10.1093/jxb/ers309.

Rubio, V., Linhares, F., Solano, R., Martín, A. C., Iglesias, J., Leyva, A. and Paz-Ares, J. (2001). A conserved MYB transcription factor involved in phosphate starvation signaling both in vascular plants and in unicellular algae. Genes & Development. 10.1101/gad.204401.

Safi, A., Medici, A., Szponarski, W., Marshall-Colon, A., Ruffel, S., Gaymard, F., Coruzzi, G., Lacombe, B. and Krouk, G. (2018). HRS1/HHOs GARP transcription factors and reactive oxygen species are regulators of Arabidopsis nitrogen starvation response.

Safrany, S. T., Ingram, S. W., Cartwright, J. L., Falck, J. R., McLennan, A. G., Barnes, L. D. and Shears, S. B. (1999). The Diadenosine Hexaphosphate Hydrolases from *Schizosaccharomyces pombe* and *Saccharomyces cerevisiae* Are Homologues of the Human Diphosphoinositol Polyphosphate Phosphohydrolase. Journal of Biological Chemistry. 10.1074/jbc.274.31.21735.

Saiardi, A., Bhandari, R., Resnick, A. C., Snowman, A. M. and Snyder, S. H. (2004). Phosphorylation of proteins by inositol pyrophosphates. Science. 10.1126/science.1103344.

Sanchez, A. M., Schwer, B., Jork, N., Jessen, H. J. and Shuman, S. (2023). Activities, substrate specificity, and genetic interactions of fission yeast Siw14, a cysteinyl-phosphatase-type inositol pyrophosphatase. mBio. Advanced Access published September 29, 2023: 10.1128/mbio.02056-23.

Schneider, R., Lami, K., Prucker, I., Stolze, S. C., Strauß, A., Langenbach, K., Kamleitner, M., Belay, Y. Z., Ritter, K., Furkert, D., Gaugler, P., Lange, E., Faiß, N., Schmidt, J. M., Harings, M., Krusenbaum, L., Wege, S., Kriescher, S., Schoof, H., Fiedler, D., Nakagami, H., Giehl, R. F. H., Lahaye, T., Jessen, H. J., Gaugler, V. and Schaaf, G. (2024). NUDIX Hydrolases Target Specific Inositol Pyrophosphates and Regulate Phosphate and Iron Homeostasis, and the Expression of Defense Genes in Arabidopsis.

Sharma, N., Chaudhary, C. and Khurana, P. (2020a). Role of *myo*-inositol during skotomorphogenesis in Arabidopsis. Scientific reports. Advanced Access published October 15, 2020: 10.1038/s41598-020-73677-x.

Sharma, N., Chaudhary, C. and Khurana, P. (2020b). Wheat *Myo*-inositol phosphate synthase influences plant growth and stress responses via ethylene mediated signaling. Scientific reports. Advanced Access published July 1, 2020: 10.1038/s41598-020-67627-w.

Steidle, E. A., Chong, L. S., Wu, M., Crooke, E., Fiedler, D., Resnick, A. C. and Rolfes, R. J. (2016). A Novel Inositol Pyrophosphate Phosphatase in *Saccharomyces cerevisiae*. Journal of Biological Chemistry. 10.1074/jbc.m116.714907.

Thibaud, M.-C., Arrighi, J.-F., Bayle, V., Chiarenza, S., Creff, A., Bustos, R., Paz-Ares, J., Poirier, Y. and Nussaume, L. (2010). Dissection of local and systemic transcriptional responses to phosphate starvation in Arabidopsis. The Plant Journal. Advanced Access published November 2, 2010: 10.1111/j.1365-313X.2010.04375.x.

Ueda, Y., Kiba, T. and Yanagisawa, S. (2020). Nitrate-inducible NIGT1 proteins modulate phosphate uptake and starvation signalling via transcriptional regulation of SPX genes. The Plant Journal. Advanced Access published January 8, 2020: 10.1111/tpj.14637.

Vance, C. P., Uhde-Stone, C. and Allan, D. L. (2003). Phosphorus acquisition and use: critical adaptations by plants for securing a nonrenewable resource. New Phytologist. 10.1046/j.1469-8137.2003.00695.x.

Wang, H., Gu, C., Rolfes, R. J., Jessen, H. J. and Shears, S. B. (2018). Structural and biochemical characterization of Siw14: A protein-tyrosine phosphatase fold that metabolizes inositol pyrophosphates. Journal of Biological Chemistry. 10.1074/jbc.ra117.001670.

Wang, H., Perera, L., Jork, N., Zong, G., Riley, A. M., Potter, B. V. L., Jessen, H. J. and Shears, S. B. (2022). A structural exposé of noncanonical molecular reactivity within the protein tyrosine phosphatase WPD loop. Nature Communications. 10.1038/s41467-022-29673-y.

Wang, Z., Zheng, Z., Zhu, Y., Kong, S. and Liu, D. (2023). PHOSPHATE RESPONSE 1 family members act distinctly to regulate transcriptional responses to phosphate starvation. Plant Physiology. 10.1093/plphys/kiac521.

Ward, J. T., Lahner, B., Yakubova, E., Salt, D. E. and Raghothama, K. G. (2008). The effect of iron on the primary root elongation of Arabidopsis during phosphate deficiency. Plant Physiology. Advanced Access published May 8, 2008: 10.1104/pp.108.118562.

Whitfield, H. L., Rodriguez, R. F., Shipton, M. L., Li, A. W. H., Riley, A. M., Potter, B. V. L., Hemmings, A. M. and Brearley, C. A. (2024). Crystal Structure and Enzymology of *Solanum tuberosum* Inositol Tris/Tetrakisphosphate Kinase 1 (StITPK1). Biochemistry. Advanced Access published December 26, 2023: 10.1021/acs.biochem.3c00404.

Yang, X., Safrany, S. T. and Shears, S. B. (1999). Site-directed Mutagenesis of Diphosphoinositol Polyphosphate Phosphohydrolase, a Dual Specificity NUDT Enzyme That Attacks Diadenosine Polyphosphates and Diphosphoinositol Polyphosphates. Journal of Biological Chemistry. 10.1074/jbc.274.50.35434.

Yoshimura, K. and Shigeoka, S. (2015). Versatile physiological functions of the Nudix hydrolase family in Arabidopsis. Bioscience, Biotechnology, and Biochemistry. Advanced Access published December 6, 2014: 10.1080/09168451.2014.987207.

Yu, X., Keitel, C. and Dijkstra, F. A. (2021). Global analysis of phosphorus fertilizer use efficiency in cereal crops. Global Food Security. 10.1016/j.gfs.2021.100545.

Zhang, Z., Li, Z., Wang, W., Jiang, Z., Guo, L., Wang, X., Qian, Y., Huang, X., Liu, Y., Liu, X., Qiu, Y., Li, A., Yan, Y., Xie, J., Cao, S., Kopriva, S., Li, L., Kong, F., Liu, B., Wang, Y., Hu, B. and Chu, C. (2021). Modulation of nitrate-induced phosphate response by the MYB transcription factor RLI1/HINGE1 in the nucleus. Molecular Plant. Advanced Access published December 11, 2020: 10.1016/j.molp.2020.12.005.

Zhou, J., Jiao, F., Wu, Z., Li, Y., Wang, X., He, X., Zhong, W. and Wu, P. (2008). OsPHR2 is involved in phosphate-starvation signaling and excessive phosphate accumulation in shoots of plants. Plant Physiology. Advanced Access published February 8, 2008: 10.1104/pp.107.111443.

Zhu, J., Lau, K., Puschmann, R., Harmel, R. K., Zhang, Y., Pries, V., Gaugler, P., Broger, L., Dutta, A. K., Jessen, H. J., Schaaf, G., Fernie, A. R., Hothorn, L. A., Fiedler, D. and Hothorn, M. (2019). Two bifunctional inositol pyrophosphate kinases/phosphatases control plant phosphate homeostasis. eLife. 10.7554/elife.43582.

Other Publications

Riemer, E., Qiu, D., Laha, D., Harmel, R. K., Gaugler, P., Gaugler, V., Frei, M., Hajirezaei, M. R., Laha, N. P., Krusenbaum, L., Schneider, R., Saiardi, A., Fiedler, D., Jessen, H. J., Schaaf, G., Giehl, R. F. H. (2021). ITPK1 is an $InsP_6$/ADP phosphotransferase that controls phosphate signaling in Arabidopsis. Molecular Plant 14(11):1864-1880. https://doi.org/10.1016/j.molp.2021.07.011

Laha, N. P., Giehl, R. F. H., Riemer, E., Qiu, D., Pullagurla, N. J., Schneider, R., Dhir, Y. W., Yadav, R., Mihiret, Y. E., Gaugler, P., Gaugler, V., Mao, H., Zheng, N., von Wirén, N., Saiardi, A., Bhattacharjee, S., Jessen, H. J., Laha, D., Schaaf, G. (2022). INOSITOL (1,3,4) TRIPHOSPHATE 5/6 KINASE1-dependent inositol polyphosphates regulate auxin responses in Arabidopsis. Plant Physis 190(4):2722–2738. https://doi.org/10.1093/plphys/kiac425

Liu, G., Riemer, E., Schneider, R., Cabuzu, D., Bonny, O., Wagner, C. A., Qiu, D., Saiardi, A., Strauss, A., Lahaye, T., Knoll, T., Jessen, J. P., Jessen, H. J. (2023). The phytase RipBL1 enables the assignment of a specific inositol phosphate isomer as a structural component of human kidney stones. RSC Chemical Biology. https://doi.org/10.1039/D2CB00235C

Acknowledgments

Completing this dissertation has been a challenging but very enlightening and rewarding journey, and it wouldn't have been possible without the support, guidance, and encouragement of many people.

First and foremost, I would like to express my deepest gratitude to my supervisor Professor Gabriel Schaaf for giving me the opportunity to continue my work after my master studies. I would like to thank you for the opportunity to develop and follow up on my own ideas, for your constructive feedback, your guidance and your patience over the past few years.

A big thank you to the current and former members of Lab Schaaf and the Department of Plant Nutrition for the shared experiences, support, and conversations, especially during the pretzel Thursdays. A very special thank you to my university friend, office mate, and lab neighbor Esther, for your mental and physical support throughout the entire journey. I already miss our lunch breaks where we talked about our work, food recipes, and the whole world. But somehow, I'm glad we didn't keep the Mon Chéri coffee breaks. I would also like to thank Verena and Philipp for all the fun times in and out of the lab. And especially Verena for proposing, constantly supporting and supervising the NUDT project during the last years. Many thanks also to Klea for completing the experiments of the NUDT project and to Brigitte for her active support with my experiments and for keeping the lab running. I would also like to thank Marília for her excellent and very helpful input and fine-tuning of my written work.

Finally, and most importantly, I would like to thank my husband, my parents and my friends, words cannot express my gratitude for your unconditional love and encouragement. Above all, I would like to thank my husband Thorsten. Thank you for your unreserved understanding, support and love, even during challenging times. I can't thank you enough for always having my back. Your motivation, encouragement and trust have been unwavering, and I truly couldn't have made it through this journey without you. I would also like to thank my parents for all their help, patience, understanding, and for giving me the opportunity and strength to study and go my academic and personal way.

Thank you all for making this milestone possible.